Impact of cigarette smoke exposure on the airway epithelium of *Drosophila melanogaster* to model COPD-like phenotypes

Dissertation

zur Erlangung des Doktorgrades

der Mathematisch-Naturwissenschaftlichen Fakultät

der Christian-Albrechts-Universität zu Kiel

vorgelegt von

Anita Bhandari

aus Freital

Kiel, 2015

Erster Gutachter:	Prof. Dr. Thomas Roeder
Zweiter Gutachter:	Prof. Dr. Holger Heine
Tag der mündlichen Prüfung:	19.01.2016
Zum Druck genehmigt:	19.01.2016

gez. Prof. Dr. Wolfgang Duschl

Table of contents

Summary ..... **I**

Zusammenfassung ..... **II**

Abbreviations and Units ..... **IV**

List of Figures ..... **IX**

List of Tables ..... **XIII**

1. Introduction **1**

1.1 Chronic obstructive pulmonary disease (COPD) 1

1.1.1 Pathogenesis and pathophysiology of COPD 1

1.1.2 Physiological role of second messengers in COPD pathogenesis 4

1.2 Modeling human diseases in *Drosophila melanogaster* 7

1.2.1 *Drosophila melanogaster* as a model to study smoke related diseases like COPD 7

1.2.2 Structure of the respiratory system of *D. melanogaster* 8

1.2.3 Respiratory defense mechanisms in *D. melanogaster* 10

1.2.4 Advantages of genetic tools for manipulation of the fly's airway epithelium 15

1.2.5 New approaches to manipulate the fly's airways using the DREADD technology and optogenetic tools to understand airway diseases 17

1.3 Aim and significance of the study 21

2. Materials and Methods **22**

2.1 Materials 22

2.1.1 Laboratory equipments 22

2.1.2 List of miscellaneous material 23

2.1.3 Chemicals 24

2.1.4 Antibodies 25

2.1.5 Plasmids and vectors 25

2.1.6 Enzymes 26

2.1.7 Bacterial strains 27

2.1.8 Antibiotics 27

2.1.9 Oligonucleotides 27

2.1.10 Solutions and media 28

2.1.11 *Drosophila* stocks 30

2.2 Methods 32

2.2.1 *Drosophila* culture and crosses 32
2.2.2 Treatment of larvae and flies 32
2.2.2.1 Cigarette smoke exposure 32
2.2.2.2 Hypoxia 33
2.2.2.3 Optogenetic manipulation of the respiratory system with blue light 34
2.2.2.4 Application of Clozapine N-oxide (CNO) 34
2.2.3 Methods for phenotypical characterization 35
2.2.3.1 Survival assay 35
2.2.3.2 Immunohistochemistry and microscopy 35
2.2.3.3 L-DOPA staining 35
2.2.3.4 β-galactosidase staining 36
2.2.3.5 Characterization of tracheal terminal cells 36
2.2.4 Molecular biological methods 36
2.2.4.1 Agarose gel electrophoresis 36
2.2.4.2 Purification of DNA from agarose gels 36
2.2.4.3 Purification of plasmid DNA 37
2.2.4.4 Restriction endonuclease digestion of DNA 37
2.2.4.5 Dephosphorylation of linearized vector 37
2.2.4.6 Ligation of DNA fragments 38
2.2.4.7 Total RNA isolation 38
2.2.4.8 Generation of cDNA and reverse transcriptase PCR 38
2.2.4.9 Quantitative real time PCR 39
2.2.4.10 Electrophoretic mobility shift assay (EMSA) 40
2.2.5 Microbiological methods 40
2.2.5.1 Growth of liquid cultures 40
2.2.5.2 Growth on solid media 40
2.2.5.3 Monitoring the bacterial growth 40
2.2.5.4 Heat-shock transformation of plasmid DNA in *E. coli* 41
2.2.5.5 Glycerol stocks of *E. coli* cultures 41
2.2.6 Protein expression and purification 41
2.2.6.1 Expression of recombinant dFoxO FH DBD 41
2.2.6.2 Preparation of cell lysates 41
2.2.6.3 Purification of dFoxO FH DBD 42
2.2.7 Protein analysis 42

2.2.7.1 SDS-polyacrylamide gel electrophoresis (SDS-PAGE) 42
2.2.7.2 Coomassie staining of protein gels 43
2.2.8 *in silico* analysis 43
2.2.8.1 Sequence collection 43
2.2.8.2 Sequence alignment and tree building 44
2.2.8.3 Structure modeling 44
2.2.8.4 Softwares 44
3. Results 45
3.1 Activation of JAK-STAT signaling in the trachea after CSE 45
3.2 Activation of the cytokine related ligands upd, upd2 and upd3 after CSE 46
3.2.1 Phylogenetic tree analysis of upd, upd2 and upd3 46
3.2.2 Recognition of a conserved helical cytokine fold of upd3 and IL-6 48
3.2.3 Expression analysis of upd, upd2 and upd3 in the trachea with and without CSE .. 49
3.2.4 Effects of CSE on upd, upd2 and upd3 gene expression in the *Drosophila* airway epithelium 51
3.3 Activation of proinflammatory transcription factors after CSE 53
3.3.1 Relish (IMD) activation after exposure to cigarette smoke 53
3.3.2 Nuclear translocation of CncC and expression of GstD after CSE 54
3.3.2 Nuclear translocation of dFoxO in response to CSE 55
3.4 dFoxO dependent regulation of cytokines upd2 and upd3 56
3.4.1 Effect of dFoxO and relish knockouts on transcription levels of upd2 and upd3 56
3.4.2 Characterization of the promoter regions of upd, upd2 and upd3 - screening for potential dFoxO binding motifs 58
3.4.3 Expression and purification of dFoxO FH DBD 59
3.4.4 Electrophoretic mobility shift assays of dFoxO and upd promoters 62
3.5 The roles of JAK-STAT signaling in the respiratory tract of *Drosophila* 63
3.5.1 Consequences of ectopic expression of upd3 in the airways 63
3.5.2 Ectopic expression of domeless in the airway epithelium 65
3.6 Cigarette smoke exposure induces local remodeling in the airway epithelium 67
3.7 Cigarette smoke exposure reduces life span of *D. melanogaster* 69
3.8 Expression of drosomycin in response to cigarette smoke exposure 72
3.9 Induction of cAMP synthesis in the airways of *D. melanogaster* by a blue light activated adenylyl cyclase of *Beggiatoa* (bPAC) 72

3.9.1 Sequence similarity between *Beggiatoa* bPAC and *Drosophila* Gyc76C 72
3.9.2 Expression and activation of bPAC controls tracheal terminal branching..... 73
3.9.3 Expression and activation of bPAC causes melanization in the airways 76
3.9.4 Expression and activation of bPAC in the airways controls growth and viability... 77
3.9.5 Expression and activation of bPAC in the trachea effects the homeobox transcription factor cut..... 78
3.9.6 Expression and activation of bPAC in the trachea leads to activation of dFoxO 82
3.10 Depolarization of the terminal cells utilizing ChR2-XXL 84
3.11 Melanotic tumor formation in the respiratory track of *D. melanogaster* 85
3.11.1 Activation of dFoxO leads into tracheal melanization..... 85
3.11.2 Activation of dFoxO in the trachea has no impact on the fruit fly's viability 86
3.11.3 Activation of dFoxO in the respiratory system triggers phenol oxidase activity required for melanin biosynthesis 87
3.11.4 dFoxO - a possible regulator of tracheal melanization 87
4. Discussion 89
4.1 Modeling of COPD in the airway epithelium of *D. melanogaster* 89
4.1.1 Activation of the JAK-STAT pathway as an autocrine signaling after CSE?..... 91
4.1.2 Role of redox-regulated transcription factors in the CSE-associated responses 93
4.1.3 Airway remodeling as a response to CSE 97
4.1.4 A possible dFoxO- mediated signaling cascade..... 97
4.2 Utilization of bPAC to study cAMP signaling in the airways of *D. melanogaster* 99
4.3 Limitations and challenges using the fruit fly as COPD-model..... 101
5. Conclusion 103
6. References 104
7. Appendix 121
7.1 Activation of Wnt signaling after CSE 121
7.2 Neighbor joining phylogenetic tree analysis of upd 1, 2 and 3 122
7.3 Secondary structure prediction for upd3 124
7.4 Expression levels of upd2 and upd3 after hypoxia 126
7.5 Cloning of dFoxO DBD into pET28a (+) 126
7.6 Induced remodeling of the terminal branches after CSE 128
7.7 Application of DREADD for targeted manipulation of the trachea..... 129
Acknowledgement i

Curriculum vitae ..... **ii**

Eidesstattliche Erklärung ..... **vi**

Summary

Chronic obstructive pulmonary disease (COPD) is currently the third leading cause of death worldwide according to the World Health Organization (WHO) and is expected to become an even more serious problem in upcoming decades. Cigarette smoking is the major risk factor for COPD and lung cancer. Although COPD is one of the most important chronic lung diseases, our knowledge about the underlying molecular framework is only fragmentary.

Hence, this study introduces *D. melanogaster* as a novel model for basic COPD research that allows testing hypotheses experimentally. Various cigarette smoke exposure (CSE) models using different exposure regimes were implemented in the course of this study and the *in vivo* impact of CSE was analyzed using 3rd instar larvae. The airways showed a strong structural modification and an activation of JAK-STAT signaling in the epithelial cells of CS treated animals. Moreover, expression of the ligands of this pathway belonging to the upd family was induced upon CSE. Both, upd2 and upd3 and the receptor dome of the JAK-STAT pathway, were strongly expressed at the posterior end of the dorsal branches, indicative for an autocrine signaling system. The exact function and role of these ligands, especially in the tracheal system of *D. melanogaster* are still poorly understood. *In silico* analysis of the structures of upd3 with IL-6 of mouse, implied an ancestral relationship between both cytokines. Moreover, an ectopic expression of these components of the JAK-STAT pathway in the airway epithelium of *Drosophila* resulted into epithelial barrier disruption in form of meta- and hyperplasia. To unravel potential upstream regulators for the expression of these upd ligands, different flies deficient in expression of either dFoxO or relish were used. Both are essential for the two major arms of the fly's airway epithelial immune system and thus were exposed to smoke. Especially, in dFoxO deficient flies, induction of upd2 and upd3 transcripts were significantly reduced. Electrophoretic mobility shift assays underline the potential role of dFoxO in directly regulating upd2 and upd3 expression. Furthermore, cigarette smoke results in structural remodeling including thickening of the epithelial layer, in parallel with activation of JAK/STAT signaling that may be triggered by dFoxO activation.

Beside this CSE based model for COPD research, destruction of the terminal airway structure via strong activation of cAMP signaling was induced.

Zusammenfassung

COPD ist derzeit nach Angaben der Weltgesundheitsorganisation (WHO) die dritthäufigste Todesursache weltweit und die Zahl der Rauchertoten nimmt in den kommenden Jahren immer mehr zu. Das Rauchen von Zigaretten oder das Passiv-Rauchen ist der größte Risikofaktor für COPD und Lungenkrebs. Obwohl COPD eine der bedeutendsten chronischen Lungenerkrankungen ist, ist unser Wissen über die zugrunde liegenden molekularen Signalwege und Gene derzeit nur bruchstückhaft.

Die vorliegende Arbeit hatte daher zum Ziel, *D. melanogaster* als ein neues Modell für die Grundlagenforschung der COPD einzuführen, um Hypothesen schnell testen zu können. Das *Drosophila*-Modell hat drei wesentliche Vorteile, zum einen, eine Fokussierung auf das Atemwegsepithel ohne Einflüsse einer adaptiven Immunantwort, die enorme zeitliche Einsparung der Experimentendauer und die recht einfache Isolierung der Tracheen. Es wurde dabei die Relevanz von Zigarettenrauch im Atemwegsepithelium von *Drosophila* untersucht und eine epitheliale Immunreaktion gezeigt. Die Applikation von Zigarettenrauch in *Drosophila* hatte eine Beeinträchtigung der epithelialen Barriere zur Folge und eine Aktivierung des JAK-STAT-Signalwegs konnte gezeigt werden. Außerdem erfolgte eine Zigarettenrauch-induzierte Expression der Liganden Upd2 und Upd3 sowie des Rezeptors Domeless, welche die Hauptkomponenten des JAK-STAT- Signalwegs sind. Die Induktion des JAK-STAT-Signalwegs erfolgte spezifisch an den doralen Verzweigungen der primären Tracheen, was für ein autokrines Signalisierungssystem spricht. Die genaue Funktion und Rolle dieser Liganden sind vor allem in den Tracheen von *D. melanogaster* noch weitgehend unverstanden. Daher wurden sowohl strukturelle Vergleiche von upd3 mit der bekannten Kristallstruktur von IL-6 als auch eine funktionelle Überexpression dieser Liganden in den Tracheen vorgenommen, um diese näher charakterisieren zu können. Eine ektopische Überexpression dieser Komponenten im Atemwegsepithel von *Drosophila* führte zu einer Störung der Epithelbarriere in Form einer Meta- und Hyperplasie.

Um mögliche Regulatorgene für die Expression dieser Upd-Liganden zu entschlüsseln, wurden Mutanten, defizient in den Transkriptionsfaktoren dFoxO und Relish verwendet und ebenfalls mit Zigarettenrauch behandelt. Insbesondere in dFoxO defizienten Fliegen war die Induktion der Upd2 und Upd3- Transkripte deutlich reduziert. *Electrophoretic Mobility Shift Assays* unterstreichen die potentielle Rolle des Transkriptionsfaktors dFoxo in seiner direkten Regulation von Upd2 und Upd3. Eine spezifische Bindung von dFoxO mit entsprechenden intakten potentiellen Bindesequenzen konnte gezeigt werden. Für die DNA-Bindungsanalysen wurde dFoxO in Form eines HIS-Fusionsproteins in *E. coli* überexprimiert und aufgereinigt.

Weiterhin konnte gezeigt werden, dass Zigarettenrauch zur Atemwegsmodelierung in Form einer verdickten Epithelschicht führt, das mit einer parallelen Aktivierung des JAK-STAT-Signalweges einhergeht, welcher vermutlich dFoxO abhängig ist.
Neben dem Zigarettenrauch-Modell für die COPD-Forschung, wurde ein alternatives Modell entwickelt, das sich der Bedeutung des cAMP-Signalings im Atemwegsepithel widmet.

Abbreviations and Units

Abbreviations

ADP	adenosine diphosphate
AC	adenylyl cyclase
amp	ampicillin
AMP	adenosine monophosphate
AMPs	antimicrobial peptides
APS	ammonium persulphate
ARE	antioxidant response element
ASM	airway smooth muscle
ATP	adenosine-5'-triphosphate
β-gal	beta-galactosidase
BLUF	sensors of blue-light using FAD
bPAC	blue light-activated adenylyl cyclase
BSA	bovine serum albumin
Btl	breathless
cAMP	cyclic adenosine monophosphate
cDNA	complimentary DNA
CCM3	cerebral cavernous malformation
ChR2	channelrhodopsin-2
ChR2-XXL	channelrhodopsin-2 D156C mutant
CnC	cap'n'collar
CNO	clozapine N-oxide
COPD	chronic obstructive pulmonary disease
CREB	cAMP response element binding
CSE	cigarette smoke exposure
CS	cigarette smoke
CT	cycle threshold
Cy5	cyanine5
DAPI	4', 6-diamidino-2-phenylindole
DBD	DNA-binding-domain
DMSO	dimethylsulfoxide
DNA	deoxyribonucleic acid

dNTP	deoxyribonucleotide triphosphate
DREADD	Designer Receptor Exclusively Activated by Designer Drugs
DSRF	*Drosophila* serum response factor
DTT	dithiothreitol
DUOX	dual oxidase
E. coli	*Escherichia coli*
EDTA	ethylenediaminetetraacetic acid
EMSA	Electrophoretic mobility shift assay
Epac	exchange protein directly activated by cAMP
FAD	flavin adenine dinucleotide
ENaCs	epithelial Na^+ channels
et al.	*et alumni*
EtOH	ethanol
FH	fork head
Fig.	figure
FoxO	forkhead box subgroup O
fwd	forward
g	acceleration due to gravity, g = 9.81 m/s^2
GFP	green fluorescent protein
GPCR	G-protein-coupled receptor
Gp130	glycoprotein 130
GST	glutathione-s-transferase
HEPES	2-(4-(2-Hydroxyethyl)-piperazine-1-yl)-ethane sulfonic acid
HL3	hemolymph-like buffer
Hop	hopscotch/JAK kinase
HPLC	high pressure liquid chromatography
IgE	immunoglobulin E
IIS	insulin/IGF (insulin-like growth factor)-like signalling
IKK-β	inhibitor of nuclear factor kappa-B kinase subunit beta
IMD	immune deficiency
IPTG	isopropyl-β-D-1-thiogalactopyranoside
IRS	insulin receptor substrate
JAK-STAT	Janus kinase signal transducers and activators of transcription
JNK	c-jun N-terminal kinase

kan	kanamycin
KO	knockout
LB	lysogeny broth
L-DOPA	L-3, 4-dihydroxyphenylalanine
MAPK	mitogen-activated protein kinase
mRNA	messenger RNA
MP1	melanization protease 1
NFκB	nuclear factor κB
NaOH	sodium hydroxide
NGS	normal goat serum
Nrf2	nuclear factor erythroid 2–related factor 2
OD_{600}	optical density at a wavelength of 600 nm
ORMDL	*orosomucoid1-like*
PAGE	polyacrylamide gel electrophoresis
PBS	phosphate buffered saline
PBT	PBS-triton-X 100
PCR	polymerase chain reaction
PDB	Protein Data Bank
PDE	phosphodiesterase
pET	plasmid for expression by T7-RNA-polymerase
PFA	paraformaldehyde
PGRP	peptidoglycan recognition protein
pH	*potentia Hydrogenii*
PI3K	phosphatidylinositol 3-kinase
PKA	protein kinase A
PLC	phospholipase C
PO	phenol oxidase
PPO	polyphenol oxidase
ppk	pick pocket
qRT-PCR	quantitative real-time PCR
rev	reverse
RCSB	Research Collaboratory for Structural Bioinformatics
RFP	Red Fluorescent Protein
RNA	ribonucleic acid

ROS	reactive oxygen species
RT	room temperature
RT-PCR	reverse transcription PCR
SEM	standard error of the mean
SDS	sodium dodecyl sulfate
TARGET	temporal and regional gene expression targeting
TBE	TRIS-Borat-EDTA buffer
TE	TRIS-EDTA-buffer
TEMED	*N, N, N', N'*-Tetramethylethylendiamine
TF	transcription factor
Tris	tris-(hydroxymethyl)-aminomethane
TritonX-100	Polyethylenglycol-mono-[p-(1, 1, 3, 3-tetramethylbutyl)-phenyl]-ether
TPRA	transient receptor potential (ankyrin)
TRPV	transient receptor potential (vanilloid)
UAS	upstream activating sequence
upd	unpaired
WHO	World Health Organization
X-Gal	5-bromo-4-chloro-3-indolyl-β-D-galactopyranoside
yw	yellow white

Units

UV	ultraviolet
°C	degree Celsius
µg	microgram
µl	microliter
µm	micrometer
aa	amino acid
bp	base pair
cm	centimeter
g	gram (weight) respective gravity (for centrifugation)
h	hour
kb	kilo base pairs
kDa	kilo Dalton
l	liter

mA	milliampere
mg	milligram
ml	milliliter
mM	millimolar
mol	mole
ng	nanogram
nm	nanometer
pmol	picomole
rpm	revolutions per minute
v/v	volume per volume
w/v	weight per volume

Abbreviations of nucleotides.

Nucleotides	Abbreviation
Adenosine	A
Cytosine	C
Guanosine	G
Thymidine	T
N	A, C, G or T

Abbreviations of amino acids, single letter code and cognate DNA codons.

Amino acid	Abbreviation	Single letter code	DNA codons
Alanine	Ala	A	GCT, GCC, GCA, GCG
Arginine	Arg	R	CGT, CGC, CGA, CGG, AGA, AGG
Asparagine	Asn	N	AAT, AAC
Aspartic acid	Asp	D	GAT, GAC
Cysteine	Cys	C	TGT, TGC
Glutamine	Gln	Q	CAA, CAG
Glutamic acid	Glu	E	GAA, GAG
Glycine	Gly	G	GGT, GGC, GGA, GGG
Histidine	His	H	CAT, CAC
Isoleucine	Ile	I	ATT, ATC, ATA
Leucine	Leu	L	TTG, TTA, CTT, CTC, CTA, CTG
Lysine	Lys	K	AAA, AAG
Methionine	Met	M	ATG
Phenylalanine	Phe	F	TTT, TTC
Proline	Pro	P	CCT, CCC, CCA, CCG
Serine	Ser	S	TCT, TCC, TCA, TCG, AGT, AGC
Threonine	Thr	T	ACT, ACC, ACA, ACG
Tryptophan	Trp	W	TGG
Tyrosine	Tyr	Y	TAT, TAC
Stop codons	–	–	TAA, TAG, TGA

List of Figures

Figure 1-1: The human respiratory system and its various different cell types. ... 3
Figure 1-2: The cAMP signaling pathway. ... 5
Figure 1-3: Phospholipase C pathway and Ca^{2+} -signaling. ... 6
Figure 1-4: The respiratory system of *D. melanogaster*. ... 9
Figure 1-5: Septate junctions of the fly's airway epithelial cells. ... 10
Figure 1-6: Respiratory defense mechanisms of *D. melanogaster*. ... 11
Figure 1-7: dFoxO expression in the respiratory track of *D. melanogaster*. ... 13
Figure 1-8: Generation cycle of *D. melanogaster*. ... 15
Figure 1-9: The GAL4/UAS system for targeted manipulation in the fly. ... 16
Figure 1-10: The Target-system of *D. melanogaster*. ... 17
Figure 1-11: UAS-DREADD transgenes of *D. melanogaster*. ... 18
Figure 1-12: Utilization of photoactivated adenylyl cyclase (bPAC), of the soil bacterium *Beggiatoa* to modulate cAMP in *D. melanogaster*. ... 19
Figure 1-13: Utilization of blue-light activated ChR2-XXL for depolarization of cells in *D. melanogaster*. ... 19
Figure 2-1: Experimental design for application of cigarette smoke on *D. melanogaster*. ... 33
Figure 2-2: Schematic view of the *in vitro* blue light stimulation. ... 34
Figure 2-3: Region of interest for characterization of terminal cells. ... 36
Figure 3-1: Cigarette smoke exposure on third instar larva of JAK-STAT reporter line. ... 45
Figure 3-2: Dissection of CS-exposed trachea of third instar larvae. ... 46
Figure 3-3: Bayesian phylogeny of the three JAK-STAT ligands upd, upd2 and upd3. ... 47
Figure 3-4: Structural model of upd3 from *D. melanogaster*. ... 48
Figure 3-5: Comparison of upd, upd2 and upd3 expression with and without CSE and under hypoxia by X-Gal staining. ... 50
Figure 3-6: Relative expression level of upd3 in response to CSE. ... 51
Figure 3-7: mRNA levels of upd2 in response to CSE. ... 52
Figure 3-8: Relative expression level of upd in response to CSE. ... 52
Figure 3-9: Translocation of the transcription factor relish after CSE. ... 53
Figure 3-10: Activation of Nrf2-signaling after cigarette smoke exposure. ... 54
Figure 3-11: Nuclear translocation of dFoxO after exposure to cigarette smoke. ... 55

Figure 3-12: Relative expression of upd3 in the trachea in dFoxO and relish deficient animals after 48 h exposure to cigarette smoke. 56
Figure 3-13: Relative expression of upd2 in the trachea in dFoxO and relish deficient animals after 48 h exposure to cigarette smoke. 57
Figure 3-14: Relative expression of upd in the trachea in dFoxO and relish deficient animals after 48 h exposure to cigarette smoke. 57
Figure 3-15: *In silico* analysis of the promoter regions of upd, upd2 and upd3. 58
Figure 3-16: Alignment of the dFoxO amino acid sequence with that of human homologues (FOXO1a, FOXO3a, FOXO4 and FOXO6). 59
Figure 3-17: Structural model of the dFoxO DBD (A) and the vector map of pET28a (+) dFoxO DBD (B). 60
Figure 3-18: SDS-PAGE analysis of pET28a (+) dFoxO FH DBD - expression in *E. coli* BL21 (DE3) cells. 61
Figure 3-19: Purification of soluble dFoxO FH DBD by NHS-chromatography. 62
Figure 3-20: EMSAs of dFoxO DBD and the promoter regions of upd2 and upd3. 63
Figure 3-21: Ectopic expression of upd3 causes remodeling of the airway epithelium. .. 64
Figure 3-22: Quantification of the thickness and obstruction of the branches after ectopic expression of upd3. 64
Figure 3-23: Ectopic expression of upd and hop^{Tum-l} cause thickening of the epithelial layer. 65
Figure 3-24: Ectopic activation of domeless in the trachea using the TARGET system causes structural changes. 66
Figure 3-25: Quantification of the cell size and number in animals ectopically expressing domeless in the trachea. 66
Figure 3-26: Ectopic expression of domeless in the fly's respiratory system causes malformation of the trachea and melanization. 67
Figure 3-27: Airway remodeling in response to cigarette smoke. 68
Figure 3-28: Activation of upd3 in the oenocytes after CSE. 69
Figure 3-29: Lifespan of male and female wild type flies after CSE. 70
Figure 3-30: Life span of flies deficient in dFoxO after CSE. 70
Figure 3-31: Life span comparison of wild type and dFoxO deficient flies. 71
Figure 3-32: CSE decreased life span of relish deficient flies. 71
Figure 3-33: Activation of the antimicrobial peptide drosomycin in response to CSE. .. 72

Figure 3-34: Sequence alignment of bPac of *Beggiatoa* with *Drosophila* Cyc76c and the human natriuretic receptor. 73
Figure 3-35: Activation of bPAC by blue light in the terminal branches under normoxic and hypoxic conditions. 74
Figure 3-36: Number of terminal branches after activation of bPAC by blue light under normoxic and hypoxic conditions. 75
Figure 3-37: Malformation of terminal branches by activation of bPAC by blue light. 75
Figure 3-38: bPAC induced activation of cAMP in the terminal branches leads into melanized lumps. 76
Figure 3-39: Activation of bPAC by blue light in the trachea driven by PPK4-GAL4 leads into melanization. 77
Figure 3-40: Activation of bPAC by blue light with the tracheal driver PPK4-Gal4 has impact on growth phenotype and viability at the L1/L2 transition. 77
Figure 3-41: Expression of the photoactive bPAC transgene using cut-Gal4 leads into malformed dorsal branches. 78
Figure 3-42: Expression of the photoactive bPAC transgene using cut-Gal4 causes thickening and melanization of the dorsal trunks. 79
Figure 3-43: Quantification of the epithelial thickness of blue-light activated animals. 79
Figure 3-44: Expression of the photoactive bPAC transgene using cut-Gal4 causes a higher number of nuclei. 80
Figure 3-45: Quantification of nuclei number. 80
Figure 3-46: Expression of the photoactive bPAC transgene using cut-Gal4 leads to proliferation of cells and decreased cell size. 81
Figure 3-47: Activation of the transcription factor dFoxO in blue-light activated bPAC animals. 82
Figure 3-48: Expression of the photoactive bPAC transgene using PPK4-Gal4 resulted into dFoxO translocation and decreased epithelial cell size. 83
Figure 3-49: Blue-light activation of ChR2-XXL in the terminal branches. 84
Figure 3-50: Ectopic expression and activation of dFoxO causes tracheal melanization. 85
Figure 3-51: Melanization of the trachea did not affect viability. 86
Figure 3-52: Phenol oxidase activity assay. 87
Figure 3-53: Schematic representation of the putative promoter region and translational start of Spn77Ba. 88

Figure 3-54: EMSA of dFoxO with the promoter of Spn77Ba. 88
Figure 4-1: Activation of JAK-STAT signaling in *Drosophila* in comparison to human lung. 92
Figure 4-2: Alignment of dFoxO binding motifs within the promoter regions of upd2 and upd3. 94
Figure 4-3: Regulatory pathways for upd2 and upd3 expression after CSE. 95
Figure 4-4: Proposed dFoxO dependent activation of JAK-STAT signaling after CSE. 98
Figure 4-5: Proposed model of cAMP- dependent inhibited differentiation of the terminal branches. 100
Figure 7-1: Activation of Wnt signaling in the respiratory track of *D. melanogaster* after CSE. 121
Figure 7-2: Neighbor joining analysis of upd upd2 and upd3 genes of *Drosophila* species. 122
Figure 7-3: Secondary structure prediction of upd3. 125
Figure 7-4: Relative expression of upd2 and upd3 in the trachea after treatment with hypoxia. 126
Figure 7-5: Double digest of pEX-A2 dFoxO DBD with NheI and HindIII and gel-purified dFoxO DBD. 126
Figure 7-6: Cloning scheme of dFoxO DBD into pET28a (+). 127
Figure 7-7: Vector pET28a (+). 127
Figure 7-8: Alignment of sequenced pET28a (+) FoxO_DBD and original dFoxO DBD sequence. 128
Figure 7-9: Remodeling of the terminal cells after CSE. 129
Figure 7-10: CNO-activation of DREADD (M1D1) receptor in the respiratory tract of the fly. 129

List of Tables

Table 1-1: Selected components of cigarette smoke and their potential role in lung injury 2
Table 2-1: List of laboratory equipments 22
Table 2-2: Summary of miscellaneous material 23
Table 2-3: Summary of chemicals and reagents. 24
Table 2-4: List of primary antibodies. 25
Table 2-5: List of secondary antibodies. 25
Table 2-6: Table of plasmids and vectors. 26
Table 2-7: List of restriction endonucleases. 26
Table 2-8: List of other enzymes. 26
Table 2-9: List of bacterial strains. 27
Table 2-10: List of antibiotics. 27
Table 2-11: List of oligonucleotides. 27
Table 2-12: List of oligonucleotides used for EMSAs. 28
Table 2-13: Solutions and media. 28
Table 2-14: Flylines used in this study. 30
Table 2-15: Details for smoke exposure. 32
Table 2-16: RT-PCR program. 39
Table 2-17: Composition of stacking and resolving gel. 42
Table 2-18: Composition of 5x SDS sample buffer. 43
Table 2-19: Composition of SDS buffer. 43
Table 2-20: Composition of coomassie staining and destaining solution. 43
Table 4-1: Comparison of Mouse, *C. elegans* & *Drosophila* as models in COPD research. .. 90
Table 4-2: COPD-features in the airways of *D. melanogaster* after CSE 102
Table 7-1: List of upd, upd2 and upd3 genes 123

1. Introduction

1.1 Chronic obstructive pulmonary disease (COPD)

1.1.1 Pathogenesis and pathophysiology of COPD

Respiratory diseases, like chronic obstructive pulmonary disease (COPD) or asthma, affect a very large proportion of people in the world in terms of morbidity and mortality (Ferkol & Schraufnagel, 2014). According to the World Health Organization (WHO) almost 329 million people (approximately 4.77% of the world's population) suffer from COPD. The impact of this disease is almost equally distributed between males (4.85%) and females (4.69%) (Pauwels & Rabe, 2004; Vos et al, 2012).

COPD, also known as chronic obstructive lung disease (COLD), is a slow progressive and irreversible lung disease characterized by the functional abnormality of airway obstruction, which makes breathing difficult (Barnes et al, 2009). The term "progressive" means the disease typically worsens over time. At first, COPD may cause no or only mild symptoms, as the disease progresses some common symptoms occur, such as shortness of breath (dyspnea), wheezing and chest tightness and an ongoing cough along with mucus hyper secretion (Agusti, 2005). COPD worsens over the time and breathing requires much more energy and its getting difficult for COPD patients to deal with routine activities. This might lead to fatigue, weight and muscle loss. COPD is largely associated with exposure to cigarette smoke as the most important risk factor but also long-term exposure to second-hand smoke like air pollutants, dust or workplace fumes and even biomass exposure such as wood smoke can contribute to COPD development (van der Vaart et al, 2004) (Salvi & Barnes, 2009). Tobacco smoke irritates the airways causing an inflammatory response and destroys the stretchy fibers in the lungs, resulting in a breakdown of the lung tissue known as emphysema (Hecht, 2003). Smoking damages mainly two parts of the lung: the airways and the small air sacs called alveoli (Eisner et al, 2005) **(Figure 1-1 A)**. The airway epithelium constitutes the first barrier of defense against the toxic effects of cigarette smoke. It is a pseudo-stratisfied barrier that consists of multiple cell types such as goblet cells, clara and ciliated cells, which are generated by the basal cells **(Figure 1-1 B)**. The bronchial tubes are lined with these tiny hair-like cilia cells which are important for secreting harmful substances out of the lungs.

Between the cilia cells there is another cell type organized called goblet cells, which are responsible for the production of mucus.

Cigarette smoke irritates the lining of the bronchial tubes causing them to swell and increase mucus production extensively. Smoking also slows down the movement of the ciliated cells causing some of the smoke components and mucus to remain and accumulate in the lungs. A selected summary of hazardous chemical compounds found in cigarette smoke and their effects on human airways are listed in **Table 1-1**.

Table 1-1: Selected components of cigarette smoke and their potential role in lung injury

Component	Effect on airways
Cadmium	Oxidative injury, promotion of emphysema, tight junction disruption
Formaldehyde	Cilia toxic; irritant
Nitrogen oxides	Oxidant activity
Hydrogen cyanide	Oxidative metabolism of cells affected
Acetaldehyde	Probable human carcinogen; irritant to respiratory tract
1,3-Butadiene	Known human carcinogen, irritant to upper respiratory tract
Acrolein	Cilia toxic; impairs lung defenses, known DNA mutagen, irritant to skin and nasal passages
N-Nitrosamines	Known human carcinogen, increases risk for lung cancer may cause reproductive damage

Most of the ciliated cells are recovering and trying to release these pollutants together with the mucus out of the lungs. The human body tries to expel this material by repeated coughing, also known as smoker's cough. Chronic bronchitis develops over time, as this detoxification process overwhelms the cilia cells and the airways become blocked with mucus thus breathing becomes difficult. Moreover, lungs become more susceptible towards airborne pathogens like viruses and bacteria. The alveoli gets overdistended and are finally damaged in their elastic fibers which makes it harder for oxygen and carbon dioxide to exchange with the blood, leading to the development of emphysema. Chronic bronchitis and emphysema are collectively called as COPD. The normal remodeling process of wound-healing is completely damaged in the lung tissue of smokers suffering from COPD. The obstruction of the airways is related to an inflammatory process that leads into thickening of the airway wall which in turn narrows the airways by depositing connective tissue **(Figure 1-1 A).**

Cigarette smoke also disrupts the tight and adherens junctions that form the epithelial barrier (Hulbert et al, 1981; Jones et al, 1980). This leads into destabilization of the epithelial integrity and permeability.

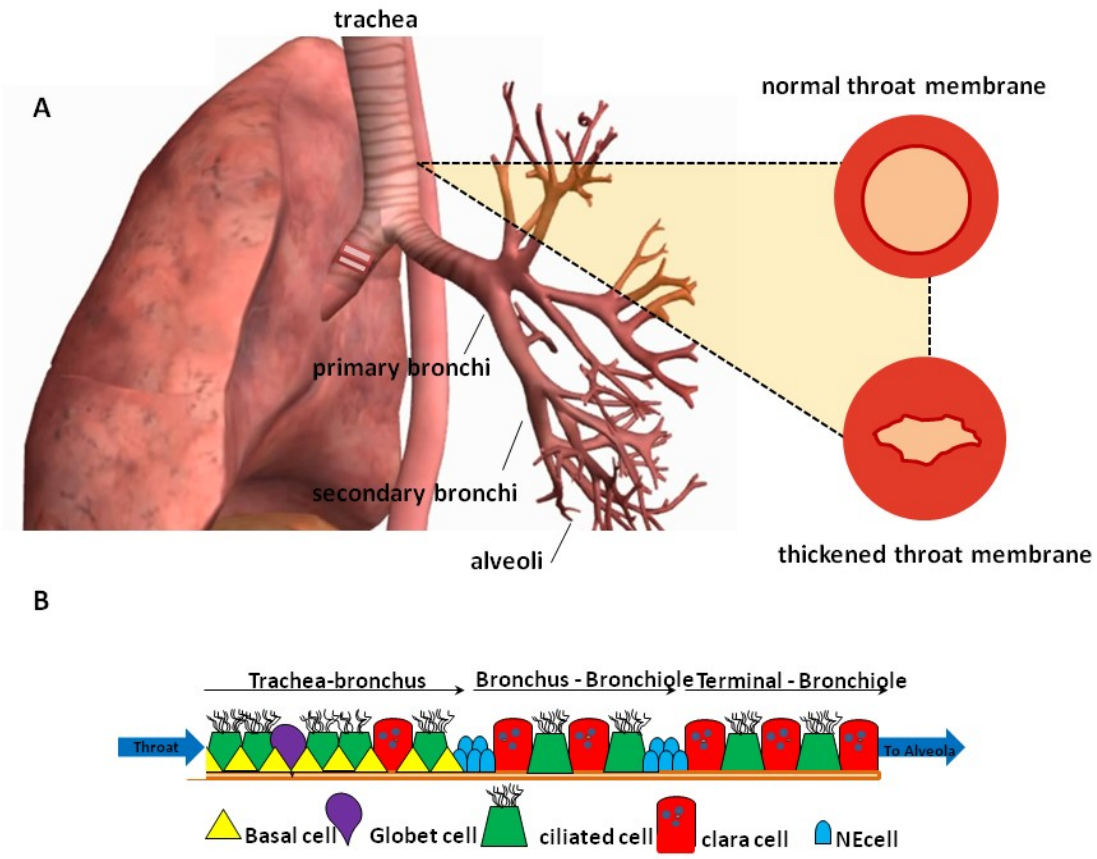

Figure 1-1: The human respiratory system and its various different cell types. (**A**) The lungs are a pair of spongy, air-filled organs located on either side of the chest (thorax). The trachea, also called windpipe, conducts inhaled air into the lungs through its tubular branches, called bronchi. The bronchi then divide into smaller branches (bronchioles), finally becoming microscopic. The bronchioles eventually end in clusters of microscopic air sacs called alveoli. In the alveoli, oxygen from the air is absorbed into the blood (source: www.webmd.com). The alveoli are lined by a delicate layer of simple squamous epithelia. Outside the epithelial lining is a delicate connective tissue containing numerous elastic fibers and a close network of blood capillaries, forming a common wall to adjacent alveoli. The epithelial membrane of smokers with and without COPD is characterized by a thickening of the airway wall, which leads into a breakdown of elastin and collagen proteins and finally into destruction of the airways. (**B**) The bronchial tubes are composed mainly of five cell types; clara (secretory) cells, tiny hair-like cells called cilia cells, pulmonary neuroendocrine (NE) cells, basal cells and goblet (mucous) cells.

The abnormal remodeling of the airway tissue is associated with deregulation of cytokines, chemokines and other growth factors. Basal cells hyperplasia and squamous metaplasia are the earliest airway epithelial lesions associated with smoking-induced carcinogenesis (Shaykhiev et al, 2013).

Smoking-induced oxidative stress due to high concentrations of free radicals leads into the generation of additional reactive oxygen species (ROS) within the airways. Naturally, ROS can also be produced intracellularly from several sources, such as mitochondrial respiration, which is the most important source of free radicals. Nevertheless, in smokers and COPD patients higher ROS levels are present compared to healthy persons.

A consequence of this higher oxidative stress is the enhanced expression of inflammatory mediators through redox-sensitive transcription factors like nuclear factor-kappa B (NF-κB). On the other hand, controlling transcription factors of cellular resistance to oxidants, like Nrf2 (the nuclear factor erythroid2-related factor 2), are getting activated (Ma, 2013).

1.1.2 Physiological role of second messengers in COPD pathogenesis

Cyclic adenosine 3′,5′-monophosphate (cAMP) was the first intracellular signaling molecule to be identified by Earl W Sutherland Jr. and Theodore W. Rall in 1956 (Sutherland & Rall, 1958). This second messenger modulates a variety of processes in the airways such as production and secretion of inflammatory mediators and extracellular matrix, proliferation, differentiation, migration, epithelial cells mucus secretion, wound healing, anion transport and ciliary beating (Billington & Hall, 2012; Giembycz & Newton, 2006; Salathe, 2002). cAMP is a critical key player by regulating the airway tone, being the major pro-relaxant effector in combating the pathophysiology of airway narrowing and remodeling (Billington & Hall, 2012; Billington et al, 2013). Thus, the decrease of cAMP levels in the human lung has a significant role in the development of COPD and asthma.

All cAMP-mediated pathways are most commonly initiated following the binding of specific ligands (e.g. hormones, neurotransmitters, growth factors, cytokines, active oxygen, drugs, toxins, etc) to G protein-coupled receptors (GPCRs) of the Gs-Protein and Gi-Protein coupled signal transduction family (Billington et al, 2013). These G-proteins are linked to an enzyme, adenylyl cyclase (AC) that dephosphorylates ATP to form cAMP. The activated Gs subunit stimulates, while the Gi subunit inhibits the AC. The resulting increase in intracellular cAMP reduces the smooth muscle tone, thus dilating the airways. cAMP then activates other cAMP dependent effectors like protein kinase A (PKA) and EPAC by binding to their regulatory subunits and allowing them to phosphorylate a wide range of cellular targets leading to bronchorelaxation (Bonnans et al, 2003) **(Figure 1-2)**.

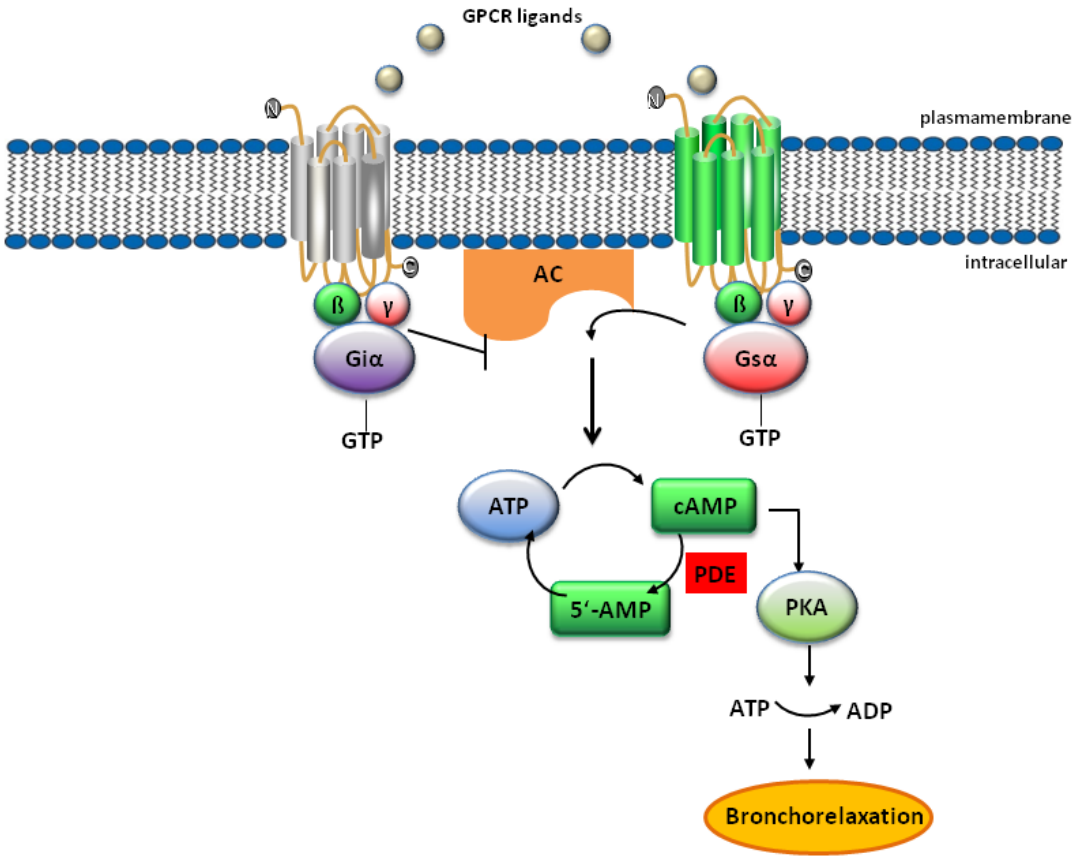

Figure 1-2: The cAMP signaling pathway. Following the binding of hormones, neurotransmitters and other lipids, the GPCR is getting activated and undergoes a conformational change that is transmitted to an attached intracellular heterotrimeric G protein complex. The Gs alpha subunit of the stimulated G protein complex exchanges GDP for GTP and is released from the complex, binds to and activates then AC. AC in turn, catalyzes the conversion of ATP into cAMP. Increased concentrations of the second messenger cAMP lead to the activation of PKA. The release of PKA phosphorylates a number of other proteins, e.g. cAMP response element binding (CREB) transcription factors, phospholipase C (PLC), inositol triphosphate receptor and β_2 adrenoreceptor leading to bronchorelaxation.

Phosphodiesterases (PDE) are enzymes responsible for cAMP degradation. In human airway smooth muscle cells (ASM), PDE4 has been found to be the major PDE subtype that is involved in cAMP degradation leading to narrowing of the airways (Nino et al, 2009). Inhibitors of the PDE4 family such as roflumilast and cilomilast have been used in clinical trials or have been licensed for use in COPD (Spina, 2008). However, to date little is known about how alterations and higher intracellular cAMP levels affect the respiratory system.

Another important second messenger, responsible for airway remodeling and extensive airway narrowing, is cytoplasmic Ca^{2+}. In response to signal molecules from other cells, the cell surface receptor protein, another G-protein coupled receptor, activates a Gq protein, which in turn activates the enzyme phospholipase C (PLC). PLC in turn hydrolyzes phosphatidylinositol 4, 5-bisphosphate (PIP2) to diacyl glycerol (DAG) and inositol trisphosphate (IP3).

DAG remains bound to the membrane and acts as a second messenger that activates protein kinase C (PKC). IP3 then diffuses through the cytoplasm to bind to IP3 receptors, particular calcium channels in the endoplasmic reticulum (ER), allowing calcium ions to flow from the ER into the cytoplasm **(Figure 1-3)** (Thore et al, 2005).

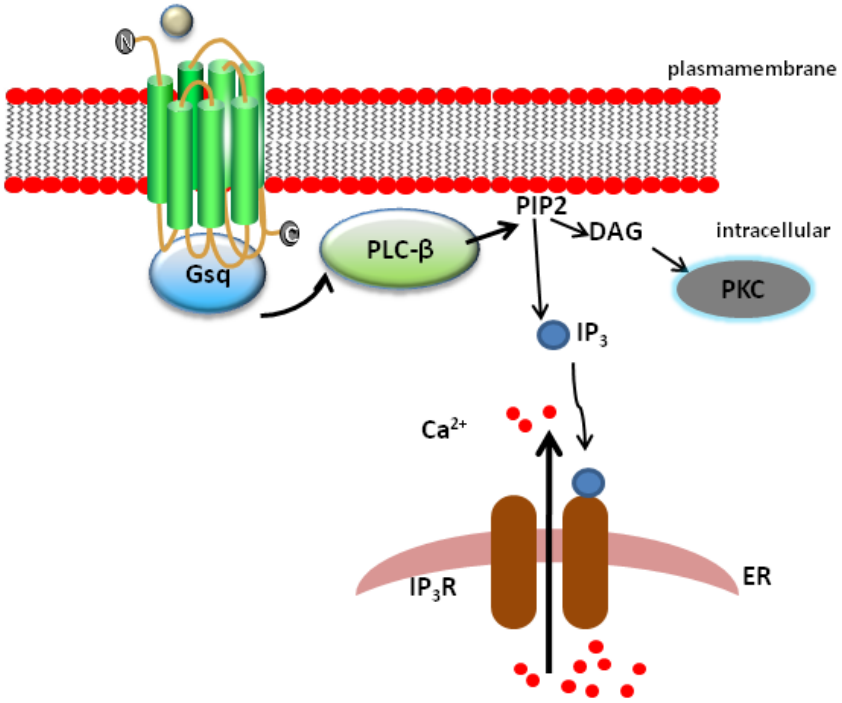

Figure 1-3: Phospholipase C pathway and Ca^{2+} -signaling. Many cell surface receptors, including G protein-coupled receptors and receptor tyrosine kinases activate the PLC enzyme. PLC hydrolyses PIP_2 into two second messengers: IP_3 and DAG. DAG activates PKC, while IP_3 diffuses to the endoplasmic reticulum (ER) and binds to the IP3 receptor, which is a Ca^{2+} channel and thereby releases Ca^{2+} from the ER into the cytoplasm.

These secreted calcium ions can further bind to epithelial NADPH oxidase family proteins like dual oxidases. Dual oxidases generate ROS by producing H_2O_2 at the epithelial cell surface. Dual oxidase 1 and 2 are expressed in the airway epithelium of smokers and patients with mild/moderate COPD (Nagai et al, 2008). A higher concentration of Ca^{2+}- ions leads into ASM contraction (Bergner et al, 2006; Jin et al, 2006; Kellner et al, 2008). Moreover, increased expression of Ca^{2+}-activated Cl^- channel 1, is associated with mucus overproduction in the airway epithelia of smokers and COPD patients (Iwashita et al, 2012).

1.2 Modeling human diseases in *Drosophila melanogaster*

1.2.1 *Drosophila melanogaster* as a model to study smoke related diseases like COPD

Progress in unraveling the role of COPD-susceptibility genes in the recent years revealed that biomedical research critically depends on suitable animal models to obtain a fast and adequate understanding of involved disease pathways and genes for development and discovery of therapeutic drugs. *Drosophila* is among the limited number of well-established and generally accepted model organisms (mice, yeast, *C. elegans*, zebra fish, rat). It is the oldest model organism that had been introduced first by Thomas Hunt Morgan and has been applied since then to a large number of human diseases (Bier, 2005; Pandey & Nichols, 2011). The fly genome has been completely sequenced and annotated and nearly 75% of human disease-related genes are believed to have a functional homolog in the fly (Adams et al, 2000; Pandey & Nichols, 2011). Among the first ones were those focusing on neurodegenerative disorders like Parkinson's disease (Feany & Bender, 2000). Chan and Bonini (Chan & Bonini, 2000) succeeded establishing *Drosophila* to model Alzheimer, which triggered a great number of follow-up studies leading to new therapeutic ideas. Further, it's not surprising that the fruit fly serves as a tremendous tool to study cerebral cavernous malformations (Song et al, 2013), as synteny analyses revealed that CCM3/PDCD10 gene shares the same genomic loci from *Drosophila* to human and the gene structure remains conserved (Kumar et al, 2014). In addition, other neuroscience studies have shown *Drosophila* to perform complex behavioral tasks such as learning and memory, sleep and even aggression (Bellen et al, 2010).

Other disease modeling approaches utilizing *Drosophila* focused on cardiovascular diseases (Wolf et al, 2006), diabetes (Baker & Thummel, 2007) and intestinal diseases (Lee & Lee, 2014). Recently, the fly has been increasingly used in cancer research.

The majority of cancers are derived from epithelial cells and misregulation of signaling pathways. Highly important was the elucidation of the Ras signal transduction cascade (Olivier et al, 1993; Simon et al, 1991). Current research shows the flies potential in understanding human inflammatory and infectious diseases exposing them to pathogens, e.g. fungi and bacteria and inquiring the release of AMPs (anti microbial peptides) in the intestine. Even in kidney-related diseases, the fly has shown to be a potential candidate to study kidney stone formation using its malpighian tubule system (Chi et al, 2015).

However, there is only a slow progress in elucidating *Drosophila* as a model to study airway related diseases such as asthma (Roeder et al, 2009; Roeder et al, 2012; Wagner et al, 2009) and not yet for either COPD or lung cancer. One of the reasons is that flies lack an adaptive immune system, including IgEs, T-cells and most aspects of interleukin signaling, which is thought to be highly relevant for understanding asthma or other lung specific diseases. A new approach in *Drosophila* genetics is the establishment of "humanized" flies carrying transgenic arrays of the corresponding human genes, or their variations. This method is successfully applied in the field of neurodegenerative diseases (Feany & Bender, 2000) and even to explore the function of asthma susceptibility genes in the respiratory track of the fly, e.g. ORMDL (Kallsen et al, 2015).

1.2.2 Structure of the respiratory system of *D. melanogaster*

Most animals possess an oxygen delivery system and the architecture of these branching networks is highly conserved throughout the animal kingdom. Respiratory epithelia are characterized as a complex network of branched tubules. In humans, the airway epithelium is a pseudo-stratified barrier that consists of multiple cell types whereas the larval trachea of *Drosophila* is a single-layered epithelium of approximately 1600 cells. It is covered by a central lumen that provides the first barrier against invading microorganisms and other environmental stimuli. The airway epithelium of the fly consists of approximately 10.000 interconnected tubes that transport the oxygen and other gases throughout the body (Affolter et al, 2003; Ghabrial et al, 2003). Green et al. has introduced *C. elegans* as an invertebrate model organism to study the impact of cigarette smoke to unravel COPD mediated responses (Green et al, 2009). Compared to the *C. elegans* model, *Drosophila* has the major advantage that it possesses an airway system, which shares similarities to those of vertebrates. Nematodes lack both specialized respiratory systems and complex circulatory organs. They must rely on diffusion from the surrounding environment into their tissues for gas exchange (Lopez Hernandez et al, 2015; Paget et al, 1987; Van Voorhies & Ward, 2000).

Although the physiology of airway epithelium of *Drosophila* larvae is simpler in structure and its organization is very delicate, cellular and molecular mechanisms resemble the overall design of the human lung (Horowitz & Simons, 2008; Roeder et al, 2012).

The air enters the trachea through specialized openings, so called posterior spiracles and passes through primary, secondary and terminal branches to reach the internal target tissues **(Figure 1-4)**.

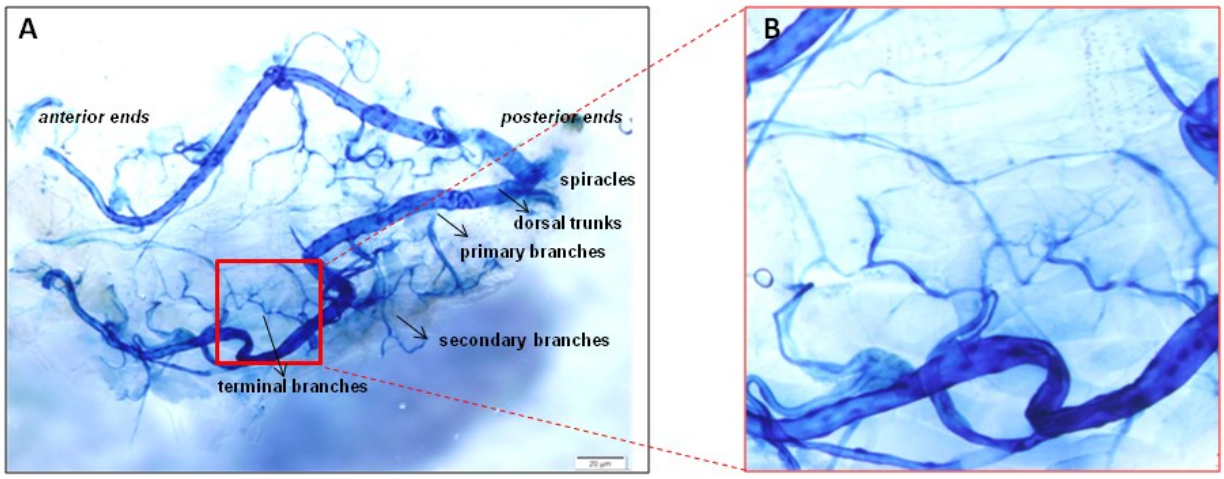

Figure 1-4: The respiratory system of *D. melanogaster*. The tracheal system of the larvae (L3) is characterized by two pairs of respiratory openings (spiracles). Both primary branches run in parallel through the entire body of the larva and split in nearly every segment to the inner and outer secondary branches. These secondary branches are finally branched into fine tertiary branches (tracheoles), which are in direct contact to other organs, e.g. gut and oenocytes to supply them with oxygen. The trachea was visualized by X-Gal staining (ppk4-Gal4::lacZ-UAS) with the ppk4-Gal4 driver line to label the entire airway system.

The terminal branches are very fine (< 1µm diameter) and terminal branching is highly variable and regulated by the oxygen supply. Their pattern is very organized, for instance terminal branches do not cross over one another and are regularly spaced. Interestingly, larvae which were grown under anoxic conditions, show dramatic increases in terminal branching in contrast to larvae grown under high oxygen levels, which have less number of terminal branches. The formation of the terminal branches are regulated by the gene DSRF/ blistered, a *Drosophila* homolog of the serum response factor. DSRF is specifically expressed in the terminal branches (Gervais & Casanova, 2011).

Liquid clearance of the tracheal system is performed by several epithelial degenerin/ Na^+ channels (ENaCs) and their family members, e.g. *PPK4* and *PPK11* are expressed quite specifically in the tracheal system (Liu et al, 2003b). They are not only important for clearing and replacing liquid by air but also contribute to proper differentiation of the tracheal cells. Most of the clinically relevant lung syndromes are caused by the failure of liquid clearance and respiratory-tube size control.

Coracle is an essential component of septate junctions of the epithelial cells, which are necessary for barrier function and extracellular matrix secretion **(Figure 1-5)** (Lamb et al, 1998).

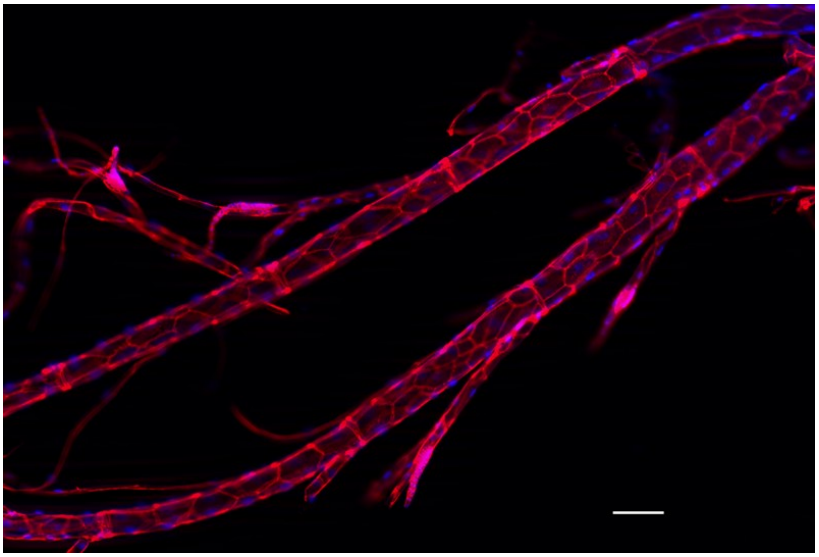

Figure 1-5: Septate junctions of the fly's airway epithelial cells. The larval trachea (L3 instar) was stained with α-coracle antibody (red) to highlight the septate junctions. DAPI (blue) was used to stain the nuclei. Scale bar: 100 µm.

1.2.3 Respiratory defense mechanisms in *D. melanogaster*

D. melanogaster lacks an adaptive immune system, but possesses an innate immune response similar to that of humans, employing three major signaling pathways namely the Toll, Immune deficiency (Imd) and Janus Kinase and Signal Transducer and Activator of Transcription (JAK/STAT) pathway (Lemaitre & Hoffmann, 2007). This is one of the advantageous aspects making *D. melanogaster* an appropriate *in vivo* model to study all innate immune related functions without the interference of the adaptive immune system.

The innate immune responses play a crucial role for maintaining inflammation and tissue destruction in COPD (Schleimer, 2005). In the early stages of the disease, the airways of smokers are bombarded with large quantities of hazardous chemical compounds. Activation of phagocytic cells occurs and results in the release of many mediators, which are believed to remodel the airways. Finally, the failure of the innate immune defense system as a result of inhalation of smoke, is likely to result in increased susceptibility towards infection by pathogenic and opportunistic organisms. Innate immunity is the oldest host defense mechanism and is highly conserved across many species. Almost all major signal transduction pathways are also found in *Drosophila*, performing the same biochemical functions and are arranged in the functional order.

This chapter describes some important genes and pathways of the fly's respiratory system which are relevant for this work. They are summarized in **Figure 1-6**.

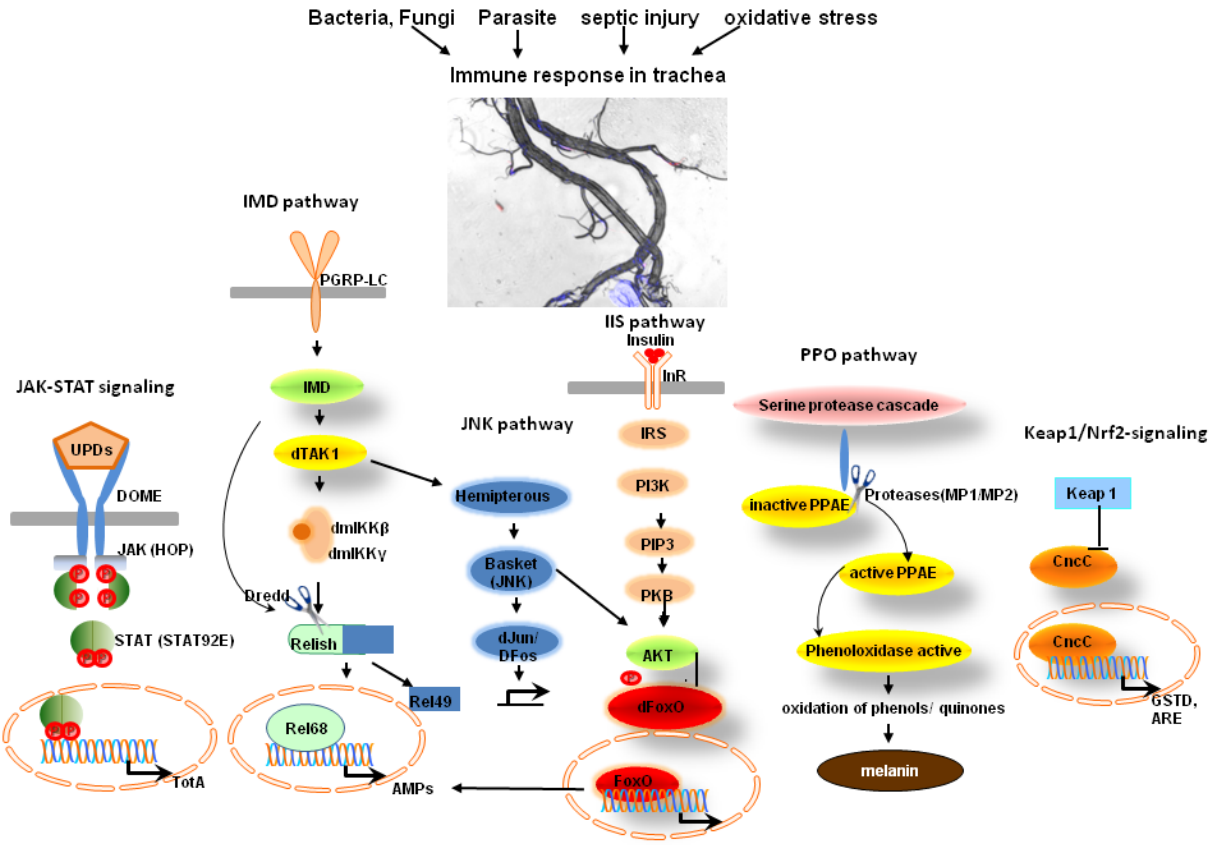

Figure 1-6: Respiratory defense mechanisms of *D. melanogaster*. Septic injury or other stressors (e.g. oxidative stress of CSE) activate several signaling pathways and transcription factors: The JAK-STAT signaling pathway is composed of 4 major components: the ligands unpaired 1-3, the receptor domeless (Dome), the JAK kinase Hopscotch/Hop and the STAT transcription factor (STAT92E). Activation of IMD and JNK signal transduction is normally initiated by gram-negative bacterial peptidoglycan directly binding to PGRP-LC, to signal to IMD. Further IMD regulates the MAPK kinase TAK1 (transforming growth factor β-activated kinase 1), which then stimulates IKK-dependent cleavage and activation of the TF relish. IMD-signaling induces AMP release, e.g. drosomycin. The FADD-Dredd pathway also activates relish. TAK1 is also another activator of the JNK pathway. The transcription factor dFoxO is controlled by JNK and insulin signaling. The dFoxO activity is repressed by insulin signaling. Another transcription factor which has been shown to activate gene expression in response to CSE (e.g. GstD) is cap-n-collar. Keap1 (Kelch-like ECH-Associated Protein 1) is its specific repressor.

The Janus Kinase-Signal Transducer and Activator of Transcription (JAK-STAT) pathway is very conserved among all species from insects to mammals and plays an important role in mediating pro-inflammatory cytokines like interleukin-6 (IL-6) in mammals (Hou et al, 2008; Levine & Wernig, 2006). JAK-STAT signaling was first discovered in mammalian systems in the transduction of a variety of cytokines and growth factor signals (Darnell, 1997). It is responsible for regulating immune responses to septic injury and infection by bacterial and viral pathogens. However, this pathway is less complex in *Drosophila* (Brown et al, 2003). In the *Drosophila* genome there are three related IL-6-like cytokines, namely upd (unpaired or outstretched), upd2 (unpaired 2) and upd3 (unpaired 3), which are secreted upon injury of infection.

They can bind to a gp130-like cytokine receptor called domeless (dome) to regulate the activity of JAK-STAT signaling (Arbouzova & Zeidler, 2006; Brown et al, 2001; Wright et al, 2011). The transmembrane receptor domeless then in turn activates the Janus Kinase (JAK) hopscotch (hop) (Binari & Perrimon, 1994). Activated hop induces phosphorylation of the signal transducer and activator of transcription STAT92E in order to activate transcription of genes that are critical to the inflammatory response. Hopscotch, the only single *JAK* gene of *Drosophila*, is most similar to human JAK2 (27% identity) and STAT92E is most homologous to human STAT5 (37% identity) (Zeidler et al, 2000).

Another signaling pathway is the IMD pathway, which shares some similarities with the vertebrate TNF-R (tumor necrosis factor receptor) pathway and is expressed in the fly's airway epithelium (Wagner et al, 2008). The pathway consists of eight additional canonical components: the PGRP-LC receptor (Choe et al, 2002), an intracellular adaptor protein containing a death domain IMD, the mitogen-activated protein 3 kinase (Map3K) TAK1 (Silverman et al, 2003; Vidal et al, 2001), which phosphorylates and activates the IKK signalosome (IKKβ - IRD5 and IKKγ - Kenny homolog) (Kleino & Silverman, 2014) and leads into phosphorylation and nuclear translocation of relish, the homolog of human NF-kB (Stoven et al, 2000; Stoven et al, 2003).

Upon direct binding of gram-negative bacteria, PGRP-LC recruits the adaptor IMD (Choe et al, 2005; Kaneko et al, 2006). IMD interacts with the *Drosophila* Fas-associated death domain ortholog (dFADD) that binds to death related ced-3/nedd2-like caspase (DREDD) (Hu & Yang, 2000). Once this caspase is phosphorylated via the IKK signaling complex (Silverman et al, 2000), it cleaves relish by removing the C-terminal inhibitor ankyrin-repeat/IκB-like domain, which remains in the cytoplasm. It allows the relish DNA-binding domain (Rel68) to translocate from the cytoplasm into the nucleus, where it induces transcription of other target genes, e.g. binding to κB-motifs of antimicrobial peptide genes (AMPs) (Engstrom et al, 1993).

The vital parts of the Toll-pathway with its core components such as the ligand spätzle, the receptor toll, the intracellular adaptors myD88 and tube and the kinase pelle, were reported to be missing in the tracheal system of *D. melanogaster* and only the NF-κB homologs dorsal (Dl) and dif are present (Wagner et al, 2008).

Beside these three major signaling pathways, transcription factors play a remarkable role in regulating the epithelial immune responses. Of central importance for proper response to oxidative stress is the activation of the transcription factor FoxO (Becker et al, 2010; Greer & Brunet, 2005; Savai et al, 2014; Varma et al, 2014).

The *Drosophila* dFoxO homolog is a highly abundant protein of the airway system (**Figure 1-7**).

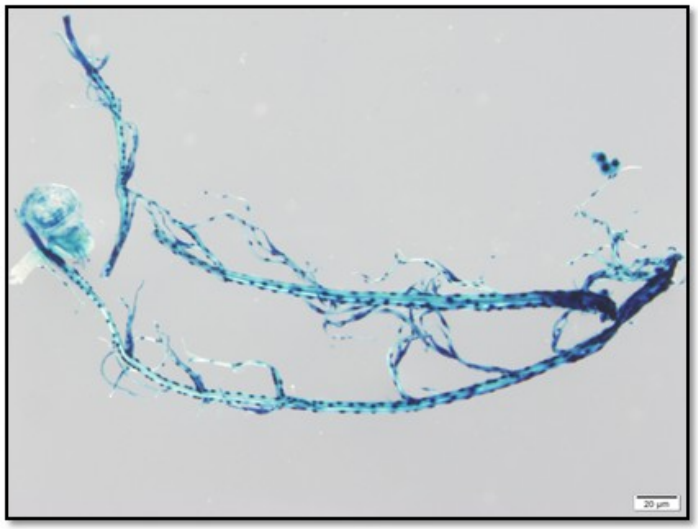

Figure 1-7: dFoxO expression in the respiratory track of *D. melanogaster*. The FoxO homolog of the fly is a highly conserved gene of the airway epithelium. Beta-galactosidase staining patterns were determined for detection of dFoxO expression by X-gal staining. Strong lacZ expression is visible in the primary, secondary and tertiary branches of the trachea.

The forkhead box O (FoxO) family of transcription factors regulates diverse gene expression programs and affects many cellular processes, including cell cycle regulation, cell survival and metabolism (van der Horst & Burgering, 2007) and are characterized by a conserved DNA-binding domain termed "forkhead box" (Kaestner et al, 2000). Stress stimuli leads into translocation of FoxO into the nucleus where it up-regulates a series of target genes.

In particular, FoxO is negatively regulated by the canonical insulin/insulin-like growth factor signaling (IIS) pathway. This cascade is highly conserved among all species possessing an insulin receptor (InR), which promotes signaling through the insulin receptor substrates (IRS), after binding of insulin or other growth factors. They further activate phosphoinositide-3-kinase (PI3K) (Coffer et al, 1998; Datta et al, 1999) that phosphorylates inositide lipids on the inner surface of the cell membrane, leading to activation of the protein kinase B (PKB) and Akt. They then lower the activation of FoxO via phosophorylation and retain it in the cytoplasm. In absence of Akt signaling, FoxO is able to activate gene transcription and cause cell death after translocation into the nucleus (Arden & Biggs, 2002; Burgering & Kops, 2002).

Moreover it was shown that different forms of stress, such as hypoxia, also lead into decreased phosphorylation of Akt and FoxO3a, correlated with an increased nuclear accumulation (Zhang et al, 2013). FoxOs are also activated in the presence of oxidative stress through Jun N‑terminal kinase (JNK) signaling (Eijkelenboom & Burgering, 2013).

Members of the core JNK signaling include hemipterous (hep), a JNKK and functional homolog of mammalian MKK7, basket (bsk), a JNK, and DJun (Glise et al, 1995; Holland et al, 1997; Hou et al, 1997; Kockel et al, 1997; Sluss et al, 1996). Activation of JNK pathway induces the expression of puc, which in turn inhibits the JNK (Adachi-Yamada, 2002). FoxO is also a key factor of signaling pathways mediating expression of AMPs (Becker et al, 2010). Eight classes of AMPs have been unraveled in *Drosophila* (Lemaitre & Hoffmann, 2007).

Another important regulation of oxidative stress and toxicity caused by chronic exposure to cigarette smoke is the Keap1/Nrf2-signaling (nuclear factor erythroid 2-related factor 2) (Motohashi & Yamamoto, 2004). Nrf2 is a transcription factor, which belongs to the cap'n'collar (cnc) subfamily of leucine zippers, and Keap1 (Kelch-like ECH-Associated Protein 1) is the specific repressor for Nrf2. The fruit fly's Nrf2-homolog is therefore called *cnc* gene. In unstressed conditions Nrf2 is tethered to its cytoplasmic inhibitor Keap1, an actin-binding protein. Keap1 suppresses the activity of Nrf2 by sequestering it in the cytoplasm, and also by targeting it for proteasomal degradation. Nrf2 is then stabilized and accumulates in the nucleus, where it binds to antioxidant response elements (ARE) in the enhancers of its target genes (Jaiswal, 2004).

Another major innate immune mechanism in *Drosophila*, and more generally in insects and other arthropods, is the melanization reaction (Cerenius & Soderhall, 2004), which is mediated by a serine protease cascade. A serine protease inhibitor protein, Spn77Ba was reported to be the regulator for tracheal melanization (Tang et al, 2008), which regulates the melanization cascade through the specific inhibition of the prophenoloxidase-activating enzymes MP1 and MP2 that activate phenol oxidase (PO), a key enzyme responsible for melanin biosynthesis. A by-product of phenol oxidase activity is ROS.

Although vertebrates do not possess an equivalent of a phenol-phenoloxidase system (PPO system), several studies indicate that the melanization cascade is triggered by injury and half a century ago melanotic tumors in *Drosophila* larvae and adults were viewed as the equivalent of cancer (Minakhina & Steward, 2006).

1.2.4 Advantages of genetic tools for manipulation of the fly's airway epithelium

A typical advantage seen for genetically tractable invertebrate model organisms is the short generation time of approximately 10-12 days at 25°C and an average life span of 50 to 60 days **(Figure 1-8).**

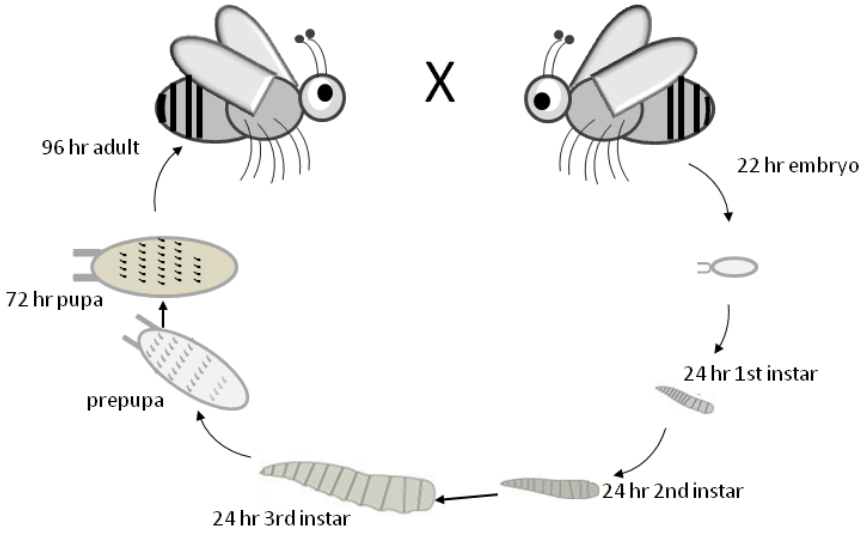

Figure 1-8: Generation cycle of *D. melanogaster*. The shortest development time (egg to adult) of 7 days is achieved at 28 °C and can increase at higher temperatures. The eggs hatch 12–15 hours after fertilization. The resulting larvae grow for about 4 days (at 25 °C) while molting twice (into second and third instar larvae) at about 24 and 48 h after hatching. Further the larvae encapsulate in the puparium and undergo a four-day-long metamorphosis, after which the adults emerge.

The maintenance of the flies requires only little labor and is very cost effective compared to other animal models. *Drosophila* offers a great number of highly relevant genetic tools and techniques for experimental design that are not found in other animal studies. They can be used for genetic manipulation of the airway system thus allowing the study of functional significance of target genes. Numerous deletions (Ryder et al, 2007), more than 12.000 transposable element insertions that can be used for genomic mutations (Bellen et al, 2004) and numerous vectors for transgenesis capitalizing on P element are readily available to researchers. One versatile and highly useful tool is the binary GAL4/UAS-system invented more than 22 years ago (Brand & Perrimon, 1993).

It is a bipartite transcription activation system that relies on the yeast transcription factor GAL4 and the corresponding DNA binding region, UAS (upstream activation sequence), used for over expression or silencing of specific genes in the tissue of interest. Both components (GAL4 and UAS) are segregated into different fly lines, called driver and effector lines, respectively.

The GAL4 line determines the location of expression and the gene of choice is under transcriptional control of UAS elements (Duffy, 2002; Roman et al, 2001). Crossing these two lines leads into activation of this system in the entire F1 generation **(Figure 1-9)**.

Remarkable numbers of GAL4 and UAS lines are available and the Barry Dickson's group established a RNAi library for all *Drosophila* genes, allowing conditional gene inactivation (Dietzl et al, 2007). Especially relevant to COPD research there are GAL4 lines that exclusively address the airway epithelium, namely btl-GAL4 and ppk4-GAL4. Until now, these lines are restricted to be specifically expressed in the respiratory system of larvae as corresponding driver lines for the adult airway system are not yet available.

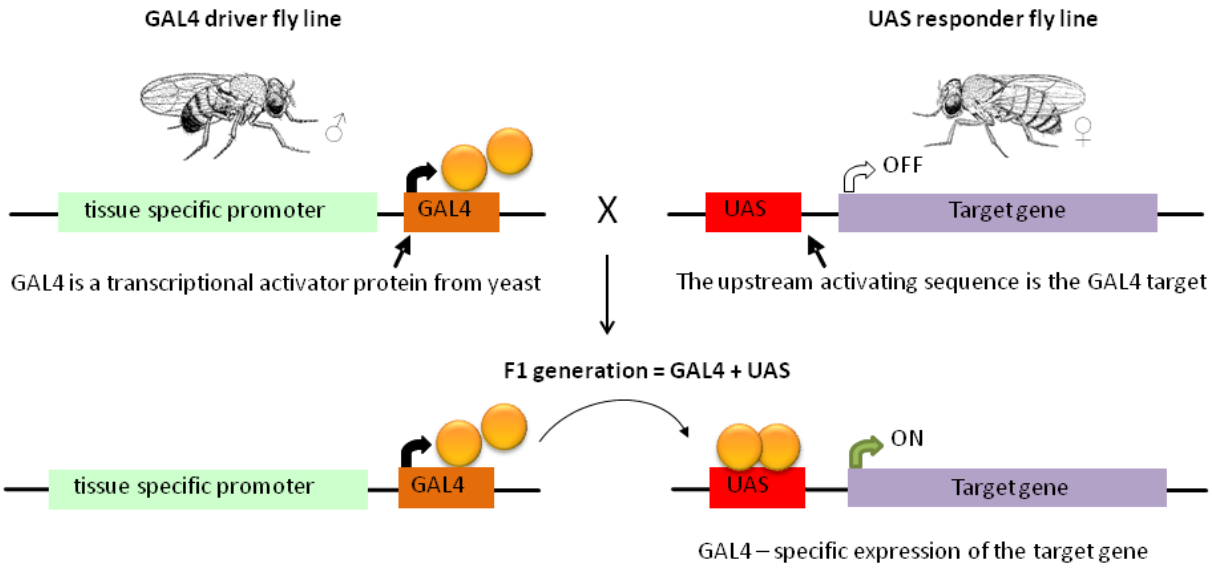

Figure 1-9: The GAL4/UAS system for targeted manipulation in the fly. The system is ideally suited for over expression or silencing (RNAi) of a target gene in a specific organ. It's a binary system, derived from yeast, consisting of a GAL4 that determines location and the UAS effector line that carries the gene to be expressed under transcriptional control of the UAS element. In the F1 generation, both factors (GAL4 and the UAS enhancer) come together to direct expression of the target gene by the expression pattern of the GAL4 line. Thereby, the target gene is only expressed in a cell- or tissue-specific pattern in their progeny.

A very useful refinement of the GAL4/UAS-system, which allows temporal control of gene expression, is the so-called TARGET system (McGuire et al, 2003). This system makes use of a temperature-sensitive repressor of GAL4, GAL80^{ts}, which is repressing expression under low temperature conditions (19° C).

Inactivation of this repressor is achieved by increasing the temperature to 29° C leading to its inhibition and expression of the target gene **(Figure 1-10)**. Such a TARGET expression system has been established for the most specific airway epithelial driver, ppk4-GAL4.

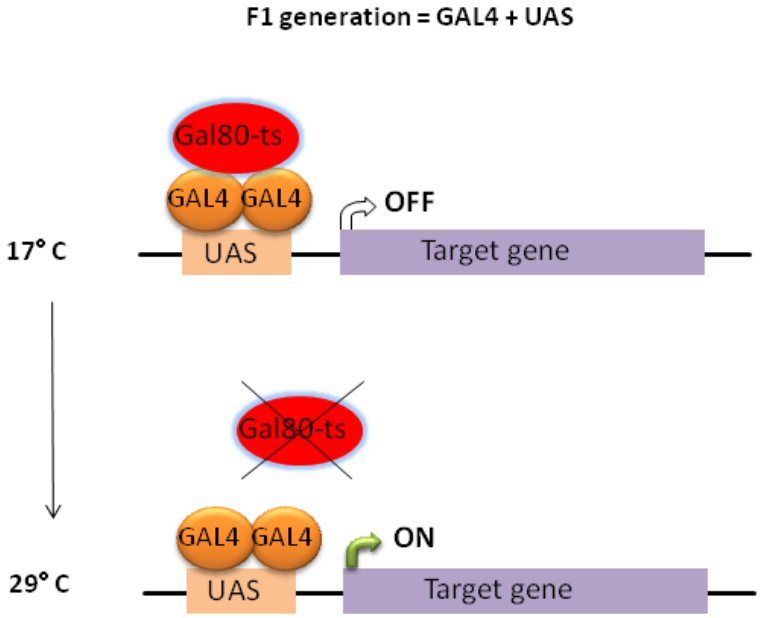

Figure 1-10: The Target-system of *D. melanogaster*. The TARGET system is a method for temporal and regional gene expression targeting (TARGET) with the conventional GAL4-upstream activator sequence (UAS) system and a temperature-sensitive GAL80 molecule, which represses GAL4 transcriptional activity at lower temperatures (19° C), inhibiting the entire system. At permissive temperatures (29° C) the sensitive repressor molecule is inhibited and allows releasing Gal4.

1.2.5 New approaches to manipulate the fly's airways using the DREADD technology and optogenetic tools to understand airway diseases

Some examples of recent advanced tools in *Drosophila genetics*, such as DREADD technology and optogenetic tools, open a new era in research to easily activate second messengers or to depolarize cell systems. There is a huge number of systems (e.g. temperature sensitive TPRA & TRPV channels etc.), thus for this work relevant tools were chosen and are described in this chapter. Designer Receptors Exclusively Activated by a Designer Drug (DREADDs) are modified muscarinic acetylcholine G-protein coupled receptors that are activated only by a synthetic ligand, namely by clozapine-N-oxide (CNO) (Armbruster et al, 2007). These specific modifications were generated by point mutations of specific amino acids within the GPCRs. DREADD technology combines genetic and pharmacology approaches, to manipulate cellular signaling in mammals and has been used for behavioral control (Nichols & Roth, 2009). Recently, the Nichols laboratory demonstrated the utility of this technology in *Drosophila* (Becnel et al, 2013). They created three important UAS-DREADD transgenes, the UAS-M1D1 that allows inducing the increase of Ca^{2+} levels, UAS-M4D1 that decreases cAMP levels and UASM5Dbar that increases the levels of cAMP **(Figure 1-11)**.

The activating ligand can be easily and conveniently administered by simply feeding or injecting CNO to the animal.

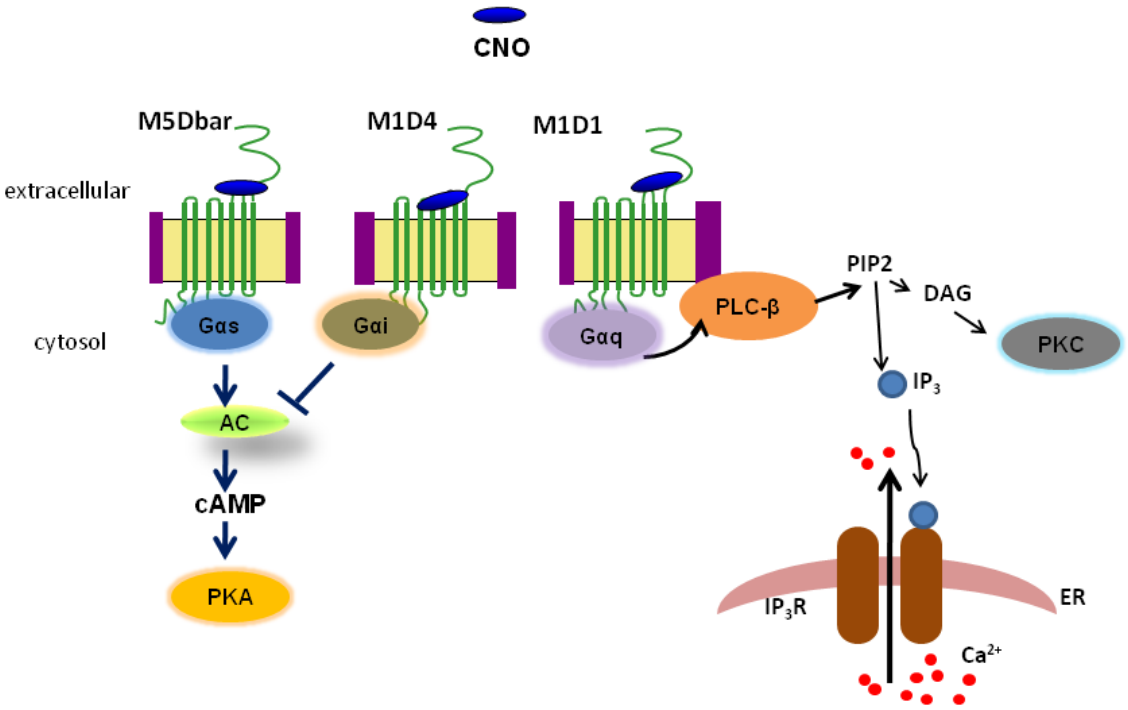

Figure 1-11: UAS-DREADD transgenes of *D. melanogaster*. There are three important UAS-DREADD transgenes: the UAS-M1D1 to increase Ca^{2+} levels, UAS-M4D1 that decreases cAMP levels and UASM5Dbar that increases the levels of cAMP.

This makes the DREADD system a beneficial tool to trigger cAMP and Ca^{2+} in the respective tissue using cell specific Gal4 drivers, e.g. PPK4-Gal4 for the tracheal system.

Another powerful technique became possible utilizing light inducible systems, such as optogenetic tools, for cell-specific targeting of effector elements.

The optogenetic approach for cAMP manipulation *in vivo* can be applied using a small bacterial photoactivated adenylyl cyclase (bPAC), of the soil bacterium *Beggiatoa*, which possesses a BLUF (blue light receptor using FAD) domain (Penzkofer et al, 2014; Stierl et al, 2011). Until now in *Drosophila* research, this system was only applied in neuronal cells and tissues and in *Drosophila* renal (malpighian) tubules for studying cAMP-dependent processes (Efetova et al, 2013; Stierl et al, 2011). Thus, utilizing Gal4-driven UAS-bPAC effector lines can be another useful tool to study blue-light dependent cAMP increase in the airways of *D. melanogaster* **(Figure 1-12)**.

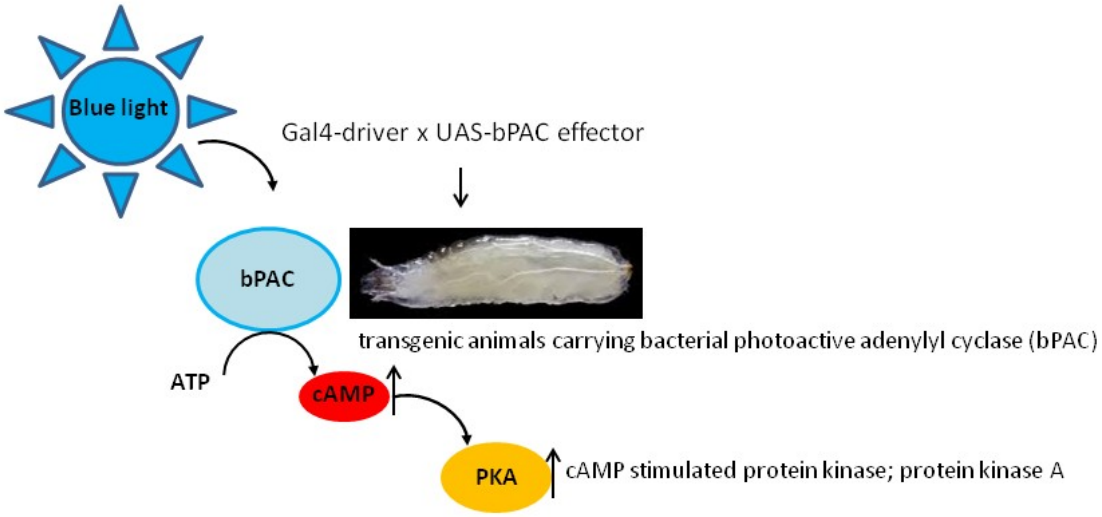

Figure 1-12: Utilization of photoactivated adenylyl cyclase (bPAC), of the soil bacterium *Beggiatoa* to modulate cAMP in *D. melanogaster*. Activation of bPAC by blue-light in the respiratory system of the fly increases cAMP levels and affects cAMP dependent effectors like protein kinase A (PKA).

Expression of the light-activated ion channel channelrhodopsin-2 (ChR2) of *Chlamydomonas reinhardtii* under UAS control allows depolarization of cells by blue light (480 nm). ChR2 modulates membrane voltage conducting H^+, Na^+, K^+, and Ca^{2+} ions and therefore was the first optogenetic system to control neuronal activity (Nagel et al, 2003). The use of a ChR2 mutant (D156C) called ChR2-XXL provides extra high expression and long open state and can be genetically expressed in any tissue using a specific Gal4-driver of choice (Dawydow et al, 2014). When the ion-channel is activated with blue light, the conformational change of the channel allows an influx of cations whereas anions cannot pass in **(Figure 1-13)**.

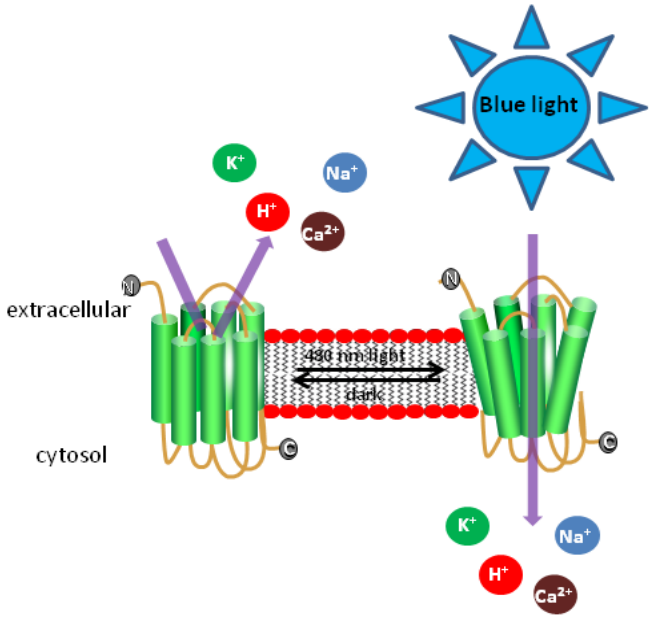

Figure 1-13: Utilization of blue-light activated ChR2-XXL for depolarization of cells in *D. melanogaster*.

The activity of voltage-gated K^+ channels in pulmonary arterial smooth muscle cells (PASMC) is pivotal in controlling membrane potential and cytoplasmic free Ca^{2+} release (Yuan et al, 1998). Cell depolarization and increased intracellular Ca^{2+} concentrations are very common in muscular pulmonary arteries of COPD patients (Shimoda et al, 2000; Weir & Olschewski, 2006). It was also reported that membrane depolarization causes activation of voltage-dependent Ca^{2+} channels, inducing Ca^{2+} release in smooth muscle cells (Liu et al, 2009). Thus, applying blue- light induced ion channels ChR2-XXL may help to understand cell polarity and depolarization of epithelial cells of the airways, which are still not fully understood.

1.3 Aim and significance of the study

The major aim of this work is to study the impact of cigarette smoke on the airway system of *D. melanogaster*. The mechanism by which cigarette smoke leads to the pathogenesis of COPD is currently unclear. Thus, this study attempts to elucidate if *D. melanogaster* can serve as a model organism for assessing the effect of cigarette smoke on airway structure and function to establish COPD models. Therefore, a further aim of this project is to analyze, which major signaling pathways or target genes play a role in the epithelial barrier immunity in response to cigarette smoke and what is their potential function for disease development. A more detailed characterization of these cigarette smoke regulated genes and their potential role for disease development were studied. To unravel transcription factors mediating this gene regulation, various fly lines defective in these transcription factors were employed and their DNA-binding property was checked by electrophoretic mobility shift assays (EMSA). Moreover, airway and lung tissue remodeling play an important role in the development of COPD. Thus, it was examined whether CSE leads into morphological changes within the airway epithelium.

Lastly, this study is focused on the roles and functions of second messengers on the physiology of the fly's airway system. By employing optogenetic tools, second messenger systems such as cAMP, was manipulated in the airway epithelium of *D. melanogaster*.

2. Materials and Methods

2.1 Materials

Standard laboratory reagents and materials were obtained from local suppliers, fine chemicals from Sigma if not otherwise indicated and instruments were supplied by the departmental facility.

2.1.1 Laboratory equipments

All equipments used for this study are listed in **Table 2-1.**

Table 2-1: List of laboratory equipments

Item	Manufacturer (location)
Agarose Gel ectrophoresis unit	Biometra GmbH, Göttingen, Germany
Analytical balance ABS	Kern & Sohn GmbH, Balingen-Frommern
Autoclave Steam Sterilizer Varioklav®	H+P Medizintechnik GmbH, Oberschleisheim, Germany
Balance MXX-412	Denver Instruments, New York, USA
Bead Ruptor 24	Omni International, Kennesaw, GA, USA
Binocular	Nikon, Düsseldorf, Germany
Casting system compact	Biometra, Göttingen, Germany
Centrifuge, 5415 D; rotor: F45-24-11	Eppendorf, Hamburg, Germany
Centrifuge 5417 R, rotor FA-45-30-11	Eppendorf, Hamburg, Germany
Centrifuge: Heraeus Fresco 17	Thermo Electron Corporation (Osterose)
Centrifuge: Sproud	Heathrow Scientific® (Illinois, USA)
Dryblock & heat bath HB-130	Unitek (Leutenbach)
Electrophoresis power supply, EV245	Consort, Parklaan, Belgium
Electrophoresis power supply, EV202	Consort Parklaan, Belgium
Flourescence microscope Axio Imager.Z1 with Axiocam MRM, HXP120 lamp, ApoTome	Zeiss, Oberkochen, Germany
Fridge Premium NoFrost CN 3056 CN 3666	Liebherr, Hamburg, Germany
Savant DNA Speed Vac® DNA 120 Thermo	Fisher Scientific Darmstadt, Germany
Thermostat cabinet 16°C	Loviband®, Dortmund, Germany
Thermostat cabinet 25°C	Aqua® Lytic, Dortmund, Germany
Icemachine Manitowoc®	Herborn, Germany
Imager FLA-5000	Fujifilm, Japan
Incubator 37°C	Memmert GmbH & Co.KG, Heilbronn, Germany
Incubation shaker, Heidolph Unimax 1010	Heidolph Instruments GmbH & Co. KG, Schwabach, Germany
Labcycler	Sensoquest, Göttingen, Germany
Labguard ES Class II Safety Cabinet	IBS Integra Biosciences, Landquart, Schweiz
Molecular Imager Gel Doc	Bio-Rad, Munich, Germany
Microscope SZX12 + camera DP 71, Olympus	Olympus GmbH, Hamburg, Germany
Microwave AFK®	Hamburg
Nanodrop ND-1000 spectrophotometer	Peqlab, Erlangen, Germany
Omni Bead Ruptor 24	Omni International Inc, Kennesaw, USA
oxygen measuring system GOX 100	Greisinger electronic
pH meter, model 330	Wissenschaftlich-Technische Werkstätten GmbH Weilheim, Germany
Platform Shaker MR Hei-Standard MR 3001	Heidolph, Schwabach, Germany

Item	Manufacturer (location)
Pipettes Research Plus	Eppendorf AG, Hamburg, Germany
pipette controller *accu-jet® pro*	Brand, Wertheim, Germany
Sonic Ruptor 400	Omni International, Kennesaw, GA, USA
StepOne Real-Time-PCR System	Applied Biosystems, Darmstadt, Germany
Table autoclave Omni Perfect	Beem® , Rosbach, Germany
Thermomixer HTMR-133	HLC-Heap Labor Consult, Bovenden
Vortex Genie-2	Scientific Industries, New York, USA
Water bath, thermostat 2761	Eppendorf, Hamburg, Germany
Ultraviolet Sterilizing PCR workstation	Peqlab Biotechnologie GmbH, Erlangen, Germany
Unitek HB 130 thermo plate	Scientific plastic, great britian

2.1.2 List of miscellaneous material

Miscellaneous material used in this work is listed in **Table 2-2**.

Table 2-2: Summary of miscellaneous material

Consumables	Manufacturer
48 wellplate and adhesive film for qRT-PCR	Applied Biosystems, Darmstadt, Germany
Ceapren plugs, 22 mm and 36 mm	Greiner Bio-One GmbH, Frickenhausen, Germany
Disposal bag autoclavable	Sarstedt, Nürnbrecht, Germany
Erlenmayer flasks 5ml, 25 ml, 300 ml	DURAN Group GmbH, Wertheim/Main, Germany
Exam gloves Rotiprotect®	Roth, Karlsruhe, Germany
Fly vials 16 ml & 68 ml	Greiner Bio-One GmbH, Frickenhausen, Germany
NHS-activated Sepharose™	GE Healthcare Life Sciences, Germany
Serological pitpettes 10ml and 25 ml	Sarstedt, Nürnbrecht, Germany
Steam Indicator Tape, Class I	Comply™ , USA
Sterile filters, ø 0.22 µm	Roth, Karlsruhe, Germany
Tubes 0,5ml, 1,5ml, 2ml	Sarstedt, Nürnbrecht, Germany
Parafilm "M"	Laboratory Film
PCR Multiply®-Pro tubes 0,2ml	Sarstedt, Nürnbrecht, Germany
PCR tubes 0,2 ml	Nerbe Plus, Winsen/Luhe
Petri dish 140x20 mm	Nerbe Plus, Winsen/Luhe
Pipette tips 20 µl, 200 µl, 1000 µl	Sarstedt, Nürnbrecht, Germany
Precision wipes, Kimberly-clark professional	Kimtech science, Canada
3R4F Research Cigarettes	University of Kentucky, Lexington, KY, USA

2.1.3 Chemicals

All chemicals used for this study are listed in **Table 2-3**.

Table 2-3: Summary of chemicals and reagents.

Chemicals	Manufacturer (Location)
1 kbp-GeneRuler™	Fermentas, St. Leon-Roth
50 bp-GeneRuler ™	Fermentas, St. Leon-Roth
Acetic acid	Carl Roth, Karlsruhe, Germany
Acryl/Bis 37.5:1; 40% (w/v) Solution	Carl Roth, Karlsruhe, Germany
Agarose	Biozym Scientific GmbH, Hessisch Oldendorf
Ammonium persulfate, > 98 %	Carl Roth, Karlsruhe, Germany
Ampicillin	Sigma, Steinheim, Germany
Antibody dilutent for IHC	Aptum Biologics Ltd., Southampton, UK
Bromophenol Blue, sodium salt	Carl Roth, Karlsruhe, Germany
Chloroform	Carl Roth, Karlsruhe, Germany
Coomassie Brilliant Blue G-250	Carl Roth, Karlsruhe, Germany
DAPI	Invitrogen, Darmstadt, Germany
Dideoxynucleotides	Promega, Mannheim, Germany
Dimethyl sulfoxide, p. a.	Carl Roth, Karlsruhe, Germany
Dithiothreitol, > 99.5 %	Invitrogen (Karlsruhe)
Ethanol, p. a.	Carl Roth, Karlsruhe, Germany
Ethidium bromide	AppliChem (Darmstadt)
Ethylene diamine tetraacetic acid	Carl Roth, Karlsruhe, Germany
Glycerol	Carl Roth, Karlsruhe, Germany
Goat serum	Sigma-Aldrich, Steinheim, Germany
Hepes	Carl Roth, Karlsruhe, Germany
Isopropyl alcohol, p. a.	Carl Roth, Karlsruhe, Germany
Isopropyl-β-d-thiogalactopyranoside	Carl Roth, Karlsruhe, Germany
Kanamycin	Sigma, Steinheim, Germany
LB agar (Lennox L agar)	Carl Roth, Karlsruhe, Germany
LB medium (Lennox L broth base)	Carl Roth, Karlsruhe, Germany
L-DOPA	Sigma, Steinheim, Germany
β-Mercaptoethanol, 98 %	Carl Roth, Karlsruhe, Germany
Methanol, p. a.	Carl Roth, Karlsruhe, Germany
Nipagin	Carl Roth, Karlsruhe, Germany
Sodium chloride	Carl Roth, Karlsruhe, Germany
Paraformaldehyde	Sigma-Aldrich, Steinheim, Germany
Potassium chloride	Merck
potassium dihydrogen phosphate	Carl Roth, Karlsruhe, Germany
dipotassium hydrogen orthophosphate	Carl Roth, Karlsruhe, Germany
RNAmagic	Bio-Budget, Kredeld, Germany
Rotiphorese® Gel 40 (29:1)	Carl Roth, Karlsruhe, Germany
Salmon Sperm DNA	Invitrogen
Section Block solution for IHC	Aptum Biologics Ltd., Southampton, UK
SeeBlue® Plus2 Prestained Standard	Thermo Fisher Scientific
Sodium dodecyl sulfate (SDS), research grade	Carl Roth, Karlsruhe, Germany
Sodium hydroxide (NaOH), p.a.	Carl Roth, Karlsruhe, Germany
N,N, N', N'-Tetramethylethylene diamine, 99 %	Carl Roth, Karlsruhe, Germany
SYBR® Green	Invitrogen, Darmstadt, Germany
Trichloroacetic acid (TCA), p.a. ≥99 %	Carl Roth, Karlsruhe, Germany
Tris-(hydroxymethyl)-aminomethane (Tris), p. a.	Carl Roth, Karlsruhe, Germany
Triton X-100	Sigma-Aldrich, Steinheim, Germany

Chemicals	Manufacturer (Location)
Washing Buffer for IHC	Aptum Biologics Ltd., Southampton, UK
Yeast extracts	Carl Roth, Karlsruhe, Germany

2.1.4 Antibodies

Antibodies, which were used for immunohistochemistry are listed in **Table 2-4** for primary antibodies and **Table 2-5** for secondary antibodies.

Table 2-4: List of primary antibodies.

Antibodies	Source	Working dilution
Mouse α-coracle	Developmental studies Hybridoma Bank, Iowa, IA, USA	1:200
Rabbit α-FoxO	Margret H. Bülow (Bulow et al, 2010)	1:200
Mouse α-WKD	gift from Amin S. Ghabrial, Dept. of Cell and Developmental Biology, University of Pennsylvania School of Medicine	1:100

Table 2-5: List of secondary antibodies.

Antibodies	Source	Working dilution
Goat α-mouse Dylight 549	Jackson ImmunoResearch Laboratories	1:500
α-mouse Alexa Flour 555	Life Technologies, Darmstadt	1:500
Goat α-rabbit Dylight 488	Jackson ImmunoResearch Laboratories	1:500

2.1.5 Plasmids and vectors

A synthetic dFoxo forkhead DNA-binding domain was obtained from *Eurofins* MWG Operon company and synthesized in a pEX-A2 vector. The product was delivered in a lyophilized state and therefore was dissolved in 100 µl 10 mM Tris-HCl (pH 8) buffer. All plasmids of this work are listed in **Table 2-6.**

Table 2-6: Table of plasmids and vectors.

Plasmid	Description	Reference
pEX-A2-FoxO FH DBD	size (bp): 2450 resistence: ampicillin insert: *dFoxO_FH* with NheI and HindIII restriction sites, size (bp): 384	Eurofins MWG operon
pET28a(+)N-X	size (bp): 5369 resistance: kanamycin IPTG-inducible *tac*-promoter His-tag desphorylated and digested with NheI and HindIII	CAU Kiel, AG Leippe*)
pET28a(+) dFoxO FH DBD	size (bp): 5689 Insert: *dFoxO FH* resistence: kanamycin	This work

**) stored at -80°C freezer*

2.1.6 Enzymes

Plasmid DNA was digested with the restriction enzymes NheI and HindIII to isolate the dFoxO FH DBD from the pEX-A2 vector and for cloning into pET28a (+) (**Section 2.1.5, Table 2-6**). All digestion reactions were incubated at 37° C for 2.5 h.

Table 2-7: List of restriction endonucleases.

Name	Concentration	Restriction site	Supplier
NheI of *Neisseria mucosa heidelbergensis*	10 U/ µl	5'…G↓CTAGC…3' 3'…CGATC↓G…5'	Thermo fisher scientific
HindIII of *Haemophilus influenzae Rd*	10 U/ µl	5'…A↓AGCTT…3' 3'…TTCGA↓A…5'	Thermo fisher scientific

Other enzymes used in this study are listed in **Table 2-8**.

Table 2-8: List of other enzymes.

Name	Supplier
Taq DNA Polymerase (5 U/µl)	Invitrogen, Darmstadt, Germany
DNAse	Thermo fisher scientific
RNAse A	Thermo fisher scientific
Proteinase K	Thermo fisher scientific
RNase inhibitor (40U/µl)	Invitrogen, Darmstadt, Germany
T4 ligase	Thermo fisher scientific
SuperScript™III Reverse transcriptase	Invitrogen, Darmstadt, Germany

2.1.7 Bacterial strains

In this work the following bacterial strains were used **(Table 2-9)**:

Table 2-9: List of bacterial strains.

Strain	Genotype	Supplier
DH5α	F- 80*lacZ* M15 (*lacZ*YA-*arg*F) U169 *rec*A1 *end*A1 *hsd*R17 (rK–, mK+) *pho*A *sup*E44 – *thi*-1 *gyr*A96 *rel*A1	Thermo Fisher Scientific (Darmstadt)
BL21 (DE3)	F^- *ompT hsd*S_B(r_B^- m_B^-) *gal dcm* (DE3)	Novagen (Darmstadt,Deutschland)

2.1.8 Antibiotics

All antibiotics applied in this work are listed in **Table 2-10** and were used with following concentrations:

Table 2-10: List of antibiotics.

Antibiotic	Stock solution	Working concentration
Ampicillin	100 mg/ml in water	100 µg/ml
Kanamycin	50 mg/ml in water	50 µg/ml
Chloramphenicol	34 mg/ml in ethanol	34 µg/ml

2.1.9 Oligonucleotides

Oligonucleotides used for RT PCR and the purpose of qRT PCR are listed in **Table 2-11** and were obtained from Eurofins MWG Operon LLC.

Table 2-11: List of oligonucleotides.

Name	Sequence
Rpl32_fwd	CCGCTTCAAGGGACAGTATC
Rpl32_rev	GACAATCTCCTTGCGCTTCT
Upd_fwd*)	CACCACAAGAAGCAGCAGAG
Upd_rev*)	AAATTGGTTGCTTCCACCAC
Upd2_fwd*)	AGCAGAAGAGCCTCAACGAG
Upd2_rev*)	CTGGCGTGTGAAAGTTGAGA
Upd3_fwd*)	GAGAACACCTGCAATCTGAA
Upd3_rev*)	AGAGTCTTGGTGCTCACTGT
OdT7 I	GAG AGA GG ATC CAA GTA CTA ATA CGA CTC ACT ATA GGG AGA (T)25
T7_fwd	TAATACGACTCACTATAGGG
T7_rev	CCCTATAGTGAGTCGTATTA

**) designed by Christina Wagner, Borstel*

Oligonucleotides for carrying out electrophoretic mobility shift assays were obtained from biomers.net GmbH and listed in **Table 2-12**:

Table 2-12: List of oligonucleotides used for EMSAs.

Name	Sequence (5` → 3`)	Decription
Upd3_for	CACATGTTTTGTTTATCTGCGAGC	Cy5 labeled, 8 bp dFoxO FH binding motif of upd3 and additionally 8 bp of the intergenic region at 5' and 3'
Upd3_rev	GCTCGCAGATAAACAAAACATGTG	Reverse complement of upd3_for
Upd2_for	CAATTAGTGTTTATGGCCTTG	Cy5 labeled, 7 bp dFoxO FH binding motif of upd2 and additionally 7 bp of the intergenic region at 5' and 3'
Upd2_rev	CAAGGCCATAAACACTAATTG	Reverse complement of upd2_for
Spn77Ba_for	GAAGTTTGTTGTTTATTGCACTTG	Cy5 labeled, 8 bp dFoxO FH binding motif of Spn77Ba and additionally 8 bp of the intergenic region at 5' and 3'
Spn77Ba_rev	CAAGTGCAATAAACAACAAACTTC	Reverse complement of Spn77Ba_for

2.1.10 Solutions and media

All media and buffers were prepared using deionized water, filtered through an ion-exchange unit (Membra Pure) **(Table 2-13)**. All media and buffers were sterilized by autoclaving at 120° C; the antibiotics were added to the media after cooling to approx. 50° C.

Table 2-13: Solutions and media.

Medium	Composition
Buffers for daily use	
10 x PBS	1,37 M NaCl 2,7 M KCl 65 mM Na_2HPO_4 15 mM KH_2PO_4 pH 7.4
HL3	70 mM NaCl 5 mM KCl 1,5 mM $CaCl_2$ 20 mM $MgCl_2$ 20 mM Glucose 10 mM $NaHCO_3$ 5 mM Trehalose 115 mM Saccharose 5 mM HEPES pH 7.2
10 x TBE	0,89 M TRIS

Medium	Composition
	0,89 M bor acid 2 mM (Na_2)-EDTA
TE	0,01 M Tris 0,25 M EDTA pH 8.0
6x DNA loading dye	50% (v/v) glycerol 60 mM EDTA 6% SDS 0.9% bromophenol blue pH 8.0
Solutions for X-GAL staining	
10 mM sodium phosphate buffer	10 mM NaH_2PO_4 10 mM Na_2HPO_4
Solution for fixation	0,75 % glutaraldehyde
Staining solution	150 mM NaCl 1 mM $MgCl_2$ 3,1 mM $K_2[Fe(CN)_6]$ 3,1 mM $K_3[Fe(CN)_6]$ 0,3% Triton X-100 in 10 mM sodium phosphate buffer
10 % x-GAL stock solution	solve 89 mg in 890 µl DMSO (store at -20° C)
X-GAL staining	25 µl x-GAL in 1 ml staining solution
Normal fly medium	
	1 % agar-agar 6.25 % cornmeal 6.25 % yeast 2 % glucose 3 % molasses 3 % sugar beet syrup 3 % nipagin (10 % v/v) 1 % propionic acid (10 % v/v)
Nipagin stock solution	10% (w/v) in 70% ethanol
Propionic acid	10% (v/v) in H_2O
Solutions for immunohistochemistry	
PFA	4% (w/v) in 1 x PBS, heat at 60-70° C; under stirring. cool it down to RT add 0,3% Triton X-100
PBT	0,1 % (v/v) Tween in 1 x PBS
NGS	10 % (v/v) in PBT

Medium	Composition
Media for cultivation of E. coli strains	
Lysogeny broth (LB) medium	1 % (w/v) tryptone 0.5 % (w/v) yeast extract 1 % (w/v) NaCl pH 7.4
SOC medium	0.5 % yeast extract 2 % (w/v) tryptone 10 mM NaCl 2.5 mM KCl 10 mM $MgCl_2$ 20 mM Glucose pH 7.0

1.5 % agar was added to the media for production of agar plates. All media were sterilized at 121° C for 30 min. LB media was stored at room temperature and SOC medium at - 20° C.

2.1.11 *Drosophila* stocks

The fly lines, which were used in this work were usually obtained from the Bloomington stock centre and are listed in **Table 2-14**.

Table 2-14: Flylines used in this study.

Wildtype flies	Genotype	Source
w^{1118}	w^{1118}	Bloomington No: 5905
yw^{1118}	y^1 w^{1118}	Bloomington No: 6598
Knockout lines		
FoxO-KO	yw;*;dfoxo24/dfoxo24	Marc Tatar**,** Rochelle**,** Yamamo-to
FoxO-KO	w[*]; P-foxo21/foxo21 homozygote	Marc Tatar, Rochelle, Yamamo-to
Imd-KO	w[1118]; Rel[E38] e[s]	Bloomington No: 9458
GFP reporter lines		
Drosomycin GFP	yw (P(w -, drom-gfp)D4, P(ry+, dipt-lacZ) (162:7)2	(Tzou et al, 2000)
10x STAT-GFP 3rd	w: 10x STAT-GFP 3rd	(Bach et al, 2007)
10xSTAT-DGFP	w[1118]; P{w[+mC]=10XStat92E-DGFP}3/TM6C, Sb[1] Tb[1]	Bloomington No: 26200
unpaired-3	upd3-Gal4;UAS-GFP	Perrimon *et al*., 2003
GST-D-Reporter	GSTD-Gal4;UAS-GFP	Gift from Dirk Bohmann, Rochester
Atf3-EGFP	w[*];;pBAC(atf3::EGFP)/TM6B	a gift from Colin Donohoe; Co-logne

dSRF-Gal4;UAS-eGFP	DSRF-Gal4;UAS-GFP	a gift from J. Casanova, IBMB CSIC/IRBB, Barcelona, Spain
Wnt-ERFP	fz3-RFP/CyO	(Olson et al, 2011)
UAS responder lines		
UAS-FoxO in II	y[1]w[*];P{w[+mC]=UASfoxo. P}2	Bloomington No: 9575
pUAS-FoxO-GFP	w[1118]; P{UAS-foxo-GFP}	BestGene (Diss. C.Wagner)
UAS-Dome^{CA}	(1;2) w; UAS-dome 2.1 TM-CYT/gowf	Perrimon *et al*., 2003
UAS-STAT92E	P{w[+mC]=UAS-STAT92E) synonym UAS-mrl	Dustin W. Perry, Univ. Kentucky
UAS-Upd3	UAS-upd3, attP40 background	BestGene 6727-2-1M
UAS- Hop^{Tum-l}	y^1v^1 hop^{Tum}/FM7c	Bloomington No: 8492
UAS M1D1	UAS M1D1, insertion on the X chromosome	Charles Nichols Lab (Becnel et al, 2013)
UAS-lacZ	P{w[+mC]=UAS-lacZ.Exel}21; 3	Bloomington No: 8530
pUAST-EYFP-relish	P{UAS-Rel.YFP}	Tony Ip's lab (Tanji et al, 2010); Bettencourt et al. 2004
UAS-pBAC	w[*];P{UAS-bPac.S}/Cyo	a gift of Martin Schwärzel; Free University Berlin
UAS-ChR2-XXL	y[1] w[1118]; PBac{UAS-ChR2.XXL}VK00018	Bloomington No:58374 (Dawydow et al, 2014)
UAS-PGRP-LE 8	DDI (Drs-GFP; Dipt.-lacZ):UAS-Flag-PGRP-LE (II)	Ihoichiro Kurata
Gal-4 driver lines		
PPK4-GAL4	yw67c23; ppk4-Gal4; +/+	(Liu et al, 2003b)
PPK4- GAL4Gal80^{Ts}	W; GAL4; GAL80, +y GAL4 GAL80	Christina Wagner Forschungszentrum Borstel
c929- GAL4	Insert of P{GawB}crc929 on 2nd chromosome	A gift from Christian Wegner (Marburg); fly line was generated by Kim Kaiser, Glasgow
Cnc- GAL4	w[1118]; P{w[+mC]=GMR36G01-GAL4}attP2	Bloomington No: 45241
Cut- GAL4	w[*]; P{w[+m*]=cut-GAL4.B}3	Bloomington No: 27327
Puc- GAL4	w[*];P{GAL4E69}puc[GAL4E69]/TM3, Sb[1] Ser[1]	Bloomington No: 6762
Upd- GAL4	Expresses Gal4 in the pattern of upd	BestGene 5070-1-1M$^{*)}$
Upd2- GAL4	Expresses Gal4 in the pattern of upd2	BestGene 5070-2-2M$^{*)}$
Upd3- GAL4	Expresses Gal4 in the pattern of upd3	BestGene 5070-3-2F$^{*)}$
Domeless- GAL4	Expresses Gal4 in the pattern of domeless	BestGene 5070-4-4M$^{*)}$

2.2 Methods

2.2.1 *Drosophila* culture and crosses

The flies were raised on standard medium, if not otherwise stated and were kept at 25° C. For crossings, 5-15 virgin females of the UAS strains and corresponding GAL4 males in a ratio 1:2 - 1:3 were used. For crosses with bPAC, 5 males of the UAS strain (straight wings) were used and mated with ten virgin females of corresponding GAL4 females. Using the temperature-dependent Gal4-tubGal80^{ts}/ UAS system, gene expression was temporarily controlled. For this purpose flies were kept at 17° C and for activating gene expression, the temperature was raised to 30° C. The F1-generation of crosses with blue-light inducible strains, were kept either in the dark, or the fly vials were covered with aluminum foil to protect them from UV-light.

2.2.2 Treatment of larvae and flies

2.2.2.1 Cigarette smoke exposure

Early third-instar larvae were collected from each genotype and placed in separate vials containing standard *Drosophila* medium for each CSE treatment. For each experiment the wild type and the mutant fly strains to be tested were placed in an air tight smoking chamber at RT. The animals were exposed to cigarette smoke by one single cigarette in intervals of 6 hours for 1 day (termed as 24 hours CSE) and 2 days, in further text termed as 48 hours CSE. After every cigarette the smoking chamber was shortly opened and closed again to ensure an air exchange. Additionally, O_2 in the smoking chamber was measured to ensure that no hypoxic conditions are created **(Figure 2-1, Table 2-15)**.

Table 2-15: Details for smoke exposure.

Animals (number)	day	Smoke exposure		Route of administration	Tissue of interest
		Number of cigarettes	Time between exposure		
25 animals each vial	1 ("24 h CSE") first dissection	4	6 h	Smoking chamber	Tracheas
	2 ("48 h CSE") second dissection	4			

For control animals, the vials for each respective genotype were placed in an identical way and were exposed to filtered air. The trachea was removed immediately after the treatment for gene expression experiments and measurement of the epithelial thickness.

The fly vials were sealed with parafilm and holes were arranged with a fine needle to ensure that flies are in contact with the smoke.

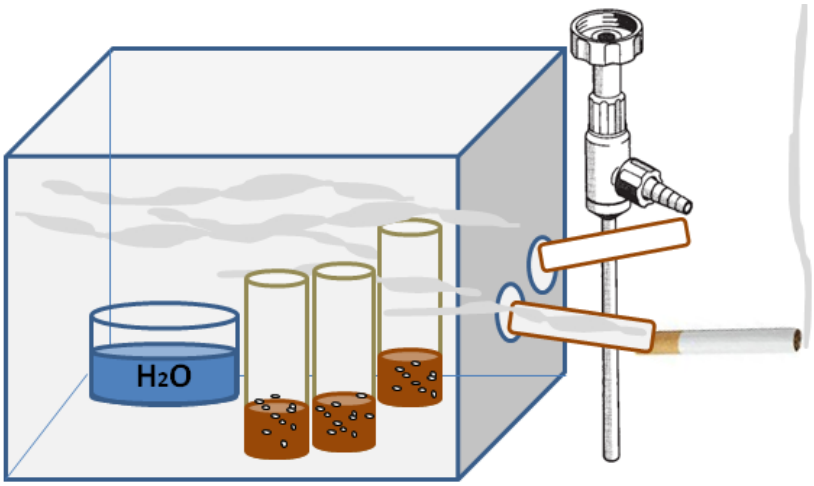

Figure 2-1: Experimental design for application of cigarette smoke on *D. melanogaster*. Flies and larvae were kept in fly vials with media and sealed with parafilm. The surface of the parafilm was punched with small holes to ensure gas exchange. Finally, smoke exposure was done by fine-regulation of the water-jet pump creating a low pressure, which led to cigarette smoke entrance into the chamber. To prevent animals from drying out, humidity was maintained with a small bowl of water inside the chamber.

For survival assays of cigarette smoke exposed adult flies, it was important to ensure that the flies were all in same age. For this purpose adult flies were kept for another 6 days at 25° C after hatching to avoid any effects of CSE on their development in the juvenile stage. The flies were subjected to smoke two times a day. Not more than 30 flies of each line were kept in a vial to avoid a too high density. The flies were transferred to fresh medium every other day, and the number of dead flies was recorded every third day.

2.2.2.2 Hypoxia

Hypoxia experiments were carried out using an air tight glass exicator, which was supplied with a N_2 gas. An oxygen electrode was used to measure the O_2 level within the exicator, until the electrode showed a reading of 3% O_2. Humidity was maintained by passing the gas over water. The exicator was sealed with parafilm to make sure that there was no exchange of air.
For gene expression experiments L3 larvae were kept for 1 h at an oxygen level of 2 %.
For branching experiments, the animals were kept for 2 to 3 days at an oxygen level of 3 %.

2.2.2.3 Optogenetic manipulation of the respiratory system with blue light

In order to investigate the physiological impact of cAMP-dependent signaling in the trachea of *D. melanogaster*, transgenic animals expressing either the photo activated adenylyl cyclase (bPAC) or the ion-channel ChR2-XXL were subjected to blue light.

Transgenic L2 instar larvae were subjected to blue light and raised until L3 in 10% glucose and then observed for phenotypic changes. The blue light lamp was arranged approximately 25 cm above the plate and a lux meter was used for measuring illumination (approximately 737 lux). Animals expressing the ChR2-XXL were treated in the same way. In order to ensure light-induction was only performed by the blue-light, the fly vials were packed in alu foil until blue-light was used **(Figure 2-2)**.

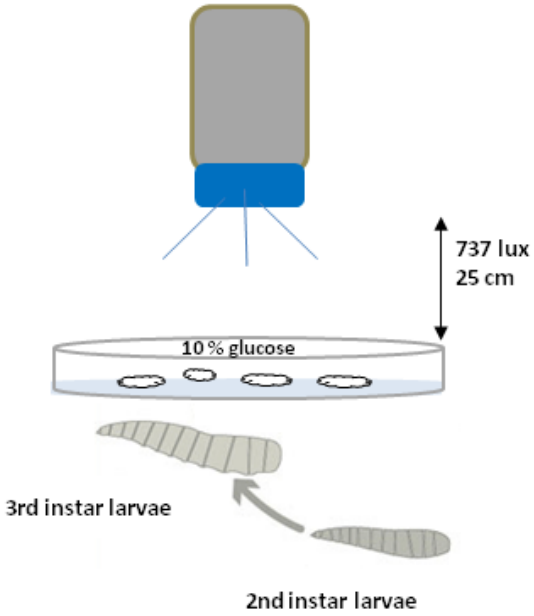

Figure 2-2: Schematic view of the *in vitro* blue light stimulation. Animals of 2nd instar were raised on 10% glucose and exposed to blue light until early 3rd instar larval stage to observe changes within the airways of the fly.

2.2.2.4 Application of Clozapine N-oxide (CNO)

To activate DREADD receptors *in vivo*, CNO was also applied to flies through food. A calculated amount of this synthetic ligand was dissolved in 1 x PBS to obtain a 10 mM stock solution. This was mixed with a calculated volume of *Drosophila* medium depending on the amount needed. The final concentration of CNO in the medium was 1 mM.

2.2.3 Methods for phenotypical characterization

2.2.3.1 Survival assay

Directly after hatching, males and females were separated. Flies hatched within 24 hrs were kept for 6 days under control conditions before exposing to cigarette smoke. These flies were kept at a density of 30 animals per vial and exposed to smoke. Cigarette smoke exposure was performed every day with two cigarettes. The flies were kept in an incubator at 25° C and were taken out only for smoke experiments. After every three days, the flies were transferred to a fresh medium. Results are represented as percentage of living flies after every 3 days of smoke exposure. The statistical analysis of lifespan was performed using the GraphPad Prism 5 analyzed by log rank test.

2.2.3.2 Immunohistochemistry and microscopy

Third instar larvae were dissected inside-out in HL3-medium and fixed over night (or for 30 min at RT) with 4% PFA at 4° C. After three rinses in PBT buffer the tissue was blocked in 10% NGS and then incubated with the primary antibody overnight at 4° C. Again three rinses in PBT followed and the secondary antibody was incubated overnight at 4 C. In all tissue samples, nuclei were stained with DAPI and mounted with 80 % glycerol in PBS. All antibodies and their dilutions used for immunohistochemistry purposes are listed in **Section 2.1.4, Tables 2-4 and 2-5**. Microscopic analysis was performed either with an Olympus SZX12 stereomicroscope, equipped with an epifluorescence support, or images were captured with the Zeiss Axio Imager Z1 with Apotome.

For fluorescent intensity measurement, Zeiss Axio Imager Z1 with Apotome was applied and the quantification of cell fluorescent intensity was measured using Image J to calculate the corrected total cell fluorescence (CTCF). CTCF= Integrated Density－Area of selected cell × Mean fluorescence of background readings (Gavet & Pines, 2010).

2.2.3.3 L-DOPA staining

Dorsal trunks of third instar larvae were dissected and, after washing in PBS, placed on a piece of filter paper pre-soaked in a saturated solution of L-DOPA in PBS.

The tracheae were submerged in a thin layer of L-DOPA solution and kept at dark room for 1–2 hrs before observation.

2.2.3.4 β-galactosidase staining

Trachea of L3 instar larvae were isolated in 1xPBS and incubated for at least 25 min in fixation solution **(Section 2.1.10, Table 2-13)**. After incubation they were rinsed two times for 5 min with 1xPBS. The tissues were transferred into pre-warmed staining solution (37° C) where X-Gal was added. For analytical purposes control flies and crosses were treated in the same way.

2.2.3.5 Characterization of tracheal terminal cells

The region marked with a red circle (3rd segment), has been used for quantification purpose of the terminal branches and to observe changes of their morphology (**Figure 2-3**).

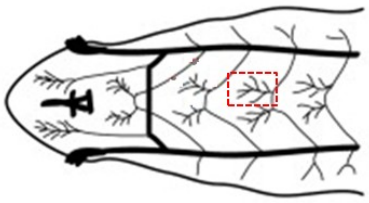

Figure 2-3: Region of interest for characterization of terminal cells. For quantification and characterization of the terminal branches, the 3rd segment of 3rd instar larva was chosen as region of interest.

2.2.4 Molecular biological methods

2.2.4.1 Agarose gel electrophoresis

Agarose gel electrophoresis was used for analytical and preparative purposes. For a casting gel, 1-2 % (w/v) agarose was dissolved by heating it in a microwave oven in 1 x TBE buffer and supplemented with 3 µl ethidium bromide. The DNA samples, mixed with 5x DNA loading buffer, were loaded into the wells. DNA size standards (100 bp or 1 kb ladder) were run in parallel. Electrophoresis was performed at a constant voltage of 100 V for 45–60 min, depending on the desired resolution. For the purposes of documentation, DNA bands were visualized under UV light (312 nm) and gels were photographed using the gel imaging system.

2.2.4.2 Purification of DNA from agarose gels

The QIAquick® gel extraction Kit (Quiagen, Hilden, Germany) was used to purify linearized vector DNA or PCR products from agarose gels. For preparative purposes selective DNA fragments were cut out from stained agarose gels with a scalpel under UV illumination.

The gel slices were weighed (= 1 volume) and each slice dissolved in 3 volumes of solubilization buffer by incubation for 10 min at 50°C. DNA was purified by using the QIAquick PCR purification Kit (Qiagen, Hilden, Germany) according to the manufacturer's instructions.

2.2.4.3 Purification of plasmid DNA

A small culture (5 ml) of bacteria was grown in order to amplify the plasmid of interest *in vivo*. The bacteria were harvested by centrifugation at 13,000 rpm for 1 min at room temperature. The resulting pellet was used for the subsequent preparation of plasmid DNA using the QIAprep® Spin Miniprep Kit (250) (Qiagen, Hilden, Germany) according to the manufacturer's instructions.

2.2.4.4 Restriction endonuclease digestion of DNA

Type II restriction endonucleases were used to digest double-stranded DNA for analytical or preparative purposes. For preparative purposes, 1-5 µg DNA and vector were digested with 1-20 U of restriction enzymes NheI and HindIII **(Section 2.1.6, Table 2-7)** in a volume of 10-50 µl. Complete digestion was confirmed by agarose gel electrophoresis. For analytical purposes, 0.2-1 µg DNA was digested with 1-5 U of enzyme in a volume of 10 -20 µl. Incubation times were varied between 1 and 3 h. Reaction buffers were supplied by the manufacturer. Enzymes were heat inactivated as recommended by the supplier or removed by purification of the digested DNA using the appropriate kit. In case of double restriction digestions, the Fermentas DoubleDigestTM Online Tool (http://www.fermentas.com/en/tools/doubledigest) was used to choose suitable conditions.

2.2.4.5 Dephosphorylation of linearized vector

In order to prevent self-ligation of vector ends in cloning strategies, 0.5 µl (0.5 U) thermosensitive alkaline phosphatase (FastAP) was added to 50 µl digested vector DNA. Dephosphorylation was performed in the respective restriction enzyme buffer. Samples were incubated for 30 min at 37° C and subsequently purified by agarose gel electrophoresis (**Section 2.2.4.1**) and gel extraction with the MinEluteTM Reaction Cleanup Kit (50), (Qiagen, Hilden, Germany).

2.2.4.6 Ligation of DNA fragments

DNA fragments bearing either sticky or blunt ends can be ligated *in vitro* with bacteriophage T4 DNA ligase (5U/µl, Fermentas, GmbH) in 1x Rapid Ligation Buffer (Promega). In a total reaction volume of 20 µL, linearized and dephosphorylated vector (50 ng) and insert DNA were mixed with a molar ratio of 1:7 **(Section 2.2.5, Table 2-6)**.

Five units of T4 DNA ligase were added and mixed thoroughly. Ligation mixtures were incubated over night at room temperature and subsequently transformed into competent *E. coli* cells **(Section 2.1.7, Table 2-9)** or stored at - 20° C.

In order to check whether the ligation was successful, the plasmid was digested as described in **Section 2.2.4.4**, analyzed by agarose gel electrophoresis and verified via sequencing by GATC biotech.

2.2.4.7 Total RNA isolation

Tracheas of 30 third instar larvae of the respective genotype were dissected in Hl-3 buffer on ice. Then 1 ml of RNA magic was added and the samples were frozen in liquid nitrogen and thawn on ice. This step was repeated for 2 to 3 times until the trachea were completely homogenized and 200 µL of chloroform was added. The samples were vortex vigorously and incubated for 10 min on ice. After the incubation the samples were centrifuged at 15,000 x g for 10 min at 4° C and the upper phase was carefully transferred into a clean tube. An equal volume of isopropanol was added for precipitating the RNA over night at - 20° C.

Then the RNA was centrifuged for 60 min at 17,000 x g, at 4° C and the supernatant was discarded. The RNA pellet was washed for 2 to 3 times with 500 µL 70% ice-cold ethanol by centrifugation at 15,000 x g for 5 - 10 min. The Pellet was dried and resolved in 10 µL RNAse free water (HPLC water) and stored at - 80 °C.

2.2.4.8 Generation of cDNA and reverse transcriptase PCR

For the generation of cDNA, 400 ng of total RNA was added into a sterile tube on ice and gently mixed with 1 µl Oligo (dT7 I) and 1 µl of 10 mM dNTPs mix (10 mM) with appropriate amount of water. The mixture was incubated at 65 °C for 5 min and immediately placed on ice for at least 1 min. Synthesis of cDNA was carried out with SuperScript III reverse transcriptase (Invitrogen) and Ribolock^{TM} ribonuclease inhibitor in each reaction as recommended in the manufacturer's protocols and incubated at 50° C for 1 h.

The reaction was terminated at 70° C for 15 min to inactivate the transcriptase. The freshly prepared cDNA could be used directly in PCR reaction or frozen at –20° C. Reverse transcriptase PCR was carried out using Taq DNA polymerase in a total volume of 25 µl with gene specific primers. The program was processed according to **Table 2-16**. Subsequently, the PCR products were checked by 1 % agarose gel electrophoresis.

Table 2-16: RT-PCR program.

Cyclus	Denaturation 95°C	Primer-Annealing 55°C	Elongation 72°C	Repeats
1	1 min	---	---	1
2	30 sec	30 sec	1 min	30
3	---	---	5 min	1
4		4°C	∞	

2.2.4.9 Quantitative real time PCR

All quantitative RT-PCR analyses were performed using StepOnePlus™ Real-Time PCR System. The total volume of 10 µl, consisting of 5 µl SYBR Green Master Mix, 0.25 µl ROX, 0.5 µl forward primer (5 µM), 0.5 µl reverse primer (5 µM), 1 µl cDNA (20 ng) and 2.75 µl water, was loaded into a 48 well plate. Primers used for qRT-PCR are listed in **Section 2.1.9, Table 2-11**. The amplification was run as below:

95 °C	10 min	
95 °C	15 sec	40 cycles
60 °C	20 sec	
72 °C	35 sec	
95 °C	5 min	
60 °C + 0.3 °C until 95°C		melting curve
95 °C	15 sec	

In a preliminary test, the primer efficiencies for both, gene of interest and reference, were analyzed based on the standard curve and the slope, which was derived from serial dilutions of cDNA from 50 ng to 3.12 ng. The primer efficiencies were calculated according to $E=10^{-1/slope}$ formula (Pfaffl, 2001). Thus, the relative expression ratio (fold change) of a target gene was determined based on E and CT values in comparison to a reference gene. In triplicates, the fold changes of each group were represented as mean ± SEM for statistical analysis. In this case, *Rpl32* served as a reference gene for all assays.

The relative expression ratio of the target gene to reference gene was calculated as follows: ΔCT = CT target – CT reference, where ΔCT is change of cycle threshold (CT) calculated by the StepOne program during amplification. All materials for qRT PCR were treated under UV light for 30 min before use.

2.2.4.10 Electrophoretic mobility shift assay (EMSA)

To create double stranded DNA fragments, an equimolar mixture of complementary Cy5-labeled oligonucleotides **(Section 2.1.9, Table 2-12)** were incubated for 5 min at 95° C and slowly cooled down to room temperature. Eighty picomoles dFoxO FH and about 10 pmol DNA fragments were mixed in binding buffer (12 mM HEPES, 6 mM KCl, 3 mM $MgCl_2$, 1 mM DTT, 4 mM Tris-HCl, 6 mM EDTA, pH 8.0) to give a final volume of 25 µl.
Salmon sperm DNA was added as competitor (50 ng/µl, final concentration). After incubation at room temperature for 30 min, the samples were separated by 7% acrylamide-bisacrylamide [29:1] gel and electrophoresis was carried out in 1xTBE buffer for 1 hour at RT and 120 V. Gels were scanned with a Fluoro Image Analyzer FLA-5000.

2.2.5 Microbiological methods

2.2.5.1 Growth of liquid cultures

For small liquid culture, 5-10 ml LB/antibiotic medium was inoculated with a single bacterial colony and incubated overnight at 37° C on a shaking platform at 250 rpm. The starter culture was incubated for 8-12 h and was used to inoculate fresh liquid medium.

2.2.5.2 Growth on solid media

Dry LB agar plates were used as solid media. Single bacterial colony or bacterial suspension was inoculated by spreading with a sterile inoculation loop or a sterile plastic spreader to achieve single colony growth. The plates were incubated inverted overnight at 37° C.

2.2.5.3 Monitoring the bacterial growth

The growth of the bacteria in liquid culture was measured at a wavelength of 600 nm (OD_{600}) in plastic cuvettes against pure medium as a blank using a spectrophotometer. Each 0.1 OD_{600} unit corresponds to approximately 10^8 cells/ ml for $OD_{600} < 1$.

2.2.5.4 Heat-shock transformation of plasmid DNA in *E. coli*

Treatment of competent bacterial cells (**Section 2.1.7, Table 2-9**) with a brief heat shock enables transformation of DNA. Plasmid DNA or a plasmid ligation reaction (not more than 25 ng) was mixed with 50 µl thawed competent bacteria and incubated for 30 min on ice.
The bacteria were treated for 90 sec by heat shock at 42° C, placed on ice for 1-2 minutes, diluted with 500 µl SOC medium and incubated for 1 h at 37° C with shaking. An aliquot of 100-300 µl or resuspended pellet was spread on a LB/antibiotic agar plate and incubated overnight at 37° C to select clones containing the desired plasmid.

2.2.5.5 Glycerol stocks of *E. coli* cultures

For long-term storage of *E. coli* clones, glycerol cultures were prepared (Sambrook and Russell, 2001). 2 mL of a fresh overnight culture was chilled on ice and the bacteria were pelleted at 10,000 x g for 1 min in a 2 mL tube. Then, 1.2 mL of the supernatants was removed and the cell pellets were resuspended in the remaining 0.8 mL.
200 µL of autoclaved 75 % glycerol were added and mixed by inverting to obtain a final glycerol concentration of 15 % (v/v). Glycerol cultures were stored at -80° C.

2.2.6 Protein expression and purification

2.2.6.1 Expression of recombinant dFoxO FH DBD

Transformed host cell BL21 (DE3) with the expression plasmid pET28 a (+) dFoxO FH **(Section 2.1.5, Table 2-6)** were deployed to inoculate 25 ml LB-broth pre-cultures. The cultures were grown overnight in an incubator shaker with 250 rpm at 37°C and then utilized to inoculate a 500 ml LB large-scale cultures (1:100). Large scale cultures were grown until an optical density between 0.6 and 0.8, induced with 0.1 mM IPTG and grown for five hours in an incubator shaker at 250 rpm and 37° C. Afterwards, the cells were collected through centrifugation in a centra CL3R centrifuge at 4000 g for 20 minutes. The resulting pellets were stored at -20° C until protein purification was done.

2.2.6.2 Preparation of cell lysates

To isolate intracellular expressed recombinant proteins, the thawed cells were resuspended in 1 x PBS. Then the cells were disrupted using the Omni Sonic Ruptor 400 Watt ultrasonic homogenizer and cell disrupter for 10 seconds in 4 cycles with a sonification power~70%.

Cell debris was removed from the crude lysate by centrifugation in a centra CL3R centrifuge at 4000 g for 1 hour at 4° C.

2.2.6.3 Purification of dFoxO FH DBD

In order to purify soluble fractions of over expressed dFoxO FH DBD, a column was filled with NHS-activated Sepharose™ and equilibrated with buffer containing 50 mM NaH_2PO_4, 300 mM NaCl and 20 mM imidazole, pH 8.0. The supernatant containing dFoxO FH DBD was applied on the equilibrated column and was washed twice with buffer.

To obtain the target protein in the flow through, an elution buffer containing 50 mM NaH_2PO_4, 300 mM NaCl and 500 mM imidazole, pH 8.0, was used and the target protein was collected in 500 µl fractions. The eluted fractions were resolved and analyzed by SDS-PAGE (**Section 2.2.7**).

2.2.7 Protein analysis

2.2.7.1 SDS-polyacrylamide gel electrophoresis (SDS-PAGE)

Protein samples were incubated under reducing conditions for analytical purposes by sodium dodecyl sulfate polyacrylamide gel electrophoresis (SDS-PAGE) performed in an electrophoresis system. SDS polyacrylamide gels were prepared according to the system instructions (**Table 2-17)**. SDS-PAGE protein samples were prepared by mixing 20 µl of the protein samples with 5 µl of 5x SDS sample buffer (**Table 2-18**). The SDS-PAGE protein samples were denatured at 95°C for 10 min and were loaded onto the gel. Electrophoresis was carried out at 150 V. The resolving gel was subsequently subjected to gel staining (Section **2.2.7.2**). By comparison with a standard protein marker (SeeBlue® Plus2 Prestained Standard), the molecular weight of the target protein was estimated.

Table 2-17: Composition of stacking and resolving gel.

Components	stacking gel 5 % SDS (1 ml final volume)	resolving gel 15 % SDS (5 ml final volume)
Water	0.68 ml	1.1 ml
30% Acrylamide mix	0.17 ml	2.5 ml
1.0 M Tris (pH 6.8)	0.13 ml	
1.5 M Tris (pH 8.8)		1.3 ml
10 % SDS	0.01 ml	0.05 ml
10 % ammonium persulfate	0.01 ml	0.05 ml

Components	stacking gel 5 % SDS (1 ml final volume)	resolving gel 15 % SDS (5 ml final volume)
TEMED	0.001 ml	0.002 ml

Table 2-18: Composition of 5x SDS sample buffer.

Components	5x SDS sample buffer
Bromphenol Blue	0.25 % (w/v)
Glycerol	50 % (v/v)
β-Mercaptoethanol	25 % (v/v)
SDS	4 % (w/v)
Tris-HCl (pH 6.8)	250 mM

Table 2-19: Composition of SDS buffer.

Components	SDS buffer
Tris (pH 8.3)	25 mM
Glycine	192 mM
Triton X-100	0.1 %

2.2.7.2 Coomassie staining of protein gels

The polyacrylamide gel was immersed in at least 5 volumes of the coomassie staining solution and placed on a slowly rotating platform for 30 min at room temperature. The gel was destained in coomassie destaining solution on a slowly rotating platform, changing the destaining solution three to four times (**Table 2-20**).

Table 2-20: Composition of coomassie staining and destaining solution.

Components	coomassie staining solution	destaining solution
Coomassie Brilliant Blue G-250	0.1 % (v/v)	-
Methanol	45 % (v/v)	10 % (v/v)
Acetic Acid	7 % (v/v)	10 % (v/v)

2.2.8 *in silico* analysis

2.2.8.1 Sequence collection

I extracted the genomic DNA/cDNA/protein sequences from flybase by scanning via BLAST suite (Altschul & Gish, 1996; Altschul et al, 1990; Altschul et al, 1997).

2.2.8.2 Sequence alignment and tree building

All sequence alignments and tree building were performed with MUSCLE (Edgar, 2004a; Edgar, 2004b) using default settings. Sequence information was obtained from the Protein Knowledgebase (UniProtKB, www.uniprot.org) available via the Expasy website (http://ca.expasy.org). Protein sequence alignments were visualized by Genedoc (Nicholas *et al*., 1997). Phylogenetic analysis was carried out using MEGA4 software (Tamura *et al.*, 2007) and using the MrBayes 3.2.1 suite (Ronquist & Huelsenbeck, 2003).

2.2.8.3 Structure modeling

Modeling of the protein structures was performed using I-TASSER (Roy et al, 2010) and subsequently, structural analysis and figure construction was carried out using PyMol (http://pymol.org).

2.2.8.4 Softwares

All softwares used in this work are summarized in **Table 2-21**.

Table 2-21: Applied softwares in this study.

Tools	Websites	Purposes
NCBI protein/DNA databases	http://www.ncbi.nlm.nih.gov/	Retrieving sequences
BLAST (NCBI)	http://www.ncbi.nlm.nih.gov/BLAST/	Homology search
ClustalW	http://www.ebi.ac.uk/Tools/clustalw/index.html	Sequence alignment
Genedoc	http://www.nrbsc.org/gfx/genedoc/index.html	Alignment editor
GenTHREADER (mGenTHREADER)	http://bioinf.cs.ucl.ac.uk/psipred/psiform.html	Fold recognition
Expasy	www.expasy.de	Protein sequence analysis
Psipred	http://bioinf.cs.ucl.ac.uk/psipred/psiform.html	Secondary structure prediction
GraphPad Prism 5	http://www.graphpad.com/scientific-software/prism/	Comparison of survival & qRT PCR data
Protein Data Bank (PDB)	www.rcsb.org/pdb/	Protein structure collections
Yasara	http://yasara.org	Protein structure visualisation

3. Results

3.1 Activation of JAK-STAT signaling in the trachea after CSE

GFP reporter lines were used to identify signaling pathways which are getting activated after cigarette smoke in the fly's respiratory track, such as Wnt signaling (**Appendix 7.1, Figure 7-1**) and JAK-STAT signaling. Third instar larvae of the 10XSTAT92E-DGFP reporter line were exposed to cigarette smoke to observe expression of the JAK-STAT pathway. The larvae were exposed to CSE after every 6 hours with 1 cigarette for 2 days, referred as 48 h CSE. It is demonstrated that JAK-STAT signaling is getting activated in the trachea in response to CSE and may play a physiological role as a key signaling pathway for smoke related disease development (**Figure 3-1**).

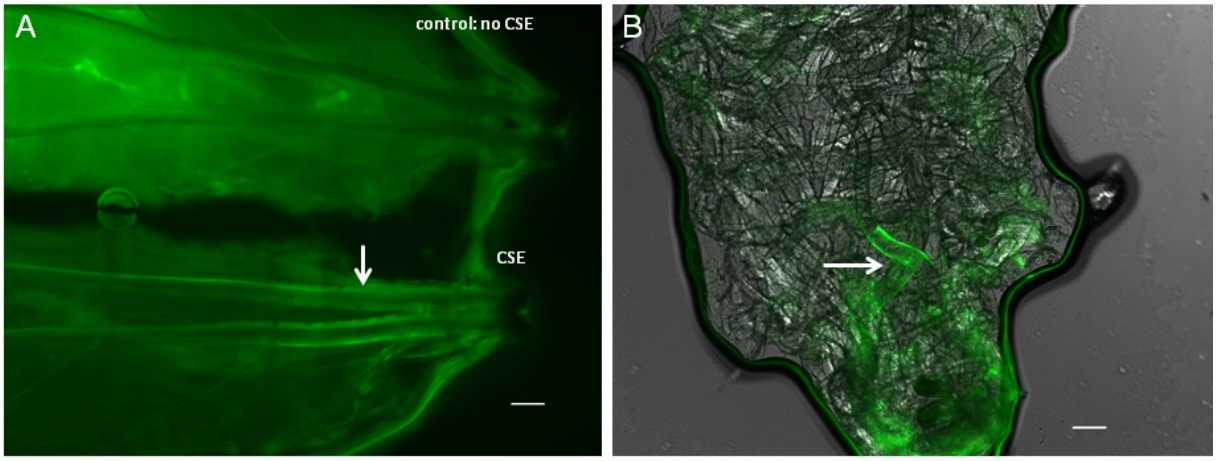

Figure 3-1: Cigarette smoke exposure on third instar larva of JAK-STAT reporter line. A) Dorsal view of cigarette smoke exposed larva. The 10XSTAT92-DGFP reporter (green) detects JAK-STAT pathway activation after CSE at the posterior end of the dorsal branches of third instar larvae. Air-exposed larvae served as a control. **B**) Filet dissection of animals carrying 10XSTAT92-DGFP confirmed JAK-STAT signaling to be occurred at the dorsal branches of the trachea. The scale bar is 100 µm.

Strong GFP expression (green) occurred in treated animals when compared to non-treated animals at the dorsal branches as illustrated in **Figure 3-1 A.** In order to examine if only the main dorsal branches were affected, the filet cutting technique was used without destroying terminal and secondary branches **(Figure 3-1 B).** This result indicates that the main affected area by cigarette smoke is limited to the dorsal trunks and to a part of the primary branches. This illustrates that *D. melanogaster* was able to absorb cigarette smoke through its airway system.

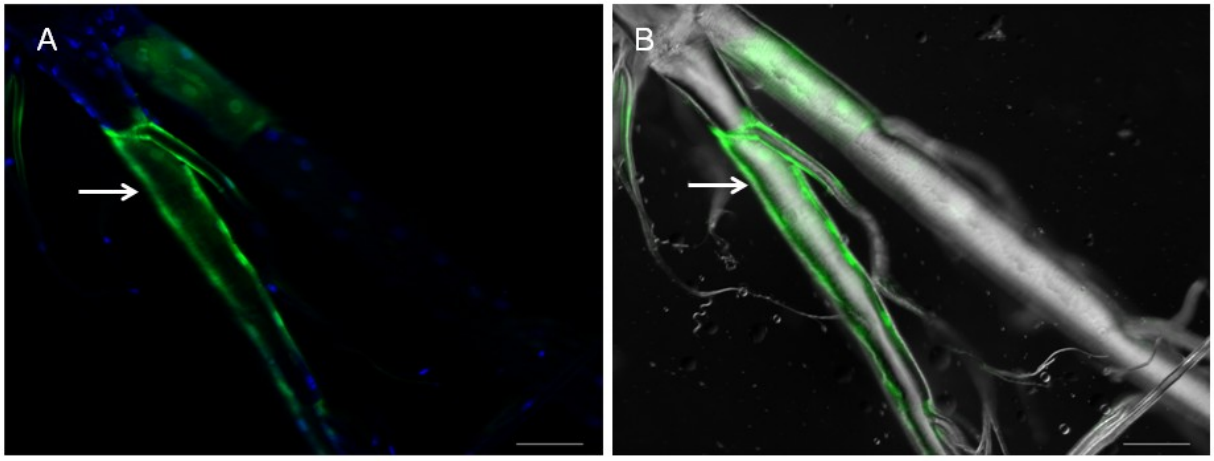

Figure 3-2: Dissection of CS-exposed trachea of third instar larvae. A) The reporter line 10XSTAT92-GFP was utilized to detect activation of JAK-STAT signaling in the epithelial layer of the dorsal branches (white arrows) after CSE. In green: GFP, blue: DAPI and **B**) DIC light.

The epithelial layer of the dorsal primary branches is the first affected area towards cigarette smoke as shown in **Figure 3-2** (white arrows). However the general organization of the air-ways as a single cell-layered epithelium was not affected, because at the parts of JAK-STAT pathway activation, cell nuclei are organized in rows along the airways. All together, these results corroborate that cigarette smoke evokes an immune response of the epithelial cells at this region.

3.2 Activation of the cytokine related ligands upd, upd2 and upd3 after CSE

3.2.1 Phylogenetic tree analysis of upd, upd2 and upd3

The fruit fly's JAK-STAT signaling pathway is simple organized and has three ligands called unpaired, namely upd (also called outstreched), upd2 and upd3. Only a few phylogenetic trees of the three cytokine-like ligands upd, upd2 and upd3 have been published. However, state of art phylogenetic analysis tools have not been used to study their evolution. To comprehend the relationship between upd, upd2 and upd3, phylogenetic trees were reconstructed using the Bayesian method with MrBayes **(Figure 3-3)** and maximum likelihood methods **(Appendix 7.2, Figure 7-2)** (Ronquist et al, 2012). Similarity searches were conducted against different genomes (see materials and method). However, I could not find any homologs in vertebrates and other close invertebrate species like *Anopheles* with the exception of *Drosophila species*. Details of all upd genes are tabulated in **Appendix 7.2 Table 7-1.**

Herein, this study reports an updated list of upd genes of other *Drosophila spec.*, which were not described earlier, especially new genomes of *D. biarmipes*, *D. bipectinata*, *D. elegans*, *D. eugracilis*, *D. ficusphila*, *D. kikkawai*, *D. rhopaloa* and *D. takahashii*.

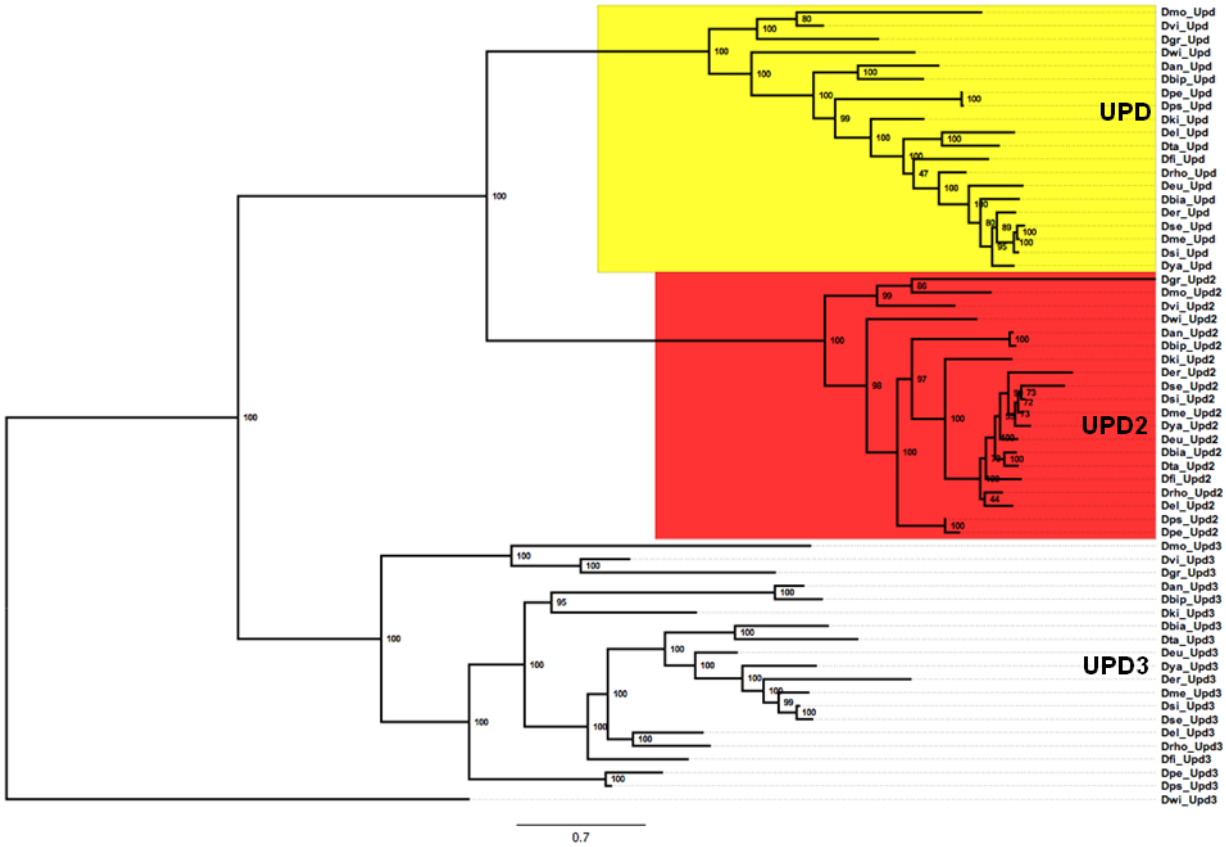

Figure 3-3: Bayesian phylogeny of the three JAK-STAT ligands upd, upd2 and upd3. Upd, upd2 and upd3 are *Drosophila* species-specific genes as depicted by Baysian phylogeny. To date no homologs are found in known insect and vertebrate genomes. Upd3 is originated first and phylogenetic analysis suggests that upd and upd2 were generated by duplication of upd3 and underwent their own evolution within *Drosophila*.

Phylogenetic analyses suggest that upd3 is ancestral and originated first to the other two upds and that upd and upd2 were generated by duplication. Upd3 underwent its segmental duplication limited to 20 genomes of *Drosophila*.

3.2.2 Recognition of a conserved helical cytokine fold of upd3 and IL-6

As suggested by phylogenetic analysis, the occurrence of invertebrate cytokine-like upds does not reflect a common evolutionary origin with other vertebrate cytokines. To date, only little is known about the structural properties of the *Drosophila* upd3. To provide insight into secondary structural elements of upd3, secondary structures were predicted by PSIPRED **(Appendix 7.3, Fig. 7-3)**. Although the upds have no sequence similarity to any other known vertebrate cytokines, the predicted α-helices are consistent with an overall structure that is similar to several cytokines. They are in high agreement with the predicted structural elements for upd3 created by I-TASSER. As illustrated in **Figure 3-4 A**, highly conserved structural parts and alpha helices (H1 - H12) are highlighted in purple. A structural part of the upd3 model, which consists of a high α-helical content (H3-H5) shares structural similarity with IL-6 of mouse **(Figure 3-4 B)**. Thus, the three-dimensional model provide an insight that upd3 is maybe distantly related to IL-6.

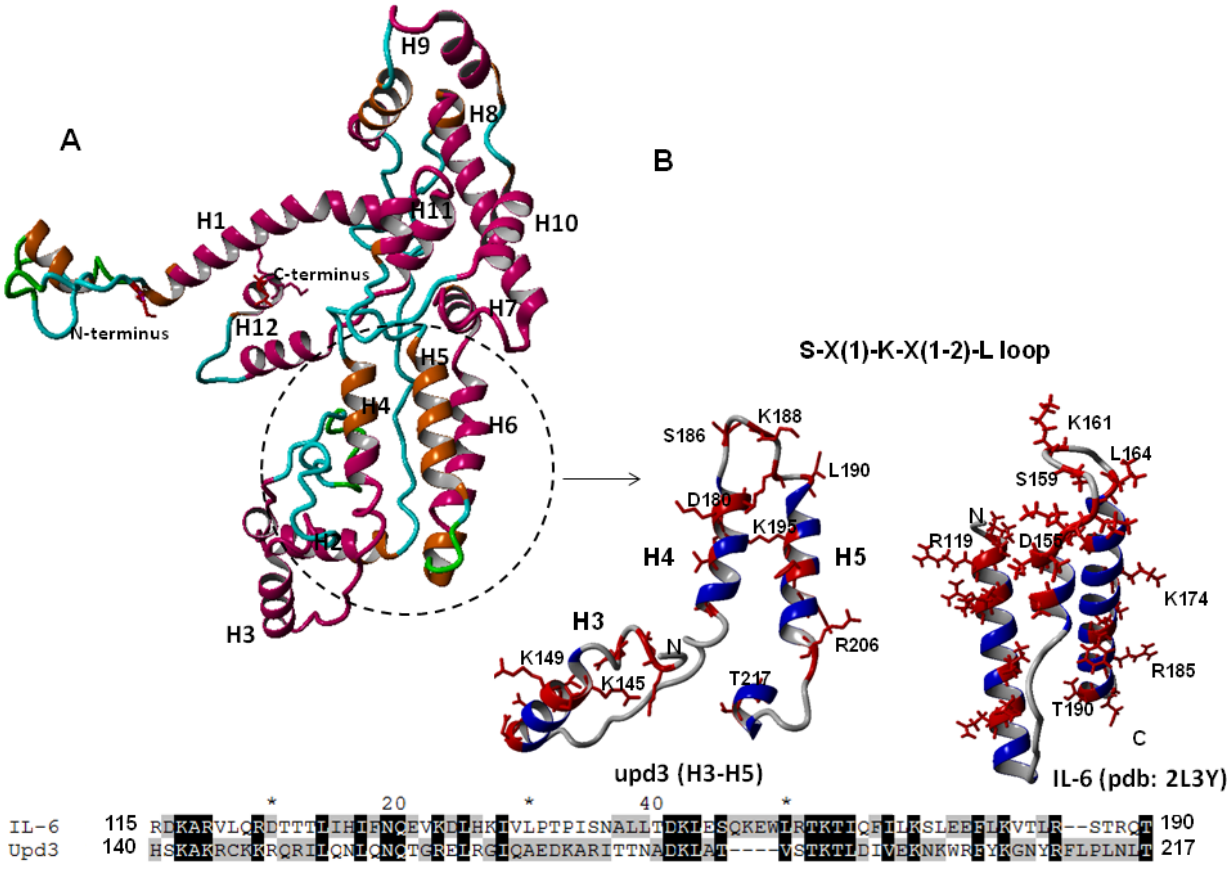

Figure 3-4: Structural model of upd3 from *D. melanogaster*. A) The predicted structural model of upd3 by I-TASSER. Secondary structure predictions by PSIPRED are colored in purple. **B**) Comparison of the crystal structure of IL-6 (PBD: 2L3Y) with upd3 indicates conserved α-helices, which are connected by an "S-X (1)-K-X (1-2)-L" loop. The alignment shows conserved amino acid residues in black. It's worthful to mention that the conserved aa residues are also similarly exposed on the surface. H = α-helices

Interestingly, common amino acids of upd3 and IL-6 are also similarly arranged and exposed on the surface of the protein.

3.2.3 Expression analysis of upd, upd2 and upd3 in the trachea with and without CSE

The *Drosophila* cytokines upd 1-3 have been reported to function as ligands of the JAK-STAT pathway. To determine whether components of the *Drososphila* cytokine cascade are expressed in the trachea, their expression patterns were examined before and after CSE of 3rd instar larvae using corresponding promoter-Gal4 lines. To determine the expression of these three ligands, the driver lines upd-Gal4, upd2-Gal4, upd3-Gal4 were mated with a LacZ reporter line to detect beta-galactosidase production by X-gal staining, without CSE treatment (**Figure 3-5 A- C**) and with CSE (**Figure 3-5 E- G**). Under control conditions upd was not detectable in the fly's airways, upd2 shows almost no expression in the trachea and upd3 is slightly expressed. Interestingly, upd2 and upd3 were strongly expressed in the dorsal trunks of the trachea after CSE. In contrast, no expression for upd was observed in the tracheal system even under CSE. These results suggest that CSE induces activation of upd2 and upd3 whereas upd plays a minor role in the cigarette smoke activated response.

To further evaluate the expression of JAK-STAT signaling, it was of interest to investigate if the transmembrane receptor domeless (dome), which is distantly related to the mammalian gp130 cytokine receptor, is getting expressed in the respiratory system of the fly. The domeless receptor got slightly expressed in the primary branches as well in the secondary branches of the airway epithelium in non-treated animals **(Figure 3-5 D)**. Strikingly, after exposure to cigarette smoke, the expression pattern of domeless-Gal4 correlates with the expression pattern of 10XSTAT92E-DGFP, upd2 and upd3 **(Figure 3-5 H)**. This result supports the hypothesis that the expression of JAK-STAT signaling at the dorsal branches occurs in an autocrine pattern after CSE.

The additional detection of beta-galactosidase by X-Gal staining demonstrated that upd2 and upd3 were differently expressed under hypoxic and CSE conditions (**Figure 3-5 E- H**).

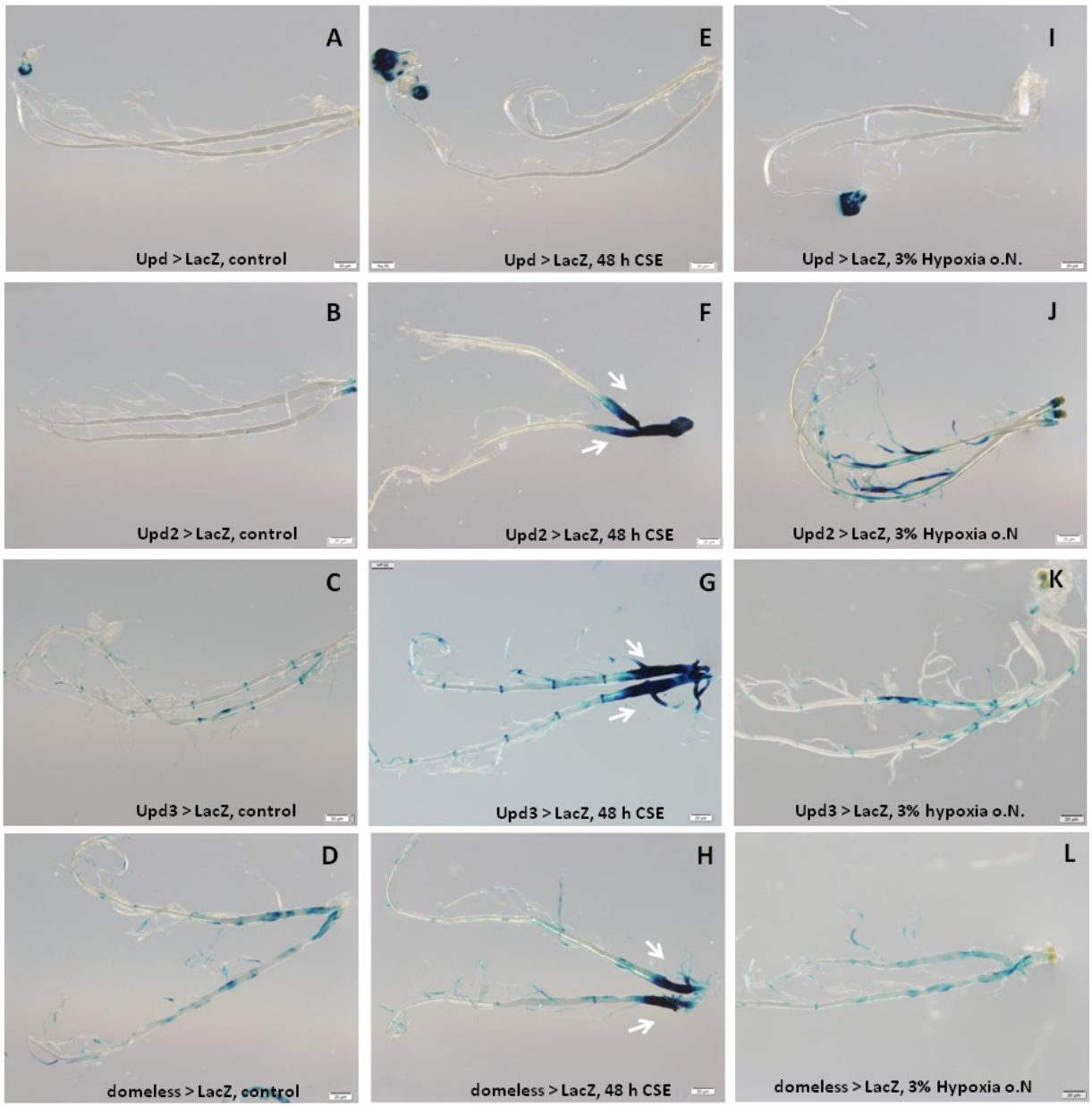

Figure 3-5: Comparison of upd, upd2 and upd3 expression with and without CSE and under hypoxia by X-Gal staining. β-galactosidase staining patterns of upd-Gal4, upd2-Gal4, upd3-Gal4 and domeless-Gal4 of larval tracheas, without (**A, B, C, D**) and with CSE treatment (**E, F, G, H**). For upd2, upd3 and domeless a strong lacZ expression was visible in CSE trachea in comparison to their controls. For upd no expression occurred under both conditions. Under hypoxic conditions no expression of upd (**I**), a strong expression of upd2 (**J**) and a slight expression of upd3 was observed in comparison their controls. The expression for domeless remain unchanged under anoxic conditions (**L**).

Under hypoxic conditions a strong expression of upd2 occured in the secondary and terminal branches (**Figure 3-5 F**). Quantitative RT PCR analysis confirmed a significant up-regulation of upd2 after hypoxia (**Appendix 7.4, Figure 7-4**).

3.2.4 Effects of CSE on upd, upd2 and upd3 gene expression in the *Drosophila* airway epithelium

To verify the results obtained from the expression pattern analysis using β-Gal staining (**Section 3.2.3**), the tracheal RNAs of control and CSE- exposed wild type animals were extracted and qRT-PCR analysis was performed, focusing on the three upd-like ligands, upd, upd2 and upd3. Their relative transcript levels of the airways were quantified using at least three independent biological samples of either control or CSE- exposed animals. To obtain a dose-dependent response, samples of trachea were taken after 24 hour and 48 h CSE treatment. As predicted from the β-Gal staining with upd-, upd2- and upd3-GAL4 (**Section, 3.2.3, Figure 3-5**), the differential transcription pattern could be verified for all three ligands by qRT-PCR. Upd2 and upd3 show a significant high transcription after CSE, whereas no increased transcription was detected for upd **(Figure 3-6)**. The response to cigarette smoke is higher when the dosage increases.

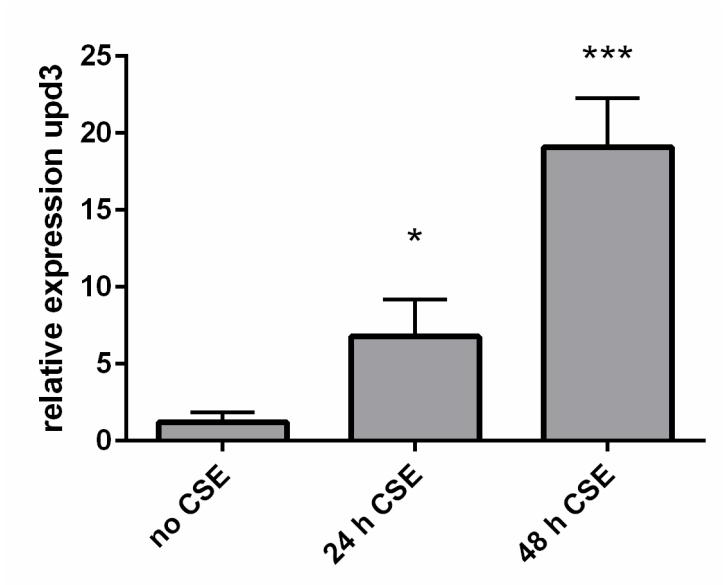

Figure 3-6: Relative expression level of upd3 in response to CSE. Transcript levels of upd3 of 3rd instar larvae (w1118) are shown after 24 h and 48 h CSE. Upd3 transcripts were significantly increased in the trachea of CSE animals compared to non-exposed animals. Values are means of at least 3 independent experiments ± SEM. Y-axis is expressed as the fold change and significances are calculated using the unpaired two-tailed student's t-test with *$p < 0.05$, **$p = 0.01$ to 0.001, ***$p < 0.001$, ns $p > 0.05$.

Similar expression was observed for upd2 after exposure to cigarette smoke. Expression levels significantly increased in comparison to non- smoke exposed animals in the respiratory system (**Figure 3-7**).

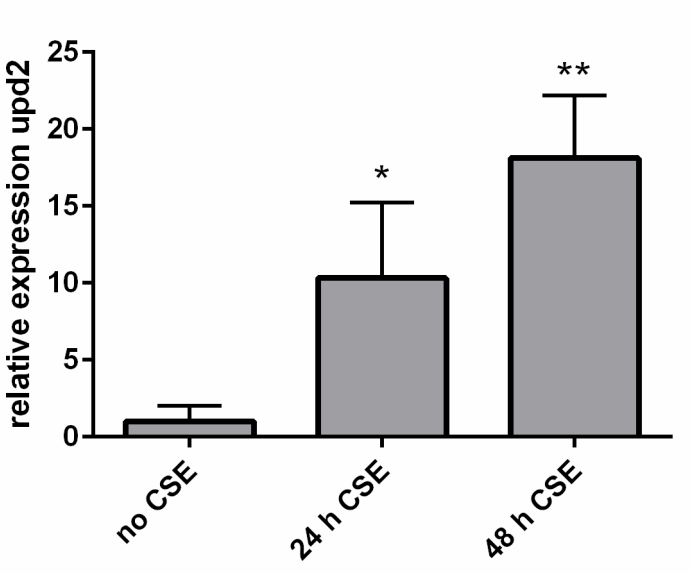

Figure 3-7: mRNA levels of upd2 in response to CSE. Transcript levels of upd2 of cigarette smoke exposed 3rd instar larva (w1118) are shown after 24 h and 48 h CSE. Upd2 transcripts were significantly increased in the trachea of CSE animals compared to non-exposed animals. Values are means of at least 3 independent experiments ± SEM. Y-axis is expressed as the fold change and significances are calculated using the unpaired two-tailed student's t-test with *p < 0.05, **p = 0.01 to 0.001, ***p < 0.001, ns p > 0.05.

There was no significant up-regulation of upd in the respiratory system of the fly in response to cigarette smoke (**Figure 3-8**).

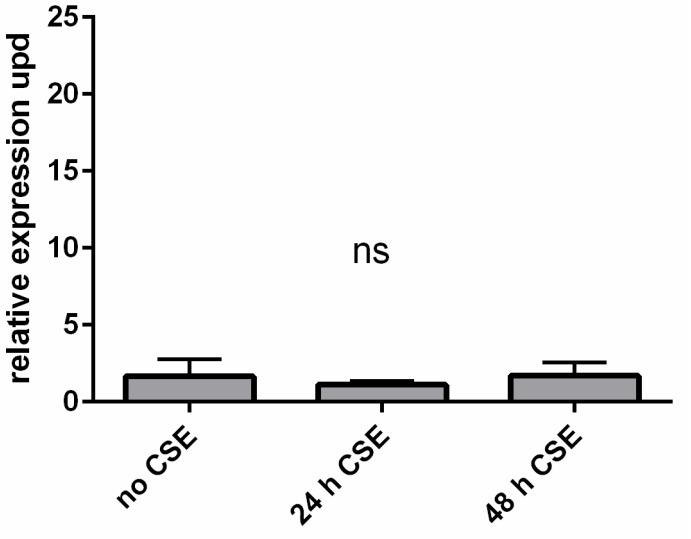

Figure 3-8: Relative expression level of upd in response to CSE. Transcript levels of upd of cigarette smoke exposed 3rd instar larva (w1118) remain unchanged after 24 h and 48 h CSE in comparison to non-exposed animals. Values are means of at least 3 independent experiments ± SEM. Y-axis is expressed as the fold change and significances are calculated using the unpaired two-tailed student's t-test with *p < 0.05, **p = 0.01 to 0.001, ***p < 0.001, ns not significant p > 0.05.

3.3 Activation of proinflammatory transcription factors after CSE

3.3.1 Relish (IMD) activation after exposure to cigarette smoke

To identify potential transcription factors, which are involved in the oxidative stress response after CSE, transgenic animals were used in which XFP tagged relish (UAS-*relish-yfp*) and dFoxO (UAS-*foxo-gfp*) are ectopically expressed in the airways. The ppk4-Gal4 driver was used to drive expression in the trachea. The nuclear factor of kappaB (NF-κB) is one of the most important transcription factor involved in airway inflammation. Thus, the expression of the fly's homolog relish was examined after CSE. Under normal conditions, relish is localized in the cytoplasm of the airway epithelial cells. In contrast, a translocation of GFP-tagged relish was detected in the nucleus after CSE (**Figure 3-7**).

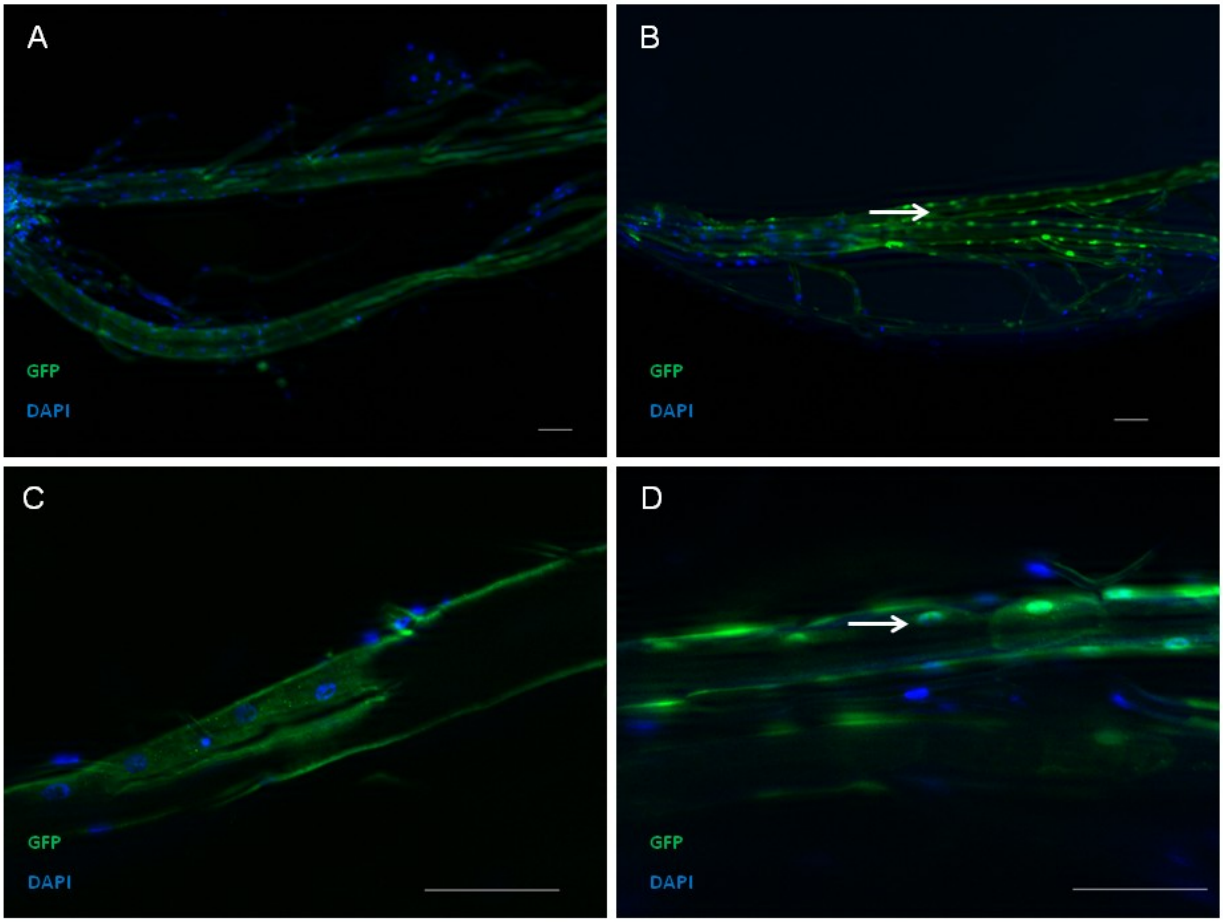

Figure 3-9: Translocation of the transcription factor relish after CSE. GFP-tagged relish shows a translocation into the nucleus (white arrows) after confrontation with cigarette smoke (**B and D**). In control animals, relish is present in the cytoplasm (**A and C**). Panels in blue indicate DAPI staining of the nuclei. Crosses were performed using UAS-*relish-yfp*::PPK4. Shown are merged images of GFP and DAPI. Scale bar is 100 µm.

3.3.2 Nuclear translocation of CncC and expression of GstD after CSE

In order to find out whether the fruit fly's Nrf2-homolog cap'n'collar is getting activated after CSE, a GAL4 (under the control of promoter elements of the cnc gene) was crossed with a UAS-GFP line, to visualize its expression pattern. A translocation of cncC into the nucleus was observed after CSE, as illustrated by nuclear GFP expression (**Figure 3-8 A-B**).

Further, a downstream gene of Nrf2, the glutathione S-transferase (GST) was investigated. GSTs are induced by Nrf2 activation and represent an important route of detoxification. The reporter line GSTD-Gal4;UAS-GFP (Zeng, 2010) was used to monitor its induction. It was observed that the GST-D expression was slightly increased in the trachea after CSE (48 h) as shown by higher GFP-expression (**Figure 3-8 C-D**). The expression of GFP was restricted to the dorsal trunks and primary branches. In control animals it was confined to the so-called fusion cells.

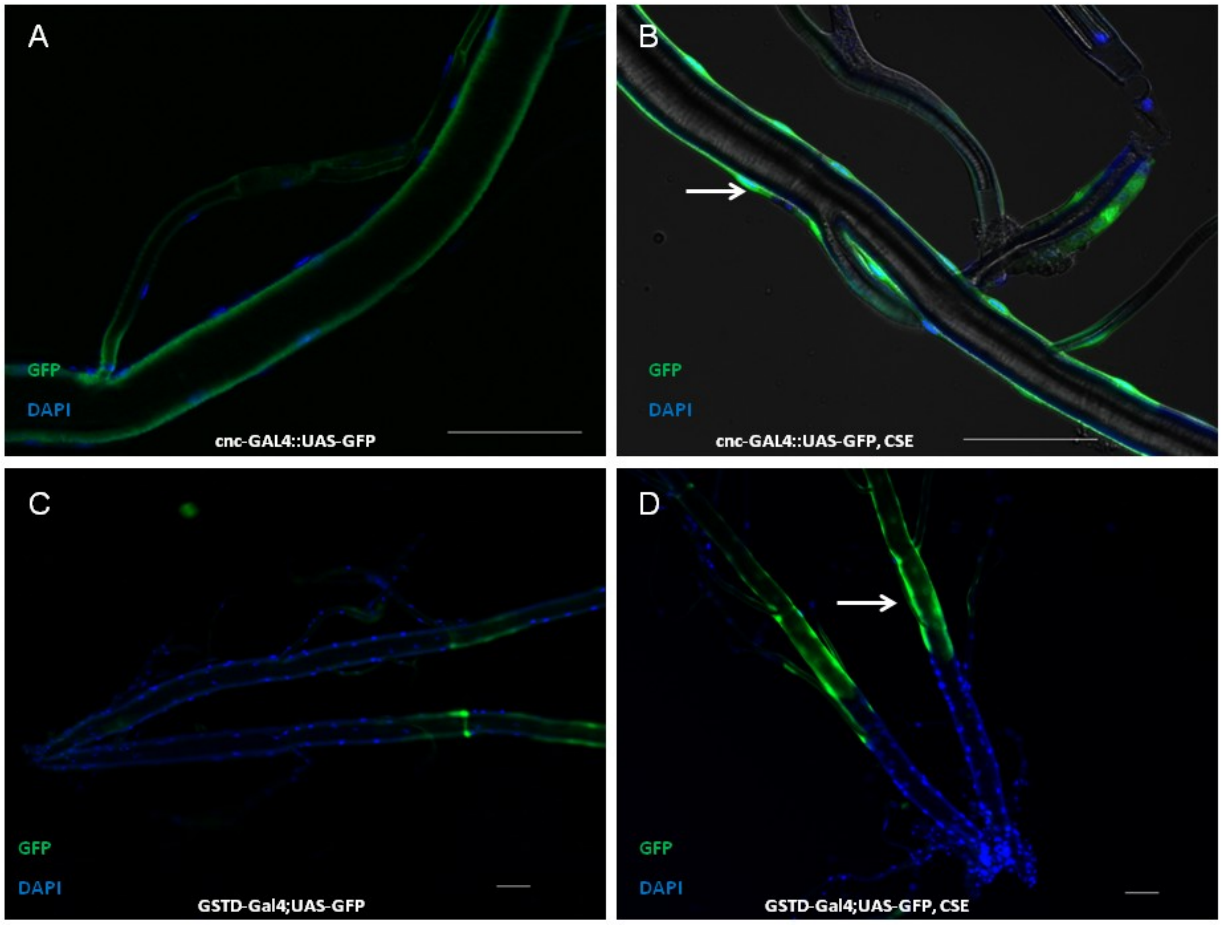

Figure 3-10: Activation of Nrf2-signaling after cigarette smoke exposure. The cap'n'collar transcription factor Nrf2 translocated into the nucleus after CSE (**B**) in comparison to control animals (**A**). Crosses were performed using cnc-Gal4::UAS-GFP. Expression of GST-D was monitored using the GFP-reporter line GSTD-Gal4;UAS-GFP without (**C**) and with CSE (**D**). Panels in blue indicate DAPI staining of nuclei. Shown are merged images of GFP and DAPI. Scale bar is 100 µm.

3.3.2 Nuclear translocation of dFoxO in response to CSE

The cellular location of dFoxO was monitored, using transgenic flies for expression of dFoxO-GFP. For tracheal localization, the tracheal specific PPK4-GAL4 line was applied. A nuclear translocation of dFoxO was observed after exposure to cigarette smoke in comparison to control animals (**Figure 3-11)**.

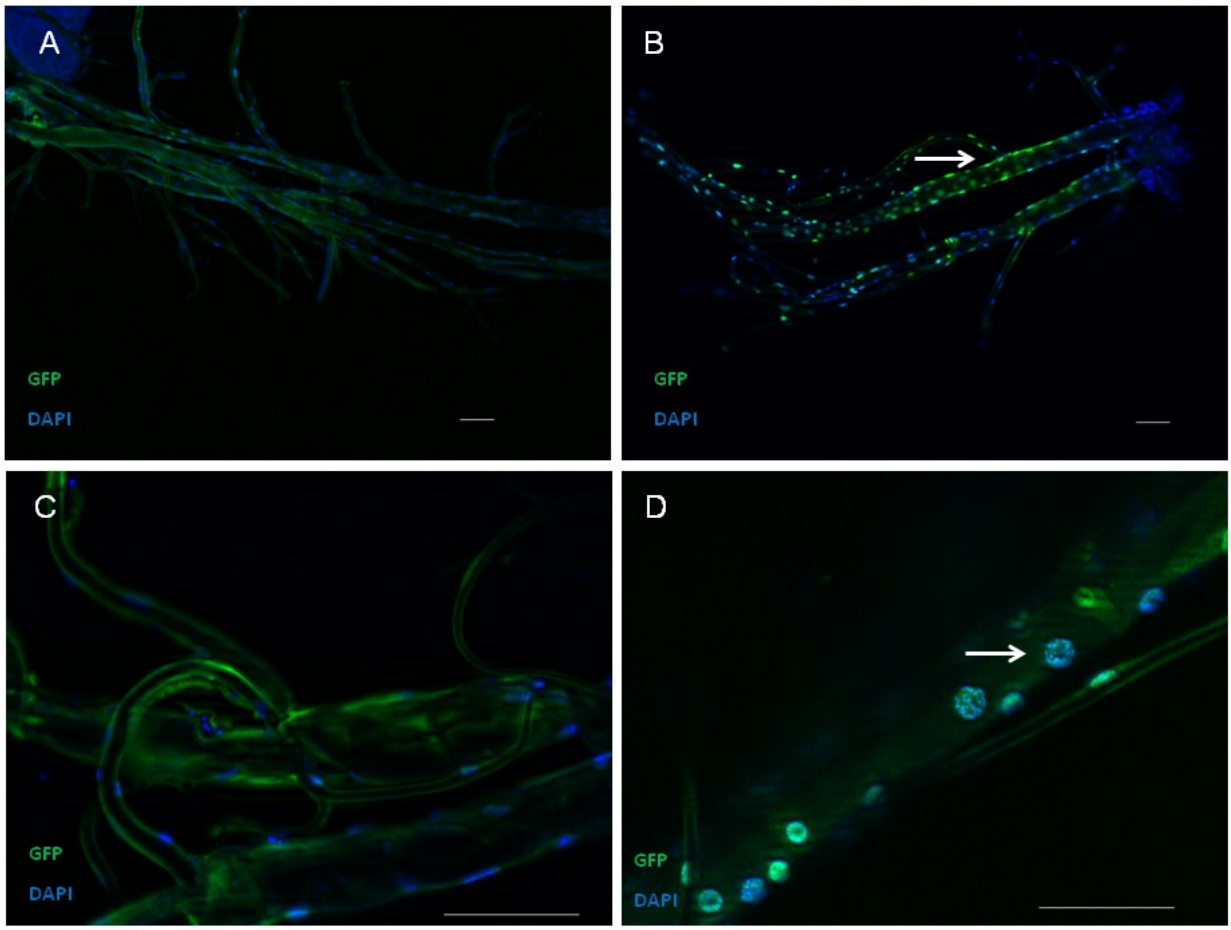

Figure 3-11: Nuclear translocation of dFoxO after exposure to cigarette smoke. The figure shows isolated trachea of control animals, expressing dFoxO-GFP in the cytosol of the airway system driven with PPK4-Gal4 (**A and C**), whereas trachea of CSE animals show a translocation of the transcription factor into the nucleus as indicated by white arrows (**B and D**). Panels in blue indicate DAPI staining of nuclei. Shown are merged images of GFP and DAPI. Scale bar is 100 µm.

3.4 dFoxO dependent regulation of cytokines upd2 and upd3

3.4.1 Effect of dFoxO and relish knockouts on transcription levels of upd2 and upd3

To unravel the molecular mechanism underlying the immune response to cigarette smoke, mutant flies, defective in either relish or devoid of functional dFoxO were used, to evaluate the regulation of the cytokine-like upd, upd2 and upd3 following cigarette smoke.

A reduced expression of upd3 was observed in relish-deficient mutant flies after CSE. No significant up-regulation of upd3 was found in dFoxO deficient animals in response to cigarette smoke treatment, indicating that dFoxO might be an essential regulatory gene (**Figure 3-12**).

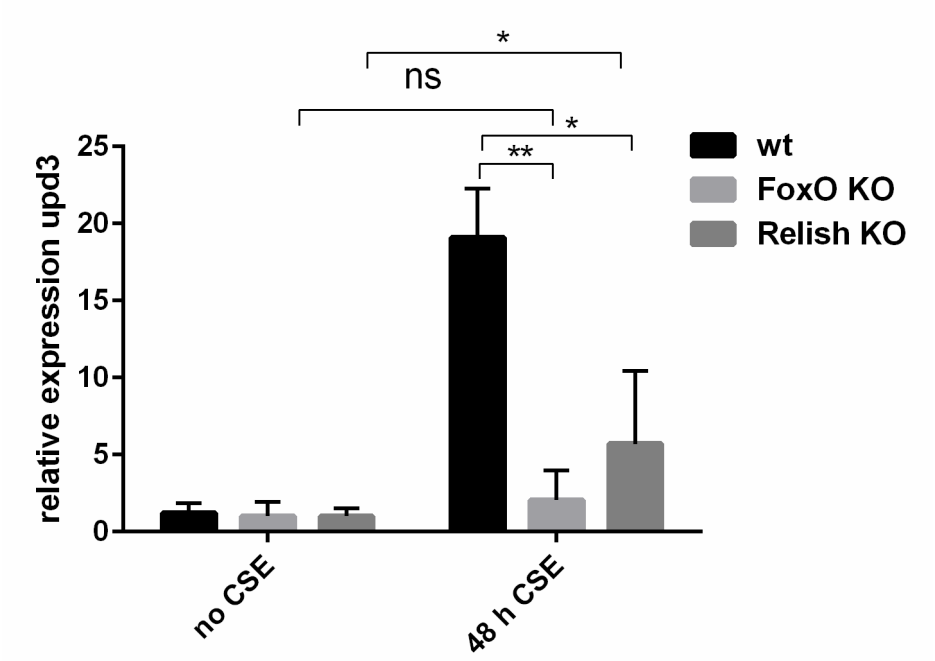

Figure 3-12: Relative expression of upd3 in the trachea in dFoxO and relish deficient animals after 48 h exposure to cigarette smoke. Upd3 transcript levels were significantly decreased in dFoxO and relish-deficient animals after exposure to cigarette smoke in comparison to CS-exposed wild type animals. Values are means of at least 3 independent experiments ± SEM. Y-axis is expressed as the fold change and significances are calculated using one-way ANOVA and the unpaired two-tailed student's t-test with *p < 0.05, **p = 0.01 to 0.001, ***p < 0.001, ns not significant p > 0.05.

Animals deficient in dFoxO or relish have shown decreased expression levels for upd2 after CSE (**Figure 3-13**).

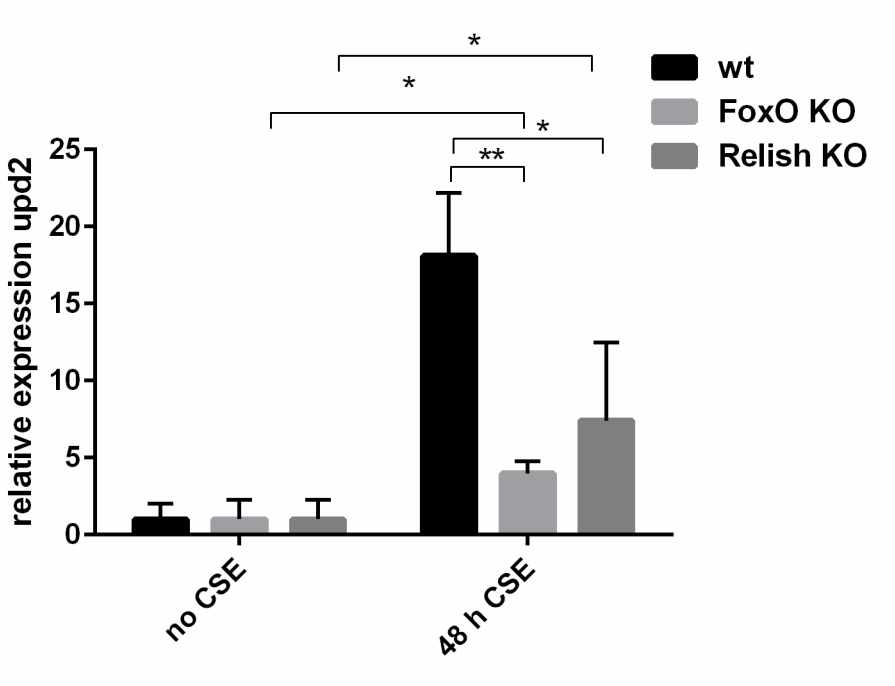

Figure 3-13: Relative expression of upd2 in the trachea in dFoxO and relish deficient animals after 48 h exposure to cigarette smoke. Upd2 transcript levels were significantly decreased in dFoxO and relish-deficient animals after exposure to cigarette smoke in comparison to CS-exposed wild type animals. Values are means of at least 3 independent experiments ± SEM. Y-axis is expressed as the fold change and significances are calculated using one-way ANOVA and the unpaired two-tailed student's t-test with *p < 0.05, **p = 0.01 to 0.001, ***p < 0.001, ns not significant p > 0.05.

Expression levels for upd remained unchanged in both mutant flies, before and after CSE (**Figure 3-14**).

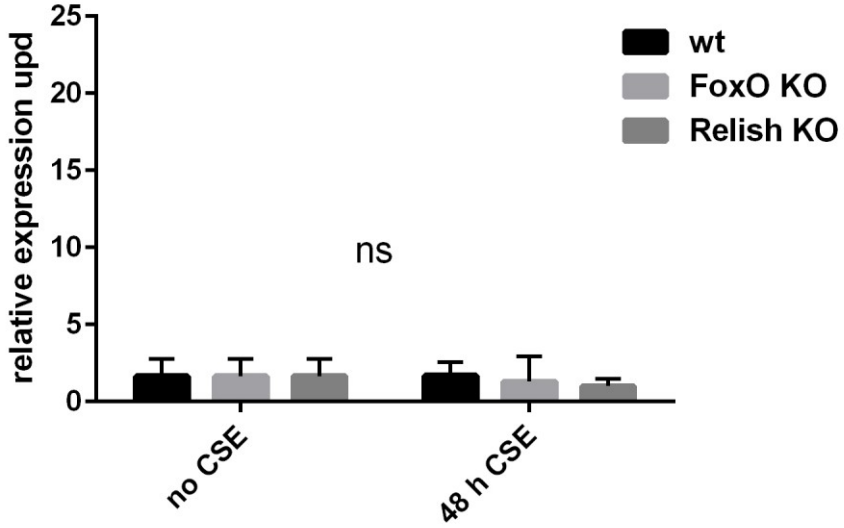

Figure 3-14: Relative expression of upd in the trachea in dFoxO and relish deficient animals after 48 h exposure to cigarette smoke. Transcript levels of upd under normal and CS-challenged conditions remained unchanged in all 3 genotypes (wild type, dFoxO and relish-deficient animals). Values are means of at least 3 independent experiments ± SEM. Y-axis is expressed as the fold change and significances are calculated using one-way ANOVA and the unpaired two-tailed student's t-test with ns not significant p > 0.05.

3.4.2 Characterization of the promoter regions of upd, upd2 and upd3 - screening for potential dFoxO binding motifs

As there were no up-regulation for upd3 and decreased transcript levels for upd2 in dFoxO deficient flies, it was interesting to examine, if there is a possible regulation of upd2 and upd3 by the transcription regulator dFoxO. Upon closer look on the promoter regions of upd2 and upd3 and after checking for possible dFoxO binding motifs (binding motif: TRTTTAY (R = A or G; Y = any with C preferred) several dFoxO DBD motifs were present in the regulatory regions of upd2 and upd3 in the forward and reverse strands (**Figure 3-15**). A highly conserved binding motif for the transcription factor was detected nearby the predicted promoter sides for upd2 and upd3 (shown in a dotted frame). No such motif was found for upd. This finding correlates with the qRT PCR data (**Section 3.2.4, Fig. 3-14**), where no expression of upd was observed. These results may indicate a strong regulatory role of dFoxO for upd2 and upd3 but not for upd.

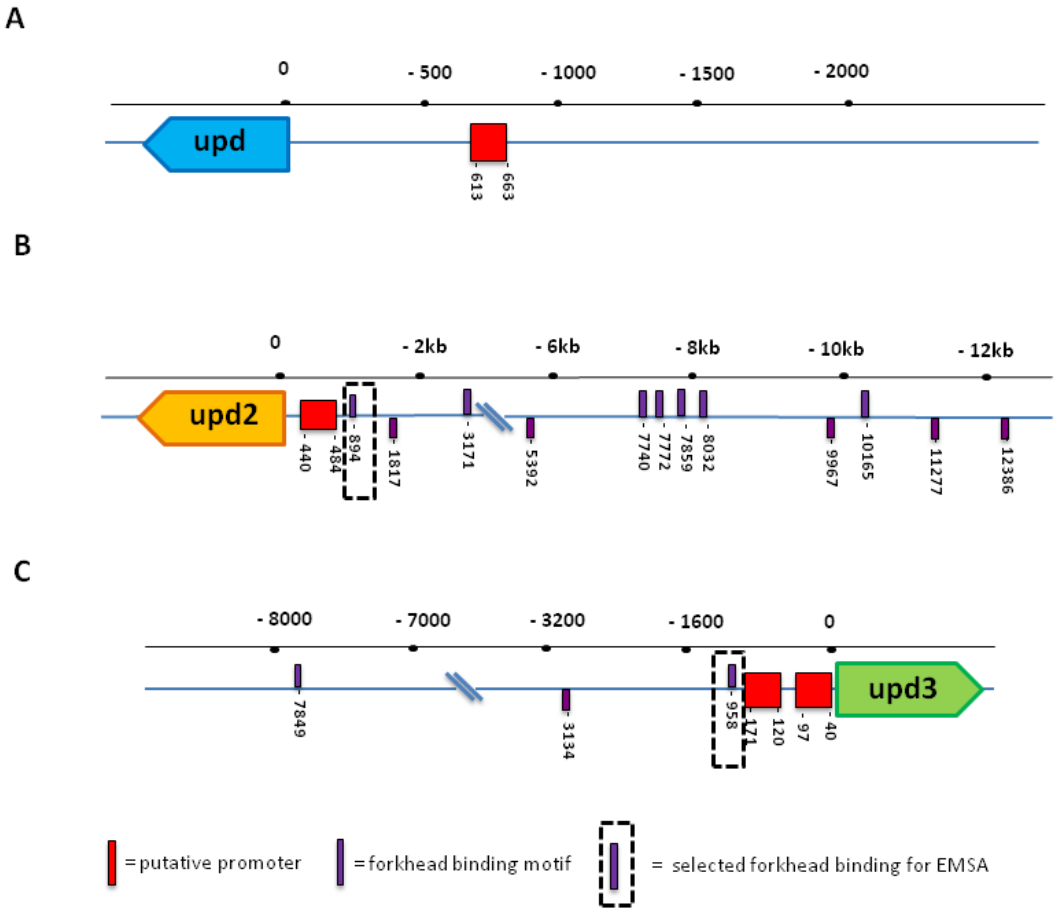

Figure 3-15: *In silico* analysis of the promoter regions of upd, upd2 and upd3. The inspected promoter regions of upd2 (**B**) and upd3 (**C**), but not that of upd (**A**) contain several putative binding sites for dFoxO at different locations. One of these putative binding sequences (dotted frame) of the promoter upd2 and upd3 was chosen to test binding ability of dFoxO FH by EMSAs.

3.4.3 Expression and purification of dFoxO FH DBD

As a next step, the forkhead DNA-binding domain of dFoxO (referred as the term dFoxO FH DBD) was cloned into a pET28a (+) expression vector carrying a N-terminal HIS-tag for further affinity purification. So far, the FoxO forkhead domain of *D. melanogaster*, encodes a protein that is highly conserved and retains important functional domains found in other FoxO homologs of human. The alignment shows dFoxO of *D. melanogaster* with human FoxOs 1, 3, 4 and 6. The highly conserved dFoxO forkhead domain (in black shades) was used for cloning. The N-terminal start and C-terminal end of the DNA-binding domain is colored in green (**Figure 3-16**).

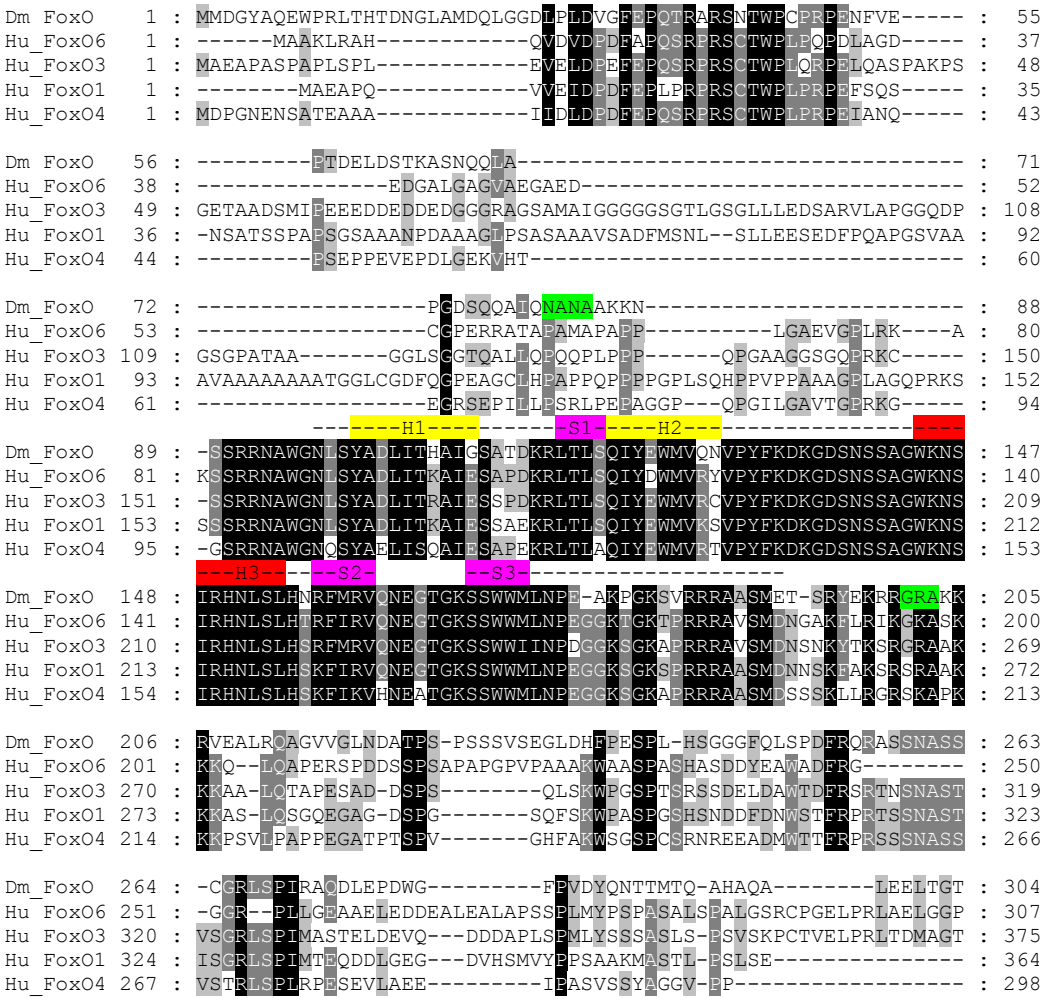

Figure 3-16: Alignment of the dFoxO amino acid sequence with that of human homologues (FOXO1a, FOXO3a, FOXO4 and FOXO6). The alignment shows the conserved FH DNA binding domain and its secondary structural elements. The major DNA binding helix is colored in red according the proposed structure. Black shades indicate amino acids that are identical in all sequences and grey shades highlight conserved substitutions. The start and ending amino acid residues of the dFoxO DBD, for cloning purposes, are highlighted in green. In yellow: Helices 1 and 2 of the dFoxO DBD and in purple: β-sheets 1-3.

So far the FoxO forkhead domain of *D. melanogaster* is structurally not yet described. Structurally it resembles to those of other species as visualized by a structural model created with I-TASSER (**Figure 3-17 A**). Especially the highly conserved helix 3 domain (in red color) was shown to be of high importance for DNA-binding in species like human and other vertebrates (Tsai et al, 2007).

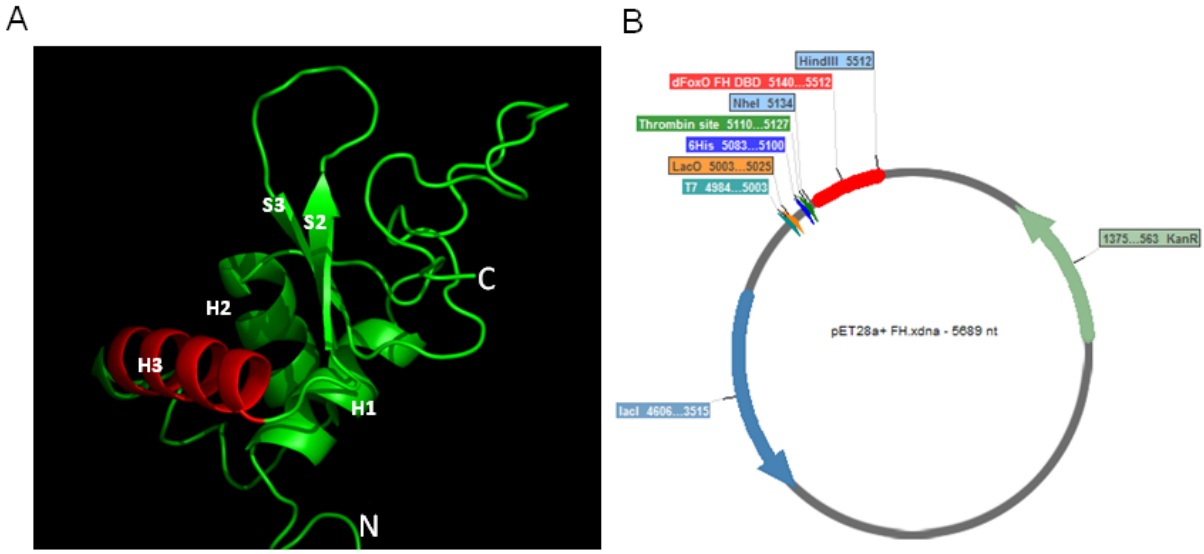

Figure 3-17: Structural model of the dFoxO DBD (A) and the vector map of pET28a (+) dFoxO DBD (B). **A**) The structural model of dFoxO was generated using I-TASSER and visualized by Pymol (http://pymol.org). The highly conserved helix 3 domain (H3), mainly important for binding to DNA, is highlighted in red. **B**) The dFoxO DNA binding domain was inserted in a pET28a (+) expression vector for further over expression and purification.

The plasmid pEX-A2 dFoxO DBD containing the synthetic gene coding for the dFoxO DBD was transformed into *E.coli* DH5α as described in **Section 2.2.5.4**. Transformation into DH5α was verified by performing agarose gel electrophoresis. The purified plasmid DNA of pEX-A2 dFoxO DBD (2450 bp) was restricted with NheI and HindIII and yielded into two fragments: a part of the unrestricted plasmid DNA pEX-A2 dFoxO DBD and the dFoxO DBD fragment of 384 bp (**Appendix 7.5, Fig. 7-5 A**). The target gene was purified from the agarose gel as described in **Section 2.2.4.2** and shown in **Appendix 7.5, Fig. 7-5 B**. Ligation of the gene into a pET28a (+) expression vector was performed as described in **Section 2.2.4.6**. The *dFoxO DBD* gene was inserted directly downstream of the translation signals into the NheI and HindIII restriction site of the pET28a (+) (**Figure 3-17 B, Appendix 7.5, Fig. 7-6)**. In order to check whether the ligation was successful, the plasmid was digested as described in **Section 2.2.4.4**, analyzed by agarose gel electrophoresis and verified via sequencing by GATC biotech (**Appendix 7.5, Figure 7-8**).

Recombinant pET28a (+) dFoxO FH DBD was transformed into BL21 (DE3) and over expressed in *E. coli* BL21. The vector pET28a (+) is under control of the lac operon. Thus, protein synthesis was induced with 0.1 mM IPTG at an OD_{600} between 0.5 - 0.7. Non-IPTG induced (t0) cells were used as a negative control.

Various expression trials were carried out initially, to promote solubility of pET28a (+) dFoxO FH DBD. Samples were taken after every hour to control the quantity of dFoxO FH DBD (**Figure 3-18, A**).

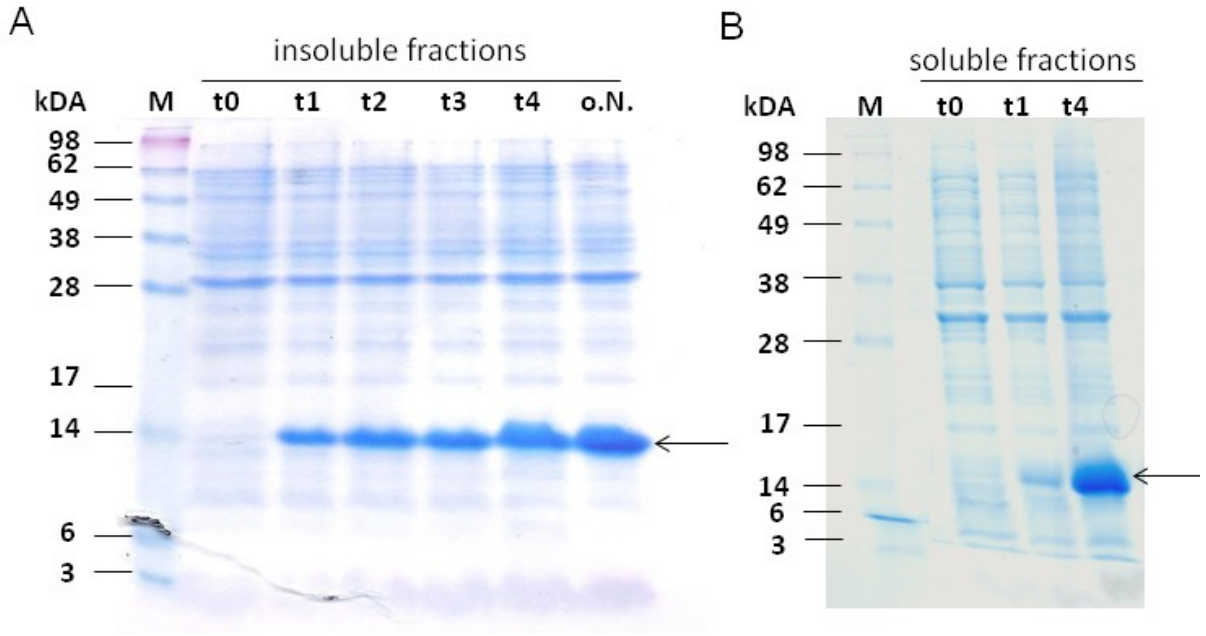

Figure 3-18: SDS-PAGE analysis of pET28a (+) dFoxO FH DBD - expression in *E. coli* BL21 (DE3) cells. **A**) Insoluble fractions of over expressed pET28a (+) FH DBD were checked on a SDS-gel after every hour. Lane 1 (M): molecular weight marker (kDa), t0: cell lysate of uninduced BL21 (DE3) cells possessing pET28a(+) dFoxO FH DBD, 1-4 h: cell lysate from induced BL21(DE3) cells containing pET28a (+) dFoxO FH DBD. **B**) Samples of soluble fractions were analyzed of t0, t1 and t4. Samples were taken after every hour and induction was carried out with 0.1 mM IPTG, in LB medium at 28°C. Black arrow: dFoxO DBD target protein. The gel was stained with coomassie.

Induction at 28°C with 0.1 mM IPTG for 4 hours turned out to be the best expression condition, which produced soluble protein of dFoxO DBD (theoretical Mw: 16 kDa) (**Figure 3-18 B**). The dFoxO FH DBD was purified using a NHS-packed chromatography column.

The flow through and the eluted fractions from the column were collected and analyzed by coomassie staining in a SDS-PAGE (**Figure 3-19 A-B**) and as described in **Section 2.2.5.4.** dFoxO FH DBD was obtained in the flow-through (**Figure 3-19 B**).

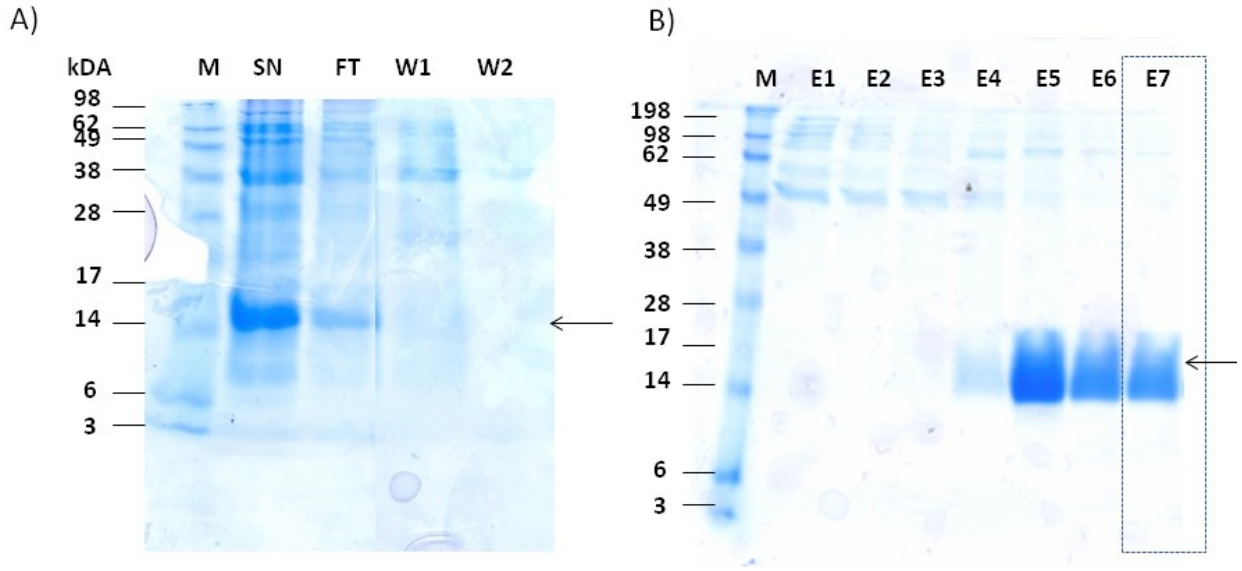

Figure 3-19: Purification of soluble dFoxO FH DBD by NHS-chromatography. A) M: molecular weight marker (kDA), SN: culture supernatant prior loading onto the NHS-column, FT: flow through, W1 and W2: fractions of wash steps. **B**) M: molecular weight marker (kDA), E1-E7: Fractions of eluted dFoxO DBD protein. Black arrow: dFoxO DBD target protein.

Fractions of purified uncontaminated dFoxO protein **(Figure 3-19 B, E7)** were used for further experiments.

3.4.4 Electrophoretic mobility shift assays of dFoxO and upd promoters

An *in silico* screening for potential dFoxO binding motifs within the promoter sequence of upd2 revealed several putative binding motifs (**Section 3.4.2, Figure 3-15**). One of these binding sequences was chosen to test the physical binding ability of dFoxO DBD. For this purpose, the conserved binding sequence nearby the predicted promoter of upd2 and upd3 was taken. The oligo contained the predicted 7 bp long binding motif plus additionally 7 bp 5' and 7 bp 3' end of the intergenic region. To determine whether the dFoxO DBD is capable of binding the - 894 bp region for upd2 and -958 bp for upd3, electrophoretic mobility shift assays were performed, using over expressed and HIS-tagged purified dFoxO DBD protein (**Section 3.4.3**). As shown in **Figure 3-20 A - B**, the cy5-labeled double-stranded probes, when incubated with dFoxO DBD, form visible DNA-protein complexes (shifts).

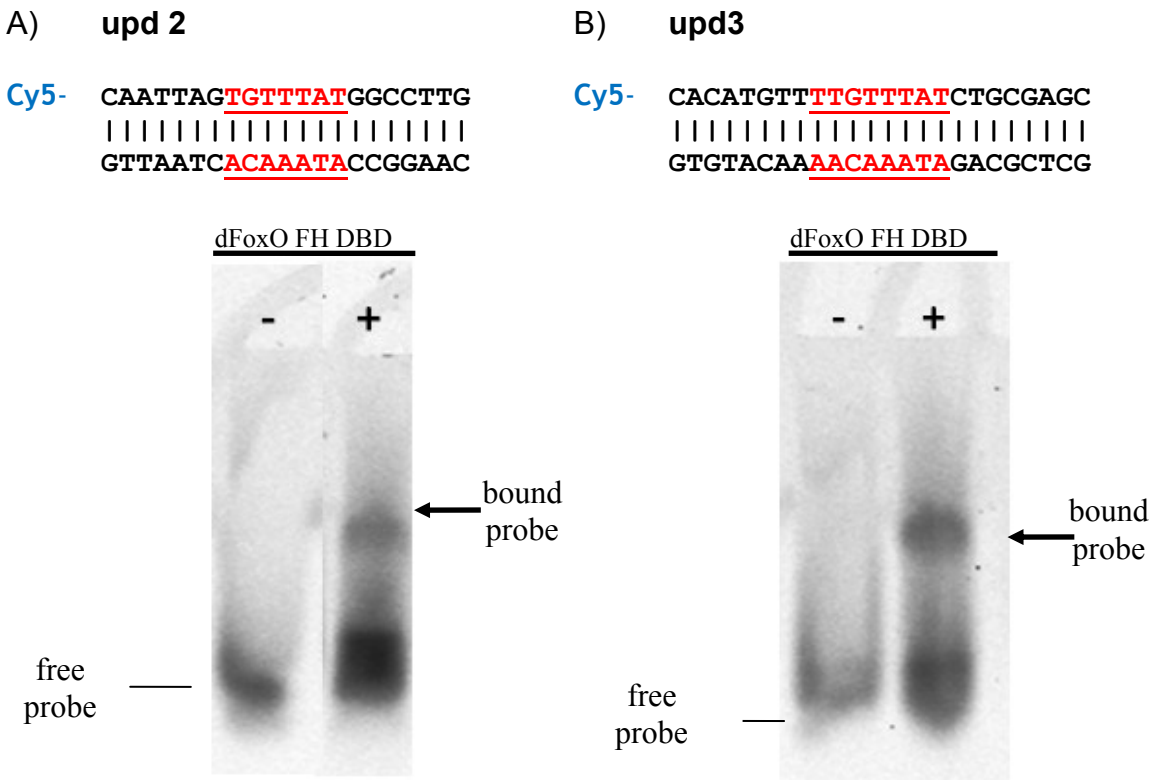

Figure 3-20: EMSAs of dFoxO DBD and the promoter regions of upd2 and upd3. EMSA was applied to detect the *in vitro* binding of the dFoxO DNA-binding domain to dFoxO motifs present in the promoter regions of upd2 (**A**) and upd3 (**B**). The shifted DNA is marked by an arrow. Protein and DNA concentrations were about 250 ng and 10 pmol, respectively. "+" with and "-" without dFoxO protein

3.5 The roles of JAK-STAT signaling in the respiratory tract of *Drosophila*

3.5.1 Consequences of ectopic expression of upd3 in the airways

To investigate the role of upd3 in the trachea of *Drosophila*, the structural and functional consequences of its ectopic expression were examined, using the tracheal driver PPK4-Gal4. It was of interest, if ectopic expression of upd3 can lead into altering of the airway epithelium. Interestingly, a remarkable thickening of the epithelial layer was observed **(Fig. 3-21 A)**. This result indicates that upd3 might play a role in thickening of the airways and may also be responsible for triggering epithelial remodeling after exposure to cigarette smoke. In some animals a narrowing of the dorsal trunks was observed **(Fig. 3-21 B)**. In these regions, the thickness of the epithelial airway layer was significantly increased.

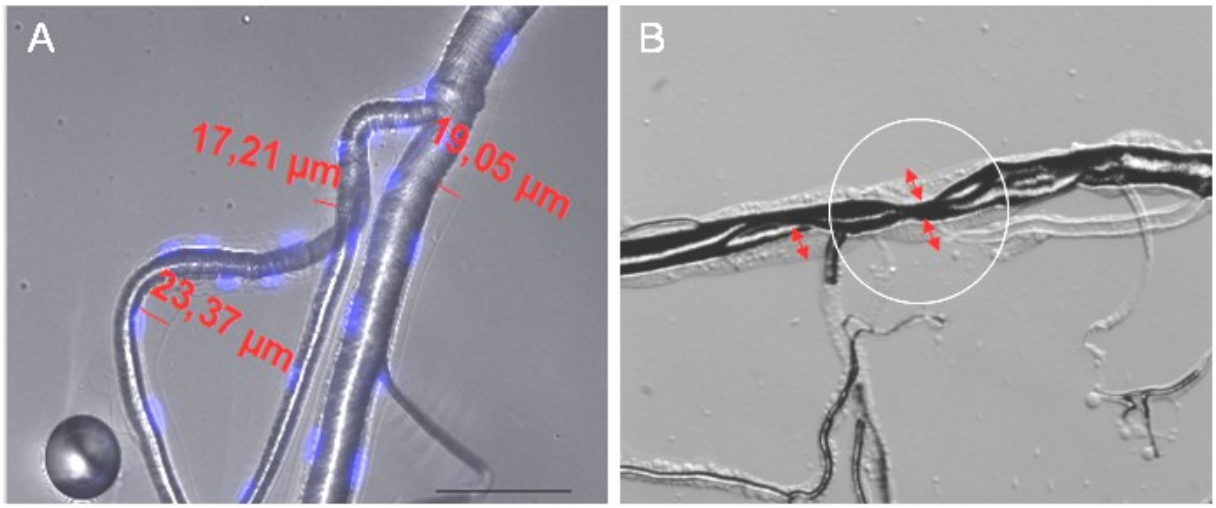

Figure 3-21: Ectopic expression of upd3 causes remodeling of the airway epithelium. A) The crossing of upd3-UAS with the trachea-specific PPK4-GAL4, induced structural remodeling in the airway epithelium. A strong thickened epithelial layer was repeatedly observed. Staining of nuclei (DAPI in blue) of those regions reveals that they are organized as a monolayer. **B**) In some animals obstructed regions caused by this thickness were visible (white circle). The scale bar is 100 µm.

Quantification of the epithelial thickness and contraction of the primary branches, in comparison to control animals, revealed a significant difference between both experimental groups **(Figure 3-22).**

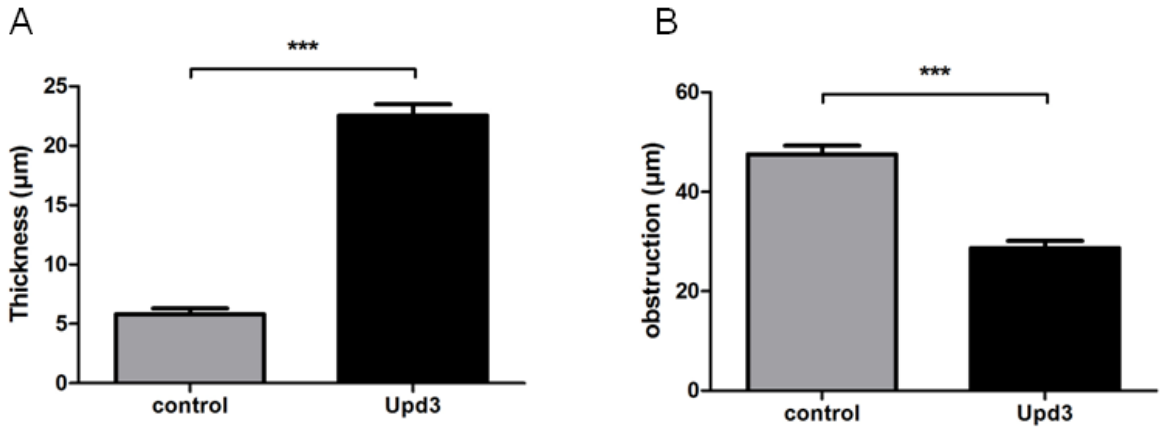

Figure 3-22: Quantification of the thickness and obstruction of the branches after ectopic expression of upd3. A) Ectopic expression of upd3 in respiratory system led into structural airway remodeling, in form of a thickened epithelial layer. Control animals are characterized by a significant thinner epithelial layer (n = 15). **B**) The primary branches are contracted in animals ectopically expressing upd3 (n = 10). Performed crossing: upd3-UAS::PPK4-Gal4. Student's t test: *: $P < 0.05$, **: $P < 0.01$, ***: $P < 0.001$, values are means ± SD.

Furthermore, it was interesting to examine, if ectopic expression of other components of the JAK-STAT signaling pathway also leads into thickening of the epithelial layer. For this purpose upd and $hop^{Tum\text{-}l}$, a dominant gain of function mutation of hopscotch (Yan et al., 1996a), were also ectopically expressed in the fly's airways. An epithelial thickness and obstruction was observed in the same pattern (**Figure 3-23**).

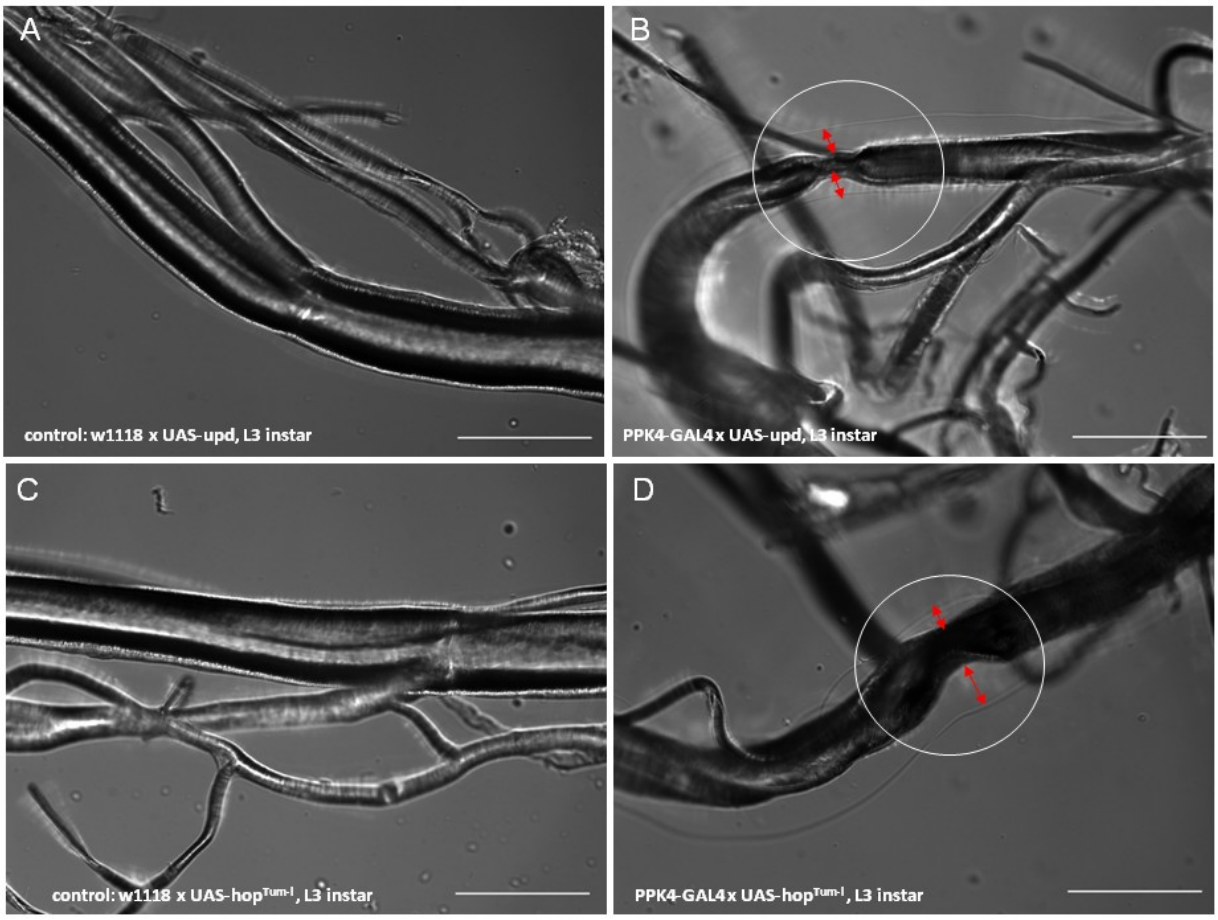

Figure 3-23: Ectopic expression of upd and hop^{Tum-l} cause thickening of the epithelial layer. The crosses of upd-UAS and hop^{Tum-l} with the trachea-specific PPK4-GAL4 induced a structural remodeling in the airway epithelium. A strong thickened epithelial layer was observed after ectopic expression of upd (**B**) in comparison to control animals (**A**). The same phenotype of epithelial thickness was observed when hop^{Tum-l} was ectopically expressed in the trachea (**D**) in comparison to control animals (**C**). The arrows indicate the thickening and obstruction of the epithelial layer. The scale bar is 100 µm.

3.5.2 Ectopic expression of domeless in the airway epithelium

During ectopic expression experiments of the constitutive active form of domeless (UAS-dome^{CA}) by using the Gal4-tubGal80^{ts}/ UAS system, an epithelial thickness, like it was observed for ectopic expression of upd3, upd and hop^{Tum-l}, was not detected. However, ectopic expression of the constitutive active form of domeless was lethal to the animals, thus a temperature sensitive system was applied for spatial and temporal expression. Once the animals reached L2 instar, the temperature sensitive system was initiated by shifting them to higher temperatures and larvae were grown until L3 to analyze epithelial cell formation. The size of tracheal epithelial cells was remarkably compressed and the number of cells increased significantly in comparison to control animals **(Figure 3-24 A-D)**.

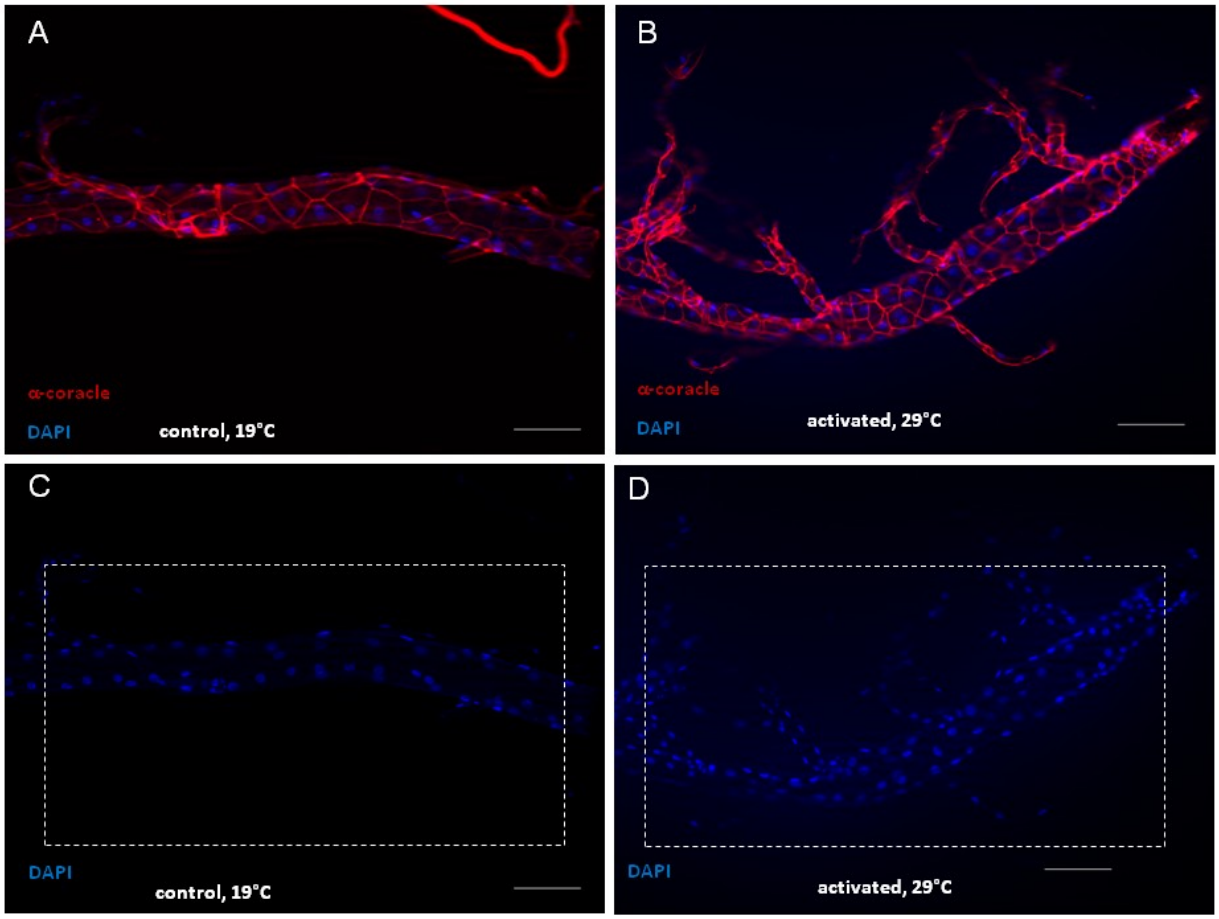

Figure 3-24: Ectopic activation of domeless in the trachea using the TARGET system causes structural changes. Temporal control of domeless expression was carried out using the temperature-sensitive driver line PPK4-Gal4-tubGal80^{ts}. Under low temperature conditions (19°C) the system was repressed by Gal80^{ts} **(A-C)**. Once the larvae reached L2 instar, a inactivation of this repressor was achieved by putting the animals to 29° C, leading to inhibition of Gal80^{ts} and expression of the constitutive active form of *domeless* gene (UAS-dome^{CA}) **(B-D)**. Expression of domeless in the respiratory system had an impact on size and number of cells. An increase of cells and decreased cell size is visualized by DAPI - (blue) and α-coracle staining (red). The scale bar is 100 μm.

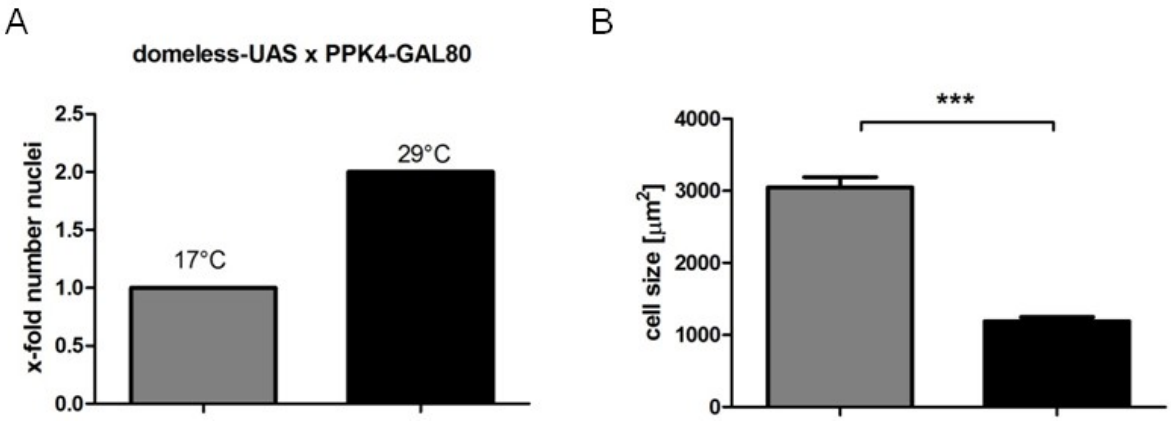

Figure 3-25: Quantification of the cell size and number in animals ectopically expressing domeless in the trachea. Ectopic expression of dome using a temperature sensitive PPK4-Gal4/Gal80^{ts} driver leads to a higher number of nuclei within the trachea (in black) in comparison to control tracheas (in grey) **(A)** and size of epithelial cells were significantly decreased in comparison to control animals **(B)**. Student's t-test: * $p \leq 0.05$; ** $p \leq 0.01$; *** $p \leq 0.001$; ns not significant. Number of animals: 20.

The number of nuclei was higher in animals ectopically expressing the constitutive active form of domeless but maintained normal size, as displayed and quantified by DAPI staining **(Figures 3-24 and 3-25 A)**. Epithelial cells were stained with α-coracle and allowed quantification of their sizes **(Figure 3-25 B)**. Other structural malformations in the respiratory tract of these larvae were strongly melanized tracheal branches, hinting that the larvae were dying due to insufficient oxygen supply **(Figure 3-26)**.

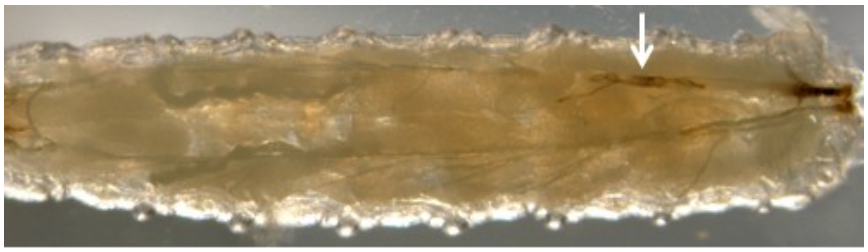

Figure 3-26: Ectopic expression of domeless in the fly's respiratory system causes malformation of the trachea and melanization. Domeless-UAS was crossed with the trachea specific PPK4-GAL4 driver, which induced a structural remodeling in the airway epithelium. The tracheal system was completely malformed and branches were characterized by strong melanization.

3.6 Cigarette smoke exposure induces local remodeling in the airway epithelium

Cigarette smoke reduces epithelial barrier function, impairs wound healing and leads into thickening of the epithelial cells. In cigarette smoke exposed larvae a thickening of the epithelial layer was observed at the same location where activation of JAK-STAT signaling occurred as displayed by the upd3-Gal4;UAS-GFP line **(Figure 3-27 A-B)**. Especially at the dorsal branches, where GFP expression was enhanced, the thickness was significantly increased compared to the control regions **(Fig. 3-27 C-D)**.

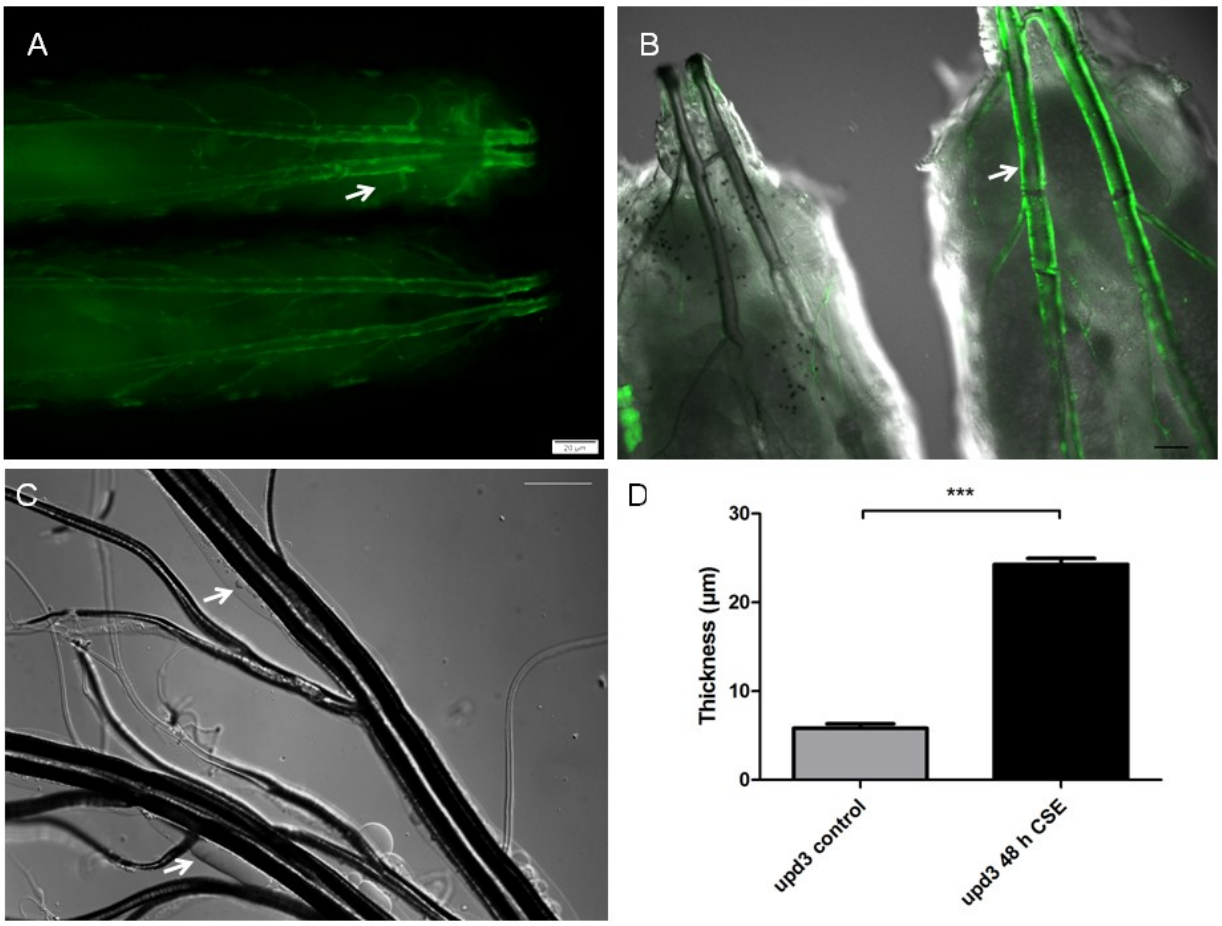

Figure 3-27: Airway remodeling in response to cigarette smoke. Strong GFP expression of CS-exposed larvae of upd3-Gal4;UAS-GFP occurred at the dorsal trunks as indicated by an white arrow (**A and B**). These regions were characterized by a strong thickening of the epithelial layer after CSE (**C**). Quantification of the thickness was performed using student's t-test: *: P< 0.05; **: P< 0.01; ***: P< 0.001 (**D**). Values are ± SD, n = 15 and the scale bar is 100 µm.

Additionally, a strong GFP expression was visible in the oenocytes of CSE animals in comparison to non-smoke exposed animals, indicative for upd3 expression **(Figures 3-28 A-B, and 3-28 D)**. A dissection of the oenocytes revealed that they are directly connected to the larvae's terminal branches **(Figure 3-28 C).** Stronger GFP signals were also detected in the fine neighboring primary branches, as indicated by a white arrow in **Figure 3-28 B.**

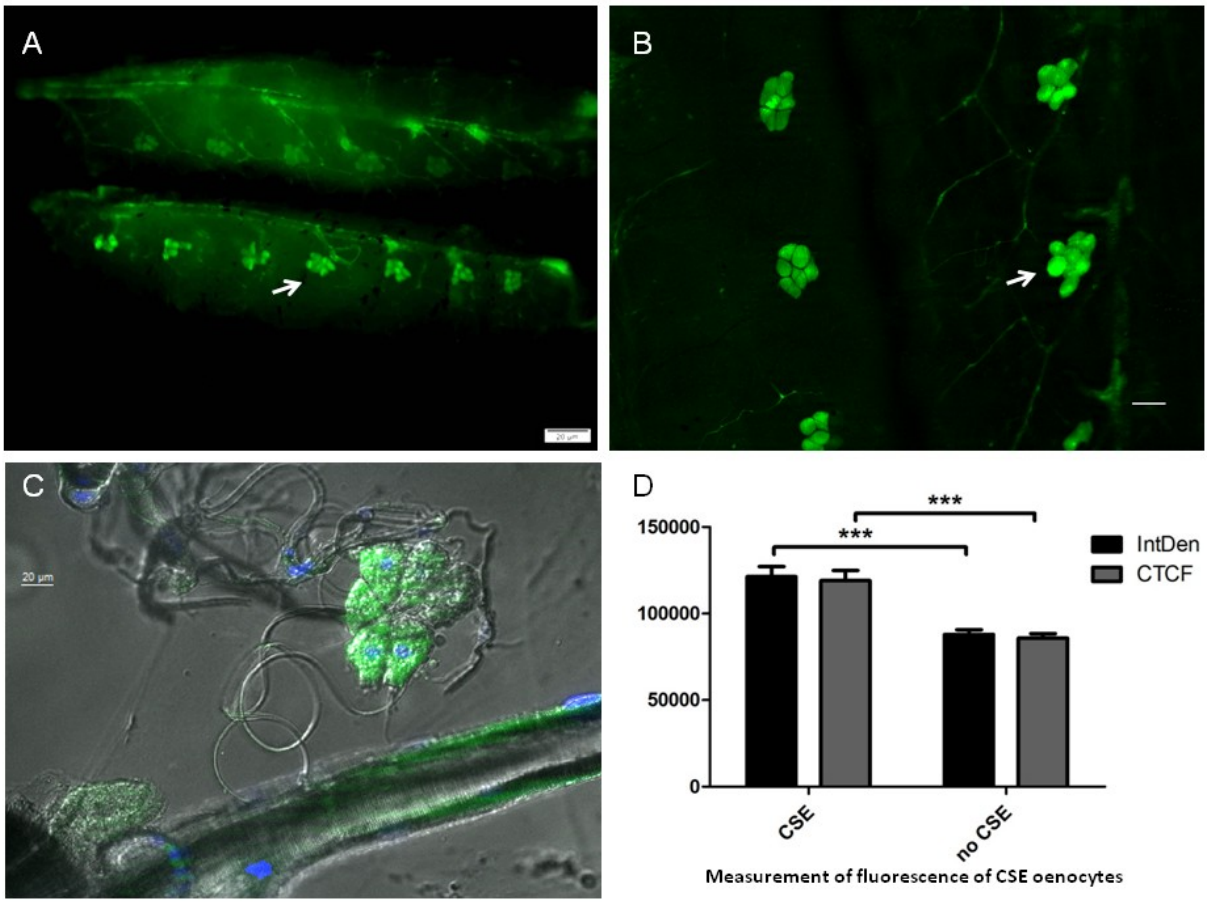

Figure 3-28: Activation of upd3 in the oenocytes after CSE. A strong GFP signal was displayed in the oenocytes in CS-exposed larvae in comparison to control animals (**A and B**). Dissection of these oenocytes shows that they are directly connected to the terminal branches of the fly's airway system (**C**). Measuring of cell fluorescence (corrected total cell fluorescence (CTCF) vs. integrated density (IntDen)) was performed using ImageJ and confirmed an increase of GFP in oenocytes of smoke-exposed larvae (**D**). Student's t-test with *: P<0.05; **: P<0.01; ***: P<0.001, values are ± SD, n=15. The scale bar is 100 µm.

Another form of airway remodeling was observed in the terminal branches of CS-exposed animals. The terminal branches occurred to be curlier after CSE in comparison to their controls, as shown by staining with α-WKD antibody (**Appendix 7.6, Figure 7-9**).

3.7 Cigarette smoke exposure reduces life span of *D. melanogaster*

In earlier studies it was shown that one cigarette each day reduces the lifespan of the fly by almost 50% (Kallsen, 2013). Therefore, it was interesting to examine, if a higher number of cigarettes enhances the toxical effect on lifespan. For this purpose, 100 flies of each genotype (wildtype and flies deficient in dFoxO or relish) were taken and exposed with two cigarettes per day. Survival curves of female and male flies of the wildtype exposed to cigarette smoke, significantly shifted to the left **(Figure 3-29 A and B)**.

For cigarette exposed male flies, the median survival was significantly decreased by 66.7%. The median survival time for CSE female flies was shortened by 66% compared to the control (Log-rank test: $p< 0.001$). The medium survival time was 15 d for smoke exposed male and 18 d for female flies. There was no change in the median survival of female and male flies under physiological conditions (45 days).

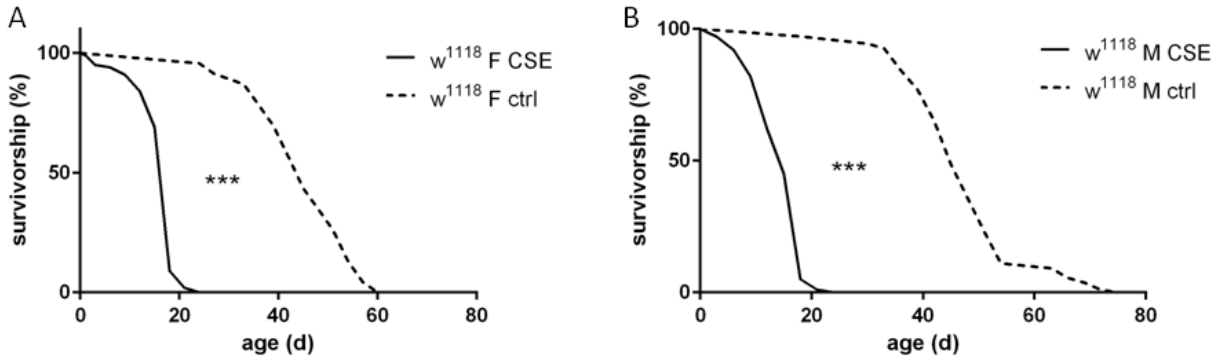

Figure 3-29: Lifespan of male and female wild type flies after CSE. Smoke exposed female (**A**) and male flies (**B**) lived 66.7% and 66.6% shorter than the control flies respectively. In smoke exposed male flies the median survival time is 15 days (n=102) and in female flies 18 days. The median survival for controls of both sexes is 45 days (n=100). Log-rank test for survival analysis showed that $p< 0.001$ for both sexes. Control flies are shown with a dotted line.

Further, it was of interest if there is any difference in mortality behaviour of flies deficient in relish or dFoxO. To rule out, if flies deficient in dFoxO may die faster, I performed a survival assay with dFoxO deficient flies. Smoke exposed dFoxO-deficient flies had a remarkable decrease in lifespan compared to their non-exposed counterpart **(Figure 3-30 A and B)**. The median survival was significantly decreased by 50% for the male and by 53.8% for female flies compared to their controls (Log-rank test: $p<0.001$).

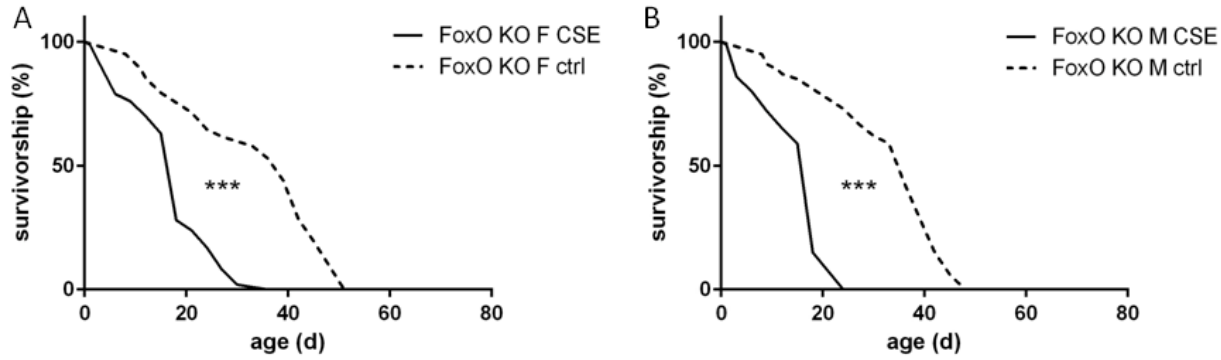

Figure 3-30: Life span of flies deficient in dFoxO after CSE. Smoke exposed female (**A**) and male flies (**B**) deficient in dFoxO lived 53.8% and 50% shorter than their controls, respectively. For both sexes the median survival time was 18 days for smoke exposed animals (n=100). The median survival was 39 days for control female (n=100) and 36 days for control male flies (n=100). Log-rank test for survival analysis showed that $p<0.001$ for both sexes.

However, under normal conditions the life span of dFoxO deficient flies is lower than that of the wild type flies (female and male) whereas after exposure to cigarette smoke, dFoxO deficient flies seems to live slightly longer than the wild type (**Figure 3-31 A - B**).

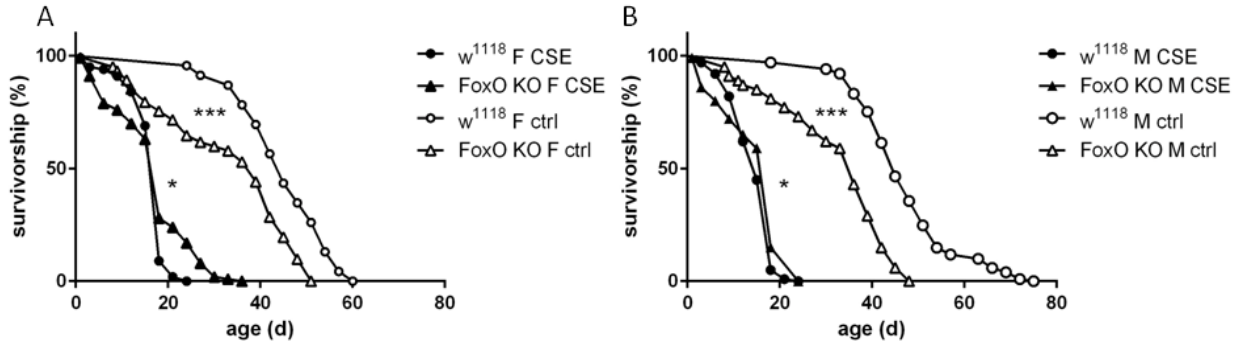

Figure 3-31: Life span comparison of wild type and dFoxO deficient flies. Female (**A**) or male (**B**) dFoxO deficient flies (white triangles) show a large decrease in lifespan under normal conditions (ctrl), when compared to wild type flies (white balls). Interestingly, dFoxO deficient animals seemed to be more tolerant towards cigarette smoke (black triangles) when compared to smoke-exposed wild type animals (black balls) for both sexes. Data derived from Log- rank analysis *: $P < 0.05$, *** $P < 0.001$.

At last, I subjected animals deficient in relish to cigarette smoke. These mutant flies showed a significantly decreased survival rate compared to wild type flies in both conditions. Relish deficient flies had a decreased natural lifespan compared to wild type flies for both sexes. In cigarette exposed male flies deficient in relish, the median survival was significantly decreased by 55.6% (Log-rank test: $p<0.001$) and shortened by 42.9% in female flies compared to non-exposed flies **(Figure 3-32 A - B)**. The medium survival time was only 12 d for both sexes.

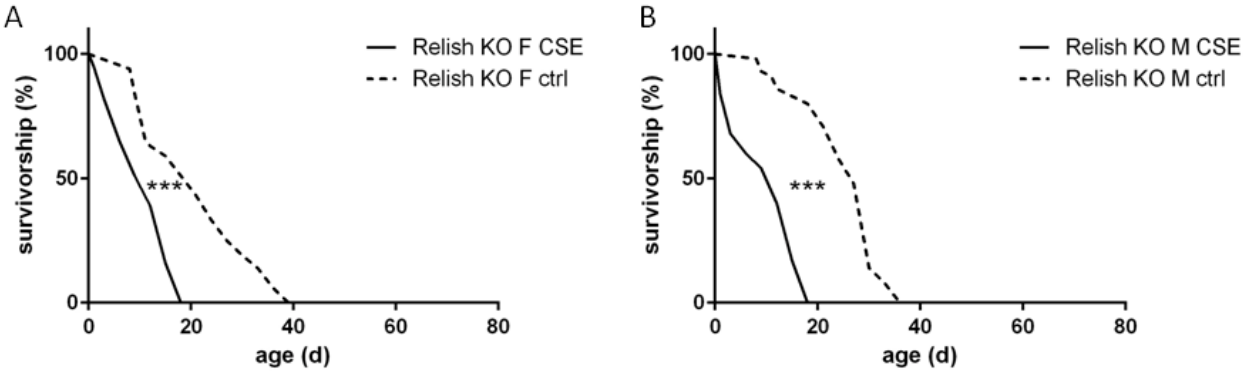

Figure 3-32: CSE decreased life span of relish deficient flies. Smoke exposed female (**A**) and male flies (**B**) deficient in relish TF lived 42.85% and 55.55% shorter than their controls, respectively. In both sexes the median survival time was only 12 days for smoke exposed animals (n=100). The median survival was 21 days for control female (n=100) and 27 days for control male flies (n=100). Data derived from Log- rank analysis ($p<0.001$) of the survival curves.

3.8 Expression of drosomycin in response to cigarette smoke exposure

To visualize expression of the major antimicrobial peptide genes in response to cigarette smoke, reporter lines were used, carrying promoter::gfp fusions of drosomycin, defensin, drosocin, attacin, metchnikowin and diptericin (Ferrandon et al, 1998; Tzou et al, 2000). The larvae were scored for the presence of GFP expression in the tracheal system after a challenging condition with smoke. Interestingly, only drosomycin was found to be expressed after CSE in the entire trachea of 3rd instar larvae **(Figure 3-33 A-B)** whereas no GFP was observed for defensin, drosocin, attacin, metchnikowin and diptericin (data not shown) neither in larvae nor in adult flies.

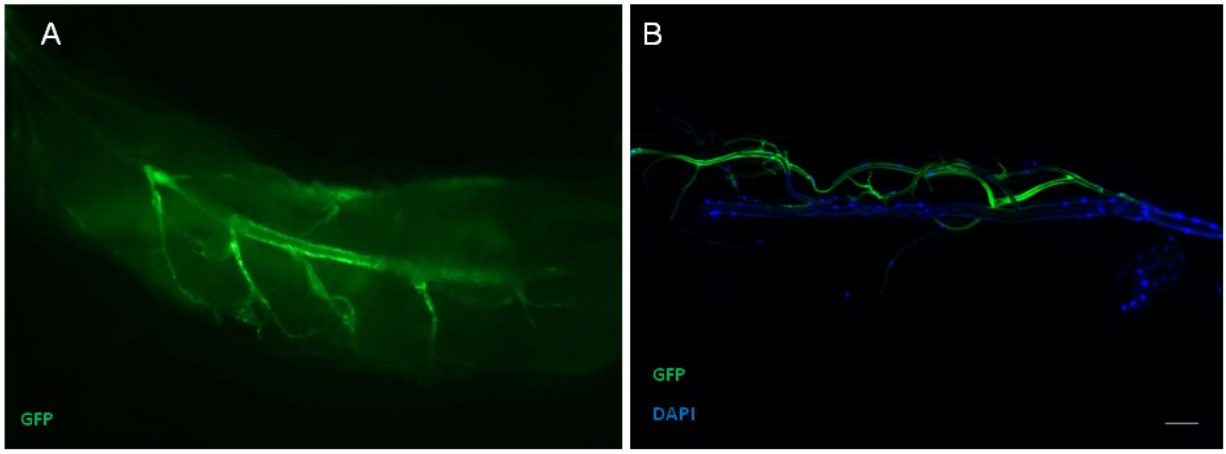

Figure 3-33: Activation of the antimicrobial peptide drosomycin in response to CSE. Following exposure to CSE, the anti-microbial peptide drosomycin was released in the trachea **(A)** and was also found to be expressed in the secondary and tertiary branches **(B)**.

3.9 Induction of cAMP synthesis in the airways of *D. melanogaster* by a blue light activated adenylyl cyclase of *Beggiatoa* (bPAC)

3.9.1 Sequence similarity between *Beggiatoa* bPAC and *Drosophila* Gyc76C

Another part of my thesis was to study, how alterations of cAMP levels affect the physiology of the airways in *Drosophila*. Until now, only little is known about how higher levels of cAMP affect the airways. In contrast much is known about cAMP degradation in context of COPD pathogenesis. The recently found adenylyl cyclase of *Beggiatoa* (bPAC) seemed to be a powerful tool for optogenetic manipulation of the fly's respiratory track via activation by blue light. Its expression and activation was tested in several tracheal parts with help of different tracheal Gal4-drivers.

A BLAST search using bPAC coding sequence of *Beggiatoa* identified a distant homologous gene in the *Drosophila* genome, the guanylyl cyclase Gyc76C and the human natriuretic receptor. The alignment of bPAC, Gyc76C and the natriuretic receptor indicates that these catalytic domains and their structural organization are tightly conserved within the adenylate and guanylate cyclase catalytic domain (Guanylate_cyc, Pfam Id - PF00211) (**Figure 3-34**).

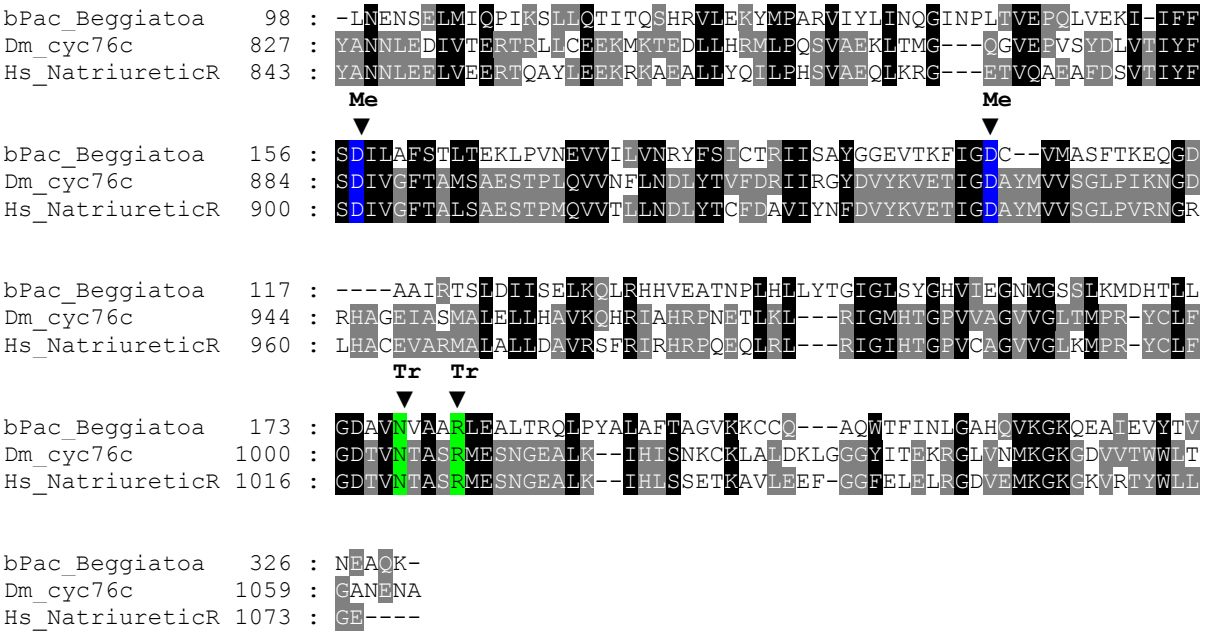

Figure 3-34: Sequence alignment of bPac of *Beggiatoa* with *Drosophila* Cyc76c and the human natriuretic receptor. A part of the bPAC sequence was aligned to the corresponding regions of other cyclases obtained from BLAST search. The closest homolog was *Drosophila* Cyc76c and the natriuretic receptor of human. The highly conserved region of all 3 proteins is highlighted in black. In grey boxes are shaded conserved substitutions, metal-binding Asps (Me) are shaded in blue and transition state-stabilizing Asn and Arg are in green (Stierl et al, 2011).

3.9.2 Expression and activation of bPAC controls tracheal terminal branching

The formation of the terminal branches is regulated by the gene DSRF/ blistered, a *Drosophila* homolog of the serum response factor. DSRF/ blistered is specifically expressed in the terminal branches. Expression and blue-light activation of bPAC in the terminal branches with help of DSRF-GAL4, had a remarkable impact on the branching phenotype of the airways. Changes in branching were observed and monitored in the 3rd segment of 3rd instar larvae in dorsal view of blue-light induced animals under normoxic (**Figure 3-35 D - F**) and hypoxic conditions (**Figure 3-35 G - I**). Blue-light exposure inhibited branching remarkably and led into disorganized pattering. The terminal branches were not properly developed nor regularly spaced.

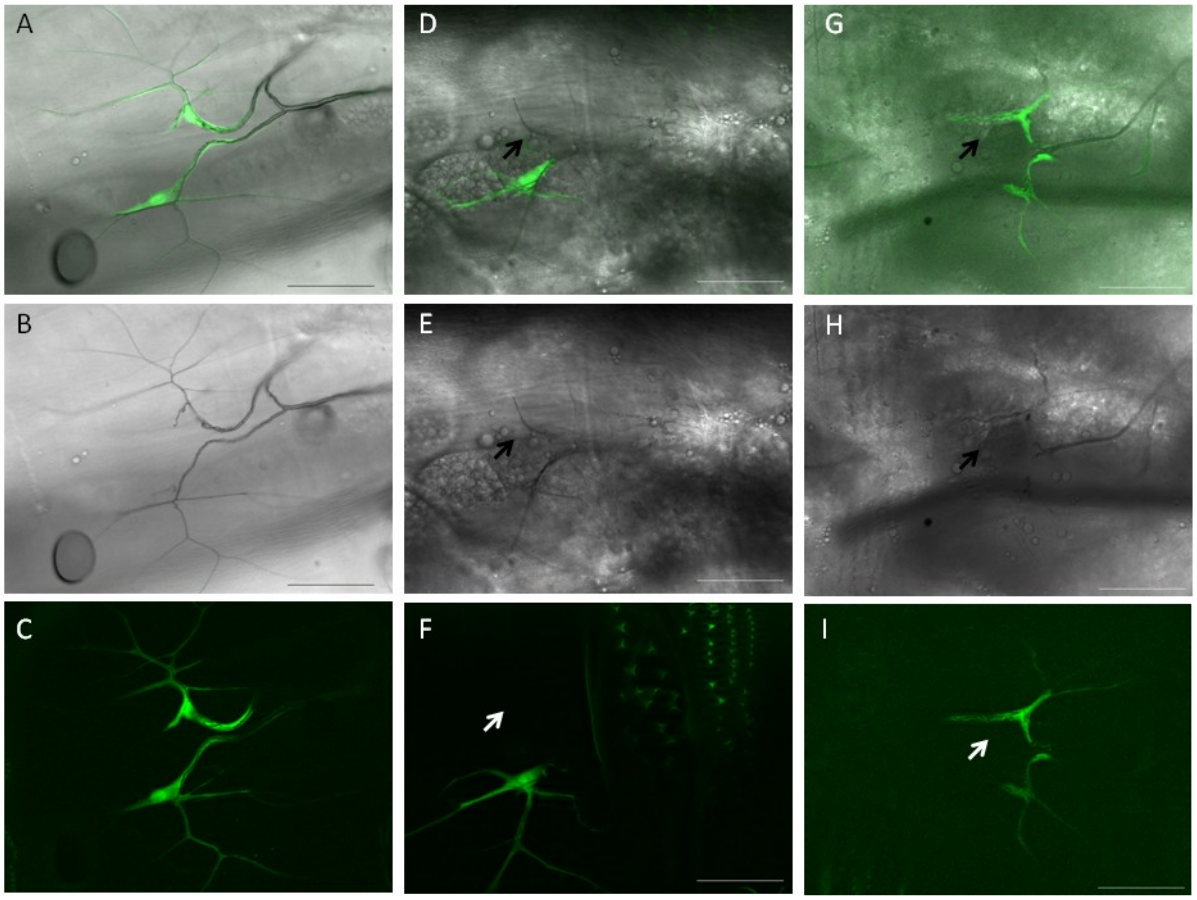

Figure 3-35: Activation of bPAC by blue light in the terminal branches under normoxic and hypoxic conditions. Blue-light activation of bPAC in the terminal cells inhibited branching and led into disorganized patterning of the terminal cells (**D, E, F**) in comparison to control animals (**A, B, C**). Subjecting these animals to hypoxic conditions could not initiate branching (**G, H, I**). For counting of branches the 3rd segment of 3rd instar larvae, dorsal view was chosen and crosses were performed using bPAC::DSRF-GAL4;UAS-GFP, scale bar: 100 µm.

Terminal branching is highly variable and regulated by the oxygen supply. Thus, bPAC activated larvae were allowed to grow under anoxic conditions in order to promote an increase in terminal branching. The result shows that hypoxia could not significantly enhance branching in blue light exposed animals **(Figure 3-36)**.

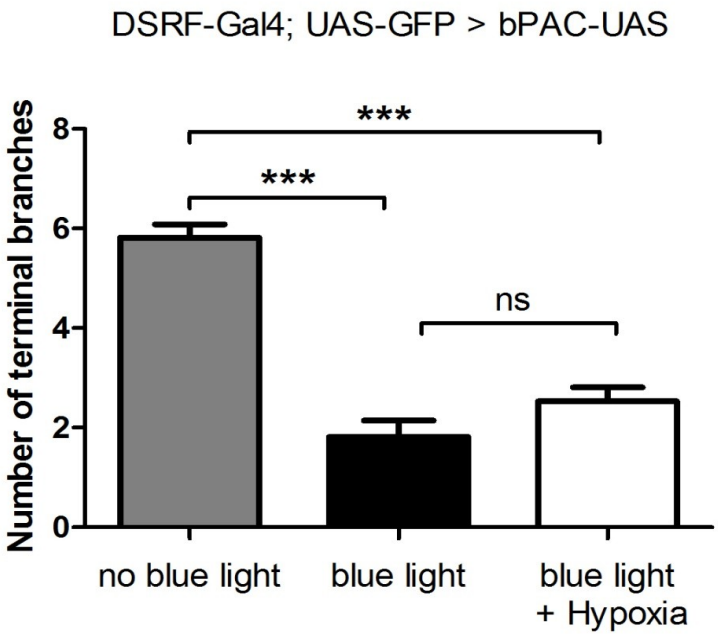

Figure 3-36: Number of terminal branches after activation of bPAC by blue light under normoxic and hypoxic conditions. The number of branches was remarkably reduced after exposure to blue light. For counting of branches: third segment of 3rd instar larvae, dorsal view. Crosses carried out were: bPAC::DSRF-Gal4; UAS-GFP. Number of animals: 20. Significances are calculated using student's t-test with * $p<0.05$, ** $p = 0.01$ to 0.001, *** $p < 0.001$, ns not significant $p > 0.05$.

In some animals an incorrect positioning of the terminal branches after activation with blue light was observed **(Figure 3-37)**.

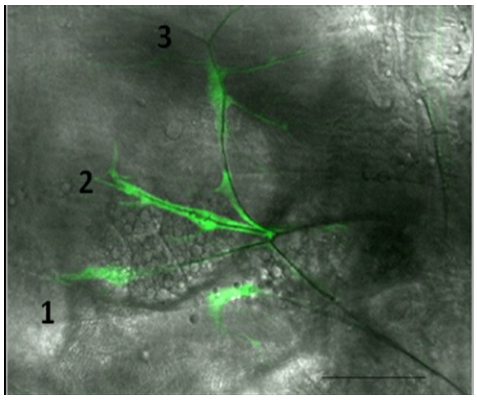

Figure 3-37: Malformation of terminal branches by activation of bPAC by blue light. Some larvae were characterized by malformed branches. The third tracheal segment of 3rd instar larva, dorsal view was used to observe morphological changes. Crosses were performed using bPAC::DSRF-GAL4;UAS-GFP, scale bar: 100 µm.

3.9.3 Expression and activation of bPAC causes melanization in the airways

Activation of bPAC in the respiratory system of the fly, using various trachea-specific GAL4-lines, resulted into melanized branches. Expression and blue-light activation of bPAC in the terminal cells displayed incorrect patterning of the terminal cells and melanized, lumpy cells **(Figure 3-38 A-D)**.

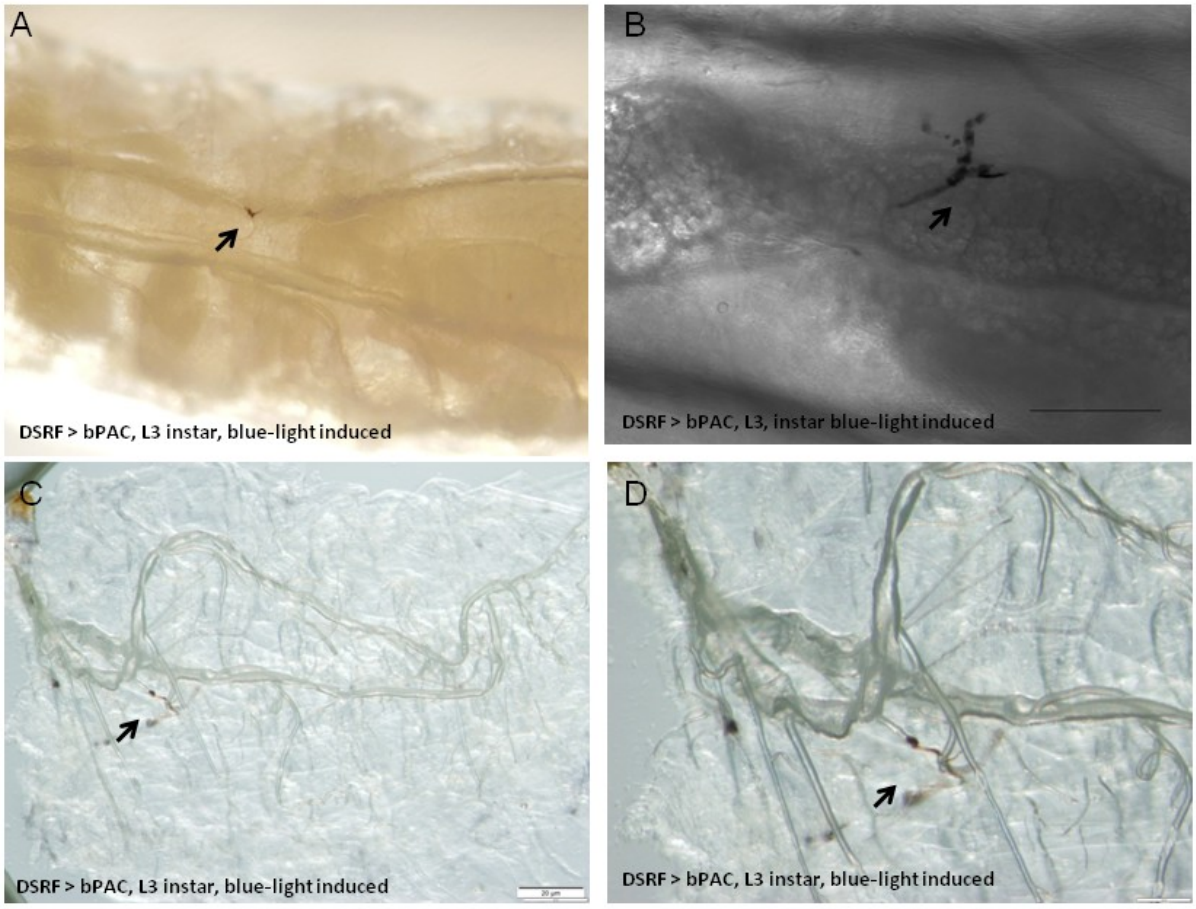

Figure 3-38: bPAC induced activation of cAMP in the terminal branches leads into melanized lumps. All animals of the crosses bPAC::DSRF-Gal4; UAS-GFP were characterized by melanized branches (**A-B**). The filet cut of tracheas show lumpy, melanized tracheal cells (**C-D**). The scale bar is 100 µm.

In addition, elevation of cAMP levels by bPAC, using a Gal4-driver specific for the inca-cells, did not induce any significant changes in the airway epithelium. This could be explained by the moderate activity of the driver line.

An expression and activation of bPAC crossed with the PPK4-driver led into tracheal melanization in instar L1-L3 **(Figure 3-39 A)**. Overall, melanization was observed in all animals carrying blue-light induced bPAC transgene **(Figure 3-39 B)**, except for crosses with the specific driver for tracheal inca-cells.

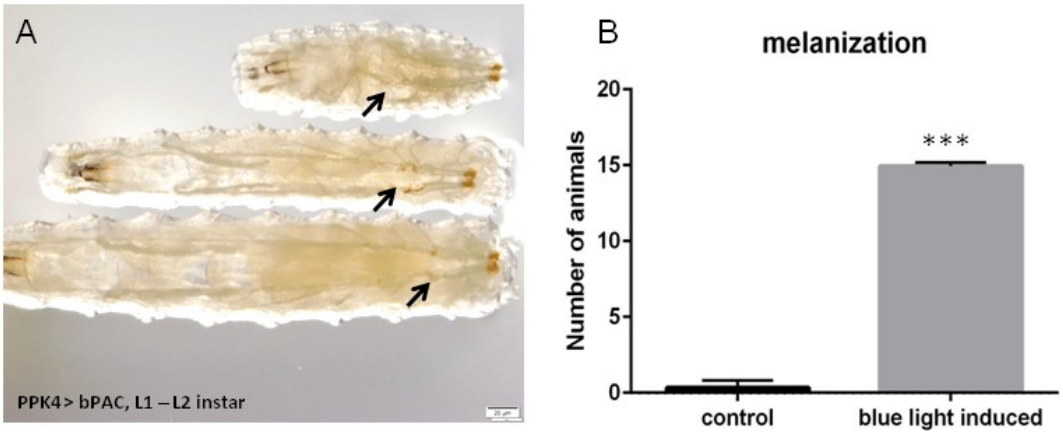

Figure 3-39: Activation of bPAC by blue light in the trachea driven by PPK4-GAL4 leads into melanization. A) Expression and blue-light activation of bPAC in the respiratory track using PPK4-Gal4 causes melanization in all instar 1-3. **B**) All animals are characterized by melanized branches and significances are calculated using student's t-test with **p = 0.01 to 0.001, ***p < 0.001, NS p > 0.05.

3.9.4 Expression and activation of bPAC in the airways controls growth and viability

Blue-light induced bPAC in the respiratory system regulates larval growth and viability. First instar larvae of bPAC::PPK4, could maximum complete L2 instar after direct exposure to blue light. In those animals, a complete larval lethality was observed **(Figure 3-40 A-B)**. The larvae show a behavior that is typically seen in animals that experience severe oxygen cutback. They left their medium prematurely and died as early larvae. **(Figure 3-40 B)**. A closer look on these larvae reveals that numerous epithelial cells are not functional any more. Damage is visible in form of melanization and a disturbed structure of the airways.

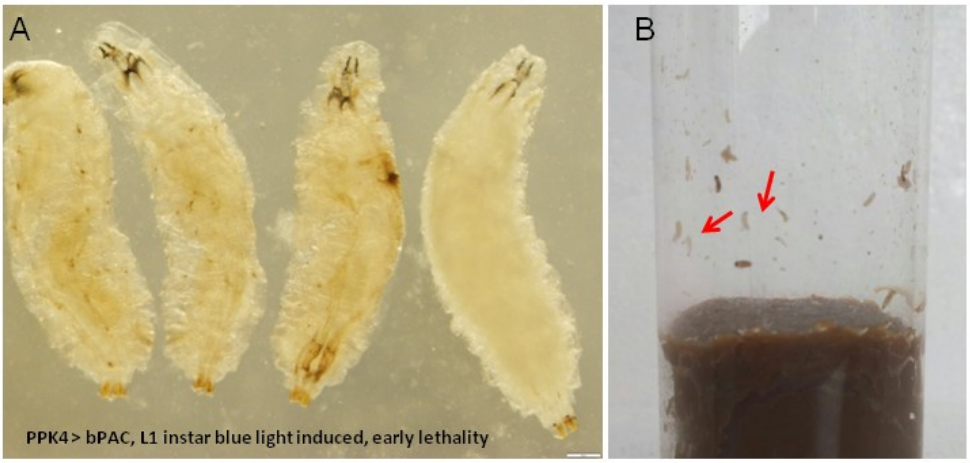

Figure 3-40: Activation of bPAC by blue light with the tracheal driver PPK4-Gal4 has impact on growth phenotype and viability at the L1/L2 transition. A) Activation of bPAC in the entire trachea using PPK4-Gal4, has remarkable effect on larvae‘s development. Most of the animals were able to reach L2 but they died as early larvae after direct application of blue light. **B**) These transgenic animals left their medium prematurely.

3.9.5 Expression and activation of bPAC in the trachea effects the homeobox transcription factor cut

Next, investigation was carried out for the role of cAMP activation with a driver line of the homeobox transcription factor cut. The homeobox transcription factor cut coordinates patterning and growth during *Drosophila* airway remodeling (Pitsouli & Perrimon, 2013). The expression and blue-light activation of bPAC in the trachea using cut-Gal4, had dramatic effects on the phenotype at the dorsal branches. This activation had a strong impact on development and growth of the branches. Branches at these regions were completely malformed and their growth was significantly suppressed **(Figure 3-41)**.

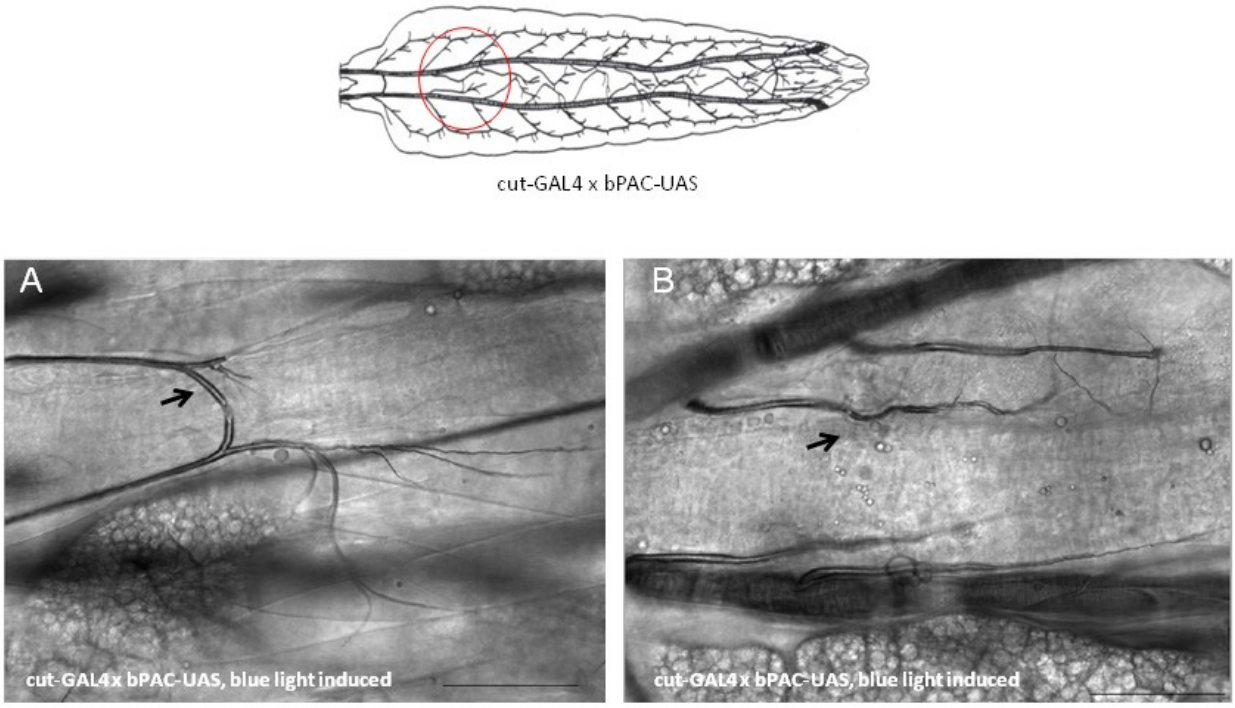

Figure 3-41: Expression of the photoactive bPAC transgene using cut-Gal4 leads into malformed dorsal branches. Activation of bPAC in the fly's airways with blue light, utilizing the cut-Gal4 driver, affects patterning and growth of the dorsal branches. Branching was significantly inhibited in the last segment of the trachea. Scale bar: 100 µm, crosses were performed using bPAC::cut-GAL4.

Additionally, regions of activated bPAC were characterized by strong epithelial thickness and melanization (**Figure 3-42 A - D and Figure 3-43**).

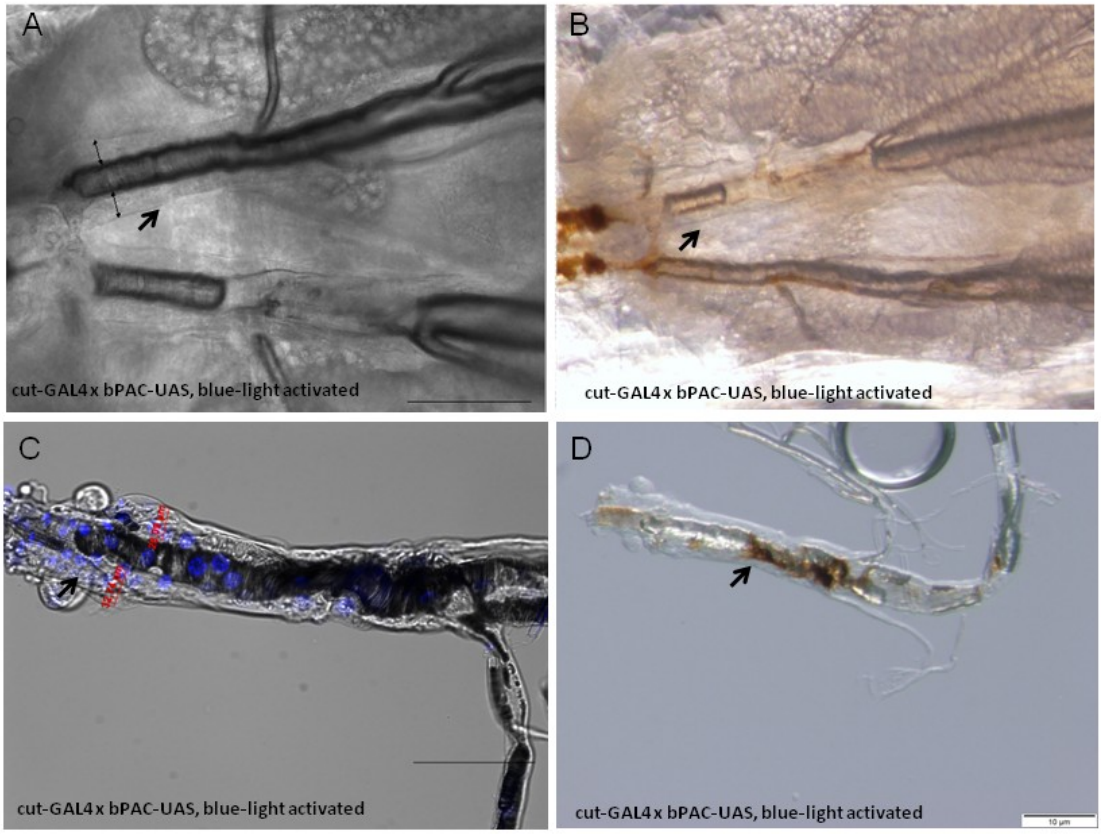

Figure 3-42: Expression of the photoactive bPAC transgene using cut-Gal4 causes thickening and melanization of the dorsal trunks. Activation of bPAC by blue light, using the cut-Gal4 driver, initiated airway remodeling in form of a thickened epithelial layer at the dorsal trunks **(A-C)**. Moreover, this part is also characterized by strong melanization **(B and D)**. The scale bar is 100 µm and crosses were performed using bPAC::cut-GAL4.

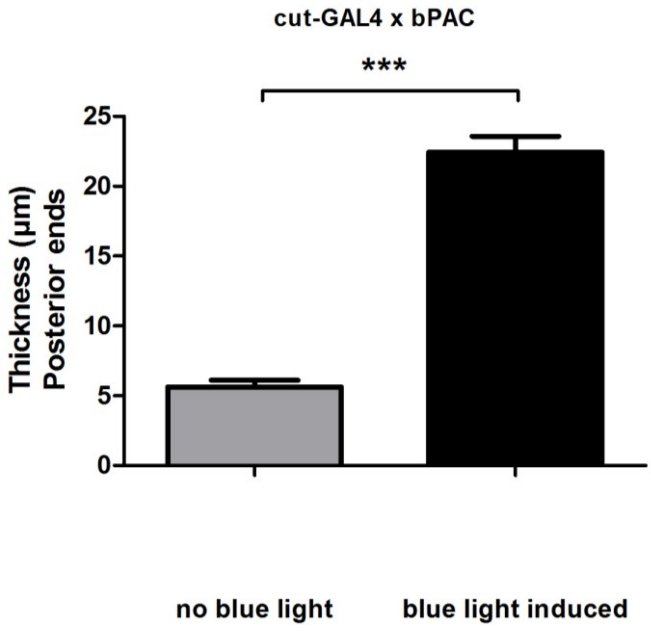

Figure 3-43: Quantification of the epithelial thickness of blue-light activated animals. Airway remodeling in form of a significant thickening was visible in blue-light exposed animals in comparison to animals not exposed to blue-light. Crosses: cut-Gal4::bPAC and data are presented as mean ± SEM, student's t-test: * $p \leq 0.05$; ** $p \leq 0.01$; *** $p \leq 0.001$. Number of animals: 15.

A closer look on these nuclei shows that transgenic animals expressing bPAC under control of cut-Gal4 possess higher number of nuclei compared to control animals **(Figures 3-44 and 3-45)**.

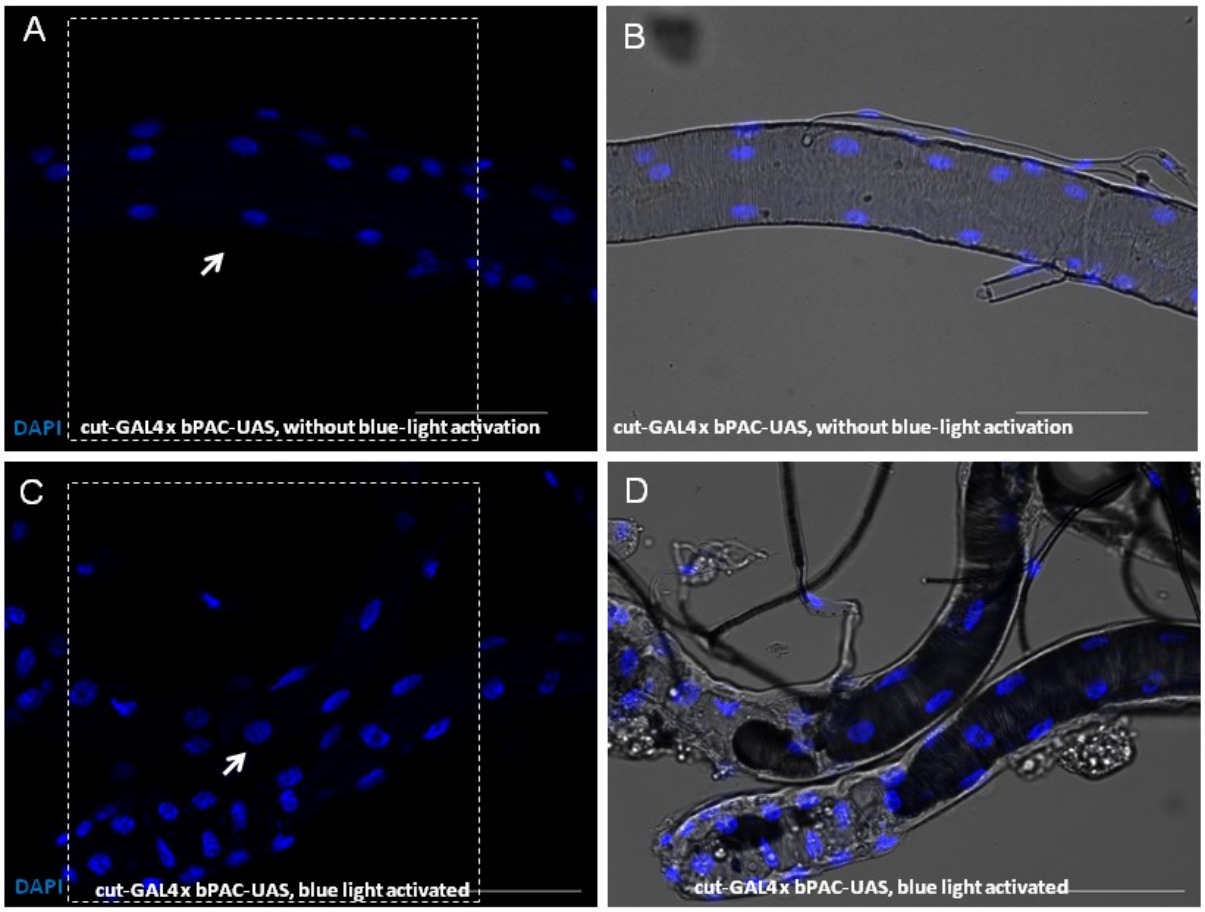

Figure 3-44: Expression of the photoactive bPAC transgene using cut-Gal4 causes a higher number of nuclei. Activation of blue-light inducible bPAC using the cut-Gal4 driver, led into an increased number of nuclei as visible by DAPI staining, which indicates higher proliferation rate of these cells **(C-D)** in comparison to control animals **(A-B)**. Scale bar: 100 µm, crosses were performed using bPAC::cut-GAL4.

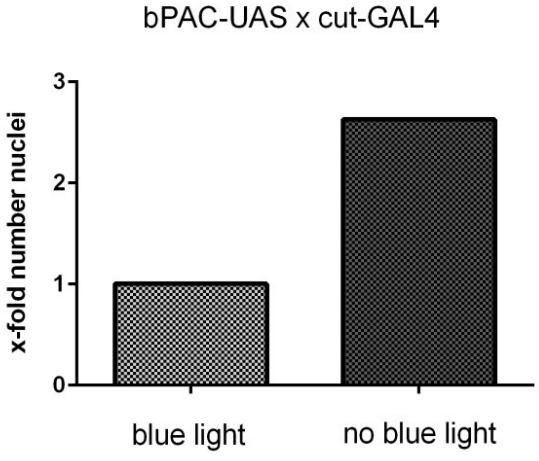

Figure 3-45: Quantification of nuclei number. Activation of blue-light inducible bPAC using the cut-Gal4 driver increased the number of nuclei 1.5-fold.

These results indicate that in these transgenic animals the proliferation of cells is increased. Cell size compaction and higher number of cells were confirmed by α-coracle staining **(Figure 3-46)**.

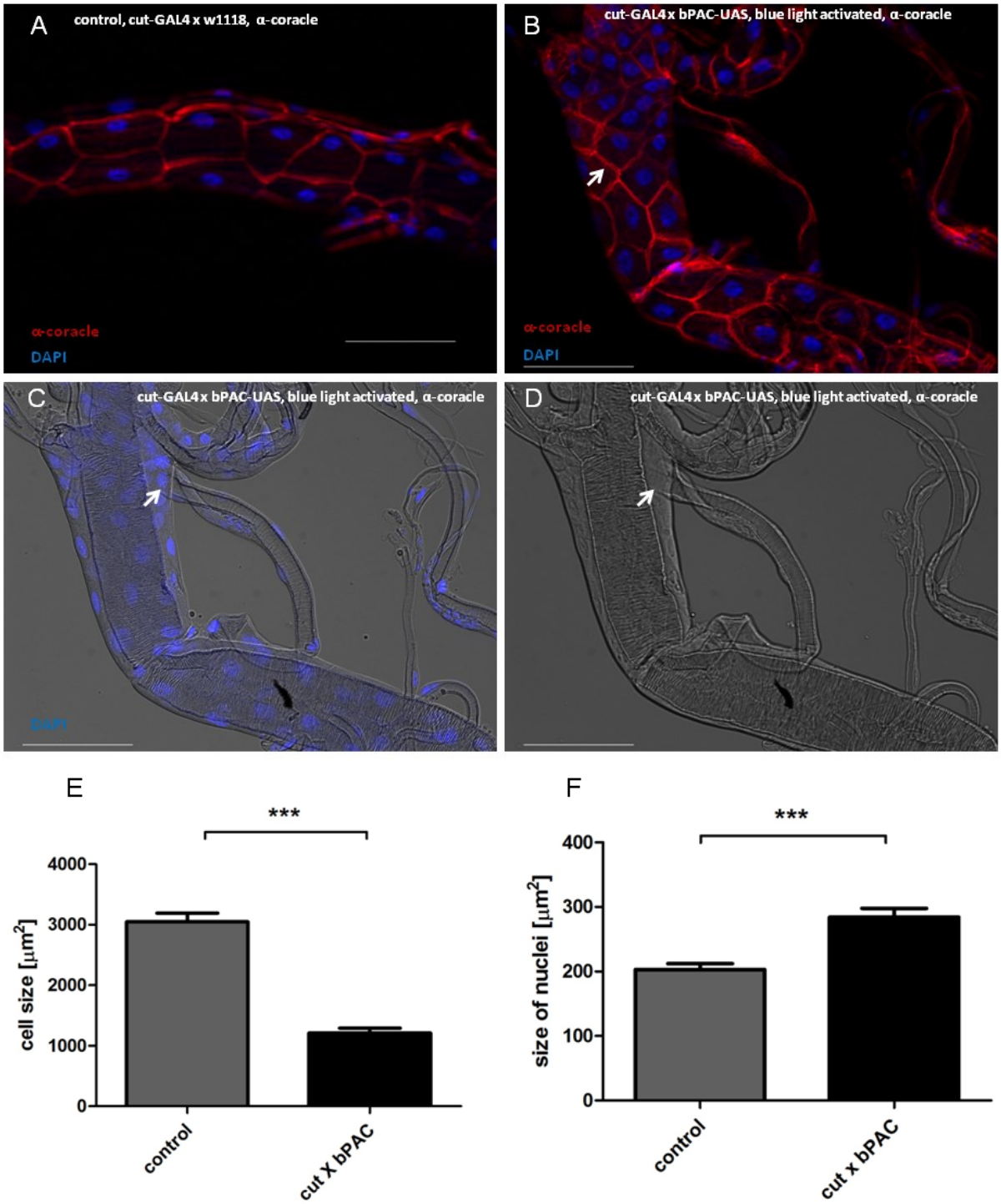

Figure 3-46: Expression of the photoactive bPAC transgene using cut-Gal4 leads to proliferation of cells and decreased cell size. Activation of bPAC by blue light, utilizing the cut-Gal4 driver, increased number of cells and decreased cell size significantly (**B** and **E**) in comparison to control animals (**A**), as observed by α-coracle staining (red). This indicates for a higher proliferation rate of these cells. A thickening of the airway epithelium was repeatedly observed and staining of nuclei by DAPI (blue) revealed that they are organized as a monolayer at these regions (**C - D**). Moreover, the size of nuclei was increased (**F**). Scale bar: 100 µm, crosses were performed using bPAC::cut-GAL4. . Number of animals: 20. Student's t-test: * $p \leq 0.05$; ** $p \leq 0.01$; *** $p \leq 0.001$.

3.9.6 Expression and activation of bPAC in the trachea leads to activation of dFoxO

Interestingly, exposure of bPAC transgenic animals to blue light utilizing cut-Gal4, had an impact on the activation of the transcription factor dFoxO in the airways. A translocation of dFoxO into nucleus was observed (**Figure 3-47**).

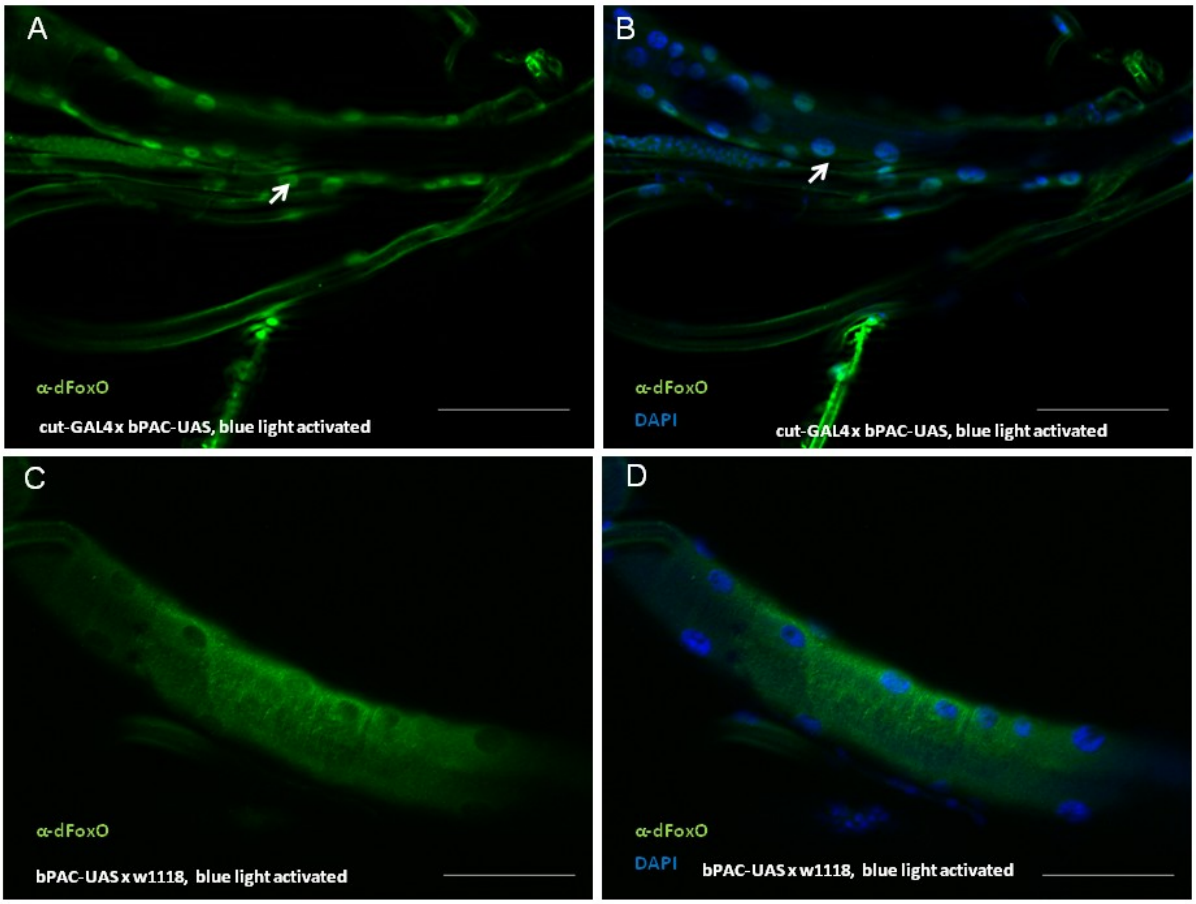

Figure 3-47: Activation of the transcription factor dFoxO in blue-light activated bPAC animals. Activation of bPAC by blue-light, utilizing the cut-Gal4 driver, resulted into nuclear translocation of dFoxO (green) (**A and B**) in comparison to control animals where dFoxO was found in the cytosol (**C and D**). DAPI-staining (blue) and α-FoxO staining (green), crosses were performed using bPAC::cut-GAL4, scale bar: 100 µm.

Similar phenotypes of cell size deduction and translocation of the transcription factor dFoxO were observed during activation of bPAC using the PPK4-Gal4 driver (**Figure 3-48**).

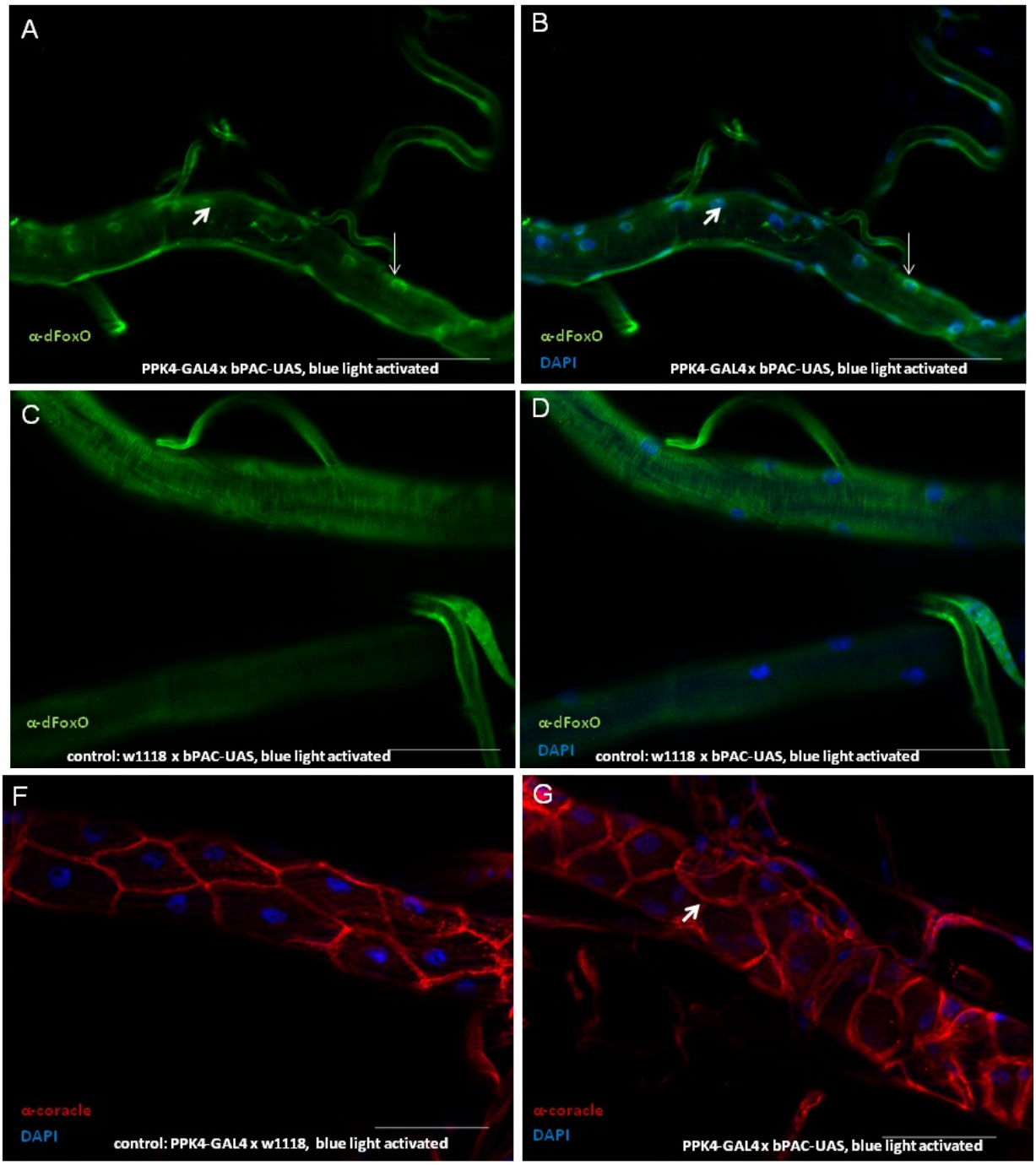

Figure 3-48: Expression of the photoactive bPAC transgene using PPK4-Gal4 resulted into dFoxO translocation and decreased epithelial cell size. Activation of bPAC by blue light in the entire trachea, using PPK4-Gal4, resulted in nuclear translocation of dFoxO into the nucleus (**A and B**) but not for control animals (**C and D**). A compressed epithelial cell size is visible as shown by α-coracle staining (red, white arrow) (**G**) in comparison to control animals (**F**), which indicates for a higher cell proliferation. DAPI-staining in blue and α-FoxO staining in green. Scale bar: 100 µm, crosses were performed using bPAC::PPK4-Gal4.

3.10 Depolarization of the terminal cells utilizing ChR2-XXL

Further, the branching plasticity after depolarization of the tracheal cells was explored, using the blue-light inducible ion-channel ChR2-XXL. Depolarization of the terminal cells by ChR2-XXL using DSRF-GAL4;UAS-GFP, leads into 3 malformed branches in comparison to all control animals possessing naturally 2 branches **(Figure 3-49)**. This result underlines the importance of a balanced cell polarity within the respiratory track. Minor changes can lead into malformations, such as inappropriate branching.

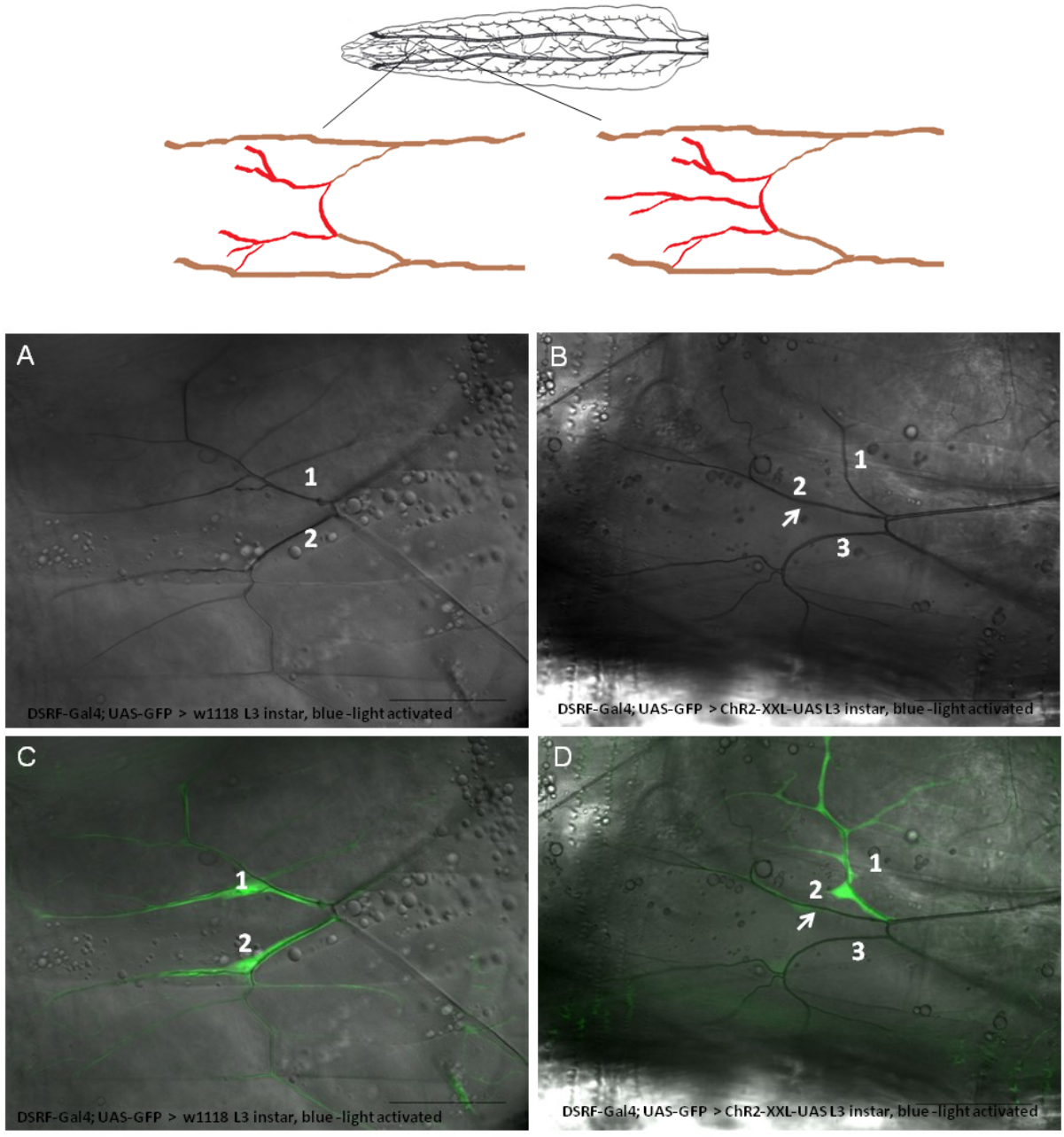

Figure 3-49: Blue-light activation of ChR2-XXL in the terminal branches. Expression of the blue-light-inducible ion channel ChR2-XXL in the terminal branches resulted in three sprouting branches (**B and D**) compared to control animals (**A and C**) with just 2 branches. Scale bar: 100 µm, crosses were performed using ChR2-XXL::DSRF-GAL4;UAS-GFP.

3.11 Melanotic tumor formation in the respiratory track of *D. melanogaster*

Until now, there is only one pathway, which fully describes how melanization can be activated in the trachea under tight negative control by a serpin protease inhibitor (Spn77Ba).

My results show that translocation of the transcription regulator dFoxO takes part in the biosynthesis of melanin within the respiratory system of the fly and thus could be a new unknown pathway to regulate melanization. Ectopic expression of dFoxO in the larvae trachea resulted into dramatic changes of the overall epithelial structure and induces melanotic tumors.

3.11.1 Activation of dFoxO leads into tracheal melanization

Ectopic expression of dFoxO in the airways of the fruit fly driven by PPK4-Gal4 resulted into melanized sections of the trachea (**Figure 3-50**). For this purpose dFoxO-UAS was mated with the driver lines PPK4-Gal4 and DSRF-Gal4. The cells expressing dFoxO were characterized by the synthesis of melanin and a translocation of dFoxO into the nucleus was detected.

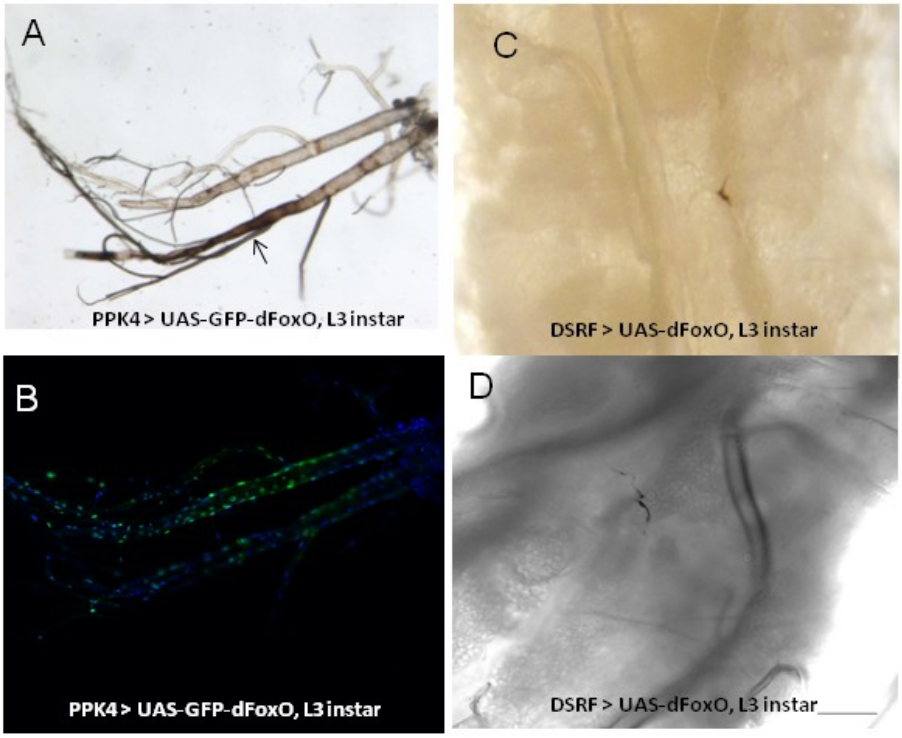

Figure 3-50: Ectopic expression and activation of dFoxO causes tracheal melanization. Melanization of the larval trachea resulted when dFoxO was ectopically expressed in the airways with the PPK4-Gal4 driver **(A-B)** and when activated in the terminal branches with the DRSF-Gal4 driver **(C-D)**. Furthermore, a nuclear translocation of the transcription factor was observed. The panel in blue indicates DAPI staining of the nuclei. Merged image of GFP and DAPI. The scale bar is 100 µm.

3.11.2 Activation of dFoxO in the trachea has no impact on the fruit fly's viability

Larvae ectopically expressing dFoxO within the trachea were able to form pupae and underwent a complete metamorphosis, turning into the adult stage. Melanization remained to be visible during pupal and adult stage **(Figure 3-51 A-C)**.

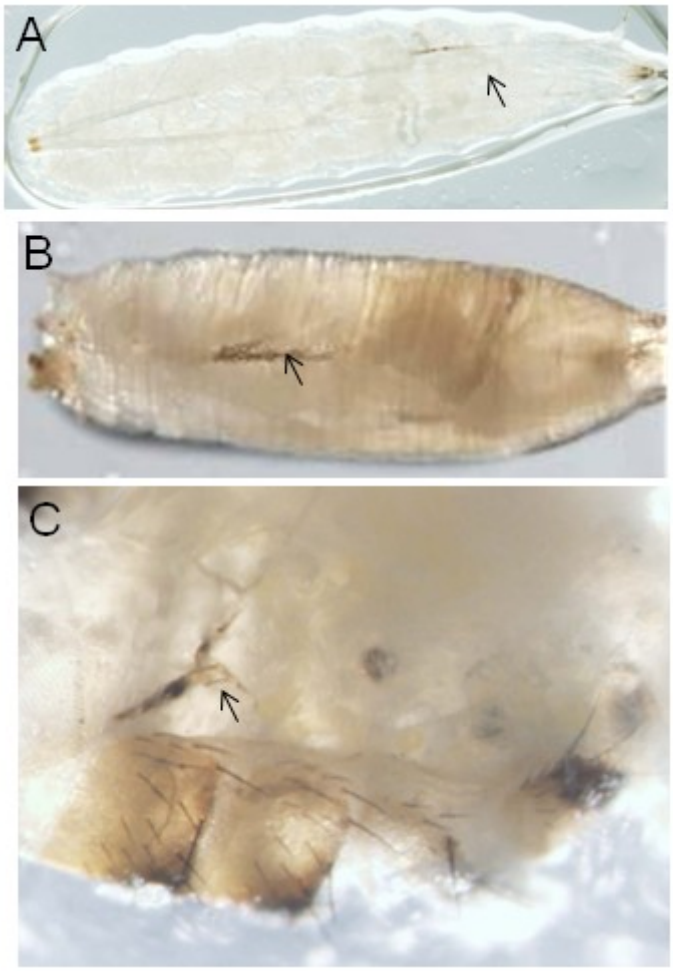

Figure 3-51: Melanization of the trachea did not affect viability. Ectopic expression of dFoxO with the tracheal specific PPK4-Gal4 driver resulted in tracheal melanization in larvae **(A)**, pupae **(B)** and adults **(C)**. It did not influence viability of the fly.

Animals were able to rescue the effect of dFoxO activation and were able to form normal generation cycle without any delay.

3.11.3 Activation of dFoxO in the respiratory system triggers phenol oxidase activity required for melanin biosynthesis

The key enzyme in the melanin biosynthetic pathway of the trachea is phenol oxidase (PO). To ensure that these blackish spots are really products of melanin and produced due to an increase in PO activity, an *ex vivo* trachea assay using L-DOPA was performed. Dorsal tracheal trunks were dissected from wildtype w^{1118}, PPK4-Gal4::UAS-dFoxO and PPK4-Gal4::UAS-dFoxO-GFP larvae and presoaked in L-DOPA. Animals of PPK4-Gal4::UAS-dFoxO were used to exclude tracheal melanization resulting from influence of GFP. After one hour of incubation, trachea from PPK4-Gal4::UAS-dFoxO and PPK4-Gal4::UAS-dFoxO-GFP, but not the control larvae, were strongly melanized, indicating a higher than normal level of PO activity (**Figure 3-52**). These results suggest that dFoxO is required to exhibit PO activity in trachea.

Figure 3-52: Phenol oxidase activity assay. PO activity was assayed ex vivo using dissected larval trachea incubated in L-DOPA solution. Trachea from wild-type (wt) larva showed no detectable melanization (**A**), but trachea from PPK4-Gal4::UAS-dFoxO-GFP and PPK4-Gal4::UAS-dFoxO showed significant melanization, indicating a high level of PO activity (**B-C**).

3.11.4 dFoxO - a possible regulator of tracheal melanization

It was reported that the serine-protease inhibitor Spn77Ba is the regulator for tracheal melanization. Until now there is no information available how this serpin is getting controlled by upstream regulators. The dFoxO transcription factor, which is characterized by a distinct forkhead DNA-binding domain, is characterized as a central regulator of many target genes involved in metabolism, life span, cell cycle, growth, and stress resistance.

In order to unravel, if dFoxO can function as a regulator of tracheal melanization and whether it could serve as a direct regulator of the serine protease inhibitor Spn77Ba, the promoter region of the serpin was examined in order to find potential binding sequences for dFoxO.

A putative binding site for dFoxO was found nearby the predicted promoter of Spn77Ba, at -462-470 of 8 bp **(Figure 3-53)**.

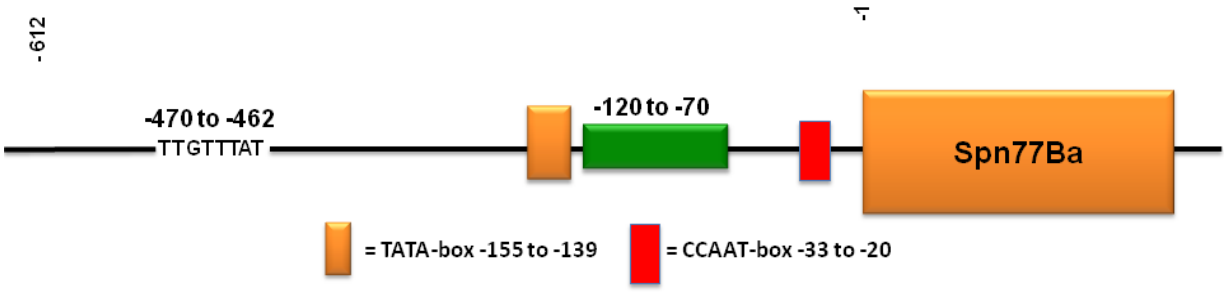

Figure 3-53: Schematic representation of the putative promoter region and translational start of Spn77Ba. The predicted putative promoter of the serpin is shown in green. An 8 bp long dFoxO binding motif was found upstream to the promoter. An enhancer binding protein, CCAAT, was predicted by the transcription factor binding site analysis software.

To confirm an *in vitro* binding of the dFoxO DNA-binding domain to this predicted dFoxO binding motif (**Figure 3-54A**), an electrophoretic mobility shift assays were performed. A clear shifting was visible (**Figure 3-54 B**).

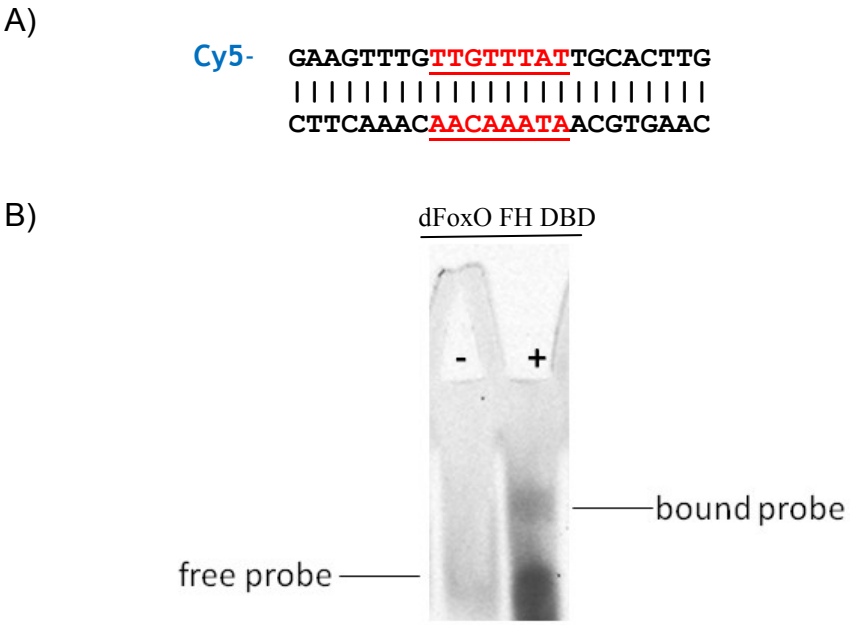

Figure 3-54: EMSA of dFoxO with the promoter of Spn77Ba. A) EMSA was applied in order to detect an *in vitro* binding of dFoxO DBD to a dFoxO binding motif within the Spn77Ba promoter. Approximately 250 ng of overexpressed and purified dFoxO protein was mixed with double stranded, labeled probe of the dFoxO binding motif. **B**) FoxO was readily binding as demonstrated by clear shifting.

4. Discussion

4.1 Modeling of COPD in the airway epithelium of *D. melanogaster*

The goal of this study was to unravel if *Drosophila* could be used as a COPD-model. This work presents one of the first reports for using *D. melanogaster* as a model organism to study the direct effects of cigarette smoke as the major risk factor for COPD. Mice, rat and guinea pigs serve as models of COPD. Nevertheless, some limitations of these models hinder the progress in our understanding of the pathogenesis, such as the complex interplay between the natural and adaptive immune responses, time consuming handling of transgenic mice to obtain COPD-phenotypes and their genetic redundancy. Therefore, simple models such as the nematode *C. elegans* (Green et al, 2009) and especially the fruit fly *Drosophila melanogaster* are considered as new models, enabling very fast and broad insight of the physiological role and function of COPD-genes and their effects on the airways. In contrast to human epithelial cell culture, which has limitations, primarily those of any *in vitro* model, *D. melanogaster*, as an *in vivo* system, can be subjected as whole animal to cigarette smoke exposure. The current work highlights the advantages of the fruit fly *Drosophila* to model COPD-like phenotypes, over two other model organisms **(Table 4-1)**. Although the fruit fly *Drosophila* has not been used previously as a smoking model for COPD research, it possess potential aspects for analyzing COPD-related target genes in the airway epithelium, except for those associated with the adaptive immune system. Moreover, the airways of the fruit fly share a comparable organ composition with striking similarities to vertebrates with respect to its physiology and reaction towards pathogens and other biotic stimuli (Wagner et al, 2008). In contrast, the invertebrate *C. elegans* model lacks an respiratory system and can only absorb chemicals from CS by converting nicotine into cotinine (Green et al, 2009).

Beside the remarkably decreased life span after exposure to cigarette smoke, *D. melanogaster* has shown several COPD-related phenotypical features (**Section 4.3, Table 4-2**).

Table 4-1: Comparison of Mouse, *C. elegans* & *Drosophila* as models in COPD research.

	Drosophila melanogaster	*Mouse*	*C. elegans*
Able to launch an immune response?	+++ innate immunity	+++ innate + adaptive immune system	+++ innate immune system (e.g. toll-like receptors, defensin-like proteins)
Speed and flexibility	+++ short life cycle, easy handling launching immune response quick	+ time consuming handling, mice require months to develop mild emphysema	+++ easy handling and short generation time
Complexity	+++ ease of genetic manipulation (Gal4-UAS system) & direct analysis of expected phenotypes possible	- generation of specific knockout and over expression studies of target genes is time consuming	++ easy to handle, simple anatomy, but less genetic tools
Genetic redundancy	+++ less genetic redundancy, direct identification of gene function possible	+ impairs the direct identification of gene function, complex task to distinguish between responses of adaptive and innate immune system	++ less genetic redundancy, but few similarity to human (ortholog genes)
Lung structure compared to human	++ lungs and tracheal system are not homologous, however comparable organ composition terminal branches = analogue to bronchioles	+++ consists of a complete lung structure, but is not identical to human, much less airway branching and no respiratory bronchioles => does not develop small airway disease	- lacks both: specialized respiratory systems and complex circulatory organs

legend: "+" - normal, "++" - advantageous, "+++" - highly advantageous, "-" - disadvantage

4.1.1 Activation of the JAK-STAT pathway as an autocrine signaling after CSE?

Until now very little is known about the early disease related response and other involved mechanisms caused by cigarette smoking. To unravel these mechanisms, the situation of cigarette smoking in the airway epithelium of the fruit fly *D. melanogaster* was mimicked.

Firstly, the current study has shown that the tracheal airway epithelium of 3rd instar larvae responds to cigarette smoke exposure. It was shown that activation of JAK-STAT signaling occurred at the posterior end of the dorsal branches of the airways as an early response towards smoke, by utilizing the 10 x STATDGFP reporter. The higher expression at the dorsal branches indicates that the windpipe in human could be the first organ of the lung system to be affected and that JAK-STAT signaling is mediating its cytokine release and activation especially at this part. Turetz et al. also showed that different regions of the airways respond in different ways towards CSE. In their studies they have shown that the trachea epithelium is more sensitive to the stress of smoking than the small airways (Turetz et al, 2009). In this study, JAK-STAT signaling is one of the important signaling mechanisms in response to cigarette smoke. In fact, recent studies have also demonstrated that JAK-STAT signaling is significantly increased in COPD patients (Chen et al, 2014; Ghosh et al, 2015; Yew-Booth et al, 2015). Furthermore Victoni *et al.* also found an activation of JAK/STAT pathway by stimulation of A549 epithelial cells after exposure to cigarette smoke (Victoni et al, 2014). Nicotine-induced JAK2/ STAT3 activation in oral keratinocytes was investigated by Arredondo et al (Arredondo et al, 2006).

Secondly, it was found that the exposure to cigarette smoke modulates gene expression of upd2 and upd3 but not that of upd, reflecting functional differences between these three cytokines. However, ectopic expression of upd and upd3 in the trachea possess the same phenotype leading to thickening of the airway epithelium. The colocalized expression of upd2 and upd3 after CSE suggests that they take related roles in response to cigarette smoking, most likely by triggering an inflammatory-like response. Upd2 and upd3 can activate the transmembrane signal transducing receptor domeless thus generating active STAT92E. The overlapping expression pattern of the major JAK-STAT components upd2, upd3, the cytokine receptor domeless and the GFP expression of 10XSTAT92E-DGFP may indicate that JAK-STAT signaling is getting activated as an early response towards cigarette smoke in the trachea in an autocrine fashion **(Figure 4-1)**. Moreover, the transcriptional activation of upd2 and upd3 at 48 h CSE is higher than after 24 h CSE, which indicates that the activation depends on the cigarette dosage.

The exact orthologs of the cytokines upd, upd2 and upd3 still remain unknown and their presence is still limited to the *Drosophila* genome as illustrated by Bayesian analysis. However, structural comparisons of upd3 to a known crystal structure of IL-6 demonstrate a similar pattern of helices. Oldefest *et al*. has also described upd3 as an ancestor of the four-helix bundle cytokines (Oldefest et al, 2013). Detailed analyses were undertaken for IL-6 and its role in lung injury and inflammation induced by cigarette smoke in mice (Halappanavar et al, 2009).

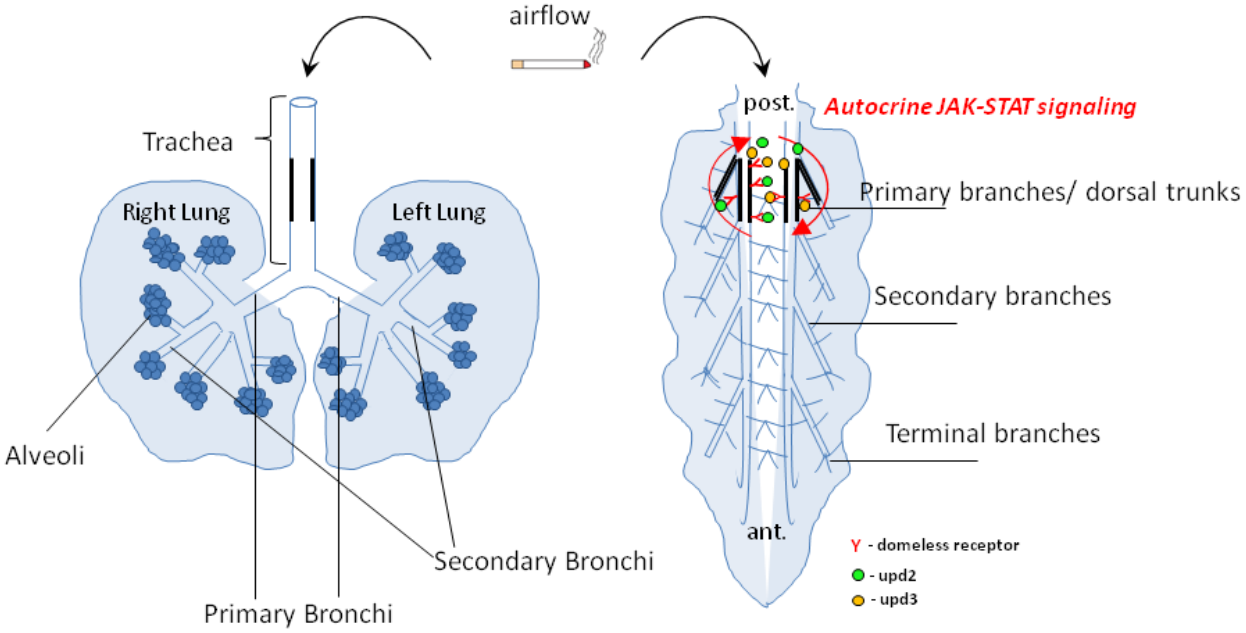

Figure 4-1: Activation of JAK-STAT signaling in *Drosophila* in comparison to human lung. JAK-STAT signaling was found to be one of the major signaling pathways in the fly's airways in response to cigarette smoke. The posterior ends of the dorsal branches were affected most probably in form of an autocrine cell signaling. Therefore our hypothetical model could be that upd2 and upd3 (as autocrine agents) are getting expressed, secreted and bound to the autocrine receptor domeless in the same affected region which finally leads to activation of JAK-STAT pathway in the trachea after CSE. In comparison to human lung it could be possible that JAK-STAT signaling is getting activated in the smokers windpipe (black line).

Sustained activation of JAK-STAT signaling is causal to human cancers and its dysregulation has been linked to several tumors in *Drosophila* (Amoyel et al, 2014). For example frequent over activation of STAT3 and STAT5 promotes a variety of tumors and blood malignancies in human and hyper activation of HOP/ STAT92E pathway which results in melanonic or leukemia-like tumor formation in larvae and adult flies (Dearolf, 1998; Hanratty & Dearolf, 1993). Activated nuclear STAT has been detected in many forms of chronic inflammation-associated diseases, including lung cancer (Wu et al, 2014). This work has presented a detailed molecular analysis of the upd-like ligands of the JAK-STAT pathway and has shown that upd2 and upd3 act in a similar fashion after CSE. Taken together, the observed expression of JAK-STAT signaling is indicative for the first response to cigarette smoke in the tracheal epithelium and that its activation is restricted to the dorsal branches.

4.1.2 Role of redox-regulated transcription factors in the CSE-associated responses

Injury of the epithelium by CSE smoke takes place due to enhanced expression of pro-inflammatory mediators through redox-sensitive transcription factors e.g. nuclear NF-κB (Barnes & Karin, 1997; Di Stefano et al, 2002; Edwards et al, 2009). Innate immune pathways that converge on activation of NF-κB factors are of more central importance for various aspects of disease development and progression (Pantano et al, 2008).
The activation of the fly's NF-κB ortholog relish was shown in cigarette smoke exposed *Drosophila* larvae by nuclear translocation. This result demonstrates the physiological function and importance of the immune deficiency (IMD)-pathway (which is homologous to the TNF-α pathway in human) as one signaling pathway involved in the response to cigarette smoke and disease. Works on guinea pigs have also shown an increased NF-κB nuclear binding after CSE in the airway epithelial cells and that it is associated with enhanced gene expression and protein release of pro-inflammatory cytokines (Nishikawa et al, 1999). Nishikawa *et al*. demonstrated an increased IL-8 gene expression and NF-kB activation in a guinea pig model after CSE. It is known that many inflammatory mediators present in COPD lungs can be induced via the actions of NF-κB. Moreover, NF-κB is constitutively active in most tumors and chronic inflammatory conditions (Wu et al, 2014). In contrast, Rastrick *et al*. showed that NF-κB/IKK-2 does not play a prominent role in the inflammatory response to CSE and its importance for COPD pathogenesis is only minor (Rastrick et al, 2013).

FoxO3 is another transcription factor, which has been shown to modulate oxidative stress (Kops et al, 2002; Marinkovic et al, 2007). This study has shown that the *Drosophila* dFoxO is involved in the cigarette smoke regulated response via an induced translocation into the nucleus. The exact role of FoxO3 in cigarette smoke (CS)-induced lung inflammation and injury has not been studied yet. Thus, the pivotal role of dFoxO was examined under physiological and CS conditions, using flies deficient in this transcription factor. Survival assays could not show that flies deficient in dFoxO possess an increased susceptibility when compared to CSE wild type flies, like it was reported for CS-induced mice deficient in FOXO3 (Hwang et al, 2011). Flies deficient in dFoxO show similar survival curves compared to wild type flies after CSE and it seems they were able to tolerate CSE slightly better. Airspace enlargement or other structural changes within the airway epithelium of CS-exposed dFoxO deficient larvae were not detected, like it was reported for mice (Hwang et al, 2011). It is well known that variation in the FOXO3A gene is associated with longevity (Anselmi et al, 2009;

Flachsbart et al, 2009; Li et al, 2009; Pawlikowska et al, 2009; Soerensen et al, 2010; Willcox et al, 2008) and also plays a role in lung cancer (Herzog et al, 2009) (Mikse et al, 2010) (Yang & Hung, 2009). However, Däumer *et al*. found that smoking does not alter the FOXO3A association with longevity (Daumer et al, 2014).

Interestingly, this work identified the transcription factors relish and dFoxO as possible potential upstream regulators of the cytokine-like upd2 and upd3. Cigarette smoke mediated induction of upd2 and upd3 was significantly decreased in dFoxO- deficient flies. Furthermore, EMSA analysis underlines the potential up-stream regulatory role of dFoxO for upd2 and upd3 through its direct DNA-binding to conserved binding motifs within their promoters **(Figure 4-2)**.

Figure 4-2: Alignment of dFoxO binding motifs within the promoter regions of upd2 and upd3. Essential nucleotides of the conserved binding motifs for binding of dFoxO are in red color.

However, qRT-PCR analysis has shown that in relish deficient flies, the transcript levels of upd2 and upd3 were also down-regulated, but not as strong as in dFoxO deficient animals. The fact that transcription of upd2 and upd3 was detected in relish deficient larvae, indicates that dFoxO is still functional in those animals.
For upd no binding motifs, neither for relish nor dFoxO, were found within its promoter. This correlates with the observation that qRT-PCR analysis did not show any transcription of upd. Also there was no expression detected by X-Gal staining after CSE, indicating that upd is not taking part in the dFoxO-mediated response towards cigarette smoke.

One way to activate dFoxO is via the JNK pathway, suggesting that this pathway may be active after CSE. To unravel if the JNK-pathway is involved, a specific puckered reporter-Gal4 line was mated to either LacZ-UAS or UAS-GFP (data not shown) (Adachi-Yamada, 2002). However, there was no detectable GFP expression or beta-galactosidase production in CS-treated animals, which gives a first indication that JNK signaling is maybe not operative for activation of dFoxO in the smoke responsive manner. Also the utilization of a reporter system with AP-1 responsive TRE elements for monitoring JNK-activity (Chatterjee & Bohmann, 2012) did not give any valuable signals. In future experiments it should be verified by qRT-PCR that JNK pathway is not getting activated on CSE.

Another possible way for activation of dFoxO is via the the phosphatidylinositol 3-kinase/Akt pathway. It plays an important role in directly phosphorylating and inhibiting transcription factors of the forkhead family (Brunet et al, 1999; Kops et al, 1999). Therefore, a decreased phosphorylation of Akt and that of dFoxO could be possibly the reason for increased nuclear accumulation of dFoxO and its binding to upd2 and upd3. Kortylewski et al. also demonstrated a crosstalk of Akt signaling and IL-6 inducible JAK/STAT3 signal transduction (Kortylewski et al, 2003). The following figure shows the proposed pathways for upd2 and upd3 expression after CSE, based upon the findings of this work (**Figure 4-3**).

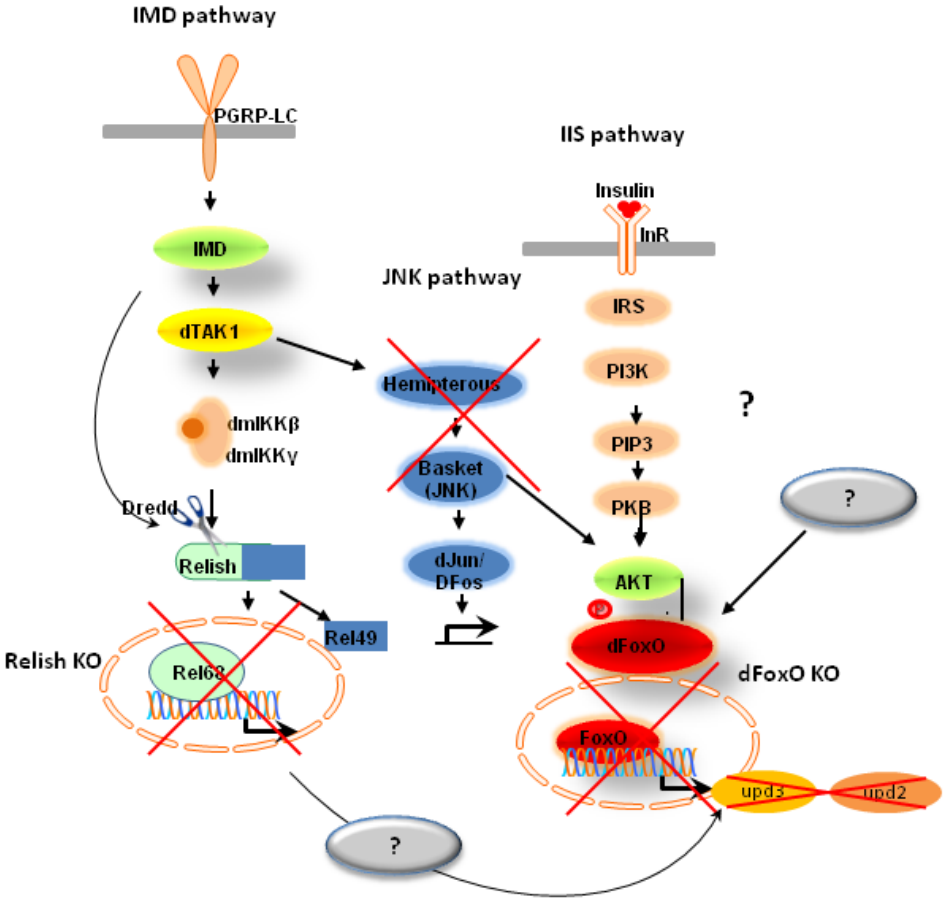

Figure 4-3: Regulatory pathways for upd2 and upd3 expression after CSE. A nuclear translocation of dFoxO and relish was observed after CSE. Deficiency of relish and dFoxO TF (red crosses) had a negative effect on the transcription levels of upd2 and upd3. Animals deficient in dFoxO have shown a strong decrease in transcription levels of upd2 and upd3. A direct binding between the TF-dFoxO and the promoters of upd2 and upd3 was observed. There was no activation of the JNK-pathway after CSE. Therefore it is very likely that dFoxO activation happens through the insulin triggered IIS-pathway or a yet unknown mechanism.

This is a new finding, which was not reported to date and it indicates that there is an existing crosstalk of dFoxO, JAK-STAT signaling and the IMD pathway in this cigarette smoke related response. This finding could be also interesting for studies working with vertebrates, in exploring the role of IL-6 in vertebrate species (e.g. mice) and to check whether transcription factors like FoxO or NF-κB are also regulating them after CSE.

STAT is another redox-sensitive transcription factor that serves as a molecular switch between inflammation and cancer (Darnell et al, 1994; Grivennikov & Karin, 2010). It was reported that STAT3 supports oncogenesis via binding to promoter regions of genes encoding inflammatory and cell cycle regulatory proteins (Yu et al, 2009; Zhong et al, 1994). In this study, translocation of STAT92E into the nucleus is most probably getting induced via activation of JAK-STAT signaling by binding of the extracellular ligands upd2 and upd3, whereas not by upd. In addition, there is increasing evidence that effective inhibitors of pro-inflammatory chemokines and cytokines are beneficial for persons who have COPD (Proudfoot 2002; Lukacs et al. 2005) and that targeting of cytokines, e.g. IL-6 and several signal transduction pathways, including JAK-STAT and Ras has been proposed to inhibit the inflammatory pathways in COPD (Roxburgh & McMillan, 2015; Schleimer, 2005).

Furthermore, this study has illustrated the activation of Nrf2 signaling in the fly's airways after CSE. Although the transcription factor Nrf2 was shown to be involved in preventing cigarette smoke- dependent lung disease (Kelsen et al, 2008), no direct evidence has been shown that smoke of cigarette is sensed by the Nrf2 activation and till now the data is partly inconsistent (Brigelius-Flohe et al, 2012; Muller & Hengstermann, 2012). This work demonstrates that the *Drosophila's* ortholog cncC (cap'n'collar) is involved in the response to oxidative stress of smoke as shown by GFP accumulation inside the nucleus. Thus, Nrf2/cncC is getting activated after exposure to CS and is therefore important for further transcriptional control of its target genes. Further, fly lines carrying Nrf2-inducible ARE elements were tested. However, no reproducible GFP signals were detected after CSE (Chatterjee & Bohmann, 2012). Still it is unclear whether the problem has to do with the reporter fly line and therefore qRT PCR experiments could be applied to address this issue in future and to confirm transcript levels of Nrf2/ cncC after CSE.

The *GstD1* gene encodes a glutathione-S-transferase which was found to be expressed in response to cigarette smoke as demonstrated by the Gst-D-GFP reporter line. GstD. It is important for the detoxification of xenobiotics and normally activated via the Keap1/Nrf2 signaling pathway (Ma, 2013; Sykiotis & Bohmann, 2008). Gst is induced in *Drosophila* during normal aging and when the flies are challenged with oxidative stress, fluctuations in redox state and electrophilic xenobiotics (Landis et al, 2004; Sykiotis & Bohmann, 2008; Zou et al, 2000). The Gst-D1 promoter region contains consensus-binding motifs for Nrf2 and dFoxO (Landis et al, 2012). In upcoming works it would be interesting to investigate, if Gst-D expression is exclusively mediated by Nrf2/ cncC, dFoxO or both.

4.1.3 Airway remodeling as a response to CSE

Chronic obstructive pulmonary disease (COPD) is characterized by extensive thickening of the airway epithelium leading into progressive and poorly reversible airflow limitation and airway distensibility (Jeffery, 2004; Postma & Timens, 2006).

Interestingly, this phenomenon of a physiologic abnormality of the airway epithelium was observed in smoke exposed animals. The epithelial layer of cigarette smoke exposed trachea was significantly thicker than in control animals. However, little is known, if thickening has a negative impact on lung function, by increasing airflow limitation or if it may serve as a protective mechanism by increasing the stiffening of the airway wall to attenuate the sporadic broncho constriction (Holgate et al, 2000; Holgate et al, 2003; Holgate et al, 2004; Pare et al, 1997; Wang et al, 2003; Ward et al, 2001). This work unraveled JAK-STAT signaling in response to cigarette smoke as an important pathway that may play a role in the pathogenesis of COPD. Several findings provide evidence that an altered airway structure has negative effects rather than playing a protective role. This study demonstrated that ectopic expression of the members of JAK-STAT signaling results into structural remodeling.

Ectopic expression of upd, upd3 or hopscotch caused epithelial hyperplasia and metaplasia in the airways and ectopic expression of the constitutive active form of domeless affected negatively on the cell size of the epithelial cells.

It was also shown in mouse lung that over expression of two closely related cytokines interleukin-6 (IL-6) and 11 leads into thickening of airway walls and sub-epithelial airway fibrosis (Kuhn et al, 2000). Works of Ochoa *et al.* describes that IL-6 promotes lung carcinogenesis and histopathologic analysis of IL-6 KO mice revealed less extensive lesions of hyperplasia (Ochoa et al, 2011). This is the first study demonstrating airway remodeling in *Drosophila* initiated by CSE and that the injured cells release cytokines at the site of injury, which could be the cause for thickening after their activation. Thus, for future works it would be of high interest to find out, if epithelial thickening occurs in upd-deficient animals after application of CSE.

4.1.4 A possible dFoxO- mediated signaling cascade

Molecular as well as functional analyses of possible candidate genes helped in gaining insight of the underlying CSE-mediated mechanisms. A possible signaling cascade mediated by dFoxO is presented in **Figure 4-4**. Taken these results under consideration one can draw the following model: CSE serves as an inflammatory stressor which leads into activation of JAK-

STAT signaling in the airways. A yet unknown upstream regulator or signaling pathway is expressing and activating the transcription factor dFoxO. DFoxO then directly binds to conserved dFoxO-binding motifs within the promoters of upd2 and upd3 as shown by Bandshift-analysis. Thus, JAK-STAT activation by CSE is mediated by local upd2 and upd3 expression whereas not by upd.

This high up-regulation of these cytokines may result in a strong and fast activation of JAK-STAT signaling and an abnormal stress response. This could be the cause for airway remodeling in the form of hyperplasia. It resembles pathotypes seen in COPD patients. Moreover, these results indicate a new crosstalk of JAK-STAT signaling and the transcription factor dFoxO, which may be operative for CSE induced structural changes in the trachea.

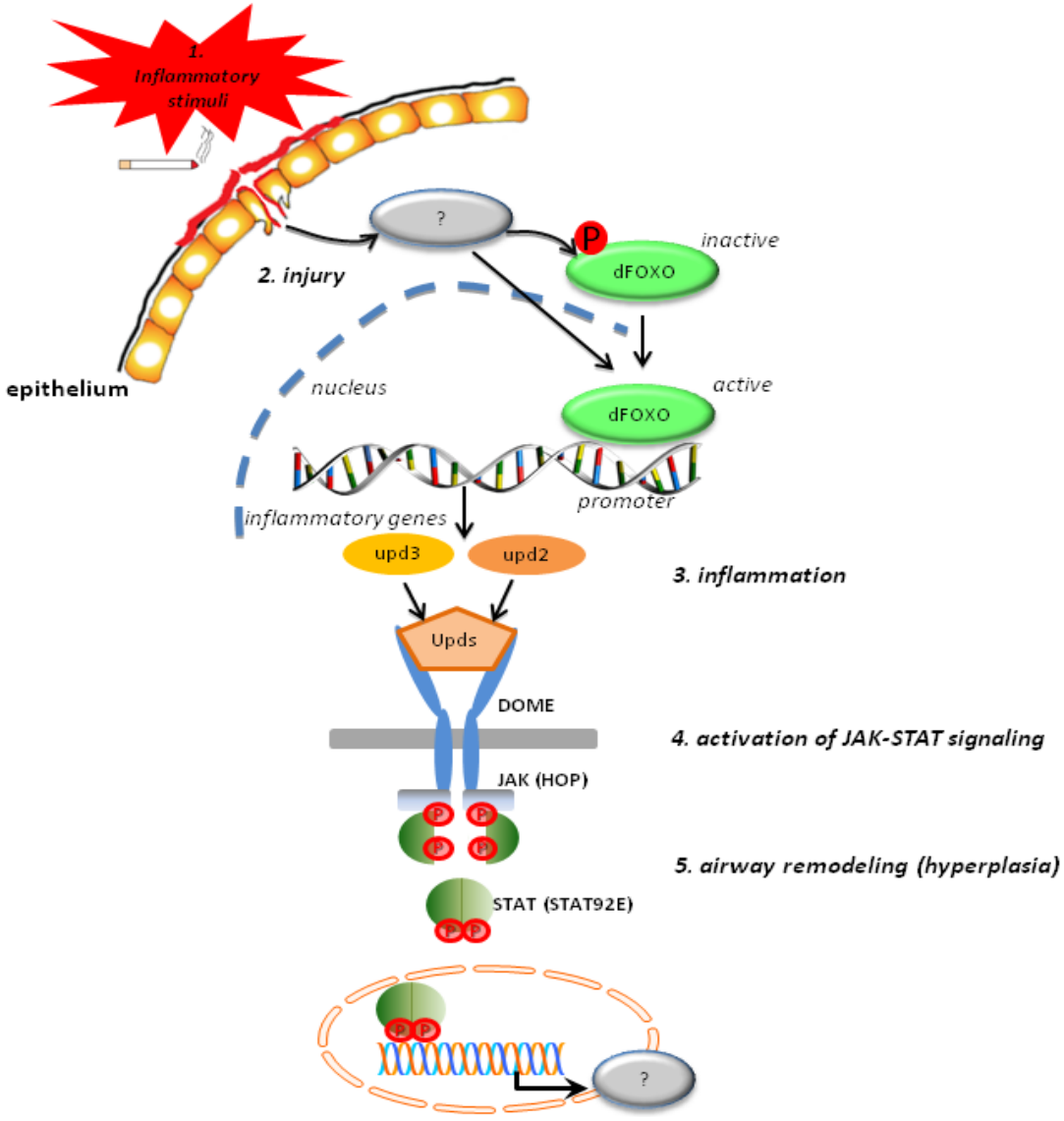

Figure 4-4: Proposed dFoxO dependent activation of JAK-STAT signaling after CSE. CSE activates JAK-STAT signaling in the airway system of the fly. dFoxO binds to conserved dFoxO binding motifs within the promoters of upd2 and upd3. JAK-STAT activation is mediated by local upd2 and upd3 expression, but not by upd. Activation of JAK-STAT signaling in the airway epithelium cause airway remodeling in the form of hyperplasia.

4.2 Utilization of bPAC to study cAMP signaling in the airways of *D. melanogaster*

Current findings of this work show novel effects of cAMP signaling and thus contribute to a better understanding of airway diseases. Up to date only little is known about how alterations and higher intracellular cAMP levels effect the respiratory system (Billington & Hall, 2012). Normally, an increase in intracellular cAMP reduces smooth muscle tone, thus dilating the airways. Moreover, it plays a key role in the functions of many airway cells including controlling ciliary beat frequency (critical for mucus clearance) (Salathe, 2002) and suppressing the pro-inflammatory activity of various immune and inflammatory cells. However, it is arguably the inhibitory effect of increased cytosolic cAMP levels on the contraction of ASM cells (Billington et al, 2013). It has been reported that cAMP leads to up-regulation and release of cytokines and chemokines such as IL-6, IL-8, and GM-CSF (Ammit et al, 2000; Lazzeri et al, 2001; Pang & Knox, 2000). Thus cAMP can have both, pro- and anti-inflammatory effects on ASM cell function.

It has been shown that cAMP dependent effectors like protein kinase A (PKA) negatively regulate serum response factor (SRF) activity, a crucial transcription factor impacting smooth muscle cell differentiation including that of ASM cells (Davis et al, 2003; Liu et al, 2003a; Miano et al, 2007). Similar effects were shown for the vascular smooth muscle cells that PKA negatively regulates SRF and inhibits differentiation (Blaker et al, 2009; Davis et al, 2003). The *Drosophila* serum response factor (DSRF) homolog is expressed in the precursor cells of terminal trachea. This work has shown that high levels of cAMP activity may have negative impact on the expression of the blistered/DSRF gene in the airway system, which in turn results in this impaired branching of the terminal branches. Thus, the current study shows that cAMP might be an important second messenger for terminal branching.

Triggering such high concentrations of cAMP within the respiratory system created a tissue-degrading phenotype. This destruction of terminal branching in the airways of the fly resembles the pathotype seen in human during COPD pathogenesis. This finding also demonstrates that the right dose of medication, e.g. asthma inhalers for asthma and COPD patients, is very crucial. Kume *et al*. highlighted this disparity by quantifying both airway relaxation and cAMP production of tracheal strips of horses in response either to forskolin (a direct activator of AC) or to isoprenaline (a non-selective β-adrenoceptor agonist) (Kume et al, 1994). Both agents were able to induce airway relaxation but interestingly forskolin induced twice as much cAMP production as isoprenaline. This emphasizes the importance of a fine tuned regulation of this second messenger within the airways.

In this work, a high cAMP production by blue-light induced bPAC is above the basal norm concentrations leading into defects of tracheal branching. Possibly it affected the expression and activity of DSRF via activation of PKA in the terminal branches. This result is similar to the finding of Mattila *et al*., where the authors describe dFoxO to regulate the expression of another AC, the AC76E, which also regulates cAMP-levels. The expression of AC76E had a remarkable effect on pupa formation, size (limits growth) and stress resistance (Mattila et al, 2009), similarly like it was observed after bPAC activation. These results show that in *Drosophila* ACs play a role in regulation of growth of several tissues.

Further I have demonstrated that blue-light activation of bPAC resulted into translocation of dFoxO into the nucleus. Additionally, higher cAMP levels had an impact on tracheal melanization. Thereby it could be possible that the translocated dFoxO functioned as an initiator for this melanization cascade by binding to a dFoxO binding motif within Spn77Ba, leading to inhibition of this serpin and thus starting melanin biosynthesis. A proposed regulation cascade is shown in **Figure 4-5.**

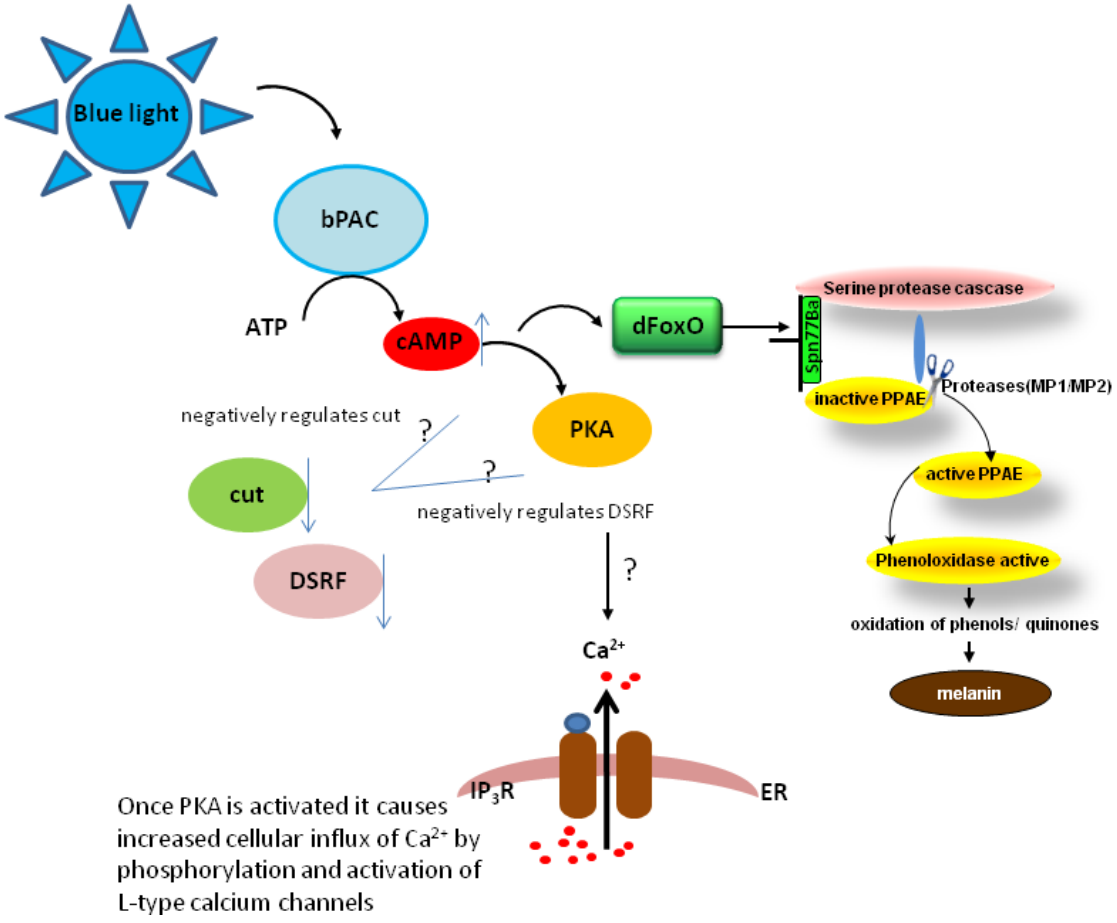

Figure 4-5: Proposed model of cAMP- dependent inhibited differentiation of the terminal branches. Activation of bPAC in the respiratory system of the fly increases cAMP levels and cAMP dependent effectors like protein kinase A (PKA) which may negatively regulate DSRF and the TF cut, leading to inhibited branching. Tracheal melanization could be possible via the cAMP/dFoxO pathway. Moreover, activation of cAMP/PKA by bPAC may lead to activation of calcium channels releasing Ca^{2+} into the cytoplasm.

It could be possible that an activation of such high cAMP levels could lead to parallel activation of Ca^{2+}-signaling via PKA in the airway epithelium of the fly. Kamp *et al*. has shown a regulation of calcium channels through the cAMP/PKA pathway (Kamp & Hell, 2000). Dixon *et al*. addressed that an elevation of free intracellular Ca^{2+} via L-type voltage-gated calcium channels is associated with contracted and tightened ASM cells (Dixon & Santana, 2013).
It was observed for few animals that expression and activation of the DREADD receptor M1D1 (for increasing Ca^{2+} in the airway epithelium), resulted into a similar phenotype seen in animals expressing bPAC. The epithelial cells of the trachea were compressed and their cell number got increased (**Appendix 7.7, Figure 7-10**).

4.3 Limitations and challenges using the fruit fly as COPD-model

While many previous studies have used *D. melanogaster* to study the innate immune response (Pandey & Nichols, 2011), this one of the initial studies to expose *D. melanogaster* to CS. The fruit fly has provided valuable insight about cigarette smoke- induced altered host defense mechanisms of the airways on molecular as well as on structural level. The experimental approach to model COPD within the fruit fly's airways was by direct inhalative challenge to CSE (Cohen & George, 2013). However, COPD pathology occurs normally after a long period of heavy smoking, thus exposure of cigarette smoke on 3rd instar larvae does not replicate the entire complexity of this disease and can only give an insight of early disease development leading to COPD (Petty & Rennard, 2000). Interestingly, major features of COPD we were able to model within the respiratory tract of the fly (**Table 4-2**). Nevertheless, cigarette smoke had only less impact on the morphology of the terminal branches. The missing emphysema development, in form of terminal cell destructions or other alterations, could be explained by the short duration of exposure of the larvae (Leberl et al, 2013). Another limitation is the missing mucus hyper secretion in the larvae's trachea. Airway secretory cells such as clara cells and goblet cells, which are important for mucus production in the human lung endothelium, are not present in the fruit fly's airways.

Table 4-2: COPD-features in the airways of *D. melanogaster* after CSE

COPD-Feature	
Airway remodeling in form of a thickened epithelial layer	+
Highly up-regulation of JAK-STAT signaling	+
Oxidative stress, indicative by redox-sensitive transcription factors	+
Reduced lifespan	+
Emphysema (small airways narrowing)	- (?)
Mucus production (sputum)	-
Cough / squeezing	-

However, the current challenge in COPD research is to identify molecular mechanisms that are involved in this pathophysiology. These understanding will help to unravel the effects of smoking and assist to the development of new treatments.

This study could unravel important signaling pathways and key enzymes after CSE in the fruitfly, which were reported to mediate acute cigarette smoke-induced inflammation in human. Therefore *D. melanogaster* offers a novel model to exclusively investigate the role of the innate immunity in host defense after cigarette smoke exposure.

5. Conclusion

The results of this current work suggest that the model organism *D. melanogaster* offers a novel *in vivo* approach to specifically study innate immune deficiencies resulting from exposure to cigarette smoke. This study paves paths for the establishments of *D. melanogaster* as a model for basic COPD research with developments on various CSE models using 3rd instar larvae of *D. melanogaster.* This work investigated the *in vivo* impact of CSE, primarily in the tracheal epithelium. After CSE the examination of expression patterns of upd ligands revealed a differential patterning. The induction of upd2 and upd3 transcripts was significantly upregulated in wildtype but strongly reduced in dFoxO deficient flies. This work depicts that cigarette smoke leads to structural remodeling including thickening of the epithelial layer in parallel with activation of JAK/STAT signaling, potentially mediated by dFoxO. Thus, these findings provide a novel crosstalk of JAK-STAT signaling and dFoxO in the trachea.
Finally, this work also illustrates an induced destruction of the terminal airway structure after strong activation of cAMP signaling in the airways of *D. melanogaster*.

6. References

Adachi-Yamada T (2002) Puckered-GAL4 driving in JNK-active cells. *Genesis* **34:** 19-22

Adams MD, Celniker SE, Holt RA, Evans CA, Gocayne JD, Amanatides PG, Scherer SE, Li PW, Hoskins RA, Galle RF, George RA, Lewis SE, Richards S, Ashburner M, Henderson SN, Sutton GG, Wortman JR, Yandell MD, Zhang Q, Chen LX, Brandon RC, Rogers YH, Blazej RG, Champe M, Pfeiffer BD, Wan KH, Doyle C, Baxter EG, Helt G, Nelson CR, Gabor GL, Abril JF, Agbayani A, An HJ, Andrews-Pfannkoch C, Baldwin D, Ballew RM, Basu A, Baxendale J, Bayraktaroglu L, Beasley EM, Beeson KY, Benos PV, Berman BP, Bhandari D, Bolshakov S, Borkova D, Botchan MR, Bouck J, Brokstein P, Brottier P, Burtis KC, Busam DA, Butler H, Cadieu E, Center A, Chandra I, Cherry JM, Cawley S, Dahlke C, Davenport LB, Davies P, de Pablos B, Delcher A, Deng Z, Mays AD, Dew I, Dietz SM, Dodson K, Doup LE, Downes M, Dugan-Rocha S, Dunkov BC, Dunn P, Durbin KJ, Evangelista CC, Ferraz C, Ferriera S, Fleischmann W, Fosler C, Gabrielian AE, Garg NS, Gelbart WM, Glasser K, Glodek A, Gong F, Gorrell JH, Gu Z, Guan P, Harris M, Harris NL, Harvey D, Heiman TJ, Hernandez JR, Houck J, Hostin D, Houston KA, Howland TJ, Wei MH, Ibegwam C, Jalali M, Kalush F, Karpen GH, Ke Z, Kennison JA, Ketchum KA, Kimmel BE, Kodira CD, Kraft C, Kravitz S, Kulp D, Lai Z, Lasko P, Lei Y, Levitsky AA, Li J, Li Z, Liang Y, Lin X, Liu X, Mattei B, McIntosh TC, McLeod MP, McPherson D, Merkulov G, Milshina NV, Mobarry C, Morris J, Moshrefi A, Mount SM, Moy M, Murphy B, Murphy L, Muzny DM, Nelson DL, Nelson DR, Nelson KA, Nixon K, Nusskern DR, Pacleb JM, Palazzolo M, Pittman GS, Pan S, Pollard J, Puri V, Reese MG, Reinert K, Remington K, Saunders RD, Scheeler F, Shen H, Shue BC, Siden-Kiamos I, Simpson M, Skupski MP, Smith T, Spier E, Spradling AC, Stapleton M, Strong R, Sun E, Svirskas R, Tector C, Turner R, Venter E, Wang AH, Wang X, Wang ZY, Wassarman DA, Weinstock GM, Weissenbach J, Williams SM, WoodageT, Worley KC, Wu D, Yang S, Yao QA, Ye J, Yeh RF, Zaveri JS, Zhan M, Zhang G, Zhao Q, Zheng L, Zheng XH, Zhong FN, Zhong W, Zhou X, Zhu S, Zhu X, Smith HO, Gibbs RA, Myers EW, Rubin GM, Venter JC (2000) The genome sequence of Drosophila melanogaster. *Science* **287:** 2185-2195

Affolter M, Bellusci S, Itoh N, Shilo B, Thiery JP, Werb Z (2003) Tube or not tube: remodeling epithelial tissues by branching morphogenesis. *Developmental cell* **4:** 11-18

Agusti AG (2005) Systemic effects of chronic obstructive pulmonary disease. *Proceedings of the American Thoracic Society* **2:** 367-370; discussion 371-362

Altschul SF, Gish W (1996) Local alignment statistics. *Methods Enzymol* **266:** 460-480

Altschul SF, Gish W, Miller W, Myers EW, Lipman DJ (1990) Basic local alignment search tool. *J Mol Biol* **215:** 403-410

Altschul SF, Madden TL, Schaffer AA, Zhang J, Zhang Z, Miller W, Lipman DJ (1997) Gapped BLAST and PSI-BLAST: a new generation of protein database search programs. *Nucleic Acids Res* **25:** 3389-3402

Ammit AJ, Hoffman RK, Amrani Y, Lazaar AL, Hay DW, Torphy TJ, Penn RB, Panettieri RA, Jr. (2000) Tumor necrosis factor-alpha-induced secretion of RANTES and interleukin-6 from human airway smooth-muscle cells. Modulation by cyclic adenosine monophosphate. *American journal of respiratory cell and molecular biology* **23:** 794-802

Amoyel M, Anderson AM, Bach EA (2014) JAK/STAT pathway dysregulation in tumors: a Drosophila perspective. *Seminars in cell & developmental biology* **28:** 96-103

Anselmi CV, Malovini A, Roncarati R, Novelli V, Villa F, Condorelli G, Bellazzi R, Puca AA (2009) Association of the FOXO3A locus with extreme longevity in a southern Italian centenarian study. *Rejuvenation research* **12:** 95-104

Arbouzova NI, Zeidler MP (2006) JAK/STAT signalling in Drosophila: insights into conserved regulatory and cellular functions. *Development* **133:** 2605-2616

Arden KC, Biggs WH, 3rd (2002) Regulation of the FoxO family of transcription factors by phosphatidylinositol-3 kinase-activated signaling. *Archives of biochemistry and biophysics* **403:** 292-298

Armbruster BN, Li X, Pausch MH, Herlitze S, Roth BL (2007) Evolving the lock to fit the key to create a family of G protein-coupled receptors potently activated by an inert ligand. *Proceedings of the National Academy of Sciences of the United States of America* **104:** 5163-5168

Arredondo J, Chernyavsky AI, Jolkovsky DL, Pinkerton KE, Grando SA (2006) Receptor-mediated tobacco toxicity: cooperation of the Ras/Raf-1/MEK1/ERK and JAK-2/STAT-3 pathways downstream of alpha7 nicotinic receptor in oral keratinocytes. *FASEB journal : official publication of the Federation of American Societies for Experimental Biology* **20:** 2093-2101

Bach EA, Ekas LA, Ayala-Camargo A, Flaherty MS, Lee H, Perrimon N, Baeg GH (2007) GFP reporters detect the activation of the Drosophila JAK/STAT pathway in vivo. *Gene expression patterns : GEP* **7:** 323-331

Baker KD, Thummel CS (2007) Diabetic larvae and obese flies-emerging studies of metabolism in Drosophila. *Cell metabolism* **6:** 257-266

Barnes PJ, Drazen MJ, Rennard IS, Thomson CN (2009) *Asthma and COPD*: Academic Press; 2 edition.

Barnes PJ, Karin M (1997) Nuclear factor-kappaB: a pivotal transcription factor in chronic inflammatory diseases. *The New England journal of medicine* **336:** 1066-1071

Becker T, Loch G, Beyer M, Zinke I, Aschenbrenner AC, Carrera P, Inhester T, Schultze JL, Hoch M (2010) FOXO-dependent regulation of innate immune homeostasis. *Nature* **463:** 369-373

Becnel J, Johnson O, Majeed ZR, Tran V, Yu B, Roth BL, Cooper RL, Kerut EK, Nichols CD (2013) DREADDs in Drosophila: a pharmacogenetic approach for controlling behavior, neuronal signaling, and physiology in the fly. *Cell reports* **4:** 1049-1059

Bellen HJ, Levis RW, Liao G, He Y, Carlson JW, Tsang G, Evans-Holm M, Hiesinger PR, Schulze KL, Rubin GM, Hoskins RA, Spradling AC (2004) The BDGP gene disruption project: single transposon insertions associated with 40% of Drosophila genes. *Genetics* **167:** 761-781

Bellen HJ, Tong C, Tsuda H (2010) 100 years of Drosophila research and its impact on vertebrate neuroscience: a history lesson for the future. *Nature reviews Neuroscience* **11:** 514-522

Bergner A, Kellner J, Silva AK, Gamarra F, Huber RM (2006) Ca2+-signaling in airway smooth muscle cells is altered in T-bet knock-out mice. *Respiratory research* **7:** 33

Bier E (2005) Drosophila, the golden bug, emerges as a tool for human genetics. *Nature reviews Genetics* **6:** 9-23

Billington CK, Hall IP (2012) Novel cAMP signalling paradigms: therapeutic implications for airway disease. *British journal of pharmacology* **166:** 401-410

Billington CK, Ojo OO, Penn RB, Ito S (2013) cAMP regulation of airway smooth muscle function. *Pulmonary pharmacology & therapeutics* **26:** 112-120

Binari R, Perrimon N (1994) Stripe-specific regulation of pair-rule genes by hopscotch, a putative Jak family tyrosine kinase in Drosophila. *Genes & development* **8:** 300-312

Blaker AL, Taylor JM, Mack CP (2009) PKA-dependent phosphorylation of serum response factor inhibits smooth muscle-specific gene expression. *Arteriosclerosis, thrombosis, and vascular biology* **29:** 2153-2160

Bonnans C, Mainprice B, Chanez P, Bousquet J, Urbach V (2003) Lipoxin A4 stimulates a cytosolic Ca2+ increase in human bronchial epithelium. *The Journal of biological chemistry* **278:** 10879-10884

Brand AH, Perrimon N (1993) Targeted gene expression as a means of altering cell fates and generating dominant phenotypes. *Development* **118:** 401-415

Brigelius-Flohe R, Muller M, Lippmann D, Kipp AP (2012) The yin and yang of nrf2-regulated selenoproteins in carcinogenesis. *International journal of cell biology* **2012:** 486147

Brown S, Hu N, Hombria JC (2001) Identification of the first invertebrate interleukin JAK/STAT receptor, the Drosophila gene domeless. *Current biology : CB* **11:** 1700-1705

Brown S, Hu N, Hombria JC (2003) Novel level of signalling control in the JAK/STAT pathway revealed by in situ visualisation of protein-protein interaction during Drosophila development. *Development* **130:** 3077-3084

Brunet A, Bonni A, Zigmond MJ, Lin MZ, Juo P, Hu LS, Anderson MJ, Arden KC, Blenis J, Greenberg ME (1999) Akt promotes cell survival by phosphorylating and inhibiting a Forkhead transcription factor. *Cell* **96:** 857-868

Bulow MH, Aebersold R, Pankratz MJ, Junger MA (2010) The Drosophila FoxA ortholog Fork head regulates growth and gene expression downstream of Target of rapamycin. *PloS one* **5:** e15171

Burgering BM, Kops GJ (2002) Cell cycle and death control: long live Forkheads. *Trends in biochemical sciences* **27:** 352-360

Cerenius L, Soderhall K (2004) The prophenoloxidase-activating system in invertebrates. *Immunological reviews* **198:** 116-126

Chan HY, Bonini NM (2000) Drosophila models of human neurodegenerative disease. *Cell death and differentiation* **7:** 1075-1080

Chatterjee N, Bohmann D (2012) A versatile PhiC31 based reporter system for measuring AP-1 and Nrf2 signaling in Drosophila and in tissue culture. *PloS one* **7:** e34063

Chen W, Hong YQ, Meng ZL (2014) Bioinformatics analysis of molecular mechanisms of chronic obstructive pulmonary disease. *European review for medical and pharmacological sciences* **18:** 3557-3563

Chi T, Kim MS, Lang S, Bose N, Kahn A, Flechner L, Blaschko SD, Zee T, Muteliefu G, Bond N, Kolipinski M, Fakra SC, Mandel N, Miller J, Ramanathan A, Killilea DW, Bruckner K, Kapahi P, Stoller ML (2015) A Drosophila model identifies a critical role for zinc in mineralization for kidney stone disease. *PloS one* **10:** e0124150

Choe KM, Lee H, Anderson KV (2005) Drosophila peptidoglycan recognition protein LC (PGRP-LC) acts as a signal-transducing innate immune receptor. *Proceedings of the National Academy of Sciences of the United States of America* **102:** 1122-1126

Choe KM, Werner T, Stoven S, Hultmark D, Anderson KV (2002) Requirement for a peptidoglycan recognition protein (PGRP) in Relish activation and antibacterial immune responses in Drosophila. *Science* **296:** 359-362

Coffer PJ, Jin J, Woodgett JR (1998) Protein kinase B (c-Akt): a multifunctional mediator of phosphatidylinositol 3-kinase activation. *The Biochemical journal* **335 (Pt 1):** 1-13

Cohen A, George O (2013) Animal models of nicotine exposure: relevance to second-hand smoking, electronic cigarette use, and compulsive smoking. *Frontiers in psychiatry* **4:** 41

Darnell JE, Jr. (1997) STATs and gene regulation. *Science* **277:** 1630-1635

Darnell JE, Jr., Kerr IM, Stark GR (1994) Jak-STAT pathways and transcriptional activation in response to IFNs and other extracellular signaling proteins. *Science* **264:** 1415-1421

Datta SR, Brunet A, Greenberg ME (1999) Cellular survival: a play in three Akts. *Genes & development* **13:** 2905-2927

Daumer C, Flachsbart F, Caliebe A, Schreiber S, Nebel A, Krawczak M (2014) Adjustment for smoking does not alter the FOXO3A association with longevity. *Age* **36:** 911-921

Davis A, Hogarth K, Fernandes D, Solway J, Niu J, Kolenko V, Browning D, Miano JM, Orlov SN, Dulin NO (2003) Functional significance of protein kinase A activation by endothelin-1 and ATP: negative regulation of SRF-dependent gene expression by PKA. *Cellular signalling* **15:** 597-604

Dawydow A, Gueta R, Ljaschenko D, Ullrich S, Hermann M, Ehmann N, Gao S, Fiala A, Langenhan T, Nagel G, Kittel RJ (2014) Channelrhodopsin-2-XXL, a powerful optogenetic tool for low-light applications. *Proceedings of the National Academy of Sciences of the United States of America* **111:** 13972-13977

Dearolf CR (1998) Fruit fly "leukemia". *Biochimica et biophysica acta* **1377:** M13-23

Di Stefano A, Caramori G, Oates T, Capelli A, Lusuardi M, Gnemmi I, Ioli F, Chung KF, Donner CF, Barnes PJ, Adcock IM (2002) Increased expression of nuclear factor-kappaB in bronchial biopsies from smokers and patients with COPD. *The European respiratory journal* **20:** 556-563

Dietzl G, Chen D, Schnorrer F, Su KC, Barinova Y, Fellner M, Gasser B, Kinsey K, Oppel S, Scheiblauer S, Couto A, Marra V, Keleman K, Dickson BJ (2007) A genome-wide transgenic RNAi library for conditional gene inactivation in Drosophila. *Nature* **448:** 151-156

Dixon RE, Santana LF (2013) A Ca2+- and PKC-driven regulatory network in airway smooth muscle. *The Journal of general physiology* **141:** 161-164

Duffy JB (2002) GAL4 system in Drosophila: a fly geneticist's Swiss army knife. *Genesis* **34:** 1-15

Edwards MR, Bartlett NW, Clarke D, Birrell M, Belvisi M, Johnston SL (2009) Targeting the NF-kappaB pathway in asthma and chronic obstructive pulmonary disease. *Pharmacology & therapeutics* **121:** 1-13

Efetova M, Petereit L, Rosiewicz K, Overend G, Haussig F, Hovemann BT, Cabrero P, Dow JA, Schwarzel M (2013) Separate roles of PKA and EPAC in renal function unraveled by the optogenetic control of cAMP levels in vivo. *Journal of cell science* **126:** 778-788

Eijkelenboom A, Burgering BM (2013) FOXOs: signalling integrators for homeostasis maintenance. *Nature reviews Molecular cell biology* **14:** 83-97

Eisner MD, Balmes J, Katz PP, Trupin L, Yelin EH, Blanc PD (2005) Lifetime environmental tobacco smoke exposure and the risk of chronic obstructive pulmonary disease. *Environmental health : a global access science source* **4:** 7

Engstrom Y, Kadalayil L, Sun SC, Samakovlis C, Hultmark D, Faye I (1993) kappa B-like motifs regulate the induction of immune genes in Drosophila. *Journal of molecular biology* **232:** 327-333

Feany MB, Bender WW (2000) A Drosophila model of Parkinson's disease. *Nature* **404:** 394-398

Ferkol T, Schraufnagel D (2014) The global burden of respiratory disease. *Annals of the American Thoracic Society* **11:** 404-406

Ferrandon D, Jung AC, Criqui M, Lemaitre B, Uttenweiler-Joseph S, Michaut L, Reichhart J, Hoffmann JA (1998) A drosomycin-GFP reporter transgene reveals a local immune response in Drosophila that is not dependent on the Toll pathway. *The EMBO journal* **17:** 1217-1227

Flachsbart F, Caliebe A, Kleindorp R, Blanche H, von Eller-Eberstein H, Nikolaus S, Schreiber S, Nebel A (2009) Association of FOXO3A variation with human longevity confirmed in German centenarians. *Proceedings of the National Academy of Sciences of the United States of America* **106:** 2700-2705

Gavet O, Pines J (2010) Progressive activation of CyclinB1-Cdk1 coordinates entry to mitosis. *Developmental cell* **18:** 533-543

Gervais L, Casanova J (2011) The Drosophila homologue of SRF acts as a boosting mechanism to sustain FGF-induced terminal branching in the tracheal system. *Development* **138:** 1269-1274

Ghabrial A, Luschnig S, Metzstein MM, Krasnow MA (2003) Branching morphogenesis of the Drosophila tracheal system. *Annual review of cell and developmental biology* **19:** 623-647

Ghosh A, Pechota A, Coleman D, Upchurch GR, Jr., Eliason JL (2015) Cigarette smoke-induced MMP2 and MMP9 secretion from aortic vascular smooth cells is mediated via the Jak/Stat pathway. *Human pathology* **46:** 284-294

Giembycz MA, Newton R (2006) Beyond the dogma: novel beta2-adrenoceptor signalling in the airways. *The European respiratory journal* **27:** 1286-1306

Glise B, Bourbon H, Noselli S (1995) hemipterous encodes a novel Drosophila MAP kinase kinase, required for epithelial cell sheet movement. *Cell* **83:** 451-461

Green RM, Gally F, Keeney JG, Alper S, Gao B, Han M, Martin RJ, Weinberger AR, Case SR, Minor MN, Chu HW (2009) Impact of cigarette smoke exposure on innate immunity: a Caenorhabditis elegans model. *PloS one* **4:** e6860

Greer EL, Brunet A (2005) FOXO transcription factors at the interface between longevity and tumor suppression. *Oncogene* **24:** 7410-7425

Grivennikov SI, Karin M (2010) Dangerous liaisons: STAT3 and NF-kappaB collaboration and crosstalk in cancer. *Cytokine & growth factor reviews* **21:** 11-19

Halappanavar S, Russell M, Stampfli MR, Williams A, Yauk CL (2009) Induction of the interleukin 6/ signal transducer and activator of transcription pathway in the lungs of mice sub-chronically exposed to mainstream tobacco smoke. *BMC medical genomics* **2:** 56

Hanratty WP, Dearolf CR (1993) The Drosophila Tumorous-lethal hematopoietic oncogene is a dominant mutation in the hopscotch locus. *Molecular & general genetics : MGG* **238:** 33-37

Hecht SS (2003) Tobacco carcinogens, their biomarkers and tobacco-induced cancer. *Nature reviews Cancer* **3:** 733-744

Herzog CR, Blake DC, Jr., Mikse OR, Grigoryeva LS, Gundermann EL (2009) FoxO3a gene is a target of deletion in mouse lung adenocarcinoma. *Oncology reports* **22:** 837-843

Holgate ST, Davies DE, Lackie PM, Wilson SJ, Puddicombe SM, Lordan JL (2000) Epithelial-mesenchymal interactions in the pathogenesis of asthma. *The Journal of allergy and clinical immunology* **105:** 193-204

Holgate ST, Davies DE, Puddicombe S, Richter A, Lackie P, Lordan J, Howarth P (2003) Mechanisms of airway epithelial damage: epithelial-mesenchymal interactions in the pathogenesis of asthma. *The European respiratory journal Supplement* **44:** 24s-29s

Holgate ST, Holloway J, Wilson S, Bucchieri F, Puddicombe S, Davies DE (2004) Epithelial-mesenchymal communication in the pathogenesis of chronic asthma. *Proceedings of the American Thoracic Society* **1:** 93-98

Holland PM, Suzanne M, Campbell JS, Noselli S, Cooper JA (1997) MKK7 is a stress-activated mitogen-activated protein kinase kinase functionally related to hemipterous. *The Journal of biological chemistry* **272:** 24994-24998

Horowitz A, Simons M (2008) Branching morphogenesis. *Circulation research* **103:** 784-795

Hou T, Tieu BC, Ray S, Recinos Iii A, Cui R, Tilton RG, Brasier AR (2008) Roles of IL-6-gp130 Signaling in Vascular Inflammation. *Current cardiology reviews* **4:** 179-192

Hou XS, Goldstein ES, Perrimon N (1997) Drosophila Jun relays the Jun amino-terminal kinase signal transduction pathway to the Decapentaplegic signal transduction pathway in regulating epithelial cell sheet movement. *Genes & development* **11:** 1728-1737

Hu S, Yang X (2000) dFADD, a novel death domain-containing adapter protein for the Drosophila caspase DREDD. *The Journal of biological chemistry* **275:** 30761-30764

Hulbert WC, Walker DC, Jackson A, Hogg JC (1981) Airway permeability to horseradish peroxidase in guinea pigs: the repair phase after injury by cigarette smoke. *The American review of respiratory disease* **123:** 320-326

Hwang JW, Rajendrasozhan S, Yao H, Chung S, Sundar IK, Huyck HL, Pryhuber GS, Kinnula VL, Rahman I (2011) FOXO3 deficiency leads to increased susceptibility to cigarette smoke-induced inflammation, airspace enlargement, and chronic obstructive pulmonary disease. *Journal of immunology* **187:** 987-998

Iwashita H, Fujimoto K, Morita S, Nakanishi A, Kubo K (2012) Increased human Ca(2)(+)-activated Cl(-) channel 1 expression and mucus overproduction in airway epithelia of smokers and chronic obstructive pulmonary disease patients. *Respiratory research* **13:** 55

Jaiswal AK (2004) Nrf2 signaling in coordinated activation of antioxidant gene expression. *Free radical biology & medicine* **36:** 1199-1207

Jeffery PK (2004) Remodeling and inflammation of bronchi in asthma and chronic obstructive pulmonary disease. *Proceedings of the American Thoracic Society* **1:** 176-183

Jin S, Tian D, Chen JG, Zhu LP, Liu SY, Wang DX (2006) Passive sensitization increases histamine-stimulated calcium signaling and NF-kappaB transcription activity in bronchial epithelial cells. *Acta pharmacologica Sinica* **27:** 708-714

Jones JG, Minty BD, Lawler P, Hulands G, Crawley JC, Veall N (1980) Increased alveolar epithelial permeability in cigarette smokers. *Lancet* **1:** 66-68

Kaestner KH, Knochel W, Martinez DE (2000) Unified nomenclature for the winged helix/forkhead transcription factors. *Genes & development* **14:** 142-146

Kallsen K (2013) Untersuchung der Relevanz unterschiedlicher Asthma-Suszeptibilitätsgene im Modellorganismus *Drosophila melanogaster*. PhD Thesis, Molecular Physiology, CAU Kiel, CAU Kiel,

Kallsen K, Zehethofer N, Abdelsadik A, Lindner B, Kabesch M, Heine H, Roeder T (2015) ORMDL deregulation increases stress responses and modulates repair pathways in Drosophila airways. *The Journal of allergy and clinical immunology*

Kamp TJ, Hell JW (2000) Regulation of cardiac L-type calcium channels by protein kinase A and protein kinase C. *Circulation research* **87:** 1095-1102

Kaneko T, Yano T, Aggarwal K, Lim JH, Ueda K, Oshima Y, Peach C, Erturk-Hasdemir D, Goldman WE, Oh BH, Kurata S, Silverman N (2006) PGRP-LC and PGRP-LE have essential yet distinct functions in the drosophila immune response to monomeric DAP-type peptidoglycan. *Nature immunology* **7:** 715-723

Kellner J, Tantzscher J, Oelmez H, Edelmann M, Fischer R, Huber RM, Bergner A (2008) Mechanisms altering airway smooth muscle cell Ca+ homeostasis in two asthma models. *Respiration; international review of thoracic diseases* **76:** 205-215

Kelsen SG, Duan X, Ji R, Perez O, Liu C, Merali S (2008) Cigarette smoke induces an unfolded protein response in the human lung: a proteomic approach. *American journal of respiratory cell and molecular biology* **38:** 541-550

Kleino A, Silverman N (2014) The Drosophila IMD pathway in the activation of the humoral immune response. *Developmental and comparative immunology* **42:** 25-35

Kockel L, Zeitlinger J, Staszewski LM, Mlodzik M, Bohmann D (1997) Jun in Drosophila development: redundant and nonredundant functions and regulation by two MAPK signal transduction pathways. *Genes & development* **11:** 1748-1758

Kops GJ, Dansen TB, Polderman PE, Saarloos I, Wirtz KW, Coffer PJ, Huang TT, Bos JL, Medema RH, Burgering BM (2002) Forkhead transcription factor FOXO3a protects quiescent cells from oxidative stress. *Nature* **419:** 316-321

Kops GJ, de Ruiter ND, De Vries-Smits AM, Powell DR, Bos JL, Burgering BM (1999) Direct control of the Forkhead transcription factor AFX by protein kinase B. *Nature* **398:** 630-634

Kortylewski M, Feld F, Kruger KD, Bahrenberg G, Roth RA, Joost HG, Heinrich PC, Behrmann I, Barthel A (2003) Akt modulates STAT3-mediated gene expression through a FKHR (FOXO1a)-dependent mechanism. *The Journal of biological chemistry* **278:** 5242-5249

Kuhn C, 3rd, Homer RJ, Zhu Z, Ward N, Flavell RA, Geba GP, Elias JA (2000) Airway hyperresponsiveness and airway obstruction in transgenic mice. Morphologic correlates in mice overexpressing interleukin (IL)-11 and IL-6 in the lung. *American journal of respiratory cell and molecular biology* **22:** 289-295

Kumar A, Bhandari A, Goswami C (2014) Surveying genetic variants and molecular phylogeny of cerebral cavernous malformation gene, CCM3/PDCD10. *Biochemical and biophysical research communications* **455:** 98-106

Kume H, Hall IP, Washabau RJ, Takagi K, Kotlikoff MI (1994) Beta-adrenergic agonists regulate KCa channels in airway smooth muscle by cAMP-dependent and -independent mechanisms. *The Journal of clinical investigation* **93:** 371-379

Lamb RS, Ward RE, Schweizer L, Fehon RG (1998) Drosophila coracle, a member of the protein 4.1 superfamily, has essential structural functions in the septate junctions and developmental functions in embryonic and adult epithelial cells. *Molecular biology of the cell* **9:** 3505-3519

Landis G, Shen J, Tower J (2012) Gene expression changes in response to aging compared to heat stress, oxidative stress and ionizing radiation in Drosophila melanogaster. *Aging* **4:** 768-789

Landis GN, Abdueva D, Skvortsov D, Yang J, Rabin BE, Carrick J, Tavare S, Tower J (2004) Similar gene expression patterns characterize aging and oxidative stress in Drosophila melanogaster. *Proceedings of the National Academy of Sciences of the United States of America* **101:** 7663-7668

Lazzeri N, Belvisi MG, Patel HJ, Yacoub MH, Chung KF, Mitchell JA (2001) Effects of prostaglandin E2 and cAMP elevating drugs on GM-CSF release by cultured human airway smooth muscle cells. Relevance to asthma therapy. *American journal of respiratory cell and molecular biology* **24:** 44-48

Leberl M, Kratzer A, Taraseviciene-Stewart L (2013) Tobacco smoke induced COPD/emphysema in the animal model-are we all on the same page? *Frontiers in physiology* **4:** 91

Lee KA, Lee WJ (2014) Drosophila as a model for intestinal dysbiosis and chronic inflammatory diseases. *Developmental and comparative immunology* **42:** 102-110

Lemaitre B, Hoffmann J (2007) The host defense of Drosophila melanogaster. *Annual review of immunology* **25:** 697-743

Levine RL, Wernig G (2006) Role of JAK-STAT signaling in the pathogenesis of myeloproliferative disorders. *Hematology / the Education Program of the American Society of Hematology American Society of Hematology Education Program***:** 233-239, 510

Li Y, Wang WJ, Cao H, Lu J, Wu C, Hu FY, Guo J, Zhao L, Yang F, Zhang YX, Li W, Zheng GY, Cui H, Chen X, Zhu Z, He H, Dong B, Mo X, Zeng Y, Tian XL (2009) Genetic association of FOXO1A and FOXO3A with longevity trait in Han Chinese populations. *Human molecular genetics* **18:** 4897-4904

Liu HW, Halayko AJ, Fernandes DJ, Harmon GS, McCauley JA, Kocieniewski P, McConville J, Fu Y, Forsythe SM, Kogut P, Bellam S, Dowell M, Churchill J, Lesso H, Kassiri K, Mitchell RW, Hershenson MB, Camoretti-Mercado B, Solway J (2003a) The RhoA/Rho kinase pathway regulates nuclear localization of serum response factor. *American journal of respiratory cell and molecular biology* **29:** 39-47

Liu L, Johnson WA, Welsh MJ (2003b) Drosophila DEG/ENaC pickpocket genes are expressed in the tracheal system, where they may be involved in liquid clearance. *Proceedings of the National Academy of Sciences of the United States of America* **100:** 2128-2133

Liu QH, Zheng YM, Korde AS, Yadav VR, Rathore R, Wess J, Wang YX (2009) Membrane depolarization causes a direct activation of G protein-coupled receptors leading to local Ca2+ release in smooth muscle. *Proceedings of the National Academy of Sciences of the United States of America* **106:** 11418-11423

Lopez Hernandez Y, Yero D, Pinos-Rodriguez JM, Gibert I (2015) Animals devoid of pulmonary system as infection models in the study of lung bacterial pathogens. *Frontiers in microbiology* **6:** 38

Ma Q (2013) Role of nrf2 in oxidative stress and toxicity. *Annual review of pharmacology and toxicology* **53:** 401-426

Marinkovic D, Zhang X, Yalcin S, Luciano JP, Brugnara C, Huber T, Ghaffari S (2007) Foxo3 is required for the regulation of oxidative stress in erythropoiesis. *The Journal of clinical investigation* **117:** 2133-2144

Mattila J, Bremer A, Ahonen L, Kostiainen R, Puig O (2009) Drosophila FoxO regulates organism size and stress resistance through an adenylate cyclase. *Molecular and cellular biology* **29:** 5357-5365

McGuire SE, Le PT, Osborn AJ, Matsumoto K, Davis RL (2003) Spatiotemporal rescue of memory dysfunction in Drosophila. *Science* **302:** 1765-1768

Miano JM, Long X, Fujiwara K (2007) Serum response factor: master regulator of the actin cytoskeleton and contractile apparatus. *American journal of physiology Cell physiology* **292:** C70-81

Mikse OR, Blake DC, Jr., Jones NR, Sun YW, Amin S, Gallagher CJ, Lazarus P, Weisz J, Herzog CR (2010) FOXO3 encodes a carcinogen-activated transcription factor frequently deleted in early-stage lung adenocarcinoma. *Cancer research* **70:** 6205-6215

Minakhina S, Steward R (2006) Melanotic mutants in Drosophila: pathways and phenotypes. *Genetics* **174:** 253-263

Motohashi H, Yamamoto M (2004) Nrf2-Keap1 defines a physiologically important stress response mechanism. *Trends in molecular medicine* **10:** 549-557

Muller T, Hengstermann A (2012) Nrf2: friend and foe in preventing cigarette smoking-dependent lung disease. *Chemical research in toxicology* **25:** 1805-1824

Nagai K, Betsuyaku T, Suzuki M, Nasuhara Y, Kaga K, Kondo S, Nishimura M (2008) Dual oxidase 1 and 2 expression in airway epithelium of smokers and patients with mild/moderate chronic obstructive pulmonary disease. *Antioxidants & redox signaling* **10:** 705-714

Nagel G, Szellas T, Huhn W, Kateriya S, Adeishvili N, Berthold P, Ollig D, Hegemann P, Bamberg E (2003) Channelrhodopsin-2, a directly light-gated cation-selective membrane channel. *Proceedings of the National Academy of Sciences of the United States of America* **100:** 13940-13945

Nichols CD, Roth BL (2009) Engineered G-protein Coupled Receptors are Powerful Tools to Investigate Biological Processes and Behaviors. *Frontiers in molecular neuroscience* **2:** 16

Nino G, Hu A, Grunstein JS, Grunstein MM (2009) Mechanism regulating proasthmatic effects of prolonged homologous beta2-adrenergic receptor desensitization in airway smooth muscle. *American journal of physiology Lung cellular and molecular physiology* **297:** L746-757

Nishikawa M, Kakemizu N, Ito T, Kudo M, Kaneko T, Suzuki M, Udaka N, Ikeda H, Okubo T (1999) Superoxide mediates cigarette smoke-induced infiltration of neutrophils into the airways through nuclear factor-kappaB activation and IL-8 mRNA expression in guinea pigs in vivo. *American journal of respiratory cell and molecular biology* **20:** 189-198

Ochoa CE, Mirabolfathinejad SG, Ruiz VA, Evans SE, Gagea M, Evans CM, Dickey BF, Moghaddam SJ (2011) Interleukin 6, but not T helper 2 cytokines, promotes lung carcinogenesis. *Cancer prevention research* **4:** 51-64

Oldefest M, Nowinski J, Hung CW, Neelsen D, Trad A, Tholey A, Grotzinger J, Lorenzen I (2013) Upd3--an ancestor of the four-helix bundle cytokines. *Biochemical and biophysical research communications* **436:** 66-72

Olivier JP, Raabe T, Henkemeyer M, Dickson B, Mbamalu G, Margolis B, Schlessinger J, Hafen E, Pawson T (1993) A Drosophila SH2-SH3 adaptor protein implicated in coupling the sevenless tyrosine kinase to an activator of Ras guanine nucleotide exchange, Sos. *Cell* **73:** 179-191

Olson ER, Pancratov R, Chatterjee SS, Changkakoty B, Pervaiz Z, DasGupta R (2011) Yan, an ETS-domain transcription factor, negatively modulates the Wingless pathway in the Drosophila eye. *EMBO reports* **12:** 1047-1054

Paget TA, Fry M, Lloyd D (1987) Effects of inhibitors on the oxygen kinetics of Nippostrongylus brasiliensis. *Molecular and biochemical parasitology* **22:** 125-133

Pandey UB, Nichols CD (2011) Human disease models in Drosophila melanogaster and the role of the fly in therapeutic drug discovery. *Pharmacological reviews* **63:** 411-436

Pang L, Knox AJ (2000) Synergistic inhibition by beta(2)-agonists and corticosteroids on tumor necrosis factor-alpha-induced interleukin-8 release from cultured human airway smooth-muscle cells. *American journal of respiratory cell and molecular biology* **23:** 79-85

Pantano C, Ather JL, Alcorn JF, Poynter ME, Brown AL, Guala AS, Beuschel SL, Allen GB, Whittaker LA, Bevelander M, Irvin CG, Janssen-Heininger YM (2008) Nuclear factor-kappaB activation in airway epithelium induces inflammation and hyperresponsiveness. *American journal of respiratory and critical care medicine* **177:** 959-969

Pare PD, Roberts CR, Bai TR, Wiggs BJ (1997) The functional consequences of airway remodeling in asthma. *Monaldi archives for chest disease = Archivio Monaldi per le malattie del torace / Fondazione clinica del lavoro, IRCCS [and] Istituto di clinica tisiologica e malattie apparato respiratorio, Universita di Napoli, Secondo ateneo* **52:** 589-596

Pauwels RA, Rabe KF (2004) Burden and clinical features of chronic obstructive pulmonary disease (COPD). *Lancet* **364:** 613-620

Pawlikowska L, Hu D, Huntsman S, Sung A, Chu C, Chen J, Joyner AH, Schork NJ, Hsueh WC, Reiner AP, Psaty BM, Atzmon G, Barzilai N, Cummings SR, Browner WS, Kwok PY, Ziv E, Study of Osteoporotic F (2009) Association of common genetic variation in the insulin/IGF1 signaling pathway with human longevity. *Aging cell* **8:** 460-472

Penzkofer A, Stierl M, Mathes T, Hegemann P (2014) Absorption and emission spectroscopic characterization of photo-dynamics of photoactivated adenylyl cyclase mutant bPAC-Y7F of Beggiatoa sp. *Journal of photochemistry and photobiology B, Biology* **140:** 182-193

Petty TL, Rennard SI (2000) Introduction: mechanisms of COPD. *Chest* **117:** 219S

Pfaffl MW (2001) A new mathematical model for relative quantification in real-time RT-PCR. *Nucleic acids research* **29:** e45

Pitsouli C, Perrimon N (2013) The homeobox transcription factor cut coordinates patterning and growth during Drosophila airway remodeling. *Science signaling* **6:** ra12

Postma DS, Timens W (2006) Remodeling in asthma and chronic obstructive pulmonary disease. *Proceedings of the American Thoracic Society* **3:** 434-439

Rastrick JM, Stevenson CS, Eltom S, Grace M, Davies M, Kilty I, Evans SM, Pasparakis M, Catley MC, Lawrence T, Adcock IM, Belvisi MG, Birrell MA (2013) Cigarette smoke induced airway inflammation is independent of NF-kappaB signalling. *PloS one* **8:** e54128

Roeder T, Isermann K, Kabesch M (2009) Drosophila in asthma research. *American journal of respiratory and critical care medicine* **179:** 979-983

Roeder T, Isermann K, Kallsen K, Uliczka K, Wagner C (2012) A Drosophila asthma model - what the fly tells us about inflammatory diseases of the lung. *Advances in experimental medicine and biology* **710:** 37-47

Roman G, Endo K, Zong L, Davis RL (2001) P[Switch], a system for spatial and temporal control of gene expression in Drosophila melanogaster. *Proceedings of the National Academy of Sciences of the United States of America* **98:** 12602-12607

Ronquist F, Teslenko M, van der Mark P, Ayres DL, Darling A, Hohna S, Larget B, Liu L, Suchard MA, Huelsenbeck JP (2012) MrBayes 3.2: efficient Bayesian phylogenetic inference and model choice across a large model space. *Syst Biol* **61:** 539-542

Roxburgh CS, McMillan DC (2015) Therapeutics targeting innate immune/inflammatory responses through the interleukin-6/JAK/STAT signal transduction pathway in patients with cancer. *Translational research : the journal of laboratory and clinical medicine*

Roy A, Kucukural A, Zhang Y (2010) I-TASSER: a unified platform for automated protein structure and function prediction. *Nature protocols* **5:** 725-738

Ryder E, Ashburner M, Bautista-Llacer R, Drummond J, Webster J, Johnson G, Morley T, Chan YS, Blows F, Coulson D, Reuter G, Baisch H, Apelt C, Kauk A, Rudolph T, Kube M, Klimm M, Nickel C, Szidonya J, Maroy P, Pal M, Rasmuson-Lestander A, Ekstrom K, Stocker H, Hugentobler C, Hafen E, Gubb D, Pflugfelder G, Dorner C, Mechler B, Schenkel H, Marhold J, Serras F, Corominas M, Punset A, Roote J, Russell S (2007) The DrosDel deletion collection: a Drosophila genomewide chromosomal deficiency resource. *Genetics* **177:** 615-629

Salathe M (2002) Effects of beta-agonists on airway epithelial cells. *The Journal of allergy and clinical immunology* **110:** S275-281

Salvi SS, Barnes PJ (2009) Chronic obstructive pulmonary disease in non-smokers. *Lancet* **374:** 733-743

Savai R, Al-Tamari HM, Sedding D, Kojonazarov B, Muecke C, Teske R, Capecchi MR, Weissmann N, Grimminger F, Seeger W, Schermuly RT, Pullamsetti SS (2014) Pro-proliferative and inflammatory signaling converge on FoxO1 transcription factor in pulmonary hypertension. *Nature medicine* **20:** 1289-1300

Schleimer RP (2005) Innate immune responses and chronic obstructive pulmonary disease: "Terminator" or "Terminator 2"? *Proceedings of the American Thoracic Society* **2:** 342-346; discussion 371-342

Shaykhiev R, Wang R, Zwick RK, Hackett NR, Leung R, Moore MA, Sima CS, Chao IW, Downey RJ, Strulovici-Barel Y, Salit J, Crystal RG (2013) Airway basal cells of healthy smokers express an embryonic stem cell signature relevant to lung cancer. *Stem cells* **31:** 1992-2002

Shimoda LA, Sham JS, Sylvester JT (2000) Altered pulmonary vasoreactivity in the chronically hypoxic lung. *Physiological research / Academia Scientiarum Bohemoslovaca* **49:** 549-560

Silverman N, Zhou R, Erlich RL, Hunter M, Bernstein E, Schneider D, Maniatis T (2003) Immune activation of NF-kappaB and JNK requires Drosophila TAK1. *The Journal of biological chemistry* **278:** 48928-48934

Silverman N, Zhou R, Stoven S, Pandey N, Hultmark D, Maniatis T (2000) A Drosophila IkappaB kinase complex required for Relish cleavage and antibacterial immunity. *Genes & development* **14:** 2461-2471

Simon MA, Bowtell DD, Dodson GS, Laverty TR, Rubin GM (1991) Ras1 and a putative guanine nucleotide exchange factor perform crucial steps in signaling by the sevenless protein tyrosine kinase. *Cell* **67:** 701-716

Sluss HK, Han Z, Barrett T, Goberdhan DC, Wilson C, Davis RJ, Ip YT (1996) A JNK signal transduction pathway that mediates morphogenesis and an immune response in Drosophila. *Genes & development* **10:** 2745-2758

Soerensen M, Dato S, Christensen K, McGue M, Stevnsner T, Bohr VA, Christiansen L (2010) Replication of an association of variation in the FOXO3A gene with human longevity using both case-control and longitudinal data. *Aging cell* **9:** 1010-1017

Song Y, Eng M, Ghabrial AS (2013) Focal defects in single-celled tubes mutant for Cerebral cavernous malformation 3, GCKIII, or NSF2. *Developmental cell* **25:** 507-519

Spina D (2008) PDE4 inhibitors: current status. *British journal of pharmacology* **155:** 308-315

Stierl M, Stumpf P, Udwari D, Gueta R, Hagedorn R, Losi A, Gartner W, Petereit L, Efetova M, Schwarzel M, Oertner TG, Nagel G, Hegemann P (2011) Light modulation of cellular cAMP by a small bacterial photoactivated adenylyl cyclase, bPAC, of the soil bacterium Beggiatoa. *The Journal of biological chemistry* **286:** 1181-1188

Stoven S, Ando I, Kadalayil L, Engstrom Y, Hultmark D (2000) Activation of the Drosophila NF-kappaB factor Relish by rapid endoproteolytic cleavage. *EMBO reports* **1:** 347-352

Stoven S, Silverman N, Junell A, Hedengren-Olcott M, Erturk D, Engstrom Y, Maniatis T, Hultmark D (2003) Caspase-mediated processing of the Drosophila NF-kappaB factor Relish. *Proceedings of the National Academy of Sciences of the United States of America* **100:** 5991-5996

Sutherland EW, Rall TW (1958) Fractionation and characterization of a cyclic adenine ribonucleotide formed by tissue particles. *The Journal of biological chemistry* **232:** 1077-1091

Sykiotis GP, Bohmann D (2008) Keap1/Nrf2 signaling regulates oxidative stress tolerance and lifespan in Drosophila. *Developmental cell* **14:** 76-85

Tang H, Kambris Z, Lemaitre B, Hashimoto C (2008) A serpin that regulates immune melanization in the respiratory system of Drosophila. *Developmental cell* **15:** 617-626

Tanji T, Yun EY, Ip YT (2010) Heterodimers of NF-kappaB transcription factors DIF and Relish regulate antimicrobial peptide genes in Drosophila. *Proceedings of the National Academy of Sciences of the United States of America* **107:** 14715-14720

Thore S, Dyachok O, Gylfe E, Tengholm A (2005) Feedback activation of phospholipase C via intracellular mobilization and store-operated influx of Ca2+ in insulin-secreting beta-cells. *Journal of cell science* **118:** 4463-4471

Tsai KL, Sun YJ, Huang CY, Yang JY, Hung MC, Hsiao CD (2007) Crystal structure of the human FOXO3a-DBD/DNA complex suggests the effects of post-translational modification. *Nucleic acids research* **35:** 6984-6994

Turetz ML, O'Connor TP, Tilley AE, Strulovici-Barel Y, Salit J, Dang D, Teater M, Mezey J, Clark AG, Crystal RG (2009) Trachea epithelium as a "canary" for cigarette smoking-induced biologic phenotype of the small airway epithelium. *Clinical and translational science* **2:** 260-272

Tzou P, Ohresser S, Ferrandon D, Capovilla M, Reichhart JM, Lemaitre B, Hoffmann JA, Imler JL (2000) Tissue-specific inducible expression of antimicrobial peptide genes in Drosophila surface epithelia. *Immunity* **13:** 737-748

van der Horst A, Burgering BM (2007) Stressing the role of FoxO proteins in lifespan and disease. *Nature reviews Molecular cell biology* **8:** 440-450

van der Vaart H, Postma DS, Timens W, ten Hacken NH (2004) Acute effects of cigarette smoke on inflammation and oxidative stress: a review. *Thorax* **59:** 713-721

Van Voorhies WA, Ward S (2000) Broad oxygen tolerance in the nematode Caenorhabditis elegans. *The Journal of experimental biology* **203:** 2467-2478

Varma D, Bulow MH, Pesch YY, Loch G, Hoch M (2014) Forkhead, a new cross regulator of metabolism and innate immunity downstream of TOR in Drosophila. *Journal of insect physiology* **69:** 80-88

Victoni T, Gleonnec F, Lanzetti M, Tenor H, Valenca S, Porto LC, Lagente V, Boichot E (2014) Roflumilast N-oxide prevents cytokine secretion induced by cigarette smoke combined with LPS through JAK/STAT and ERK1/2 inhibition in airway epithelial cells. *PloS one* **9:** e85243

Vidal S, Khush RS, Leulier F, Tzou P, Nakamura M, Lemaitre B (2001) Mutations in the Drosophila dTAK1 gene reveal a conserved function for MAPKKKs in the control of rel/NF-kappaB-dependent innate immune responses. *Genes & development* **15:** 1900-1912

Vos T, Flaxman AD, Naghavi M, Lozano R, Michaud C, Ezzati M, Shibuya K, Salomon JA, Abdalla S, Aboyans V, Abraham J, Ackerman I, Aggarwal R, Ahn SY, Ali MK, Alvarado M, Anderson HR, Anderson LM, Andrews KG, Atkinson C, Baddour LM, Bahalim AN, Barker-Collo S, Barrero LH, Bartels DH, Basanez MG, Baxter A, Bell ML, Benjamin EJ, Bennett D, Bernabe E, Bhalla K, Bhandari B, Bikbov B, Bin Abdulhak A, Birbeck G, Black JA, Blencowe H, Blore JD, Blyth F, Bolliger I, Bonaventure A, Boufous S, Bourne R, Boussinesq M, Braithwaite T, Brayne C, Bridgett L, Brooker S, Brooks P, Brugha TS, Bryan-Hancock C, Bucello C, Buchbinder R, Buckle G, Budke CM, Burch M, Burney P, Burstein R, Calabria B, Campbell B, Canter CE, Carabin H, Carapetis J, Carmona L, Cella C, Charlson F, Chen H, Cheng AT, Chou D, Chugh SS, Coffeng LE, Colan SD, Colquhoun S, Colson KE, Condon J, Connor MD, Cooper LT, Corriere M, Cortinovis M, de Vaccaro KC, Couser W, Cowie BC, Criqui MH, Cross M, Dabhadkar KC, Dahiya M, Dahodwala N, Damsere-Derry J, Danaei G, Davis A, De Leo D, Degenhardt L, Dellavalle R, Delossantos A, Denenberg J, Derrett S, Des Jarlais DC, Dharmaratne SD, Dherani M, Diaz-Torne C, Dolk H, Dorsey ER, Driscoll T, Duber H, Ebel B, Edmond K, Elbaz A, Ali SE, Erskine H, Erwin PJ, Espindola P, Ewoigbokhan SE, Farzadfar F, Feigin V, Felson DT, Ferrari A, Ferri CP, Fevre EM, Finucane MM, Flaxman S, Flood L, Foreman K, Forouzanfar MH, Fowkes FG, Franklin R, Fransen M, Freeman MK, Gabbe BJ, Gabriel SE, Gakidou E, Ganatra HA, Garcia B, Gaspari F, Gillum RF, Gmel G, Gosselin R, Grainger R, Groeger J, Guillemin F, Gunnell D, Gupta R, Haagsma J, Hagan H, Halasa YA, Hall W, Haring D, Haro JM, Harrison JE, Havmoeller R, Hay RJ, Higashi H, Hill C, Hoen B, Hoffman H, Hotez PJ, Hoy D, Huang JJ, Ibeanusi SE, Jacobsen KH, James SL, Jarvis D, Jasrasaria R, Jayaraman S, Johns N, Jonas JB, Karthikeyan G, Kassebaum N, Kawakami N, Keren A, Khoo JP, King CH, Knowlton LM, Kobusingye O, Koranteng A, Krishnamurthi R, Lalloo R, Laslett LL, Lathlean T, Leasher JL, Lee YY, Leigh J, Lim SS, Limb E, Lin JK, Lipnick M, Lipshultz SE, Liu W, Loane M, Ohno SL, Lyons R,

Ma J, Mabweijano J, MacIntyre MF, Malekzadeh R, Mallinger L, Manivannan S, Marcenes W, March L, Margolis DJ, Marks GB, Marks R, Matsumori A, Matzopoulos R, Mayosi BM, McAnulty JH, McDermott MM, McGill N, McGrath J, Medina-Mora ME, Meltzer M, Mensah GA, Merriman TR, Meyer AC, Miglioli V, Miller M, Miller TR, Mitchell PB, Mocumbi AO, Moffitt TE, Mokdad AA, Monasta L, Montico M, Moradi-Lakeh M, Moran A, Morawska L, Mori R, Murdoch ME, Mwaniki MK, Naidoo K, Nair MN, Naldi L, Narayan KM, Nelson PK, Nelson RG, Nevitt MC, Newton CR, Nolte S, Norman P, Norman R, O'Donnell M, O'Hanlon S, Olives C, Omer SB, Ortblad K, Osborne R, Ozgediz D, Page A, Pahari B, Pandian JD, Rivero AP, Patten SB, Pearce N, Padilla RP, Perez-Ruiz F, Perico N, Pesudovs K, Phillips D, Phillips MR, Pierce K, Pion S, Polanczyk GV, Polinder S, Pope CA, 3rd, Popova S, Porrini E, Pourmalek F, Prince M, Pullan RL, Ramaiah KD, Ranganathan D, Razavi H, Regan M, Rehm JT, Rein DB, Remuzzi G, Richardson K, Rivara FP, Roberts T, Robinson C, De Leon FR, Ronfani L, Room R, Rosenfeld LC, Rushton L, Sacco RL, Saha S, Sampson U, Sanchez-Riera L, Sanman E, Schwebel DC, Scott JG, Segui-Gomez M, Shahraz S, Shepard DS, Shin H, Shivakoti R, Singh D, Singh GM, Singh JA, Singleton J, Sleet DA, Sliwa K, Smith E, Smith JL, Stapelberg NJ, Steer A, Steiner T, Stolk WA, Stovner LJ, Sudfeld C, Syed S, Tamburlini G, Tavakkoli M, Taylor HR, Taylor JA, Taylor WJ, Thomas B, Thomson WM, Thurston GD, Tleyjeh IM, Tonelli M, Towbin JA, Truelsen T, Tsilimbaris MK, Ubeda C, Undurraga EA, van der Werf MJ, van Os J, Vavilala MS, Venketasubramanian N, Wang M, Wang W, Watt K, Weatherall DJ, Weinstock MA, Weintraub R, Weisskopf MG, Weissman MM, White RA, Whiteford H, Wiersma ST, Wilkinson JD, Williams HC, Williams SR, Witt E, Wolfe F, Woolf AD, Wulf S, Yeh PH, Zaidi AK, Zheng ZJ, Zonies D, Lopez AD, Murray CJ, AlMazroa MA, Memish ZA (2012) Years lived with disability (YLDs) for 1160 sequelae of 289 diseases and injuries 1990-2010: a systematic analysis for the Global Burden of Disease Study 2010. *Lancet* **380:** 2163-2196

Wagner C, Isermann K, Fehrenbach H, Roeder T (2008) Molecular architecture of the fruit fly's airway epithelial immune system. *BMC genomics* **9:** 446

Wagner C, Isermann K, Roeder T (2009) Infection induces a survival program and local remodeling in the airway epithelium of the fly. *FASEB journal : official publication of the Federation of American Societies for Experimental Biology* **23:** 2045-2054

Wang L, McParland BE, Pare PD (2003) The functional consequences of structural changes in the airways: implications for airway hyperresponsiveness in asthma. *Chest* **123:** 356S-362S

Ward C, Johns DP, Bish R, Pais M, Reid DW, Ingram C, Feltis B, Walters EH (2001) Reduced airway distensibility, fixed airflow limitation, and airway wall remodeling in asthma. *American journal of respiratory and critical care medicine* **164:** 1718-1721

Weir EK, Olschewski A (2006) Role of ion channels in acute and chronic responses of the pulmonary vasculature to hypoxia. *Cardiovascular research* **71:** 630-641

Willcox BJ, Donlon TA, He Q, Chen R, Grove JS, Yano K, Masaki KH, Willcox DC, Rodriguez B, Curb JD (2008) FOXO3A genotype is strongly associated with human longevity. *Proceedings of the National Academy of Sciences of the United States of America* **105:** 13987-13992

Wolf MJ, Amrein H, Izatt JA, Choma MA, Reedy MC, Rockman HA (2006) Drosophila as a model for the identification of genes causing adult human heart disease. *Proceedings of the National Academy of Sciences of the United States of America* **103:** 1394-1399

Wright VM, Vogt KL, Smythe E, Zeidler MP (2011) Differential activities of the Drosophila JAK/STAT pathway ligands Upd, Upd2 and Upd3. *Cellular signalling* **23:** 920-927

Wu Y, Antony S, Meitzler JL, Doroshow JH (2014) Molecular mechanisms underlying chronic inflammation-associated cancers. *Cancer letters* **345:** 164-173

Yang JY, Hung MC (2009) A new fork for clinical application: targeting forkhead transcription factors in cancer. *Clinical cancer research : an official journal of the American Association for Cancer Research* **15:** 752-757

Yew-Booth L, Birrell MA, Lau MS, Baker K, Jones V, Kilty I, Belvisi MG (2015) JAK-STAT pathway activation in COPD. *The European respiratory journal*

Yu H, Pardoll D, Jove R (2009) STATs in cancer inflammation and immunity: a leading role for STAT3. *Nature reviews Cancer* **9:** 798-809

Yuan XJ, Wang J, Juhaszova M, Golovina VA, Rubin LJ (1998) Molecular basis and function of voltage-gated K+ channels in pulmonary arterial smooth muscle cells. *The American journal of physiology* **274:** L621-635

Zeidler MP, Bach EA, Perrimon N (2000) The roles of the Drosophila JAK/STAT pathway. *Oncogene* **19:** 2598-2606

Zhang S, Zhao Y, Xu M, Yu L, Zhao Y, Chen J, Yuan Y, Zheng Q, Niu X (2013) FoxO3a modulates hypoxia stress induced oxidative stress and apoptosis in cardiac microvascular endothelial cells. *PloS one* **8:** e80342

Zhong Z, Wen Z, Darnell JE, Jr. (1994) Stat3: a STAT family member activated by tyrosine phosphorylation in response to epidermal growth factor and interleukin-6. *Science* **264:** 95-98

Zou S, Meadows S, Sharp L, Jan LY, Jan YN (2000) Genome-wide study of aging and oxidative stress response in Drosophila melanogaster. *Proceedings of the National Academy of Sciences of the United States of America* **97:** 13726-13731

7. Appendix

7.1 Activation of Wnt signaling after CSE

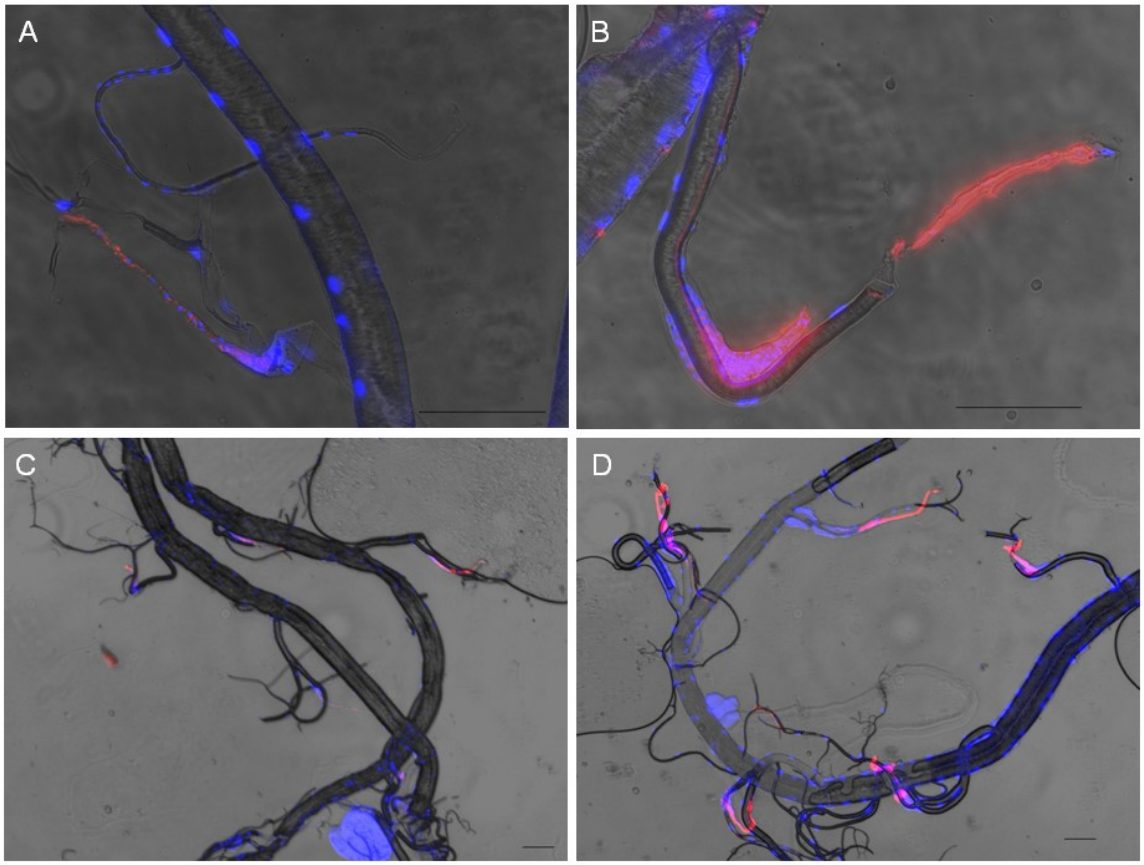

Figure 7-1: Activation of Wnt signaling in the respiratory track of *D. melanogaster* after CSE. The inidicator fly line for Wnt-pathway activity, which expresses a RFP under the native promotor of frizzled 3, was investigated under physiological conditions (**A and C**) and after CSE (**B and D**). Wnt signaling got expressed in the secondary and tertiary branches after CSE. The scale bar is 100 µm.

7.2 Neighbor joining phylogenetic tree analysis of upd 1, 2 and 3

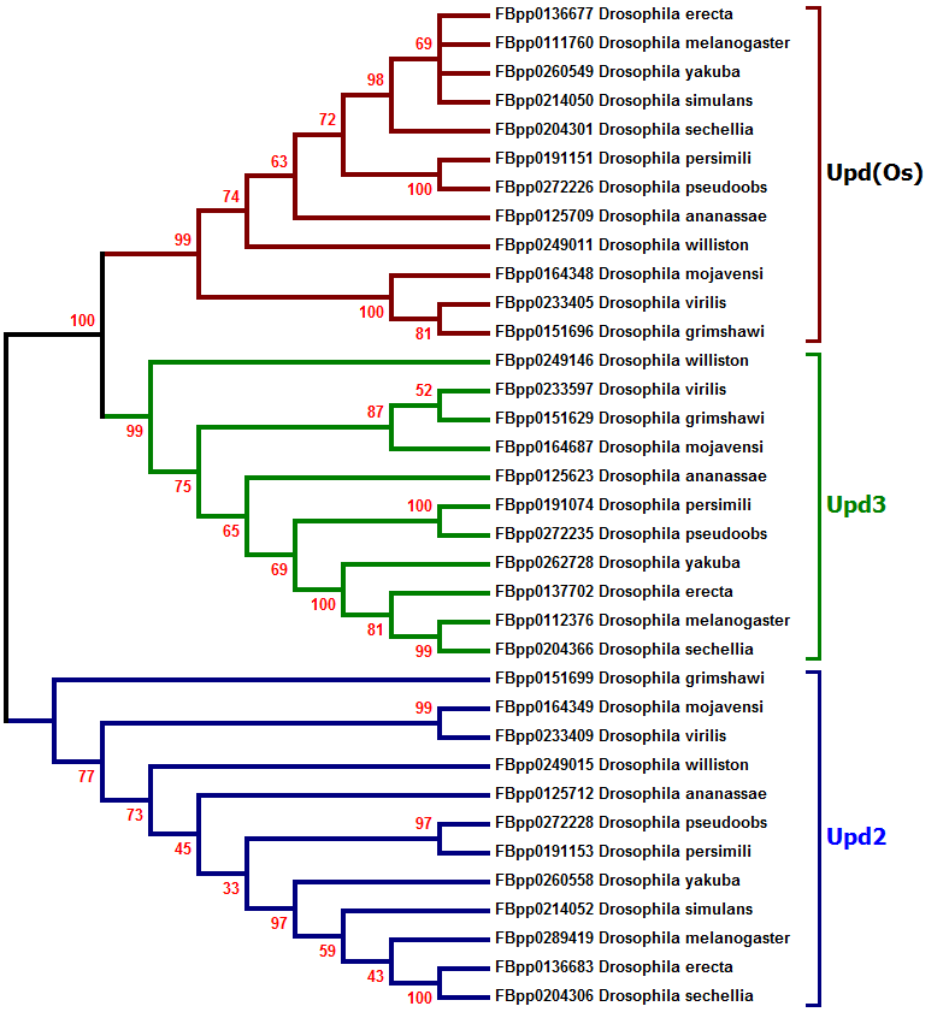

Figure 7-2: Neighbor joining analysis of upd upd2 and upd3 genes of *Drosophila* species. Upd, upd2 and upd3 are *Drosophila* species specific genes as depicted by NJ. However, NJ method could not extract that upd3 originated first as depicted by Bayesian phylogeny.

Table 7-1: List of upd, upd2 and upd3 genes

Upds short name	Accession numbers Flybase
Dwi_Upd3	FBpp0249146_*Drosophila_williston*
Dan_Upd3	FBpp0125623_*Drosophila_ananassae*
Dya_Upd3	FBpp0262728_*Drosophila_yakuba*
Der_Upd3	FBpp0137702_*Drosophila_erecta*
Dme_Upd3	FBpp0112376_*Drosophila_melanogaster*
Dsi_Upd3	CG33542_*Drosophila_simulans*
Dse_Upd3	FBpp0204366_*Drosophila_sechellia*
Dps_Upd3	FBpp0272235_*Drosophila_pseudoobscura*
Dpe_Upd3	FBpp0191074_*Drosophila_persimilis*
Dmo_Upd3	FBpp0164687_*Drosophila_mojavensis*
Dvi_Upd3	FBpp0233597_*Drosophila_virilis*
Dgr_Upd3	FBpp0151629_*Drosophila_grimshawi*
Dgr_Upd2	FBpp0151699_*Drosophila_grimshawi*
Dmo_Upd2	FBpp0164349_*Drosophila_mojavensis*
Dvi_Upd2	FBpp0233409_*Drosophila_virilis*
Dwi_Upd2	FBpp0249015_*Drosophila_williston*
Dan_Upd2	FBpp0125712_*Drosophila_ananassae*
Dps_Upd2	FBpp0272228_*Drosophila_pseudoobscura*
Dpe_Upd2	FBpp0191153_*Drosophila_persimilis*
Der_Upd2	FBpp0136683_*Drosophila_erecta*
Dse_Upd2	FBpp0204306_*Drosophila_sechellia*
Dya_Upd2	FBpp0260558_*Drosophila_yakuba*
Dsi_Upd2	FBpp0214052_*Drosophila_simulans*
Dme_Upd2	FBpp0289419_*Drosophila_melanogaster*
Dmo_Upd	FBpp0164348_*Drosophila_mojavensis*
Dvi_Upd	FBpp0233405_*Drosophila_virilis*
Dgr_Upd	FBpp0151696_*Drosophila_grimshawi*
Dwi_Upd	FBpp0249011_*Drosophila_williston*
Dan_Upd	FBpp0125709_*Drosophila_ananassae*
Dpe_Upd	FBpp0191151_*Drosophila_persimilis*
Dps_Upd	FBpp0272226_*Drosophila_pseudoobscura*
Der_Upd	FBpp0136677_*Drosophila_erecta*
Dya_Upd	FBpp0260549_*Drosophila_yakuba*
Dse_Upd	FBpp0204301_*Drosophila_sechellia*
Dme_Upd	FBpp0111760_*Drosophila_melanogaster*
Dsi_Upd	FBpp0214050_*Drosophila_simulans*

7.3 Secondary structure prediction for upd3

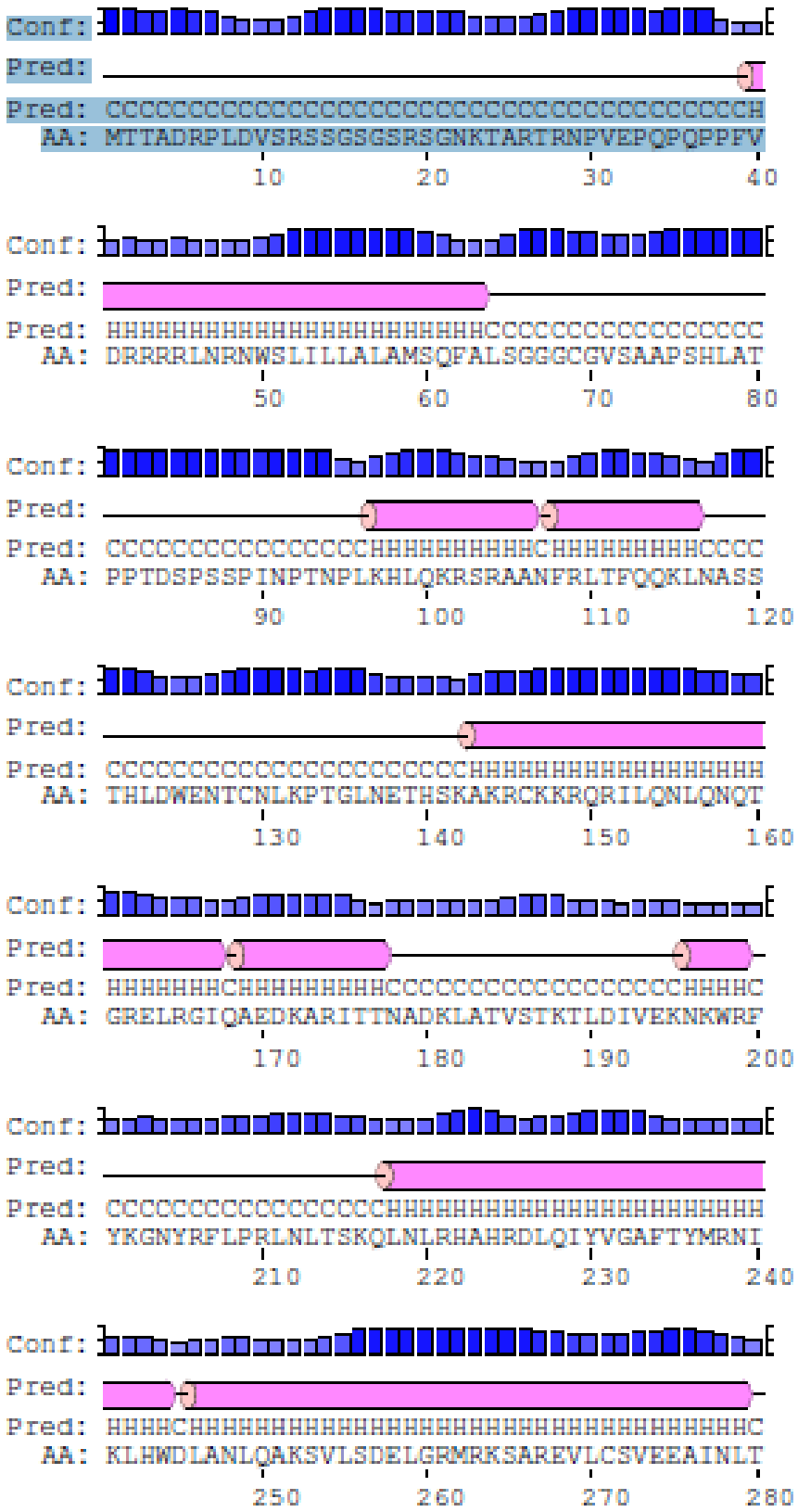

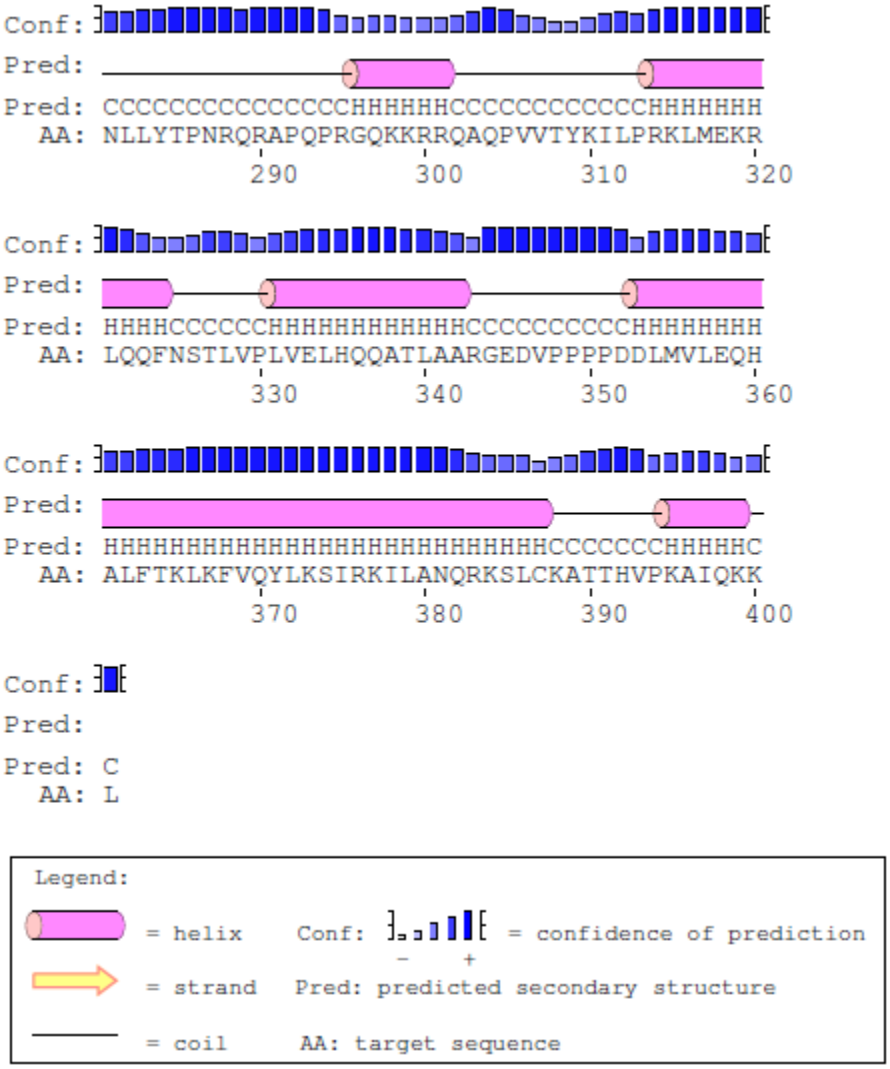

Figure 7-3: Secondary structure prediction of upd3. Secondary structure prediction was performed by PsiPred.

7.4 Expression levels of upd2 and upd3 after hypoxia

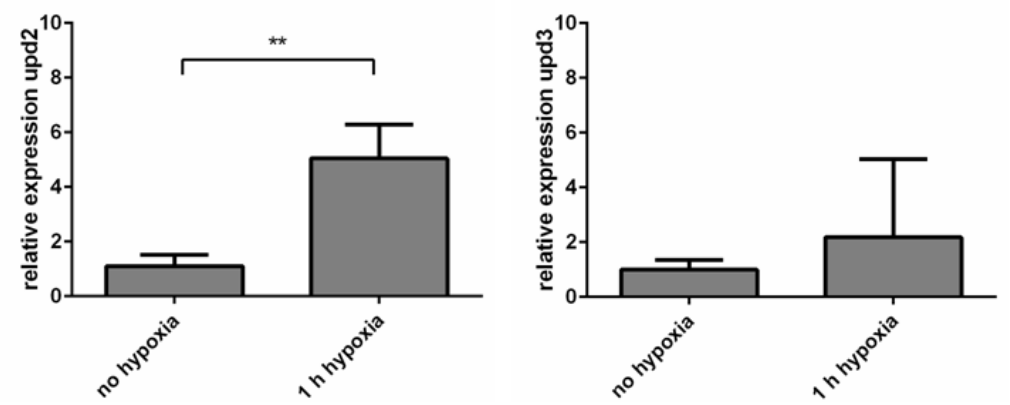

Figure 7-4: Relative expression of upd2 and upd3 in the trachea after treatment with hypoxia. Upd2 transcript levels were significantly increased in the trachea after hypoxia (3% O_2, 1 h). Whereas, only a slight increase of upd3 was observed for hypoxia treated animals. Upd transcripts remained unchanged in tracheas of animals with and without hypoxia treatment (data not shown). Values are means of at least 3 independent experiments ± SEM. Y-axis is expressed as the fold change and significances are calculated using t-test with **p = 0.01 to 0.001, ***p < 0.001, NS p > 0.05.

7.5 Cloning of dFoxO DBD into pET28a (+)

pEX-A2 dFoxO DBD

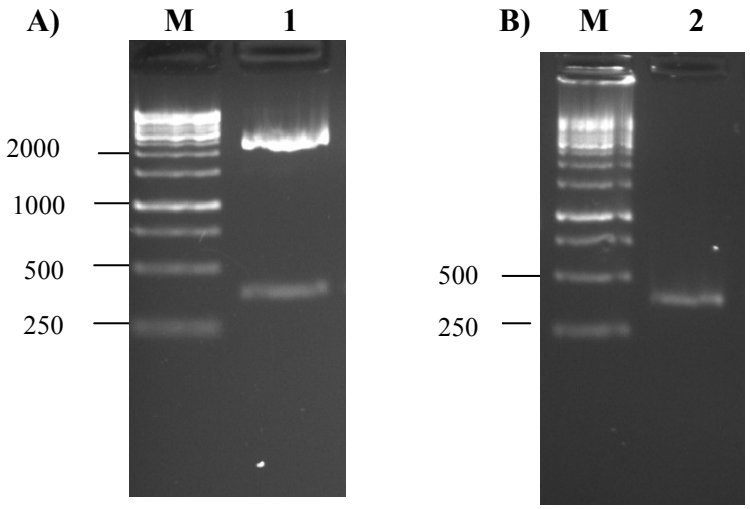

Figure 7-5: Double digest of pEX-A2 dFoxO DBD with NheI and HindIII and gel-purified dFoxO DBD. The plasmid pEX-A2 dFoxO DBD containing the synthetic gene coding for the dFoxo DNA binding domain was transformed into *E.coli* DH5α. The purified plasmid DNA of pEX-A2 dFoxO DBD (2450 bp) was restricted with NheI and HindIII and yielded into 2 fragments: a part of unrestricted plasmid DNA pEX-A2 dFoxO DBD and the dFoxO DBD fragment of 384 bp. The target gene was purified from the agarose gel as described in **Section 3.2.5**.

pET28a(+)FoxO_DBD

SD
AAGGAGATATACCATGGGCAGCAGCCATCATCATCATCATCACAGCAGCGGC ...
M G S S H H H H H H S S G …
NheI
CTGGTGCCGGCGGGCAGCCATATGGCTAGCAATGCGAATGCAGCCAAGAAGAAC
L V P R G S H M A S N A N A A K K N..
HindIII
N-terminus…GGCAGGGCCTAGAAGCTT
G R A

Figure 7-6: Cloning scheme of dFoxO DBD into pET28a (+). The start methionine is highlighted in a frame, the HIS-tag in red and the STOP codon in green color.

Vector map of pET28a (+) FoxO_DBD

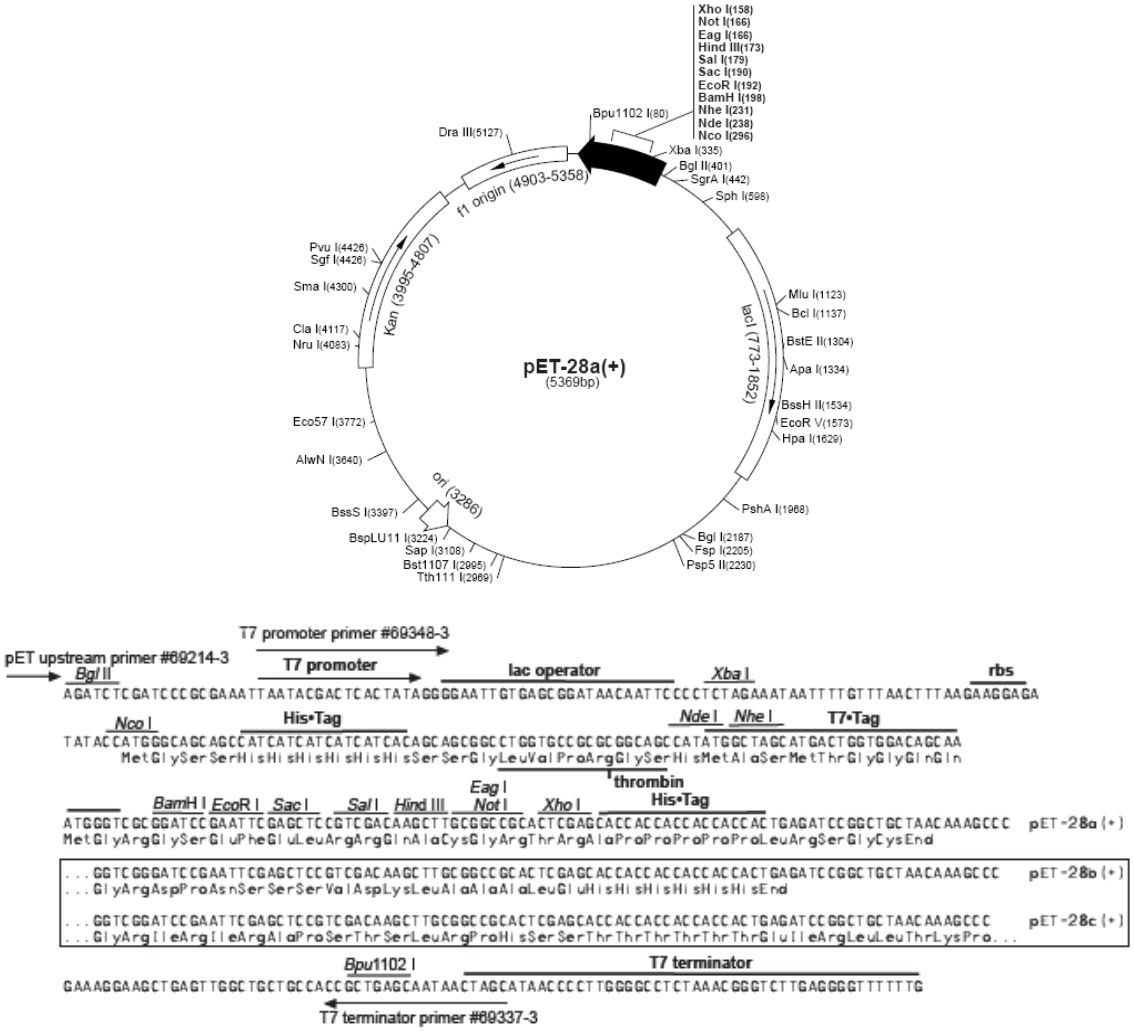

Figure 7-7: Vector pET28a (+). The pET28a (+) vector contains kanamycin resistance. Unique sites are shown on the map. The cloning/expression region of the coding strand transcribed by T7 RNA polymerase is shown. The pET28a (+)dFoxO DBD vector was constructed by cloning the dFoxO DBD codon sequence into the vector's multiple cloning site, using NheI and HindIII restriction sites. This cloning strategy allows N-terminal His-tag affinity purification.

Sequencing result of pET28a (+) FoxO_DBD

```
dFoxO_DBD_seq   1 : AATTTNGNTTAACTTTAAGAAGGAGATATACCATGGGCAGCAGCCATCAT
dFoxO_DBD       - : -------------------------------------------------

dFoxO_DBD_seq  51 : CATCATCATCACAGCAGCGGCCTGGTGCCGCGCGGCAGCCATATGGCTAG
dFoxO_DBD       1 : ----------------------------------------GCTAG

dFoxO_DBD_seq 101 : CAATGCGAATGCAGCCAAGAAGAACTCATCGCGTCGCAATGCATGGGGAA
dFoxO_DBD       5 : CAATGCGAATGCAGCCAAGAAGAACTCATCGCGTCGCAATGCATGGGGAA

dFoxO_DBD_seq 151 : ATCTATCCTATGCGGATCTCATCACGCATGCCATTGGATCGGCCACCGAC
dFoxO_DBD      55 : ATCTATCCTATGCGGATCTCATCACGCATGCCATTGGATCGGCCACCGAC

dFoxO_DBD_seq 201 : AAACGATTGACACTGAGTCAGATTTACGAGTGGATGGTCCAGAATGTGCC
dFoxO_DBD     105 : AAACGATTGACACTGAGTCAGATTTACGAGTGGATGGTCCAGAATGTGCC

dFoxO_DBD_seq 251 : ATATTTCAAGGACAAGGGCGATTCGAATAGCAGTGCCGGATGGAAGAACT
dFoxO_DBD     155 : ATATTTCAAGGACAAGGGCGATTCGAATAGCAGTGCCGGATGGAAGAACT

dFoxO_DBD_seq 301 : CCATACGTCACAATCTGTCGCTGCACAACCGCTTTATGAGGGTCCAAAAC
dFoxO_DBD     205 : CCATACGTCACAATCTGTCGCTGCACAACCGCTTTATGAGGGTCCAAAAC

dFoxO_DBD_seq 351 : GAGGGCACCGGCAAGTCATCCTGGTGGATGCTCAACCCGGAGGCCAAGCC
dFoxO_DBD     255 : GAGGGCACCGGCAAGTCATCCTGGTGGATGCTCAACCCGGAGGCCAAGCC

dFoxO_DBD_seq 401 : CGGCAAGTCTGTGCGCCGCCGTGCCGCTTCCATGGAGACGTCCCGGTACG
dFoxO_DBD     305 : CGGCAAGTCTGTGCGCCGCCGTGCCGCTTCCATGGAGACGTCCCGGTACG

dFoxO_DBD_seq 451 : AGAAGCGGCGCGGCAGGGCCTAG
dFoxO_DBD     355 : AGAAGCGGCGCGGCAGGGCCTAG
```

Figure 7-8: Alignment of sequenced pET28a (+) FoxO_DBD and original dFoxO DBD sequence. The sequencing result obtained from https://www.gatc-biotech.com/en/index.html confirms the correct insertion of dFoxO DBD into pET28a (+) vector. The start methionine is highlighted in a frame, the HIS-tag in red and the STOP codon in green color.

7.6 Induced remodeling of the terminal branches after CSE

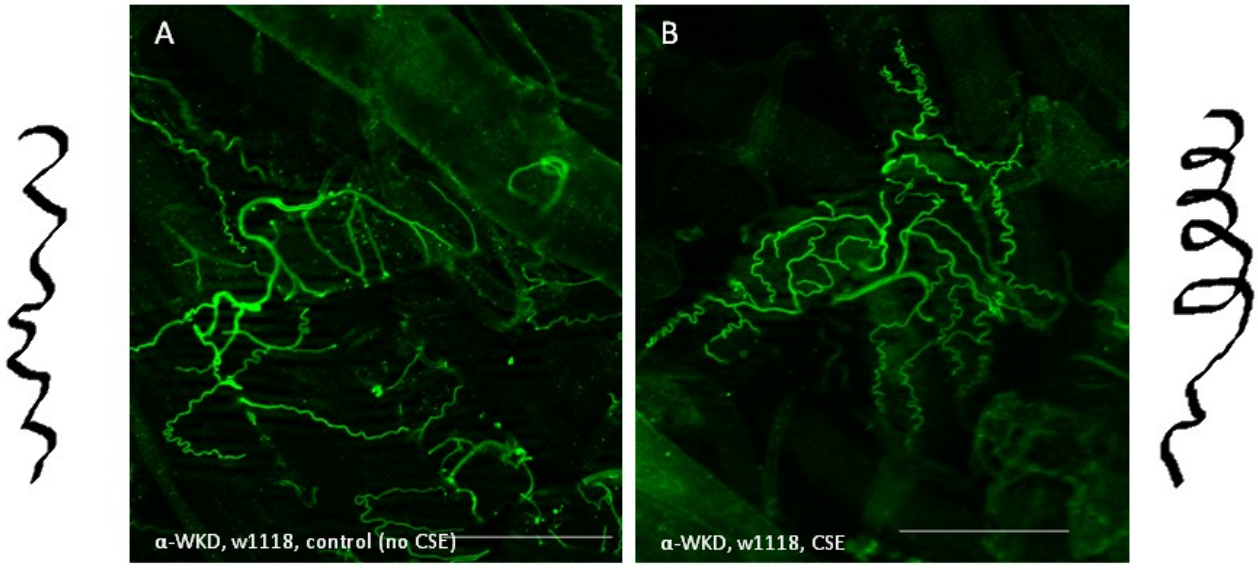

Figure 7-9: Remodeling of the terminal cells after CSE. The terminal branches of CS-exposed 3rd instar larvae looking curlier (**B**) in comparison to control animals (**A**). In green: α-WKD antibody, scale bar is 100 µm.

7.7 Application of DREADD for targeted manipulation of the trachea

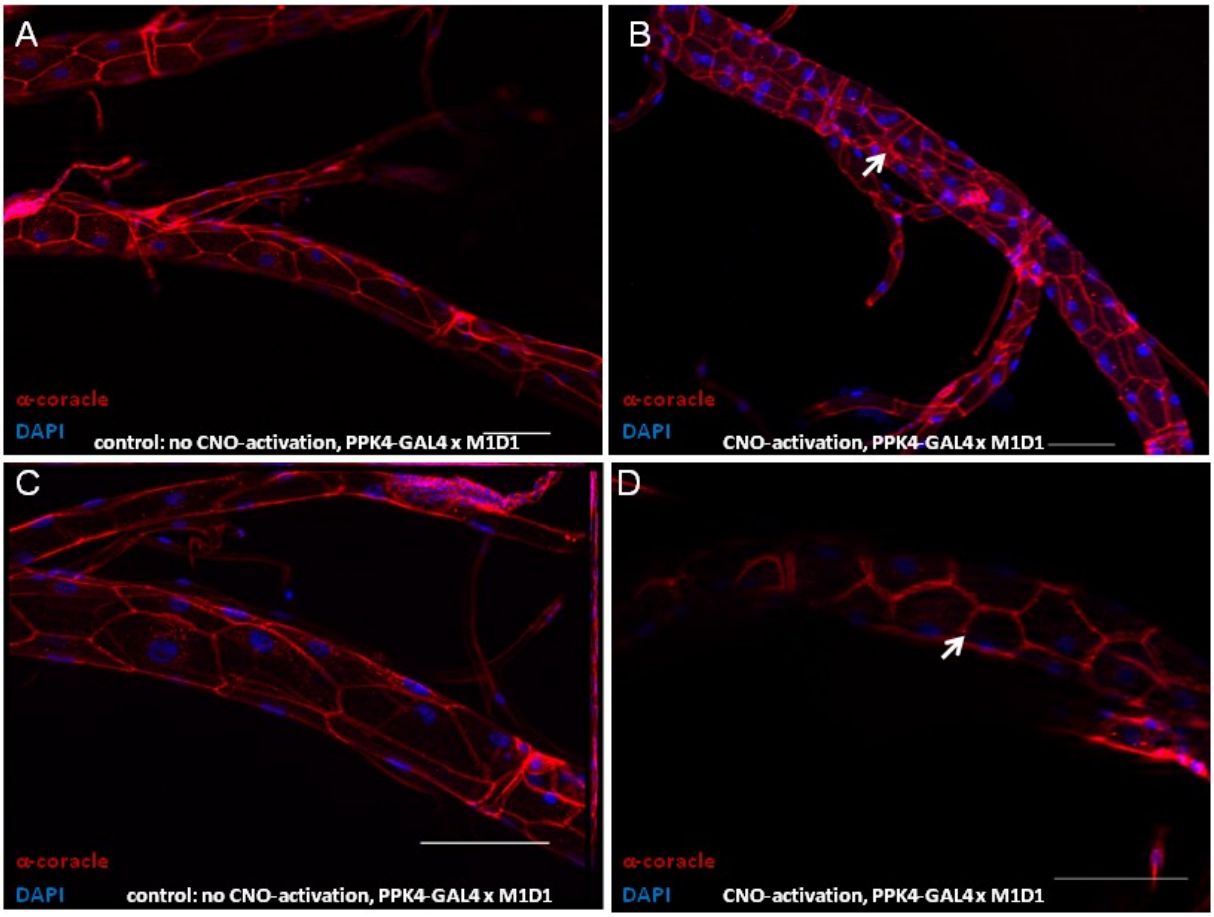

Figure 7-10: CNO-activation of DREADD (M1D1) receptor in the respiratory tract of the fly. The DREADD receptor (M1D1) was activated *in vivo* in the trachea using PPK4-Gal4 and by feeding animals CNO. Activation of DREADD, leads into decreased cell size as visualized by DAPI (blue) and α-coracle staining (red) (**B and D**) in comparison to control animals (**A and C**). Scale bar: 100 µm, crosses were performed using UAS-DREADD-M1D1 x PPK4-Gal4.

Acknowledgement

First and foremost, I want to express my biggest thanks to Prof. Dr. Thomas Roeder for making this interesting PhD thesis possible at his lab and for his extended scientific support and supervision! I sincerely appreciate his warm guidance throughout my work. It was a great experience for me to work with *Drosophila melanogaster*.

I cordially thank Dr. Abhishek Kumar for teaching me so many useful skills over the years, which I could apply in my thesis and for giving me the chance to shape my personality as a researcher by collaborative work.

I want to express my special thanks to all members of the Molecular Physiology department for the good working environment and Dr. Christine Fink, for the stuff ordering and organization of the lab. Many thanks goes to Dr. Flora Stephano and Dr. Li Yong, it has been a pleasure to work alongside with you. I will always remember our nice conversations and laughing which we had beside the work. I want to also say thanks to Dr. Julia Hoffmann for her helpful contributions during the lab meetings. I thank Tian, Ali, and Yang for the nice atmosphere in our room! Thanks also to our "little" lab member Justus for the hearty connection, his nice drawings and for providing me ice cream and sweets.

Special thanks go to the technical assistants Britta Laubenstein and Christiane Sandberg for the lab maintenance that helped in smooth running of our lab. Thanks also to Heidi and Heidrun.

I thank my previous bachelor student Dörte Nitchkowski for the nice time we have spent together in the lab.

Thanks to Dr. Sreemukta Acharya and Dr. Zhiyi Lv for the cheerful time during the EDRC in Heidelberg.

I also thank my cousin sister Kitty Choudary, Rosemarie and my neighbor Maria for their care, support and positivity. The acknowledgements would be incomplete without the mention of my dear Harish.

I thank the German Center for Lung Research (DZL) and the Airway Research Center North (ARCN) for funding this project.

Most importantly, none of this would have been possible without the love and patience of my parents, my opa and brother - they have been a constant source of love, concern, support and strength all these years.

THANK YOU!

Curriculum vitae

Date of birth	01.02.1983
Place of birth	Freital
Nationality	German
Marital Status	Single

Professional education/ Work experience

01/13 - 12/15 Research Associate & Doctoral thesis, Zoological institute, Department of Molecular Physiology, workgroup of Prof. Dr. Thomas Roeder, Christian-Albrechts-University at Kiel

- Research focus: Development of COPD (Chronic Obstructive Pulmonary Disease) models using the fruit fly *Drosophila melanogaster*
- Unraveling signaling pathways and molecular characterization of genes of the airway epithelium after exposure to cigarette smoke
- Applied methods: Real-time PCR, Immunohistochemsitry, EMSA etc.

08/11 – 12/12 Researcher, Institute of Phytopathology, Department of Molecular Phyto-pathology and Biotechnology, Christian-Albrechts-University at Kiel

- Research focus: Enhancing the resistance of rape (*Brassica napus*) against *Sclerotinia* stem rot disease
- Applied methods: RNAseq, Real-time PCR, cloning

04/11 - 07/11 Researcher, Department of Gynecology and Obstetrics, Faculty of Medicine, University of Greifswald

- Research focus: Effect of Malaria on the Placental vascular development
- Applied methods: Isolation and cell culture of primary cell line of HUVECS (Human umbilical vein endothelial cells), stem cells of umbilical cord blood, trophoblast cells of cotyledons of human placenta and abortion material and immunomagnetic purification via MACS-technology

Academic education

01/09 - 03/11 **Master of Science (M.Sc.) Biotechnology and Applied Ecology** at the Dresden university of technology (TU Dresden) - International Institute (IHI) Zittau, central academic unit of TU Dresden

Master thesis: ***Modification of Human Cationic Trypsinogen Reduces Autoactivation***, Center for Biotechnology and Biomedicine (BBZ) Leipzig, Research group: Structural analysis of biopolymers & Junior Research Group:

Ultrasensitive Protein Detection Unit (USPDU)

- Research focus: Modification, Expression and Purification of Human Cationic Trypsinogen for its application in a sensitive two-enzyme cascade

09/05 - 01/09 **Bachelor of Science (B.Sc.) Biotechnology**, at the University of Applied Sciences Zittau/ Görlitz

Bachelor thesis: ***Characterization of the operator region of the transcriptional repressor FrrA of Bradyrhizobium japonicum***,

Department of Biology, Institute of Genetics, Dresden university of technology (TU Dresden)

- Research focus: Analysis of the interaction of the transcription regulator FrrA with its palindromic typical operator motifs through DNA-binding assays (EMSA)

Publications

1. Kumar A., **Bhandari, A.**, Sarde, S. J., Muppavarapu S. & Tandon, R. (2015). Understanding V(D)J recombination initiator RAG1 gene using molecular phylogenetic and genetic variant analyses and upgrading missense and non-coding variants of clinical importance. Biochem. Biophys. Res. Commun. (in Press)

2. El-Kholy S., Stephano F., Li Y., **Bhandari A.**, Fink C., Roeder T. (2015) Expression analysis of octopamine and tyramine receptors in *Drosophila. Cell and Tissue Research*; DOI:10.1007/s00441-015-2137-4

3. Kumar A., **Bhandari, A.**, Krishnaswamy, S. (2015). Sequence and Structural Perspectives of bacterial β-Stranded Porins. Proteins & Peptide Letters, 22(1), 8–22. DOI: 10.2174/0929866521666140827110755.

4. Kumar A., **Bhandari, A.**, & Goswami, C. (2014). Surveying genetic variants and molecular phylogeny of cerebral cavernous malformation gene, CCM3/PDCD10. *Biochem. Biophys. Res. Commun.*, 455(5), 98–106. DOI: 10.1016/j.bbrc.2014.10.105.

5. Kumar A. & **Bhandari, A.** (2014) Urochordate serpins are classified into six groups encoded by exon-intron structures, microsynteny, sequence and Bayesian phylogenetic analyses. *J. Genomics,* 2:131-140. doi:10.7150/jgen.9437 (New Journal).

6. Kallsen K., Fink C., **Bhandari A.**, Kabesch M., Heine H., Roeder T. (2014) Deregulation of ORMDL3 expression induces stress responses and modulates repair pathways, Pneumologie 06/2014; 68(06). DOI:10.1055/s-0034-1376771

7. Kumar A., **Bhandari, A.**, Sarde, S. J., & Goswami, C. (2014). Molecular phylogeny of C1 inhibitor depicts two immunoglobulin-like domains fusion in fishes and ray-finned fishes specific intron insertion after separation from zebrafish. *Biochem. Biophys. Res. Commun.* 450, 219–226.

8. Kumar A., **Bhandari, A.**, Sarde, S. J., & Goswami, C. (2014). Genetic variants and evolutionary analyses of heparin cofactor II. *Immunobiology,* 219, 713–728

9. Kumar, A., Sarde, S. J., & **Bhandari, A.** (2014). Revising angiotensinogen from phylogenetic and genetic variants perspectives. *Biochem. Biophys. Res. Commun.*, 446, 504–518. doi:10.1016/j.bbrc.2014.02.139.

10. Kumar A., **Bhandari, A**., Sarde, S. J., & Goswami, C. (2013). Sequence, phylogenetic and variant analyses of antithrombin III. *Biochem. Biophys. Res. Commun.*, *440*(4), 714–724. doi:10.1016/j.bbrc.2013.09.134

11. Kumar A.†, **Bhandari A.**†, Sinha R., Sardar P., Sushma M., *et al*. (2012). Molecular *Phylogeny of OVOL Genes Illustrates a Conserved C2H2 Zinc Finger Domain Coupled by Hypervariable Unstructured Regions*. PLoS ONE 7(6): e39399. doi:10.1371/journal.pone.0039399

12. Sardar P., Kumar A., **Bhandari A.**, Goswami C. (2012). *Conservation of Tubulin-Binding Sequences in TRPV1 throughout Evolution*. PLoS ONE 7(4): e31448. doi:10.1371/journal.pone.0031448

13. Wenzel M.†, Lang K.†, Günther T., **Bhandari A.**, Weiß A., Lulchev P., Szentgyörgy E., Kranzusch B., and Göttfert M. (2012). *Characterisation of the Flavonoid-Responsive Regulator FrrA and its Binding Sites*. Journal of Bacteriology, May;194(9):2363-70.

14. Kumar A.†, **Bhandari A.**†, Sinha R., Goyal P., Grapputo A. (2011). *Spliceosomal Intron Insertions in Genome Compacted Ray-Finned Fishes as Evident from Phylogeny of MC Receptors, Also Supported by a Few Other GPCRs*. PLoS ONE 6(8): e22046. doi:10.1371/journal.pone.0022046
(† shared first authors)

Manuscripts under preparation

Bhandari, A., Nitschkowski, D., Fedders, H. & Roeder, T. (2015). Activation of JAK-STAT signaling in the airway epithelium of *Drosophila melanogaster* in response to cigarette smoke - new insight in COPD

Bhandari, A. & Roeder, T. (2015). Utilization of optogenetics to study cAMP signaling in the airways of *D. melanogaster*

Kumar, A., **Bhandari, A.**, Sarde, S. J., & Goswami, C. (2015). Molecular evolution, sequence and genetic variant analyses of collagen chaperone protein HSP47.

Patents

Title: **"FrrA and flavonoide-inducible expression system"**
Patent ID: **DE102008062285A1**
Author names: **Bhandari, A.,** Göttfert, M., Günther T., Lang K., Mäbert K., Wenzel M.
Year: 2010

Talks

Anita Bhandari, S. Rietz und Daguang Cai: RNAseq-basierte Analysen und Identifizierung von Resistenzmechanismen gegen die Weißstängeligkeit (*Sclerotinia sclerotiorum*) in Wildkohlarten (*Brassica spec*.), 58. Deutsche Pflanzenschutztagung, Technische Universität Braunschweig, 10. - 14. September 2012

Bhandari A.: Molecular Identification of *Sclerotinia sclerotiorum* resistance mechanisms in *Brassica spec*. by use of RNAseq strategy, James D. Watson Institute of Genome Sciences, Institute of Bioinformatics & Crop Sciences Zhejiang University Hangzhou, china, 17. - 27. September 2011 (invited talk)

Posters

Bhandari A. & Roeder T.: JAK-STAT signaling in response to cigarette smoke in the respiratory epithelia of *Drosophila melanogaster* - induction of an autocrine immune related signaling system. 24th European *Drosophila* Research Conference (EDRC), September 9th - 12th 2015, Heidelberg

Bhandari A. & Roeder T.: Activation of JAK-STAT signaling in the airway epithelium of *Drosophila melanogaster* in response to cigarette smoke. Regional *Drosophila* Meeting 2014, 27th - 28th may 2014, Heidelberg

Bhandari A., Gu T., Kallsen K. & Roeder T.: Development of COPD models using the fruit fly *Drosophila melanogaster*. Annual Meeting of German Center for Lung Research (*DZL*), 26th - 27th January 2015, Hamburg

Kumar, A. **Bhandari, A.** Sushma, M. Kumar, U., Goyal, P. Sequence, Structure and Evolution of Metazoan Ovo-like genes. National Symposium on Modern Approaches and Innovations in Biotechnology, (November 14-15, 2010), Meerut, India. Published in conference proceeding

Eidesstattliche Erklärung

Hiermit erkläre ich, dass die vorliegende Dissertation, abgesehen von der Beratung durch die Betreuer, in Inhalt und Form selbständig von mir angefertigt wurde. Es wurden ausschließlich die ausdrücklich benannten Hilfsmittel und Quellen verwendet. Wörtlich oder sinngemäß übernommenes Gedankengut habe ich als solches kenntlich gemacht. Zudem versichere ich, dass die Arbeit noch keiner anderen Fakultät oder Universität zur Prüfung vorgelegt wurde, dass sie noch nicht veröffentlicht ist und ich eine Veröffentlichung vor Abschluss des Promotionsverfahrens nicht vornehmen werde. Diese Arbeit ist unter Einhaltung der Regeln guter wissenschaftlicher Praxis der Deutschen Forschungsgemeinschaft entstanden.

Kiel, 05.11.2015

Ort, Datum	Unterschrift